EUROPEAN UNION
EUROPEAN FUND FOR
MARITIME AFFAIRS AND FISHERIES

MINISTRY OF AGRICULTURE, FOOD AND FORESTRY

ПРОГРАМА ЗА
МОРСКО ДЕЛО И
РИБАРСТВО

PELAGIC TRAWL SURVEYS IN THE BULGARIAN MARINE AREA 2017-2019

Violin St. Raykov et al., 2020

2020

www.eufunds.bg

Project proposal № BG14MFOP001-3.003-0001 "Collection, management and use of data for the purposes of scientific analysis and implementation of the Common Fisheries Policy for the period 2017-2019", funded by the Maritime Affairs and Fisheries Program, co-financed by the European Union through the European Maritime and Fisheries Fund

EUROPEAN UNION
EUROPEAN FUND FOR MARITIME AFFAIRS AND FISHERIES

MINISTRY OF AGRICULTURE, FOOD AND FORESTRY

ПРОГРАМА ЗА
МОРСКО ДЕЛО И РИБАРСТВО

This study was carried out thanks to the financial support of the European Commission under Regulation (EC) No 199/2008 and Regulation (EU) 2017/1004 of the European Parliament and of the Council on the establishment of a Union framework for the collection, management and use of data in the fisheries sector and support for scientific advice regarding the common fisheries policy and repealing Council Regulation (EC) No 199/2008, the National Agency for Fisheries and Aquaculture – Ministry of Agriculture, Food and Forestry, Bulgaria and

Institute of Oceanology – BAS, Varna, Bulgaria

Project No BG14MFOP001-3.003-0001, "Collection, management and use of data for the purpose of scientific analysis and implementation of the Common Fisheries Policy for the period 2017-2019", funded by the Maritime and Fisheries Program and co-financed by the European Union through the European Maritime and Fisheries Fund

The survey was carried out during the period 2017 – 2019 in the Bulgarian Black Sea area on board of R/V *HAITHABU* in execution of the National Program of Bulgaria for data collection.

BULGARIAN ACADEMY OF SCIENCES

INSTITUTE OF OCEANOLOGY

VARNA

Assoc. Prof. Violin Raykov (project leader), Assoc. Prof. Maria Yankova, Assoc. Prof. Petya Ivanova, Assoc. Prof. Veselina Mihneva, Assoc. Prof. Dimitar Dimitrov, Assoc. Prof. Kremena Stefanova, Chief Asst. Elitsa Stefanova,Ilian Kotsev, Chief Asst. Nina Dzembekova, Chief Asst.Ivelina Zlateva, Nelly Valcheva (technician), Dobroslav Dechev (technician), Hristiyana Stamatova (technician), Svetla Koleva (technician), Petar Trandafilov (logistics), Snejina Bacheva (editor)

https://doi.org/10.7546/IO.BAS.2020.5

ISBN 978-619-245-070-0
e-book 978-619-245-071-7

www.eufunds.bg

Project proposal № BG14MFOP001-3.003-0001 "Collection, management and use of data for the purposes of scientific analysis and implementation of the Common Fisheries Policy for the period 2017-2019", funded by the Maritime Affairs and Fisheries Program, co-financed by the European Union through the European Maritime and Fisheries Fund

Contents

Project proposal № BG14MFOP001-3.003-0001 "Collection, management and use of data for the purposes of scientific analysis and implementation of the Common Fisheries Policy for the period 2017-2019", funded by the Maritime Affairs and Fisheries Program, co-financed by the European Union through the European Maritime and Fisheries Fund

Project proposal № BG14MFOP001-3.003-0001 "Collection, management and use of data for the purposes of scientific analysis and implementation of the Common Fisheries Policy for the period 2017-2019", funded by the Maritime Affairs and Fisheries Program, co-financed by the European Union through the European Maritime and Fisheries Fund

1. Results from pelagic surveys in 2017-2019

1.1. Summary

Pelagic Trawl Surveys were accomplished in October-December 2017; Ocober-December 2018; June 2019 and October-November 2019 in the Bulgarian Black Sea zone. A scientific team has produced a biological analysis of the results obtained from the surveys. The biological analysis is based on the biomass of the species found during the study. Besides, an analysis of the distribution and abstraction of the other species caught as by-catch is presented. Sprat (*Sprattus sprattus*) is a key species for the Black Sea ecosystem. Together with the anchovy, sprat is one of the most abundant, planktivorous, pelagic species. The level of its stocks depends on the conditions of the environment mainly and on the fishing effort (Raykov, 2007; Raykov et al., 2007; Raykov et al., 2011).

The changes in the environment due to anthropogenic impact affect the dry land as well as the world ocean. The level of sea pollution and its "self-purifying" ability is completely different. There is a clear indication of changes in the natural equilibrium in the corresponding ecological niches (Prodanov et al., 1997). The greatest impact on the world ocean has commercial fishery, which directly devastates a significant part of the given species populations. As a result of this, some of the species stocks are declined or depleted. As a result of the excessive exploitation, altered habitats and climatic variations numerous of the commercial species are critically endangered or vulnerable. The abundance of the given fish species generations is dependent on different abiotic and biotic factors. With great importance is the level of fishing mortality, changes in trophic levels due to mass occurrence of the ctenophore *Mnemiopsis leidyi*, algal blooms which lead to hypoxia in the shallower waters with mass mortality of the bottom-dwelling organisms, etc. The recent state of the sprat stock biomass (aggregations) off the Bulgarian Black sea coast show relative stability, i.e. taking into consideration the almost constant level of exploitation (in the western and north-western part of the Black Sea) in recent years, the stock has not yet been sufficiently exploited. Estimates of the number and size distributions of fish stocks based on experimental

trawling have become a necessity in fisheries management (GodØ et al., 1990). The main assumption in these studies is that the level of catches is constant, no matter how long the trawling is. Any deviation from the linear dependence between the catch and the magnitude of the effort applied to the fishery can have a significant impact on the composition of the catches and the estimates of the numbers and deviate from the results of the trawl studies (Wassenberg et al., 1998). The duration of the fishing effort during the trawling period may last up to 200 min (GodØ et al., 1990), but for economic reasons, together with the need for multiple reps and maintaining statistical validity, the duration of trawling is reduced. Thus, the standard trawl duration varies from 30 to 120 minutes for each selected station. Some authors (Godø et al., 1990; Somerton et al., 2002; Wassenberg et al., 2002) allow larger specimens to swim in the trawl without entering the bag and that trawls of varying lengths may affect the levels of the catches and the size distribution of the trawl. In this way, some size groups may not be captured in short-haul trawls. The average catch per unit of effort or unit area is the inventory of the stock (assumed to be proportional to the stock) (Beverton and Holt, 1957). These indices can be converted into an absolute measure for biomass by the so-called "area method" which is also referred to as a holistic method (www.fao.org). All analyses are based on biomass and density estimates and geographical strata. All the teams calculated their standard statistical estimates using the same software.

This report presents successively the results obtained at these two levels. The regional reports are presented in order following the coast, from the northern to the southern part of the Black Sea. The document is completed by a series of tables and figures related to the biomass/abundance indices and length-frequency distributions of the species included in the reference list.

2. Research vessel and gears

The Pelagic Trawl survey (PT) was accomplished on the board of research vessel *HaitHabu* (Pic. 2.1; 2.2). The main characteristics of the ship are listed below.

Pic. 2.1. R/V *HaitHabu*

R/V *HaitHabu*

IMO: 8862686
MMSI: 207139000
Call sign: LZHC
Flag: Bulgaria [BG]
AIS Vessel Type: Other
Gross Tonnage: 142
Length Overall x Breadth Extreme:24.53m × 8m Crew: 6

Pic. 2.2. a,b Catch of the OTM

3. Material and Methods

Pelagic Trawl surveys were accomplished following National Programs for Data Collection in the Fisheries sector of Bulgaria for 2017-2019. The study was conducted during the period June and October-November 2017- 2019, in the area enclosed between Durankulak and Ahtopol (Bulgaria) with a total length of the coastline of 370 km. The study area encloses waters between 42^{o}05’ and 43^{o}45’ N and 27^{o}55 and 29^{o}55 E.

During the survey, a total of 37mid-water hauls were carried out in the Bulgarian area (October-November 2019). The survey took place during the day and the following types of data were collected:

- Coordinates and duration of each trawl
- Sprat total catchweight
- Separation of the by-catch by species
- Composition of by-catch
- Conservation of the samples

Project proposal № BG14MFOP001-3.003-0001 "Collection, management and use of data for the purposes of scientific analysis and implementation of the Common Fisheries Policy for the period 2017-2019", funded by the Maritime Affairs and Fisheries Program, co-financed by the European Union through the European Maritime and Fisheries Fund

3.1. Sampling design

To establish the abundance of the reference species (*Sprattus sprattus*) in front of the Bulgarian coast a standard methodology for stratified sampling was employed (Gulland, 1966). To address the research objectives the region was divided into 3 strata according to depth: Stratum 1 (15 - 30 m), Stratum 2 (35 – 50 m) and Stratum 3 (50 – 100m).

The study area in Bulgarian waters was partitioned into 128 equal in size, not overlapping fields, situated at a depth between 16 - 92 m. At 37of the fields chosen at random, sampling employing mid-water trawling was carried out (Pic. 3.1.1).

Pic. 3.1.1. Trawling operation

Each field was a rectangle with sides 5' Lat × 5' Long and area around 62.58 km^2 (measured by application of GIS), large enough for a standard lug extent in meridian direction to fit within the field boundaries. The fields were grouped in larger sectors, so-called strata, in which geographic and depth boundaries were selected according to the density distribution of the species under study. At each of the fields, only one haul with duration between 30 - 40 min at speed 2.7-2.9 knots was carried out.

As a result of the trawling survey, a biomass index was calculated.

3.2. Onboard sample processing

The number of processed individuals is presented in Table 3.2.1.

Table 3.2.1. Number of processed individuals

Species	Number
Sprat	1326
Whiting	893
Red Mullet	925

Species	Numbs
S.sprattus	2565
M.merlangius	1084
M.barbatus	1195

Species	Numbs
M.barbatus	750
T.mediterraneus	1800
P.saltatrix	550
E.encrasicolus	1550
S.sprattus	98

Species	Numbs
(*S.sprattus*)	1250
(*T.mediterraneus*)	750
(*M.barbatus*)	680
(*M.merlangus*)	744

The data recorded and samples collected at each haul include (Gulland,1966):

- Depth, measured by the vessel's echo sounder
- GPS coordinates of start/end haul points
- Haul duration
- An abundance of sprat caught
- Weight of total sprat catch
- Abundance and weight of other large species
- Species composition of by-catch
- 4% Formaldehyde solution with marine water was used for the conservation of sprat for stomach content examination.

Project proposal № BG14MFOP001-3.003-0001 "Collection, management and use of data for the purposes of scientific analysis and implementation of the Common Fisheries Policy for the period 2017-2019", funded by the Maritime Affairs and Fisheries Program, co-financed by the European Union through the European Maritime and Fisheries Fund

3.3. Laboratory analyses

The samples collected onboard were processed in a laboratory for determination of age and food composition.

The age was established in otoliths under the binocular microscope.

The food spectrum was determined by separation of the stomach contents into taxonomic groups identified to the lowest possible level.

3.4. Statistical analyses

Swept area method

This method is based on bottom trawling across the seafloor (area swept), weighted with chains, rock-hopper, and roller gear, or steel beams. Widely used a direct method for demersal species stock assessment (Foote,1996).

The main point of the method: the trawl doors are designed to drag along the seafloor for defined distance. Trawling area was calculated as follows:

(1) $$a = D * hr * X2$$
$$D = V * t$$

(Where: a – trawling area, V – trawling velocity, hr* X2 – trawl door distance, t – trawling duration (h), D – dragged distance on the seafloor;

(2) $$D = 60 * \sqrt{(Lat_1 - Lat_2)^2 + (Lon_2 - Lon_1) * \cos(0.5 * (Lat_1 + Lat_2))}$$

(3) $$D = \sqrt{VS^2 + CS^2 + 2 * VS * CS * \cos(dirV - dirC)},$$

Where, VS is vessel velocity, CS - present velocity (knots), dir$V$ vessel course (degrees), and $dirC$- present course (degrees).

Stock biomass is calculated using catch per unit area, as a fraction of catch per unit effort from the dragged area:

(4) $$\left(\frac{C_{w/t}}{a/t}\right) = C_{w/a} kg / sq.km$$

Where: *Cw/t* – catch per unit effort, a/t – trawling area (km^2) per unit time;

Stock biomass of the given species per each stratum could be calculated as follows:

(5) $B = (\overline{C_{w/a}}) * A$

Where: $\overline{C_{w/a}}$ - mean CPUA for total trawling number in each stratum, A- area of the stratum.

The variance of biomass estimate for each stratum is (equation 4):

(6) $VAR(B) = A^2 * \frac{1}{n} * \frac{1}{n-1} * \sum_{i=1}^{n} \left[Ca(i) - \overline{Ca}\right]^2$

The total area of the investigated region is equal to the sum of areas of each stratum:

$A = A1+A2+A3$

Average weighted catch per whole aquatic territory is calculated as follows:

(7) $\overline{Ca}(A) = Ca1 * A1 + Ca2 * A2 + Ca3 * A3 / A$

Where: Ca1- catch per unit area in stratum 1, A1 – an area of stratum 1, etc., A- size of total area.

Accordingly, total stock biomass for the whole marine area:

(8) $B = \overline{Ca}(A) * A$

Where: $\overline{Ca}(A)$ - average weighted catch per whole investigated marine area, A – total investigated marine area.

Estimation of Maximum Sustainable Yield (MSY)

The Gulland's formula for virgin stocks is used (equation 7):

(9) MSY = 0.5*M*Bv

where: M – coefficient of natural mortality; Bv – virgin stock biomass.

A relative yield-per-recruit model with uncertainties

$$Y'/R = E * U^{M/k}\left\{1 - \frac{3U}{(1+m)} + \frac{3U^2}{(1+2m)} - \frac{U^3}{(1+3m)}\right\}$$ (10)

where: U = 1-(Lc/L∞)

m = (1-E)/(M/k) = k/Z

E = F/Z – exploitation coefficient.

Lenght-converted catch curve

Several methods are available with the help of which total mortality (Z) can be estimated from length-frequency data. Thus, it is possible to obtain reasonable estimates of Z from the mean length in a representative sample or the slope of Jones' cumulative plot. In this article, a variety of approaches for analyzing length-frequency data are presented which represent the functional equivalent of [age structured] catch curves. These "length-converted catch curves" are built around assumptions similar to those involved in age-structured catch curves.

3.5. Age estimation

As it is well known, the Calcified Structures (CS) are usually used to assign age useful to obtain their growth model and so, to reconstruct age composition of exploited fish populations. Fish aging implies the presence in the CS of a structural pattern, in terms of succession of opaque and translucent zones and the knowledge of the periodicity of this deposition pattern. Calcified structures available for fish aging are different: otoliths (sagittal, lapilli, asterischi), scales, vertebrae, spines, and opercular bones (Panfili et al., 2002). For the selected stocks the CS utilized is the sagittae. The most important aspects (difficulties, extraction, storage, preparation method, aging criteria) regarding the age analysis are addressed by species. Otoliths are important for fish and fisheries scientists. Otoliths are playing role of balance, motion, and sound. These structures are effective from growth to death in the entire life cycle. They are most commonly used to determine growth age and for mortality studies. Research on otoliths began in the 1970s and continued to 21st century. Periodic growth increments in scales, vertebrae, fin rays, in cleithra, opercula, and otolith are used to determine annual age in many fish species.

Researchers used otolith reference collections and photographs in publications to aid in identification (Pic. 3.5.1). Otoliths have a distinctive shape that is highly specific but varies widely among species.

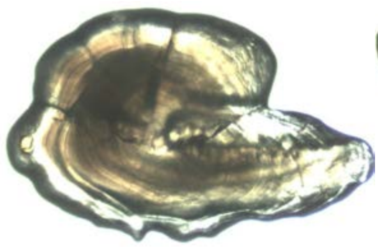

6 cm (0+)

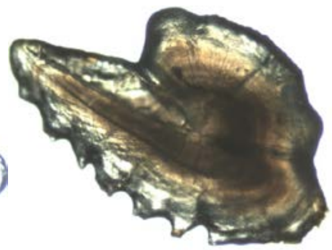

7.5 cm (1+)

8.2 cm (1+)

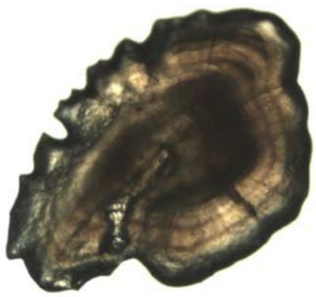

9 cm (2+)

9.5 (3+) 10.7 (4+)

Pic. 3.5.1. Otoliths of sprat

Biologists, taxonomists, and archaeologists, based on the shape and size of otoliths determine fish predators feeding habits (Kasapoglu and Duzgunes, 2014). In teleost fishes, otoliths are the main CS for age determination and it is widely used in fisheries biology. On the other hand, analyzing O_2 isotopes in their structure is useful to determine fish migrations between freshwater and sea as well as species and stock identification. Otoliths are the balance and hearing organs for the fish. They are three types located on the left and right side of the head in semi rings: “sagitta” in the saccular, “lapillus” in the lagenar, and “asteriskus” in the utricular channels. Place, size, and shape of these three types are different by species, the biggest one is sagitta and the smallest one is asteriscus. So, sagitta is the one mostly used in age determination in bony fishes. Other reasons for the preference to otoliths are:

- Their formation in the embryonic phase which shows all the changes in the life cycle of the fish.
- Existence in the fish which have no scales.
- Giving better results than the scales and more successful age readings in older fish
- than their scales.
- No restoration or regeneration.
- Having the same structure in all the individuals in the same species (Jearld, 1983).

On the other hand, their disadvantages are the obligation of dissecting the fish and some failures in age determination due to crystal-like formations by irregular $CaCO_3$ accumulations on the otoliths.

3.5.1. Otolith preparation for sprat

For the sampling of fish for otolith extraction from the overall samples is very important to have representative samples for the catch. The number of otoliths needed is lower for the species having a smaller size range than the species having a larger size range. According to the availability, 5 fish for each length group may be better for age readings to be representative of the population. Each of the individuals should be recorded individually with the place of catch, date, and ID number. These steps are useful for the process:

- For each fish total length (±0,1 cm), total weight (±0,01g), sex, maturation stage (I-V), gonad weight (±0,01g) are recorded.
- Sagittal otoliths of each fish are removed by cutting the head over the eyes after all individual measurements. Then, rinsed and immersed in 96% ethyl alcohol to get rid of organic wastes/residuals and finally kept in small chambers in plastic roomed boxes with the sample number and other operational information.

3.5.2. Preparation of the otoliths for the age determination

Otoliths are put into small black convex glasses containing 96% ethyl alcohol for age readings under the binocular stereo microscope which is illuminated from top and sides (Fig. 3.5.2.1) (Polat and Beamish, 1992). The magnifying level depends on the size of the otolith; X4 is good for sprat and X1 for turbot.

Fig. 3.5.2.1. Binocular stereo microscope with top and side illumination

3.5.3. Age readings and commenting on annuluses

To prevent bias, during age reading reader should not refer the length and weight of that fish. But information on the date of the catch and gonadal state is very important. The first step is to clarify the place of the center and the first age ring. After that, observation of the successive rings, whether they are continuous or not is important.

Finally, determination of the fish in growth or just at the end of the growth period by checking characteristics of the ring at the edge of the otolith to decide it is opaque or hyaline. After these procedures otoliths can be read under these protocols which are very important to provide data on age to determine realistic population parameters and reduce uncommon procedures and biases by standardized age reading criteria.

3.5.4. Sprat (Sprattus sprattus)

In sprat left and right otoliths show isometric growth. They are small and transparent (Fig. 3.5.4.1). Age readings can be done over the otolith surface by clear ring views. Due to summer and winter growths, there are two different nucleus formations in the center; spring recruits have opaque, late fall recruits have hyaline rings which are taken into consideration during age readings (Pısıl, 2006).

a

b

TL: *a* – 6.2 cm; *b* – 6.7 cm

S. sprattus

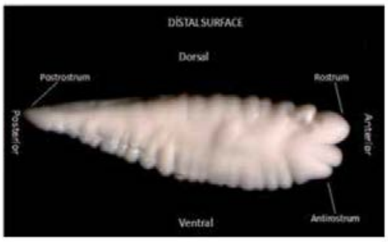

Merlangius merlangus

Trachurus mediterraneus

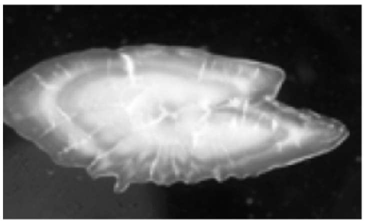

E.encrasicolus

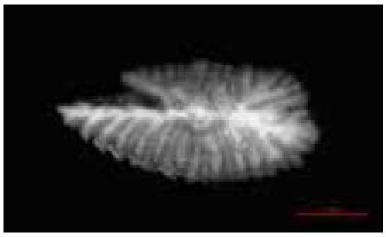

P.salstarix

Project proposal № BG14MFOP001-3.003-0001 "Collection, management and use of data for the purposes of scientific analysis and implementation of the Common Fisheries Policy for the period 2017-2019", funded by the Maritime Affairs and Fisheries Program, co-financed by the European Union through the European Maritime and Fisheries Fund

M.barbatus

Fig. 3.5.4.1. Sprat, anchovy, horse mackerel, red mullet, bluefish otoliths

3.5.5. Age reading protocol

1. Dissected otoliths rinsed and treated with 96% ethyl alcohol and stored dry.
2. Readings were carried out by inspecting the whole otolith in 96% ethyl alcohol in black colored convex glass bowl under reflected light against a dark background.
3. Magnification was set considering the biggest otolith size which fitted the visual capacity of the lens. It was aimed not to change magnification rate which might enable false rings visible in bigger otoliths and permitted to see true rings (hyalines) better by unchanging the color contrasts. That's why magnification rate X4 was selected for the sprat otoliths.
4. Otolith samples were observed from the distal surface as a whole, broken ones were not used.
5. Birthday of the sprat is accepted as 1st of January as the common principle for the fish living in the Northern hemisphere in line with the sub-tropic fish growth models.
6. Central point surrounded by the hyaline rings which is one in some cases or two for the others is formed after the end of consumption of yolk sac and starting of free feeding, known as “stock rings”. Next opaque accumulation is known as “first-year growth ring”. This ring keeps its circular form in the postrostrum region. Both, this ring and the next hyaline ring forming “V” shape in the rostrum, are accepted as first age rings.
7. Tiny and continuous concentric rings prolonged close to the real hyaline ringe are counted together with the real one as one age. This ring may be either a very tiny and opaque one inside the hyaline band or tiny hyaline ring near the outer edge of the opaque ring.

8. Sprat and some other short-lived species have a very fast growth rate, especially in the first two years. Width of the growth bands after 2nd year ring becomes relatively narrower. This issue should be kept in mind in the older age ring readings.

The number of tiny and weak hyaline rings, known as false rings, in the opaque region, is not so high and their separation from age rings is rather easy. When they are so much and inseparable, these otoliths should not be used.

3.6. Sex and maturity estimation

3.6.1. Sprat

The European sprat (*Sprattus sprattus* L.) is a small short-lived pelagic species from the family Clupeidae. Sprat has a wide distribution including shelf areas of the Northeast Atlantic, the Mediterranean Sea, and the Baltic Sea. Sprat is most abundant in relatively shallow waters and tolerates a wide range of salinities. Spawning is pelagic in coastal or offshore waters and occurs over a prolonged period that may range from early spring to late autumn. Sprat is an important forage fish in the North Sea and Baltic Sea ecosystems. Commercial catches from pelagic fisheries are mainly used for fish meal and fish oil production. Three subspecies of sprat have been defined, i.e. *Sprattus sprattus sprattus* L., distributed along the coasts of Norway, the North Sea, Irish Sea, Bay of Biscay, the western coast of the Iberian peninsula down to Morocco, *Sprattus sprattus phalericus*, R. in the northern parts of the Mediterranean and the Black Sea and *Sprattus sprattus balticus* S. in the Baltic Sea. Knowledge about stock structure, migration of sprat, and mixing of populations among areas is limited. Questions have been raised about the geographic distribution and separation of stocks and their interaction with neighboring stocks (ICES 2011). The apparent overlap, e.g. between North Sea sprat and English Channel sprat seems very strong, whereas the overlap between North Sea sprat and Kattegat sprat is not as strong and varies between years. A distribution wide phylogeographic study showed that sprat in the western Mediterranean is a subgroup of the Atlantic group and that these two populations are closer to each other than to sprat in the eastern Mediterranean and Black Sea (Debes et al., 2008).

Project proposal № BG14MFOP001-3.003-0001 "Collection, management and use of data for the purposes of scientific analysis and implementation of the Common Fisheries Policy for the period 2017-2019", funded by the Maritime Affairs and Fisheries Program, co-financed by the European Union through the European Maritime and Fisheries Fund

3.6.2. Maturity Stages of Sprat

It is very important to use standardized maturity scales for sprat (and all species) to evaluate sampling strategies and timing for accurate classification of maturity to provide reliable maturity determination for both sexes. For sprat, small gonad size and the batch spawnings by several cohorts of eggs over a long period are the main challenges for standardizing a maturity scale.

According to the ICES (2011), present standardized maturity scales of sprat include 6-stages for both sexes (Fig. 3.6.2.1, Table 3.6.2.1)

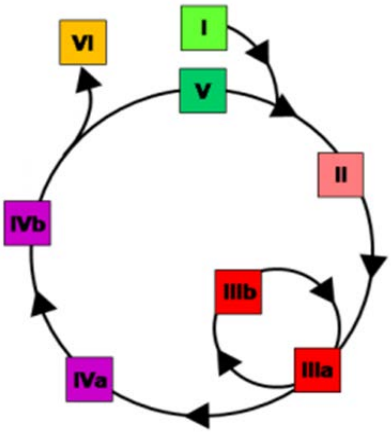

Fig. 3.6.2.1. Scale with six maturity stages in sprat (Name of the stages are given in Table 3.6.2.1)

In particular, specimens without visible development have been combined into Immature and Preparation, whereas the spawning stage has been sub-divided into a non-active spawning stage (maturing and re-maturing characterized by visible development of gametes) and an active spawning stage indicated by hydrated eggs/running milt. The integration of maturing and re-maturing into the spawning stage allows an accurate determination of maturing and spawning specimens and reliable assessment of the spawning fraction of the population.

Table 3.6.2.1. Macroscopic and histological characteristics of gonadal development stages

Stages	*Macroscopic Characteristics*	*Histological characteristics*
FEMALES (OG: Oogonia, PG1: Early previtellogenic oocytes, PG2: Late previtellogenic oocytes, CA: Cortil alveoli oocytes, VT1: Early vitellogenic oocytes, VT2: Mid vitellogenic oocytes, VT3: Late vitellogenic oocytes, HYD: Hydrated oocytes, POF: Postovulatory follicles, SSB: Spawning stock biomass).		
I-Immature	*Juvenile: ovaries threadlike and small; transparent to wine red and translucent in color; sex difficult to determine; distinguishable from testes by a more tubular shape; oocytes not visible to the naked eye*	*OG+/-PGI*
II-Preparation	*The transition from immature to early maturing; oocytes not visible to the naked eye; ovaries yellow-orange to bright red; ovaries occupy up to half of the abdominal cavity. This stage is not included in SSB.*	*PG1, PG2, CA*

III. Spawning *a. Spawning(inactive)* *b. Spawning (active)*	*Maturing and re-maturing: yolked opaque oocytes visible to the naked eye; ovaries change from semi-transparent to opaque yellow-orange or reddish as more oocytes enter the yolk stage; ovaries occupy at least half of the body cavity; re-maturing ovaries may be red to grey-red or purple in color and less firm than an ovary maturing the first batch, few hydrated oocytes may be left* *Spawning active. Hydrated eggs are visible among yolked opaque oocytes; hydrates oocytes may be running; ovaries fill the body cavity; overall color varies from yellowish to reddish.*	*PG1, PG2, CA, VT1, VT2, VT3, +/- POF* *PG1, PG2, CA, VT1,VT2, VT3, HYD, POF*
IV.a Cessation IV.b. Recovery	*Baggy appearance; bloodshot; grey-red translucent in color; atretic oocytes appear as opaque irregular grains; few residual eggs may remain* *Ovaries appear firmer and membranes thicker than in sub-stage IV.a; these characteristics together with the slightly larger size distinguish this stage from the virgin stage; ovaries appear empty and there are no residual eggs; transparent to wine red translucent in color*	PG1, PG2, POF, atretic oocytes, residual HYD PG1, PG2, atretic VT oocytes

V. Resting	*Ovaries appear more tubular and firmer; oocytes not visible to the naked eye; transparent or grey-white to wine red with well-developed blood supply; this stage leads to stage II.*	PG1, PG2 +/- atretic oocytes
VI. Abnormal	*a) infection; b) intersex - both female and male tissues can be recognized; c) one lobe degenerated; d) stone roe (filled with connective tissue); e) other*	Abnormal tissue
MALES (SG: Spermatogonia; PS: Primary spermatocytes; SS: Secondary spermatocytes; ST: Spermatids; SZ: Spermatozoa; SSB: Spawning stock biomass)		
I. Immature	*Juvenile: Testes threadlike and small; white-grey to grey-brown; difficult to determine sex, but distinguishable from ovaries by a more lanceolate shape (knife-shaped edge of the distal part of the lobe).*	SG, PS
II-Preparation	*The transition from immature to mature: Testes easily distinguishable from ovaries by lanceolate shape; sperm development not visible; reddish grey to creamy translucent in color; testes occupy up to ½ of the abdominal cavity; this stage is not included in SSB.*	SG, PS, SS, potentially few ST

III. Spawning a. Spawning(inactive)	*Maturing and re-maturing: Testes occupy at least half of the body cavity and grow to almost the length of the body cavity; the empty sperm duct may be visible; color varies from reddish light grey, creamy to white; edges may still be translucent at the beginning of the stage, otherwise opaque; re-maturing testes may be irregularly colored with reddish or brownish blotches and grey at the lower edge with partly whitish remains of sperm*	*SG, PS, SS, ST, SZ*
c. Spawning (active)	*Spawning active: testes fill the body cavity; Sperm duct filled and distended throughout the entire length; sperm runs freely or will run from the sperm duct, if transected; color varies from light grey to white..*	*SG, PS, SS, ST, SZ*

IV.a. Cessation IV.b. Recovery	*Baggy appearance (like an empty bag when cut open); bloodshot; grey to reddish-brown translucent in color; residual sperm may be visible in the sperm duct.* *Testes appear firmer and the testes membrane appears thicker than in stage IVa due to contraction of the testes membrane; these characteristics together with the slightly larger size distinguish this stage from the virgin stage; testes appear empty and no residual sperm is visible in the sperm duct; reddish grey to greyish translucent in color.*	*SG, PS, atretic SS,* *ST and SZ* *SG, PS, potentially SS, atretic SZ*
V. Resting	*Testes appear firmer, development of a new line of germ cells; grey in color; this stage leads to stage II.*	*SG, PS, SS*
VI. Abnormal	*a) infection; b) intersex - both female and male tissues can be recognized; c) one lobe degenerated; d) other.*	*e.g. oocytes visible among spermatogenic tissues*

3.6.3. Batch fecundity

All fish were measured to the nearest 1 mm in the Total Length (TL) and weighted to the nearest 1 g. Gonads of the fish were examined under a dissecting microscope for its external features such as turbidity and color to determine a maturity stage. The sex ratio was also calculated in this study (i.e., No. of males/No. of females (Simon et al., 2012). The female was determined by the macroscopic observation of mature ovary (Laevastu, 1965).

Project proposal № BG14MFOP001-3.003-0001 "Collection, management and use of data for the purposes of scientific analysis and implementation of the Common Fisheries Policy for the period 2017-2019", funded by the Maritime Affairs and Fisheries Program, co-financed by the European Union through the European Maritime and Fisheries Fund

Batch fecundity can vary considerably during the short spawning season, low at the beginning, peaking during high spawning season and declining again towards the end.

Annual egg production is the product of the number of batches spawned per year and the average number of eggs spawned per batch.

Batch fecundity of sprat was determined using the 'Hydrated Oocyte Method' (Hunter et al., 1985). Oily hydrated females were used. After sampling their body cavity was opened and they were preserved in a buffered formalin solution (Hunter et al., 1985). The ovary-free female weight and the ovary weight were determined. Three tissue samples of ca. 50 mg were removed from different parts of the ovary and their exact weight determined. Under a binocular, the number of hydrated oocytes in each of the three subsamples was determined.

Hydrated oocytes can easily be separated from all other types of oocytes because of their large size, their translucent appearance and their wrinkled surface which is due to formalin preservation. Batch fecundity was estimated based on the average number of hydrated oocytes per unit weight of the three subsamples.

Gonadosomatic Index (GSI) was determined monthly. GSI was calculated as:

$$GSI = \frac{GW}{SW} X\ 100$$

where GW is gonads weight and SW is the somatic weight (represents the BW without GW)

For the estimation of sprat growth rate, the von Bertalanffy growth function (1938) is used, (according to Sparre, Venema, 1998):

$$L_t = L_\infty \left\{1 - \exp\left[-k\left(t - t_0\right)\right]\right\} \quad (11)$$

$$W_t = W_\infty \left\{1 - \exp\left[-k\left(t - t_0\right)\right]\right\}^n \quad (12)$$

where

L_t, W_t are the length and weight of the fish at age t years; L_∞, W_∞ - asymptotic length and weight, k – curvature parameter, t_o - the initial condition parameter.

The length-weight relationship is obtained by the following equation:

(13) $W_t = qL_t^{\ n}$

where

q – condition factor, constant in a length-weight relationship; *n* – constant in a length-weight relationship.

Coefficient of natural mortality (M)

Pauly's empirical formula (1979, 1980) was applied:

(14) $\log M = -0.0066 - 0.279 * \log L_\infty + 0.6543 * \log k + 0.4634 * \log T^oC$

(15) $\log M = -0{\cdot}2107 - 0{\cdot}0824 \log W_\infty + 0{\cdot}6757 \log K + 0{\cdot}4627 \log T°C$

where

L_∞, W_∞ and κ – parameters in von Bertalanffy growth function, T^oC - an average annual temperature of the water, ambient of the investigated species.

3.7. Feeding of sprat (*Sprattus sprattus*, L)

The study of the food of the sprat and horse mackerel in front of the Bulgarian Black Sea coast is based on the analysis of stomach content of 80 sprat and 80 horse mackerel spesimens, reported in the interval 27 October – 11December 2017. Mesozooplankton in the high seas, with this group comprised the basic nutritional base of the sprat and the young stages of horse mackerel.

The study was based on analysis of stomach content composition of 30 sprat, 119 horse mackerel and 10 red mullet specimens, collected in front of the Bulgarian Black Sea coast during the period 24 November- 08December 2018. This study encompassed also analysis of the zooplankton species composition and biomass in the marine environment, as these pelagic organisms formed the main food source of planktivorous fish species.

The study included analysis of stomach content composition of 110 sprat specimens, collected in front of the Bulgarian Black Sea coast during the period 08 June – 20June 2019, and it encompassed additional analyses of the zooplankton species composition and biomass in the marine environment.

The study included analysis of stomach content composition of 110 sprat specimens, collected in front of the Bulgarian Black Sea coast during the period 28 October – 08 November 2019, and it encompassed additional analyses of the zooplankton species composition and biomass in the marine environment (Mihneva et al., 2015).

ata	Trawl №	Coordinates	Bottom depth (m)	Zooplankton stations	Sprat feeding data	Horse mackerel feeding data
).2017	2.1	42.36.59 N - 27.46.44 E	34	Zoo1		T1
).2017	5.1	42.28.29 N - 27.49.12 E	36	Zoo2		T2
1.2017	13.1	42.30.70 N - 27.55.04 E	24	Zoo3	S1	
1.2017	18.1	42.21.77 N - 27.49.58 E	20	Zoo4		T3
1.2017	20.1	42.48.93 N - 28.09.98 E	54	Zoo5	S2	
1.2017	2.2	43.21.12 N - 28.22.91 E	30	Zoo6		T4
1.2017	3.2	42.24.20 N - 27.59.49 E	24	Zoo7		T5
1.2017	8.2	43.01.24 N - 28.00.98 E	53	Zoo8	S3	
.2017	27.2	42.16.56 N - 28.01.34 E	35	Zoo9	S4	
.2017	29.2	42.15.72 N - 27.59.02 E	34	Zoo10	S5	
.2017	30.2	42.31.63 N - 27.55.47 E	34	Zoo11	S6	
2.2017	34.2	42.18.14 N - 27.01.74 E	36	Zoo12	S7	
2.2017	36.2	43.31.06 N - 28.42.98 E	30	Zoo13	S8	

A B

Date	№	Coordinates	Depth (m)	Zooplankton stations	Sprat food	Red mullet food	Horse mackerel food
24.11.2018	3	42.261 N - 27.854 E	57	Zoo1			Tr1
25.11.2018	6	42.423 N -27.837 E	37	Zoo2			Tr2
25.11.2018	7	42.395 N - 27.919 E	38	Zoo3			
25.11.2018	8	42.309 N - 27.971 E	37	Zoo4			
25.11.2018	11	42.278 N - 27.841 E	50	Zoo5			Tr3
26.11.2018	17	42.410 N - 27.803 E	39	Zoo6			Tr4
26.11.2018	18	42.447 N - 27.758 E	40	Zoo7			Tr5
27.11.2018	19	42.467 N - 27.715 E	38	Zoo8		M1	
27.11.2018	20	42.494 N - 27.708 E	35	Zoo9			Tr6
27.11.2018	21	42.494 N - 27.690 E	36	Zoo10			Tr7
27.11.2018	22	42.485 N - 27.671 E	36	Zoo11			Tr8
03.12.2018	24	42.898 N - 28.144 E	62	Zoo12			Tr9
03.12.2018	25	43.003 N - 28.312 E	64	Zoo13			Tr10
04.12.2018	28	43.348 N - 28.755 E	81	Zoo14	Sp1		
04.12.2018	30	43.370 N - 28.272 E	18	Zoo15	Sp2		
07.12.2018	33	42.746 N - 28.133 E	57	Zoo16			Tr11
07.12.2018	34	42.708 N - 28.133 E	64	Zoo17			Tr12
08.12.2018	36	42.638 N - 27.875 E	28	Zoo18	Sp3		

C

Date	№	Coordinates	Depth (m)	Zooplankton stations	Sprat food	Red mullet food
14.12.2018	1	42.53 N - 27.75 E	36	Zoo1	Sp1	
14.12.2018	2	42.55 N - 27.79 E	35	Zoo2	Sp2	
14.12.2018	4	42.51 N - 27.75 E	35	Zoo3		Mb1
15.12.2018	8	42.45 N - 27.78 E	36	Zoo4	Sp3	
15.12.2018	10	42.45 N - 27.70 E	37	Zoo5	Sp4	
21.12.2018	16	42.58 N - 27.87 E	34	Zoo6	Sp5	
21.12.2018	18	42.64 N - 28.09 E	52	Zoo7	Sp6	
23.12.2018	26	42.57 N - 27.73 E	30	Zoo8	Sp7	
27.12.2018	28	43.05 N - 27.98 E	22	Zoo9	Sp8	
28.12.2018	32	42.84 N - 28.05 E	33	Zoo10	Sp9	
29.12.2018	34	42.65 N - 27.85 E	25	Zoo11	Sp10	
29.12.2018	36	42.59 N - 27.74 E	31	Zoo12	Sp11	

D

Date	№	Coordinates	Depth (m)	Zooplankton stations	Sprat food
08.06.2019	1	42.46; 27.83	37	1	Sp1
08.06.2019	2	42.34; 27.92	39	2	Sp2
08.06.2019	5	42.25; 28.11	60	3	Sp3
09.06.2019	7	42.39; 27.81	42	4	Sp4
09.06.2019	9	42.25; 27.90	41	5	Sp5
11.06.2019	13	42.47; 27.81	36	6	Sp6
12.06.2019	18	42.62; 27.84	27	7	Sp7
12.06.2019	22	42.65; 27.79	31	8	Sp8
18.06.2019	27	43.36; 28.43	16	9	Sp9
19.06.2019	35	43.21; 28.09	21	10	Sp10
20.06.2019	37	43.03; 27.97	22	11	Sp11

E

Fig. 3.7.1. Investigated area 2017-2019

Per trawl catch, about 10 fish specimens were separated and preserved in 10% formaldehyde-seawater solution. The absolute length (TL, to the nearest 0.1 cm) and weight (to the nearest 0.01 g) of fish specimens were measured. Under laboratory conditions, the stomachs of the selected animals were weighted with analytical balance (to the nearest 0.0001 g). The food mass of each individual was calculated as a difference between the weights of a full and empty sprat stomach.

The stomach content was investigated under a microscope for the estimation of species composition and prey number. The prey biomass was estimated by multiplication of the number of consumed mesozooplankton species by their weights.

The following indices were calculated:

1. Index of stomach fullness (ISF) as a percent of body mass: (stomach content mass/fish mass) *100; and

2. Index of relative importance - IRI, Pinkas et al. (1971): IRI = (N+M) x FO; where N - the proportion of prey taxa (species) in the diet by numbers (abundance); M - the percentage of prey taxa (species) in the diet by mass; FO - frequency of occurrence among fish.

The zooplankton samples in the marine environment were gathered from the whole water layer (bottom- surface) with a plankton set (opening diameter d = 36 cm; mesh size 150 µm). The samples were fixed onboard the ship in 4% formaldehyde-seawater solution (Korshenko and Aleksandrov, 2012). The mesozooplankton species composition was identified by

"Guides for the Black and Azov Seas" (Mordukhay-Boltovskoy et al., 1968; Alexandrov and Korshenko, 2006; Korshenko and Aleksandrov, 2013) and its quantity - by the method of Bogorov (Dimov, 1959; Korshenko & Aleksandrov, 2013).

3.8. The selectivity of the fishing gear

The change in mesh size of the codend is the basis of the analysis of the selectivity in the calculations. The mesh size (a, mm) of the trawl bag is shown in Fig. 3.8.1. The study of the variation in the trawl selectivity is based on calculations at the corresponding change in the size of the "eye" side.

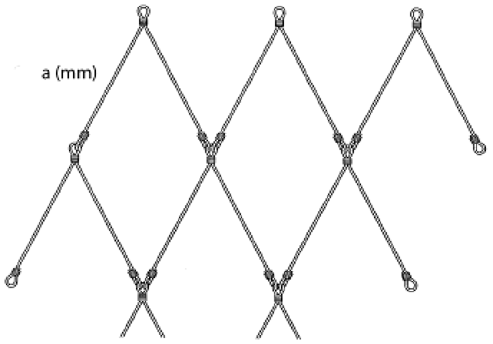

Fig. 3.8.1. "Eye" of the codend and size a (mm)

Using the model of Treschev (1974), an additional trawl bag for experimental study of the change in selectivity was made (Fig. 3.8.2).

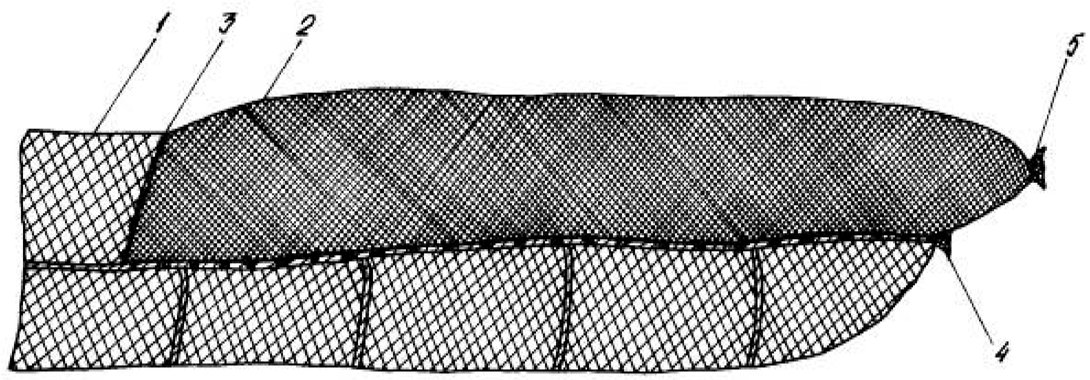

Fig. 3.8.2. Codend bag scheme: 1 - main bag 2 - apron; 3 - connector, 4 - the main bag 5 - the trailer outer bag connection

Linear size measurements were used to evaluate the following biological parameters:

- L50, L25, and L75 - the amount at which 50%, 25% and 75% of the individuals entered into the fishing gear are detained therein
- selectivity factor
- extent of selectivity

The dimensional selectivity of the trawl bag is determined by the relationship between the probability p, the fish entering the bag and its size l (Holden, 1971). This link is described by the logistic function (Fryer, 1996):

$$p = \frac{e^{(v_1 + v_2 l)}}{(1 + e^{(v_1 + v_2 l)})}$$

Where, v_1 represents the intersection of the abscissa, v_2 is the slope of the curve following log-transformation. L50, L25 and L75 function values can be estimated from the following expressions:

$$L_{50\%} = \frac{v_1}{v_2} \qquad L_{25\%} = \frac{(-Ln(3) - v_1}{v_2} \qquad L_{75\%} = \frac{(Ln(3) - v_1}{v_2}$$

$$SR = L_{75} - L_{25} \qquad SF = \frac{L_{50}}{meshsize}$$

Suppose that fish of size l1, l2,. . .1N enter the trawl bag. Small fish may loose through the mesh (i.e., have a low probability of retention), but as they grow in length, the chance to get rid of the net decreases. At some point, because of their increased size, they can not get out of the net (their probability of retention equals 1).

4. Results

4.1. Selectivity of the fishing gear

The possibilities of holding individuals from sprat of mesh size a = 8 mm, 7.5 mm and 6.5 mm are presented on Table 4.1.1 to trace the change in the probability of retention of individuals when changing the mesh size of the network.

Table 4.1.1. Possibilities for holding individuals from twine in a midwater otter trawl of different mesh sizes; Selectivity factor (SF) and Selectivity Spectrum (SR)

		8		7,5		6,5
"EYE" size	selectivity	mm	selectivity	mm	selectivity	mm
	L25%	**6,2cm**	L25%	**5,4cm**	L25%	**5,2cm**
Retention	L50%	**7.0cm**	L50%	**6,2cm**	L50%	**5,7cm**
capability						
	L75%	**7,8cm**	L75%	**7,0cm**	L75%	**6,2cm**
	SF	**4,4**		**4,13**		**4,77**
	SR	**1,6**		**1,6**		**1**

In the trawl bag of mesh size a = 8.00 mm, the probability is that 25% of the specimens remained in the bag should have a size of 6.2 cm (L25 = 6.2 cm). With 50% probability

(L50%), individuals with a size of 7.00 cm and larger ones will be retained, with probability of retention (L75%) are individuals with a linear size of 7.8 cm (Table 4.1.1, Fig. 4.1.1).

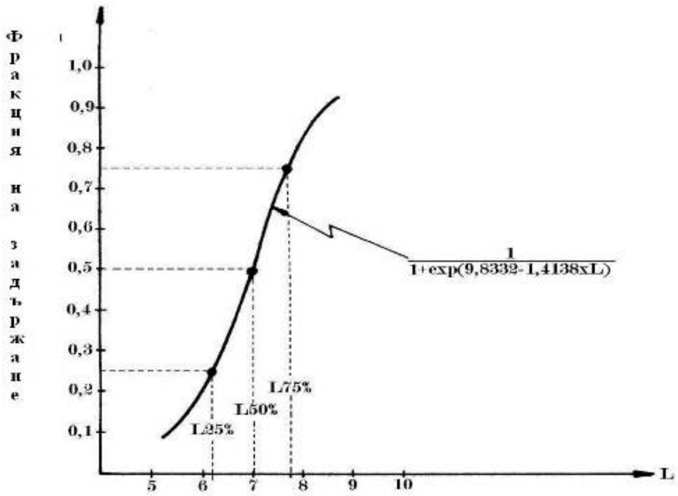

Fig. 4.1.1. Graphical presentation of L25%, L50%, L75% at the mesh size of the "bag" a = 8.00 mm

The next scenario examines the change in selectivity with 0.5 mm smaller mesh size,i.e. 7.5 mm. In this case, 6.2 cm individuals will retain a probability of 50% in the trawl net (L50% = 6.2 cm, Table 4.1.1), which is 0.8 mm less than the case of mesh size a = 8mm. In this case, it reduces the size of the specimens that would be retained in the trawl with a probability of 25%, namely L25% = 5.4 cm. Reducing the network mesh from 8.00 to 7.5 cm results in a 75% retention probability of 7.00 cm specimens, which is 0.8mm less than the previous case. The selectivity factor for this particular case decreases to 4.13 and the SR selectivity range is maintained at the mesh size a = 8.00 cm. The proportion of the magnitude in both cases examined so far is the same, but with decreasing mesh size, the size of the retained specimens also diminishes. In the third case, the mesh size is a = 6.5 mm. Such a network will retain in a proportion of 50% individuals with TL = 5.7 cm, which is 1.3 cm less than in the case of mesh size of the net - a = 7mm.

Project proposal № BG14MFOP001-3.003-0001 "Collection, management and use of data for the purposes of scientific analysis and implementation of the Common Fisheries Policy for the period 2017-2019", funded by the Maritime Affairs and Fisheries Program, co-financed by the European Union through the European Maritime and Fisheries Fund

In this case, the difference between the individuals of the trickles of certain dimensions retained in the bag (inner) with an eye of 6.5 mm in the proportion of 25, 50 and 75% will be 0.5 cm.

A codend of mesh size a = 6.5mm (the actual mesh size measured in the present research, and length distribution of sprat caught in such a codednd (Fig. 4.1.2) will retain fish of size 6.2 cm and size of 5.2 cm in a proportion of 75% and a proportion of 25%, respectively. The selectivity factor, in this case, increases to 4.77 (from 4.4 and 4.5) and the selectivity range is equal to one (SR = 1). It can be seen that in all cases with a mesh size of 6.5 mm, the change in the size of the detainees varies within a smaller range, but in all variants, the holdings are very much below the minimum allowable harvest size (2001) spatula, namely 7.00 cm. We should note the fact that active trawl-fishing gears are using nets with mesh sizes from 6.0 to 6.5 cm. This fact undoubtedly speaks of the fact that there are specimens that have not reached sexual maturity in different proportions. Not least, the fact that active fishing activity related to the use of trawls takes place in the near coastal strip at a lower depth. It is well-known from the biology of species that large individuals, respectively senior age groups, migrate to greater depths in search of favorable temperature and nutritional conditions.

According to the calculations made on the selectivity of the trawl bag of different mesh sizes, it can be seen that at a = 8mm, 50% of the TL = 7cm individuals have a chance of being trapped while the TL = 7.8 cm 75% retention capability. A further reduction in mesh size leads to a reduction in the selectivity of the trawl. In eye mesh a = 7.0cm, L50% = 6.2cm and L75% = 7cm. For nets with a mesh size of 6.5mm, the size of the trait-retained individuals drops to 5.7cm at L50%. As the mesh of the bag grows, the number of small individuals that escape the trawl increases. At the same time, the average length of the fish caught, i.e. this is part of the breeding biomass that has already participated in the reproduction. The Regional Fisheries Commissions are aiming for maximum mesh sizes, which would allow maximum "extraction" of juvenile individuals.

The minimum allowable catch for sprat referred to in the Fisheries and Aquaculture Act (2001) is 7 cm. This fact is indicative that to comply with the measure of resource use

Project proposal № BG14MFOP001-3.003-0001 "Collection, management and use of data for the purposes of scientific analysis and implementation of the Common Fisheries Policy for the period 2017-2019", funded by the Maritime Affairs and Fisheries Program, co-financed by the European Union through the European Maritime and Fisheries Fund

referred to in the law, the mesh size of the trawl should be a = 8 mm, which would result in the proportion of individuals in the proportion of L75% = 7.8cm. This measure is essential to protect the exploited resource from overloading and undermining stocks in a longer term.

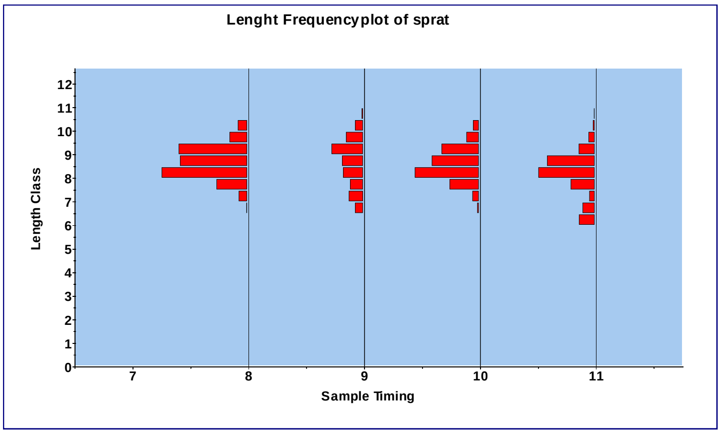

Fig. 4.1.2. Linear dimensions of the sprat in the codend of the trawl

5. Results

5.1. Abundance and biomass

For the three-year observation period, 72-74 trawls per year were carried out in the Bulgarian part of the Black Sea on board of the R/V *Haithabu*. The observation period covered the period October-December 2017 (Fig. 5.1.1), November-December 2018 (Fig. 5.1.2) and June, November-December 2019 (Fig. 5.1.3).

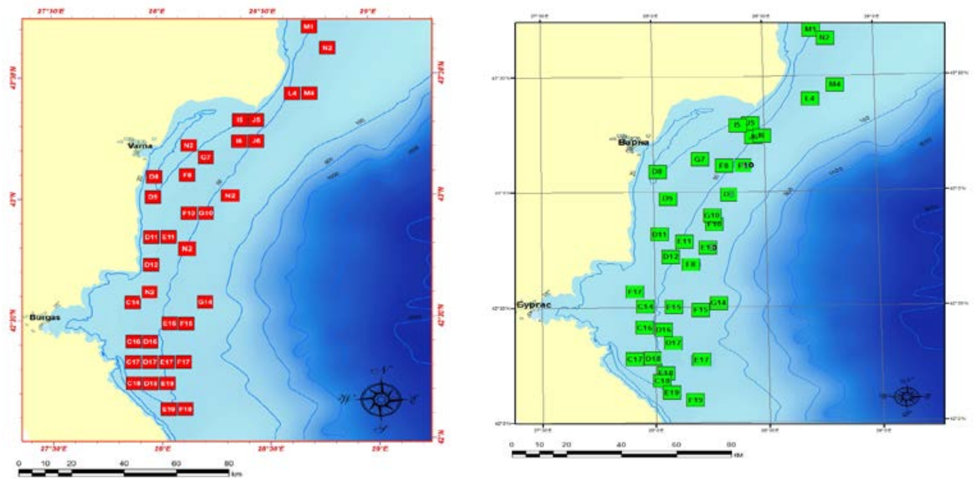

A B

Fig. 5.1.1. Location of the stations in 2017, October-November (A) and November-December (B)

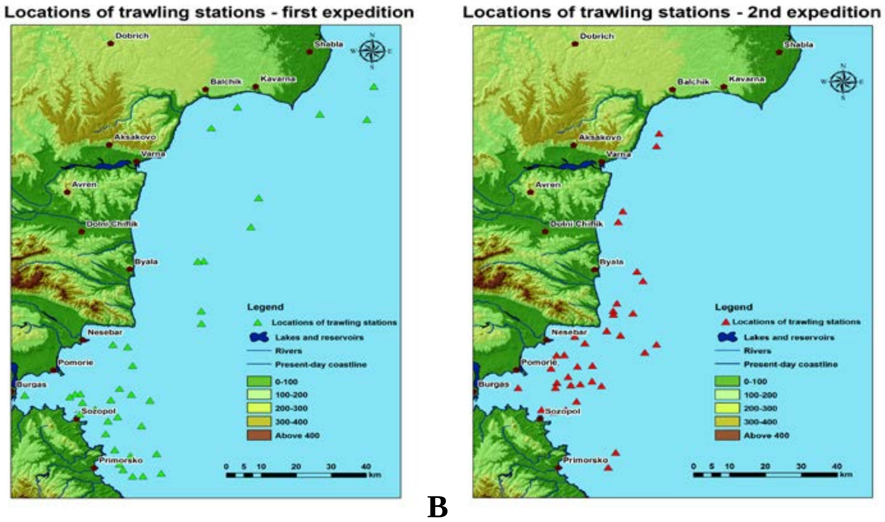

A B

Fig. 5.1.2. Location of the stations in 2018, November (A) and December (B)

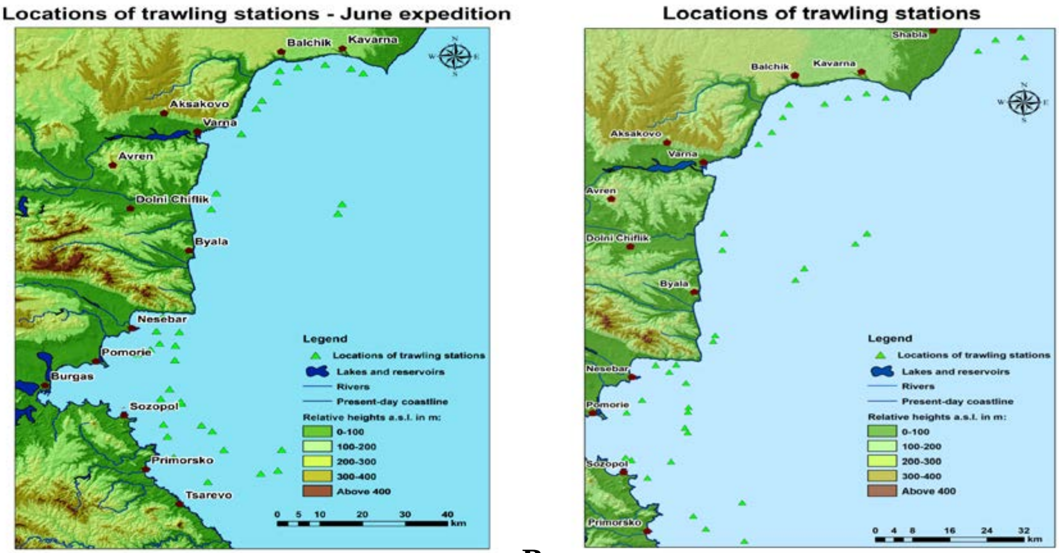

A **B**

Fig. 5.1.3. Location of the stations in 2019, June (A) and November-December (B)

Trawling time for the period was between 25 and 40 min at depths between 15.8 m and 92 m, in the area between Ahtopol, Kiten and Durankulak. The studied area in Bulgarian waters was about 8135.40 km^2 (2017), 6633.48 km^2 (2018), and 8010.24 km^2 (2019). The sprat was observed in depth exceeding 18 m.

The total number of identified species in 2017 was 11, of which 10 fish and 1 macrozooplankton. The most common species detected in October - November survey (in terms of presence/absence) were: *A. aurita* (28.4%), *M. barbatus* (16.4%), *P. saltatrix* (7.5%), *Tr. mediterraneus* (20.9%), *S. sprattus* (20.9%), *M. merlangius* (5.97%), and the rest of the species *A. immaculata, N. melanostomus, G.niger, Sq.acanthias u P. maxima* were detected rarely in the catch. In terms of weight, the largest share held *Aurelia aurita* (264 kg), *H.mackerel* (230.5 kg), *S. sprattus* (188 kg), *M. barbatus* (67.85 kg), *M. Merlangius* (32.2 kg) and *P. saltatrix* (13.5 kg). In the second study (November-December 2017) the presence of the species was as follows: *S. sprattus* (31.25%), *A. aurita* (28.13%), *M. merlangius* (15.63%), *Tr. mediterraneus* (12.5%), *M. barbatus* (10.94%), *P. saltatrix* (1.56%). *Aurelia aurita* (200 kg), *H. mackerel* (97.5 kg), *S. sprattus* (250.5 kg), *M. barbatus* (16.8 kg), *M. Merlangius* (86 kg) and *P. saltatrix* (0.3 kg).

The total number of identified species in November 2018 was 18, of which 14 were fish, crustaceans - 1, molluscs - 1 and two macrozooplankton species. The most common types of trawl operations (in terms of presence/absence) were: *Tr. mediterraneus* (52.13%), *M. barbatus* (25.66%) and *E. encarsicolus* (8.11%), *P. saltatrix* (14.1%). Other species such as *S. sprattus*, *M. merlangius*, *A. immaculata*, *N. melanostomus*, *G. niger, Mugil cephalus,* etc. were rarely present in the catches. Single specimens from family Sparidae, *Scorpaena porcus*, *Pegusa lascaris* were caught. During the studied period, the largest abundance had the jellyfish *Aurelia aurita*, which dominated in the pelagic society.

In December 2018 the total number of identified species was 19, of which 15 fish, crustaceans - 2, molluscs - 1 and one macrozooplankton species. With the highest abundance was sprat *S. sprattus*, which dominated the pelagic society, followed by *M. merlangius* (68%) and horse mackerel *Tr. mediterraneus* (11%). The other species as *Raja clavata*, *Dasyatis pastinaca* and *Scophthalmus maximus* were represented by single specimens.

The total number of identified species in June 2019 was 24, of which 16 fish, 2 crustaceans, molluscs - 2 and 4 macrozooplankton species. The most common species in trawl operations (in terms of presence/absence) were: *S. sprattus* (76.5%), *M. barbatus* (9.66%) and *M. merlangius* (4.86%); other species such as: *A. immaculata*, *N.melanostomus*, *G.niger*, etc. were rarely presented in the catch. Single specimens of *A. stellatus*, *S. maximus* , family Sparidae, *Scorpaena porcus*, *Pegusa lascaris* and others were caught.

In October-November 2019 with the largest abundance was sprat, which dominated the pelagic society. The total number of identified species was 34, of which 26 fish, 2 crustaceans, molluscs - 2 and 4 macrozooplankton species. The most common types of trawl operations (in terms of presence/absence) were: *S. sprattus* (82.99%), *M. merlangius* (9.44%) and *M. barbatus* (6.54%). Other species, such as *Tr. mediterraneus*, *A. immaculata*, *N. melanostomus*, *G. niger*, *N. melanostomus*, *M. batrachocephalus*, *At. boyeri*, *H. guttulatus*, *R. clavata, D. pastinaca, P. lascaris, Sc. umbra, U. scaber, Tr. draco, A. guldensaedtii, A. stellatus, Sq. acanthias, Sc .maximus, B. gymnotrachelus, C. ocellatus, C. tinca, C. kessleri pontica, S. tenuirostris,* had a negligible catch presence compared to June 2019. Single specimens from *A. stellatus*, *S. maximus*, species from family Sparidae, *Tr. draco, Scorpaena porcus, Pegusa lascaris* and other were caught.

6. Sprat (*Sprattus sprattus* L.)

6.1. Distribution

In the first stage of the survey (October-November), the densest clusters of sprat were found at 50-75 m depth with an average catch per unit area of CPUA = 1446.46 kg. km^{-2} (depth 50m), followed by a depth of 30-50m (CPUA = 1396.58 kg.km^{-2}). During the November-December 2017 survey, the 30-50m deep strip of CPUA of the sprat was 333.70kg.km$^{-2.}$ The lower average catch values per unit area compared to the previous survey were due to the fact that many trawls did not record catches of sprat.

6.2. Sprat biomass from different depths

In 2017 the biomass in the studied areas was not high, no dense clusters were observed, rather the passages were quite scattered. In October-November 2017, low levels of catches per unit area and, respectively, of sprat biomass (CPUA 50-75m = 353 kg.km^{-2}; biomass = 970kg) were established (Fig. 6.2.1).

A
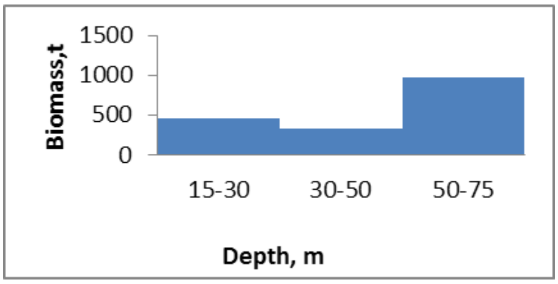

Project proposal № BG14MFOP001-3.003-0001 "Collection, management and use of data for the purposes of scientific analysis and implementation of the Common Fisheries Policy for the period 2017-2019", funded by the Maritime Affairs and Fisheries Program, co-financed by the European Union through the European Maritime and Fisheries Fund

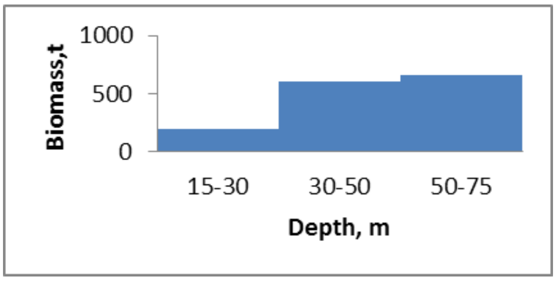

B

Fig. 6.2.1. Sprat biomass by depths in A. October-November and B. November-December 2017

In November 2018 only single specimens in catches were detected. A slightly higher abundance and clusters of sprat were observed in December. Hydrometeorological conditions, the presence of large predators, strong underwater currents and large accumulations of the jellyfish *Aurelia aurita* were probably factors that had a very negative impact on the species' accumulations. The catch per unit area in December 2018 was predominant at 15-30m (2065 $kg.km^{-2}$). At a stratum of 30-50 m, it was 1815 $kg.km^{-2}$ and the highest catch per unit area in the depth band 50-75m - 2754 $kg.km^{-2}$ on the species assemblages.

The species had the highest recorded biomass and catch per unit area in June and October-November 2019. At stratum 15-30 m CPUA = 1867.7 $kg.km^{-2}$ and biomass12 497 t (June 2019) and respectively at the same depths much higher CPUA = 11 537 $kg.km^{-2}$ and biomass 23 825 t were recorded during the autumn period. In deep layer 30-50m CPUA=1731 $kg.km^{-2}$ and biomass 7557 t (June 2019) and 10 641 $kg.km^{-2}$ and 19 311 t (October 2019), for stratum (combined) 50-100m clusters were CPUA = 1416 $kg.km^{-2}$ and biomass 5850 t (June 2019) and CPUA = 7 131 $kg.km^{-2}$ and biomass 2945 t (October-November 2019).

Comments on the *Sprattus sprattus* biomass from different depth layers

The sprat total biomass in December 2018 estimated by the area method (Table 1) amounted to 10 898.18 t for the Bulgarian Black Sea area. The biomass in stratum 15-30m was 3857 kg. Similar values were recorded in the 30-50 m and 50-75 m layers, 3141kg and 3900 kg, respectively. The total biomass in June 2019 was 2511.64t for the Bulgarian Black Sea area, and in October - November 2019 it was 46 081.41t for the Bulgarian Exclusive Economic

Zone (Tables 6.2.1and 6.2.2).

The highest values of sprat biomass were recorded at a depth range of 15-30 m (Fig.6.2.2).

Table 6.2.1. Area method in December 2018, June and October - November 2019, calculated average catch per unit area (CPUA, average), Biomass - weight in kg, Ah-area and number of fields per area

Stratum	December 2018				June 2019				October-November 2019	
	Area (Ax)	Number of fields	CPUA average	Biomass (kg)	Area (Ax)	Number of fields	CPUA average	Biomass (kg)	CPUA average	Biomass (kg)
15-30	2065.14	33	1867.74	3857.14	2065.14	33	1867.74	12496.6	11536.8	23825.06
30-50	1814.82	29	1730.74	3140.98	1814.82	29	1730.74	7556.84	10640.8	19311.14
50-100	2753.52	44	1416.39	3900.06	4130.28	66	1416.39	5850.08	7130.8	2945.2
Total	6633.48	106		10898.2	8010.24	128		25903.5		46081.41

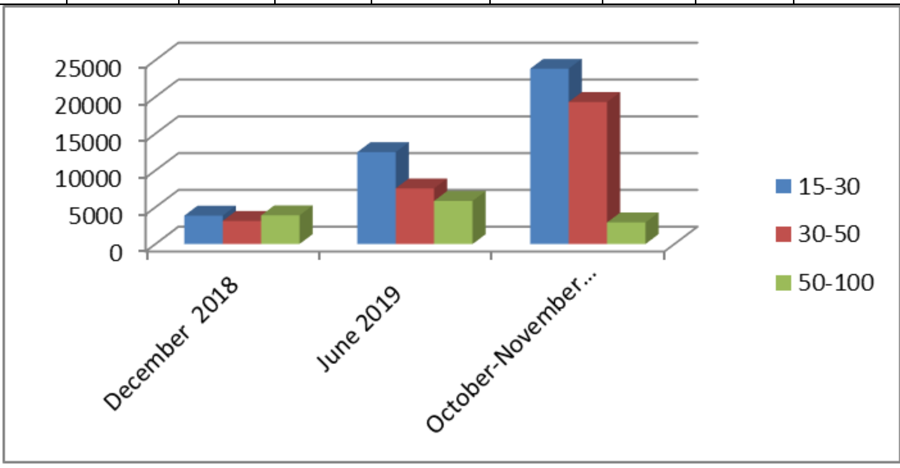

Fig. 6.2.2. Comparison of sprat biomass (kg) during the monitoring period

Table 6.2.2. Descriptive statistics on the biomass indices (t) of sprat in December 2019 and June and October-November 2019

Parameters	December 2018			June 2019			October-November 2019		
	15-30м	*30-50м*	*50-75м*	*15-30м*	*30-50м*	*50-75м*	*15-30м*	*30-50м*	*50-75м*
Mean	1867.739	1730.739	1416.389	12496.6	7556.837	4972.173	11536.777	11079.193	7130.762
Standard Error	471.2985	231.7836	228.9086	1843.06	872.043	1556.601	1504.1474	1515.8932	1354.2061
Median	1512.81	1466.262	1489.536	13223.9	7405.364	4760.591	10579.091	10579.091	5289.5455
Mode	#N/A	2792.88	#N/A	15868.6	7405.364	#N/A	7934.3182	#N/A	#N/A
Standard Deviation	1333.033	1087.162	605.6353	5212.95	4090.244	3480.666	6556.4265	5027.6491	3582.8927
Sample Variance	1776978	1181920	366794.1	2.70E+07	16730096	12115033	42986729	25277255	12837120
Kurtosis	2.283527	7.921022	-0.61944	0.55498	5.109744	1.785545	1.7391695	0.7654725	-0.298885

Project proposal № BG14MFOP001-3.003-0001 "Collection, management and use of data for the purposes of scientific analysis and implementation of the Common Fisheries Policy for the period 2017-2019", funded by the Maritime Affairs and Fisheries Program, co-financed by the European Union through the European Maritime and Fisheries Fund

Skewness	1.408772	2.403399	0.149215	-0.80827	1.654978	1.234005	1.192791	0.31593	0.9256806
Range	4142.772	5213.376	1768.824	16397.6	19412.63	8992.227	26976.682	18513.409	9962.3209
Minimum	512.028	465.48	558.576	2644.77	1745.55	1586.864	2115.8182	2644.7727	3261.5428
Maximum	4654.8	5678.56	2327.4	19042.4	21158.18	10579.09	29092.5	21158.182	13223.864
Sum	14941.91	38076.26	9914.724	99972.4	166250.4	24860.86	219198.77	121871.13	49915.334
Count	8	22	7	8	22	5	19	11	7
Largest(1)	4654.8	5678.856	2327.4				29092.5	21158.182	13223.864
Smallest(1)	512.028	465.48	558.576				2115.8182	2644.7727	3261.5428
Conf. Level (95.0%)	1114.444	482.0204	560.1192	4358.14	1813.513	4321.817	3160.0964	3377.6206	3313.6231

6.3. Catch per unit area

The catch per unit area (CPUA kg.km^{-2}) and species biomass were low and no characteristic clusters were formed. The dispersed behavior of sprat during the in 2017 (October - December) was due to adverse weather and hydrological conditions. The densest passages were registered in front of c. Emine and Sozopol, and in the other regions the sprat was scattered (Fig. 6).

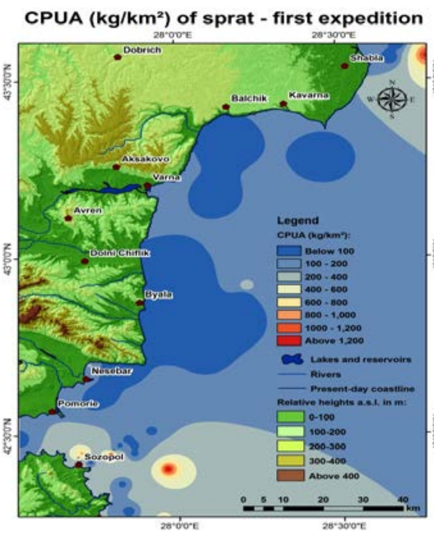

A

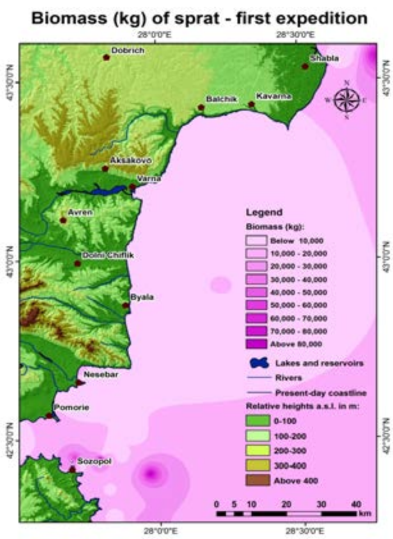

B

Project proposal № BG14MFOP001-3.003-0001 "Collection, management and use of data for the purposes of scientific analysis and implementation of the Common Fisheries Policy for the period 2017-2019", funded by the Maritime Affairs and Fisheries Program, co-financed by the European Union through the European Maritime and Fisheries Fund

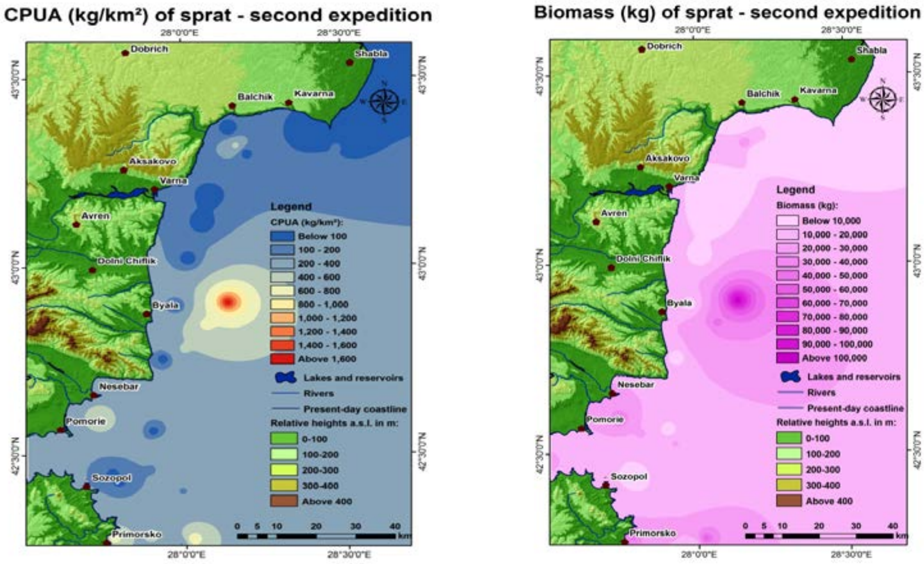

A **B**

Fig. 6.3.1. A. Catch per unit area (CPUA kg.km^{-2}) and B. Sprat biomass from the deep layers of the study areas during the period October-November and November-December 2017

The highest CPUA kg.km^{-2} of sprat in December 2018 was recorded in a depth strip of 30-50 m (21 158), followed by a strip of 15-30 m (15868.64) in the southern part of the surveyed area, north of Tzarevo. Similar high values were observed in Primorsko and south of Sozopol. Relatively lower CPUA values were found at greater depths of 50-100 m, an average CPUA of 3552 kg.km^{-2} (Fig. 6.3.2).

The highest CPUA was recorded in June 2019 at a depth of 50 m southeast of Pomorie (5679 kg.km^{-2}). In Nessebar Bay and in c. Maslen Nos area, at a depth of 29-30 m, CPUA = 2560 kg.km^{-2} and at a depth of 62 m - CPUA = 1955 kg.km^{-2} were reported (Fig. 6.3.3).

The highest values of CPUA kg.km^{-2} of sprat in October-November 2019 were recorded in a depth strip of 15-30 m (29 093), followed by a strip of 30-50 m (21 158) in the southern part of the surveyed area - in front of the town of Nessebar, in the region of Emine village and NW of Pomorie. Lower values were registered in areas near Sozopol and Kavarna. Relatively lower CPUA values were found in shallow depths in front of the mouth of Kamchia River, in Aladzha Bank area (<5000 kg.km^{-2}) (Fig. 6.3.4).

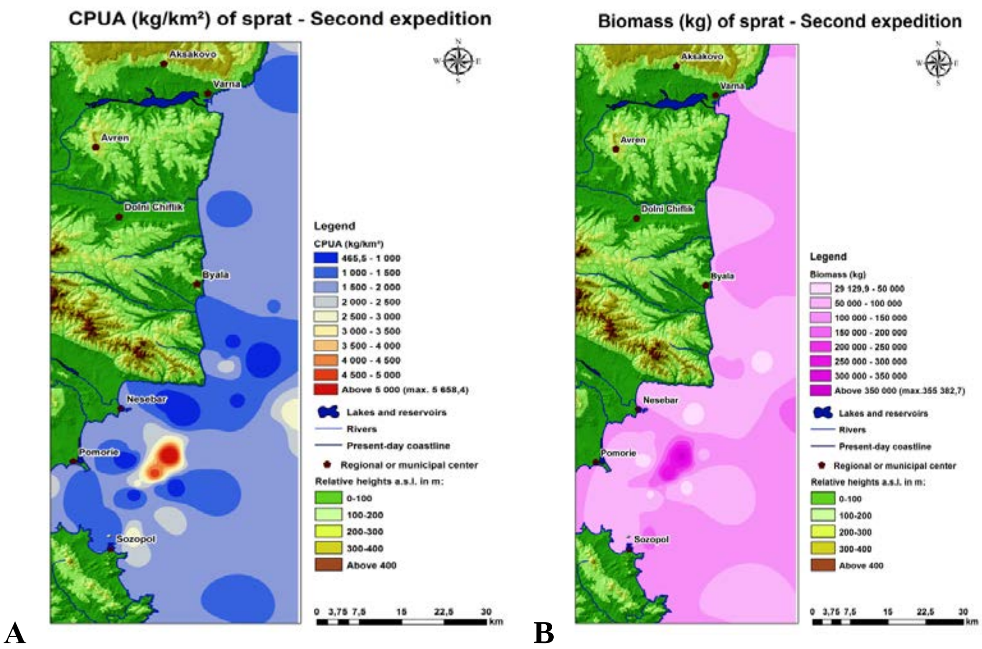

Fig. 6.3.2. A. Catch per unit area (CPUA kg.km^{-2}) and B. Sprat biomass from the deep layers of the studied areas in December 2018

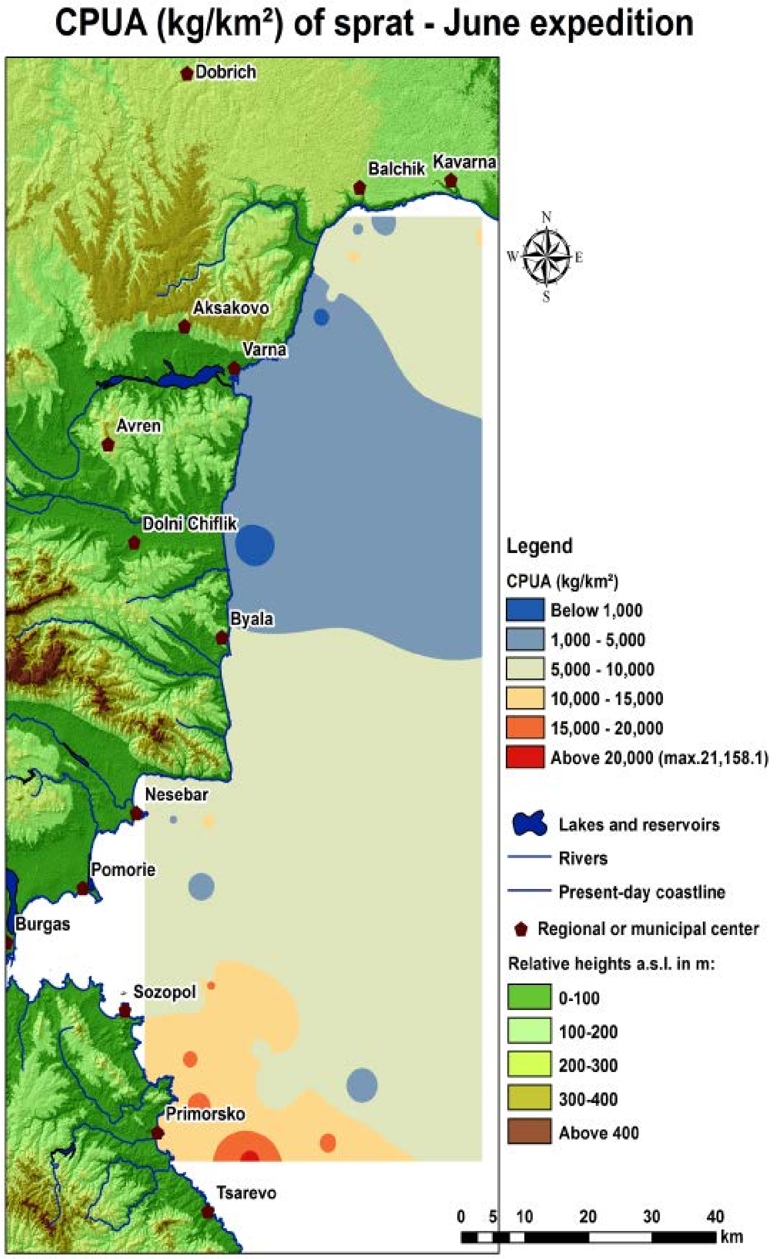

Fig. 6.3.3. Catch per unit area (CPUA kg.km^{-2})

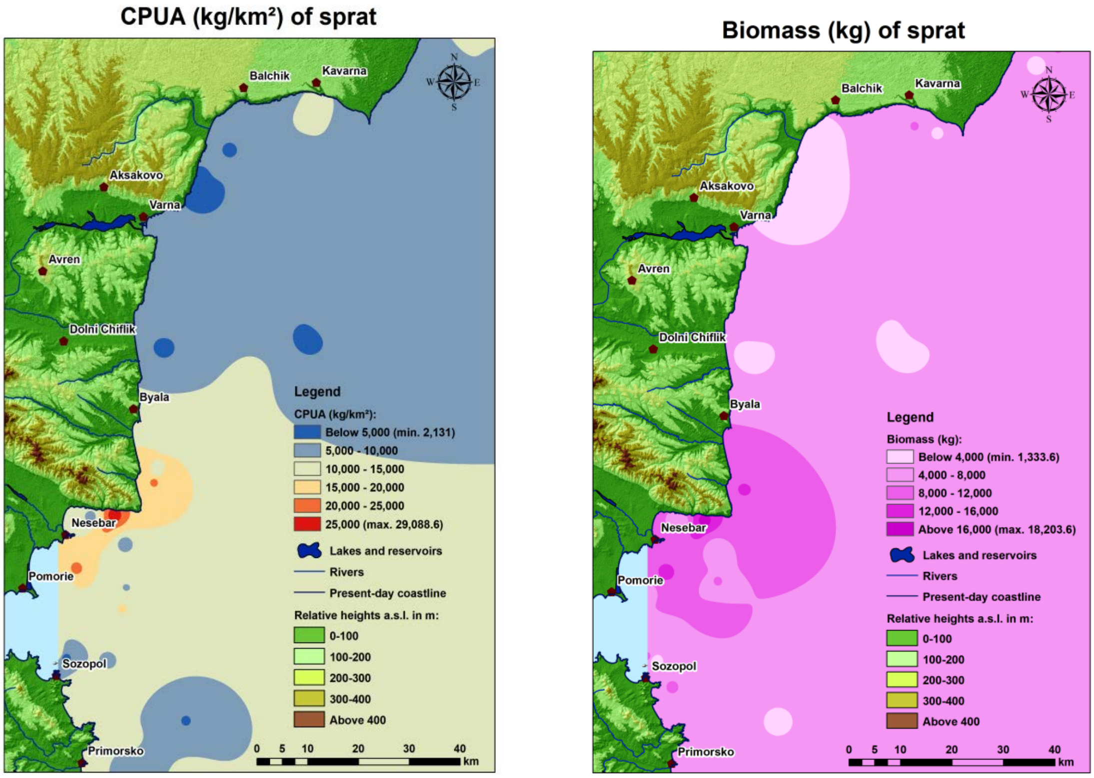

Fig. 6.3.4. A. Catch per unit area (*CPUA kg.km*$^{-2}$) and B. Sprat biomass from the deep layers of the studied areas in October-November 2019

6.4. Catch per unit effort

The catch per unit effort (CPUE) for identified species is presented graphically and spatially identified and analyzed by GIS (Fig. 6.4.1).

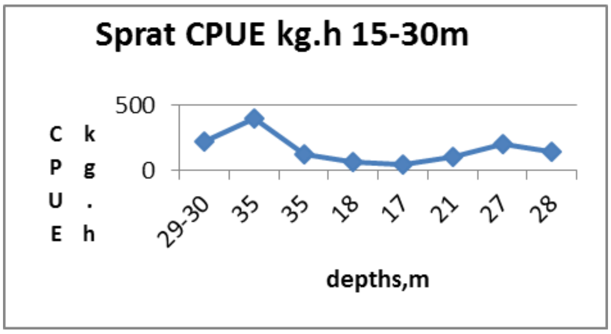

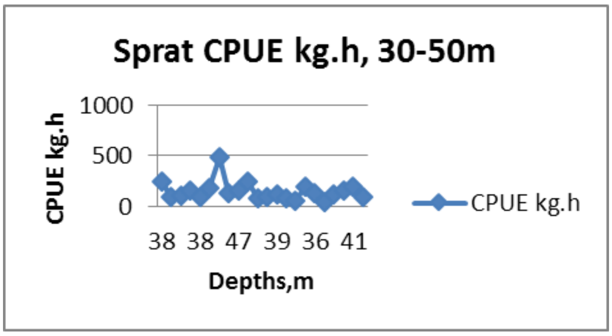

Fig. 6.4.1. Catch per unit effort (CPUE kg.h^{-1}) of sprat in December 2018 in the studied area

Catches per unit effort (CPUE kg.h^{-1}) for sprat in June 2019 are presented on Fig. 6.4.2.

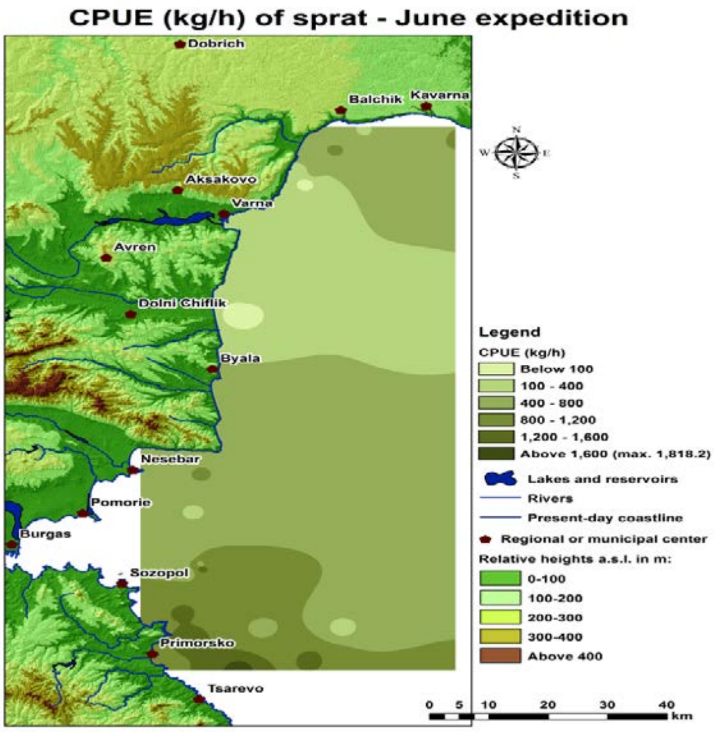

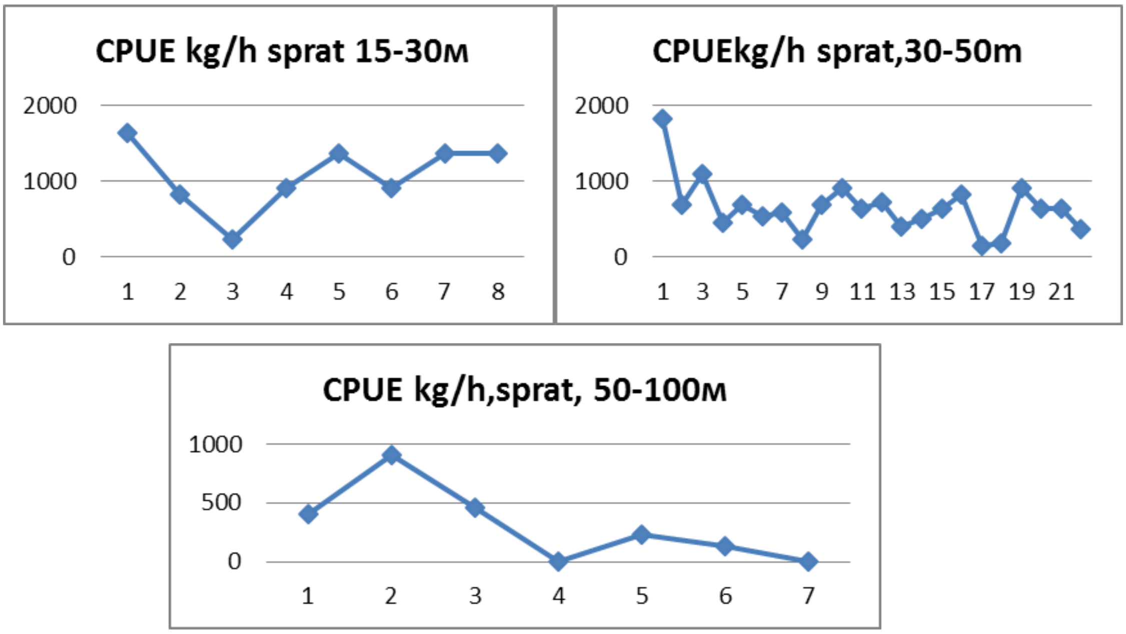

Fig. 6.4.2. Catch per unit effort (CPUE) for sprat, June 2019, along deep horizons

CPUE kg.h^{-1} values for sprat, October-Novembder 2019, is presented on Fig. 6.4.3. Maximums of this parameter were established in the shallow coastal zone (15-30m) (Fig. 6.4.3).

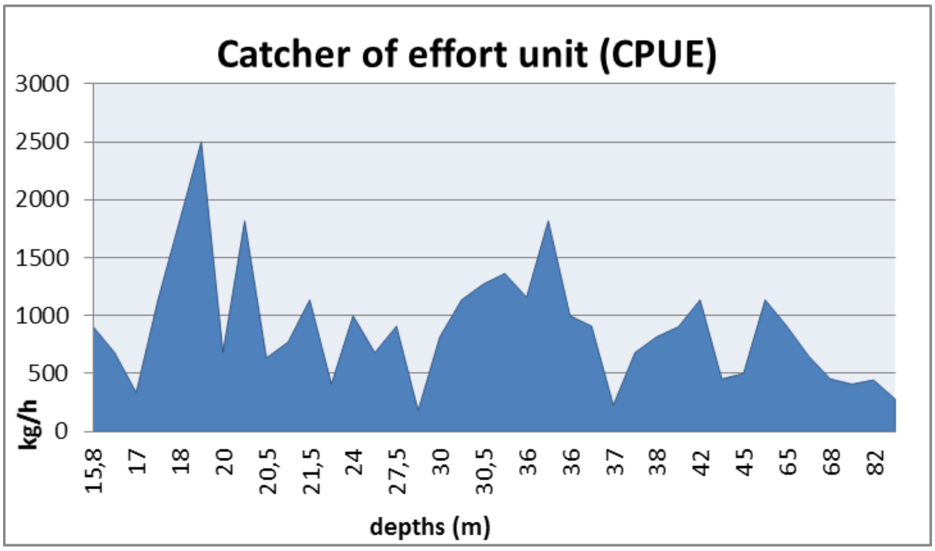

Fig. 6.4.3. Catch per unit of effort (CPUE) for sprat in deep-sea for the period October-November 2019

7. Whiting (*Merlangius merlangus*)

7.1. Distribution

The whiting inhabits the layer near the bottom and feeds mainly sprat. The species is a predator and is an important component of food web for the largest predators such as turbot and dolphins. The whiting was not presented in the catch. This might be related to relatively high temperatures.

7.2. Whiting biomass from different depths

The highest value of biomass was 248t (in the stratum 30-50 m) in November - December 2017. In the other fields, CPUA and biomass were very low and ranged from 0 to 49t (Fig.7.2.1).

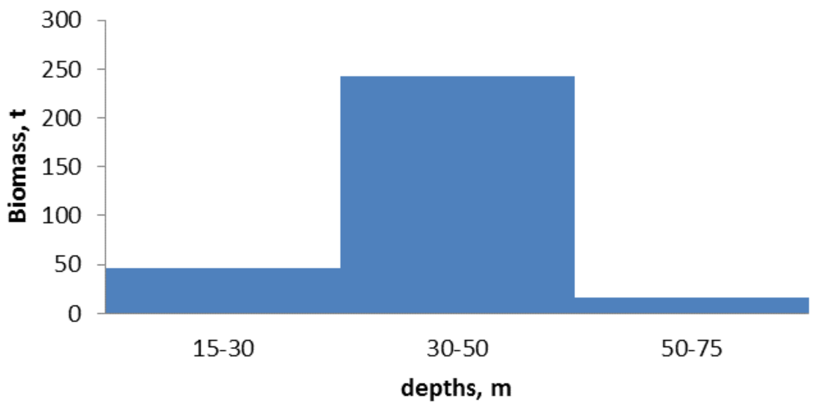

Fig. 7.2.1. Whiting biomass at different depth layers in November-December 2017

In November - December 2018, the catch of whiting was sporadic, with the presence of individual specimens, which might be related to the relatively high temperatures. The catch size of this species was small. In December, the species was present together with sprat (overlapping ecological niches).

Comments on whiting biomass

The total survey area was 8010.24 km^2. The total whiting biomass in the Bulgarian Black Sea area in June 2019 was 1426.5t, and in October-November it was above 14 times higher (21

174.59 t), (Table 7.2.1, Fig. 7.2.2), which was expected, given the biology of the species that is winter-breeding.

Table 7.2.1. The Area method in December 2018, June and October-November 2019 calculated average catch per unit area (CPUA, average), biomas, weight in kg, Ah-area and number of fields per area

Stratum	December 2018				June 2019				October-November 2019	
	Area (Ax)	Number of fields	CPUA average	Biomass (kg)	Area (Ax)	Number of fields	CPUA average	Biomass (kg)	CPUA average	Biomass (kg)
15-30	2065.14	33	1611.73	3328.44	2065.14	33	269.767	557.106	495.55	1023.4
30-50	1814.82	29	924.613	1678.01	1814.82	29	218.194	395.982	171.91	311.99
50-100	2753.52	44	824.565	2270.46	4130.28	66	114.607	473.358	4803.4	19839
Total	6633.48	106		7276.9	8010.24	128		1426.45		21174.59

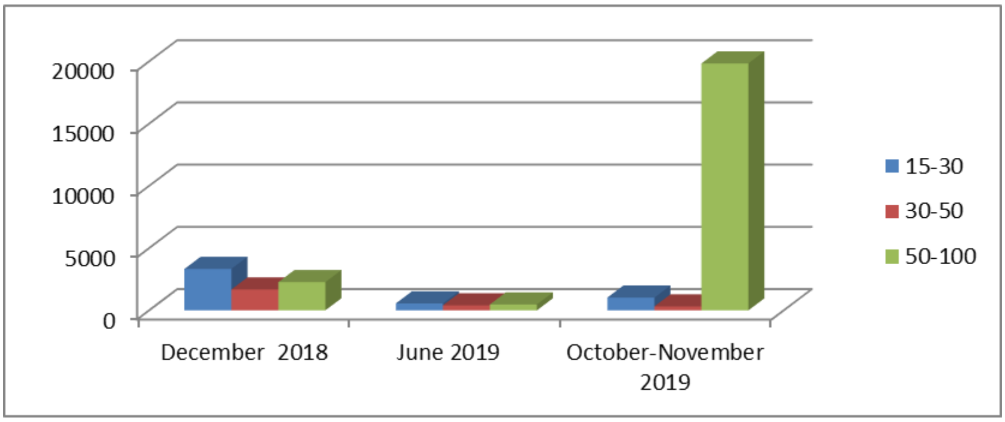

Fig. 7.2.2. Comparison of whiting biomass (kg) during the monitoring period

Table 7.2.2. Whiting. Descriptive statistics on the biomass indices (t) of whiting in December 2018, June and October-November 2019

Parameters	**December 2018**			**June 2019**			**October-November 2019**		
	15-30м	*30-50м*	*50-75м*	*15-30м*	*30-50м*	*50-75м*	*15-30м*	*30-50м*	*50-75м*
Mean	1611.725	924.6126	824.5646	168.6043	158.6864	98.23442	495.54689	171.91023	4803.362
Standard Error	472.0778	83.27297	196.6263	95.35045	33.92143	33.51087	184.00204	74.840881	969.95272
Median	1280.07	861.138	930.96	66.11932	132.2386	52.89545	105.79091	0	5183.7546
Mode	#N/A	837.864	#N/A	0	264.4773	52.89545	0	0	#N/A
Standard Deviation	1335.238	390.5849	520.2242	269.6918	159.1056	88.66143	802.0463	259.25642	2566.2537
Sample Variance	1782859	152556.5	270633.2	72733.67	25314.6	7860.849	643278.27	67213.889	6585657.9
Kurtosis	4.671846	0.092315	-0.512	5.168391	0.727612	1.268084	4.2273986	1.9566644	1.0687864

Skewness	2.028315	0.341692	0.110074	2.207363	1.050908	1.201291	2.1071513	1.5756641	-0.9287209
Range	4142.772	1582.632	1536.084	793.4318	528.9545	264.4773	2909.25	793.43182	7511.1546
Minimum	512.028	232.74	93.096	0	0	0	0	0	105.79091
Maximum	4654.8	1815.372	1629.18	793.4318	528.9545	264.4773	2909.25	793.43182	7616.9455
Sum	12893.8	20341.48	5771.952	1348.834	3491.1	687.6409	9415.391	2062.9227	33623.534
Count	8	22	7	8	22	7	19	12	7
Largest(1)	4654.8	1815.372	1629.18				2909.25	793.43182	7616.9455
Smallest(1)	512.028	232.74	93.096				0	0	105.79091
Conf. Level (95.0%)	1116.287	173.1756	481.1271	225.468	70.54348	81.99814	386.57394	164.72367	2373.3888

7.3. Catch per unit area

The whiting was recorded in the catches in the second half of the survey in 2017, with the densest clusters found in front of c. Kaliakra (Fig. 7.3.1).

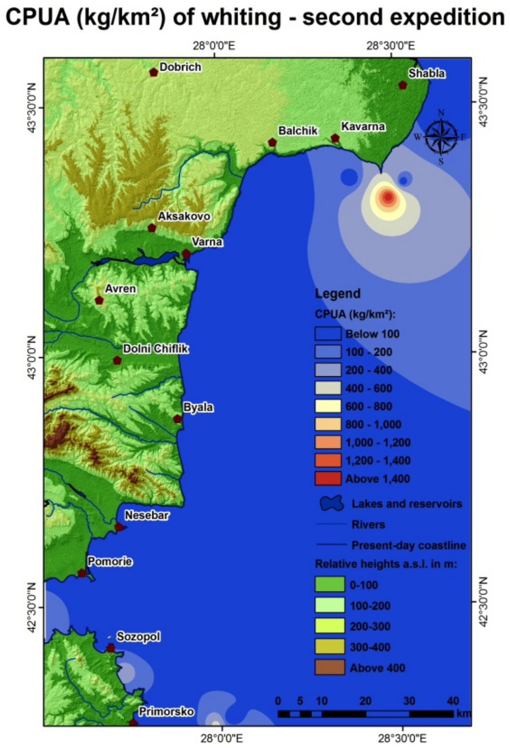

A

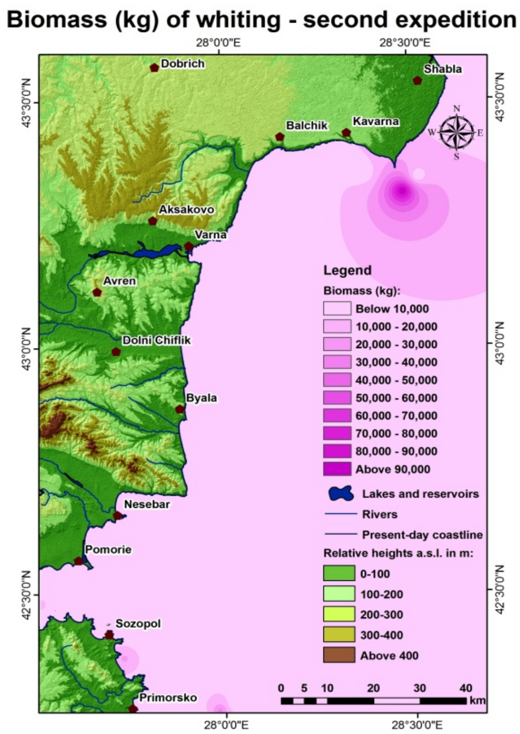

B

Fig. 7.3.1. A. Catch per unit area (CPUA kg.km^{-2}) and B. Whiting biomass in November-December 2017 from

the studied areas

In the 15-30 m depth layer, the highest CPUA was 2050 kg.km^{-2}, average for the layer 1612 kg.km^{-2} , in December 2018. In the 30-50m and 50-75m layers, the CPUAs were with close values of 925 kg.km^{-2} and 825 kg.km^{-2}. The biomass in the coastal zone was 7277t. Species clusters were registered in all tested sites. The highest values of CPUA and biomass of the species were found in front of c. Maslen Nos, Nessebar Bay and in front of Pomorie (Fig.7.3.2).

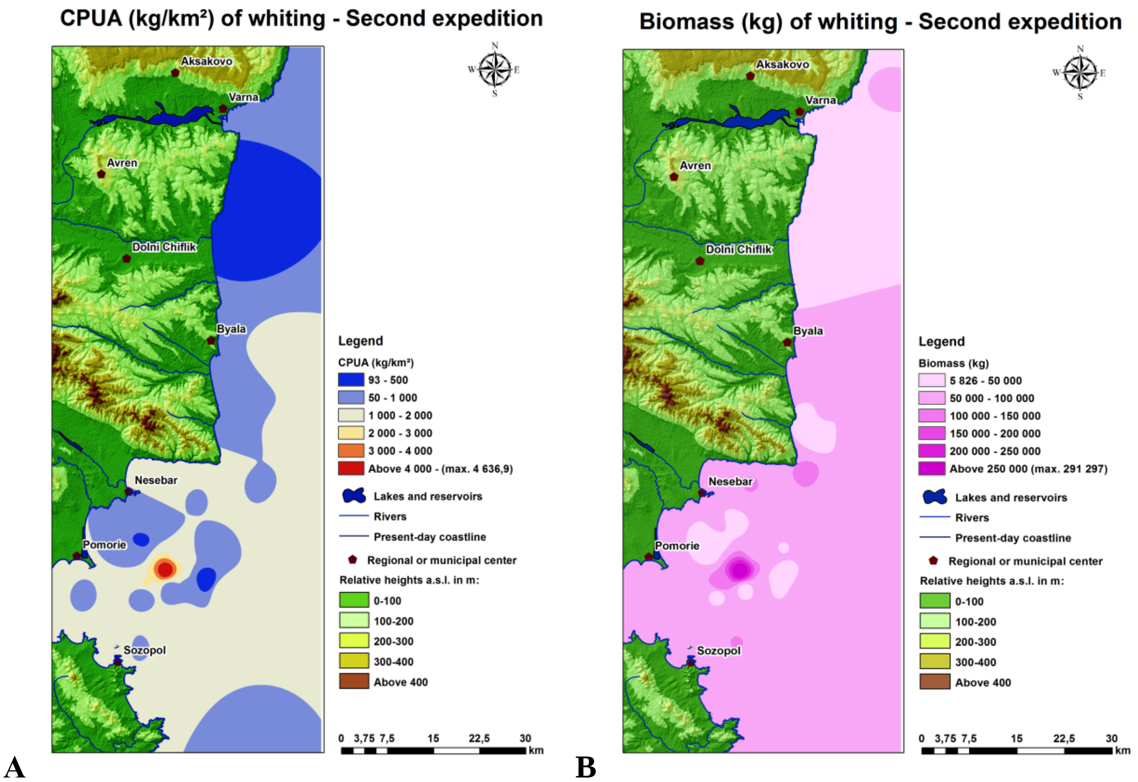

Fig. 7.3.2. A. Catch per unit area (CPUA kg.km^{-2}) and B. Whiting biomass in December 2018 from the studied areas

In June 2019, whiting was most strongly represented in the shallow coastal zone 15-30m with a CPUA = 270 kg.km^{-2} and biomass of 557 t, followed by a depth strip of 30-50m with a CPUA of 218 kg. km^{-2} and biomass 396 t, 115 kg.km^{-2} for CPUA and 473 t biomass at depths of 50-100m. The average CPUA was significantly lower than 98 kg.km^{-2} (Fig. 17).

In June 2019, the highest values> 700 kg.km^{-2} of whiting CPUA were regressed in front of Nessebar and Primorsko (Fig.17). In the 30-50m depths, the highest CPUA was 528 kg.km^{-2}, again in the area described in this study. At depths of 50-100m, the average CPUA was significantly lower - 98 kg.km^{-2} (Fig. 7.3.3).

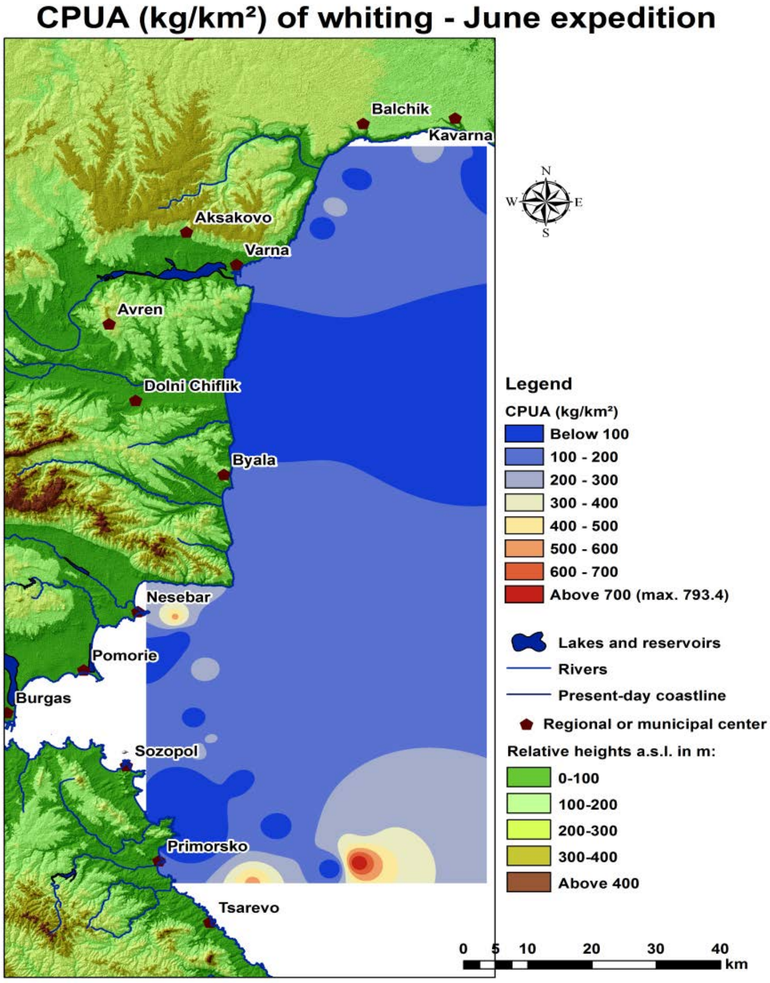

Fig. 7.3.3. Catch per unit area (CPUA kg.km^{-2}) of whiting in June 2019

In October-November 2019, whiting was most strongly represented in the deepest coastal zone 50-100 m with a CPUA = 4803 kg.km^{-2} and biomass of 19 839 t, followed by a depth strip of 30-50 m with a CPUA (the lowest) of 172 kg.km^{-2}, biomass 312 t, 496 kg.km^{-2} for CPUA and 1023 t biomass at depths of 15-30 m.

In October-November 2019, the highest values > 9415 kg.km^{-2} of whiting CPUA were registered southwest of Balchik and in front of Albena (Fig. 7.3.4). In the 30-50 m strip, the highest CPUA was 2063 kg.km^{-2}, again in the described area during the present study. At depths of 50-100 m, the average CPUA was significantly higher than 33624 kg.km^{-2}, which clearly indicated concentrated clusters of the species in the deepest coastal zone during the described period (Fig. 7.3.4).

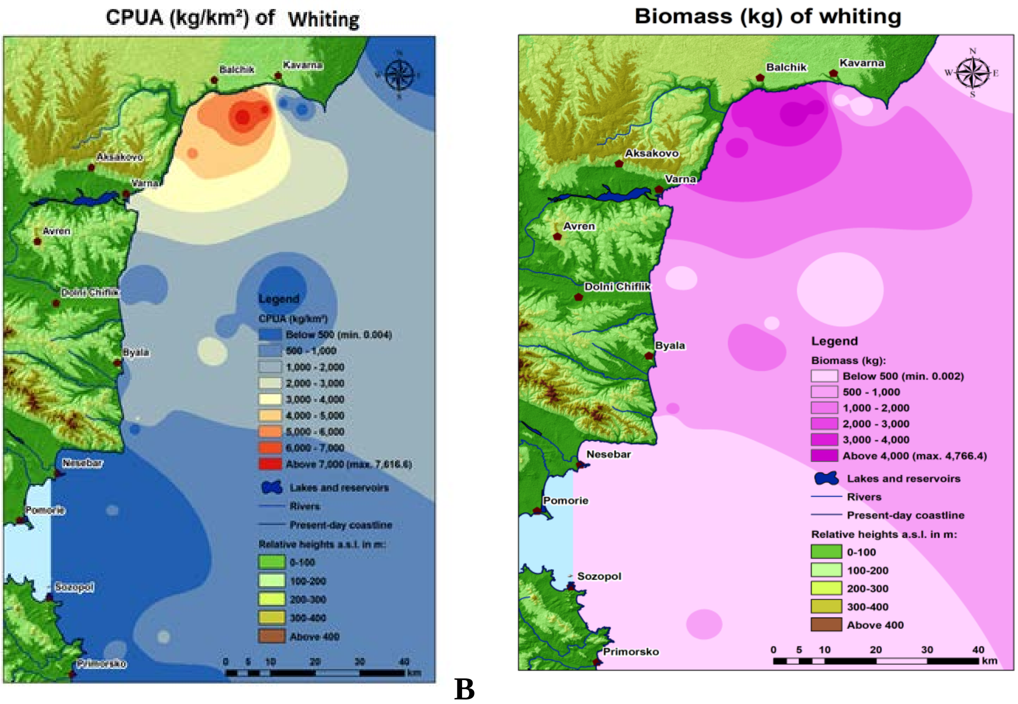

A **B**

Fig. 7.3.4. A. Catch per unit area (CPUA, kg.km^{-2}) and B. whiting biomass (kg) in October-November 2019

7.4. Catch per unit effort

The catch per unit effort for the identified species is presented graphically on Fig. 7.4.1.

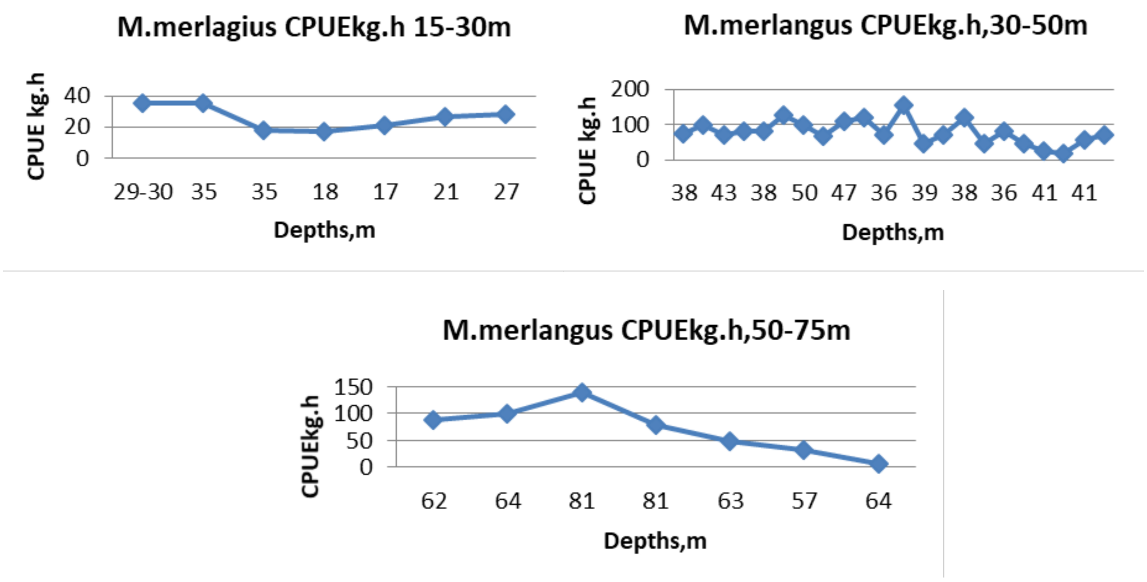

Fig. 7.4.1. Catch per unit effort (CPUE kg.h^{-1}) of whiting in December 2018

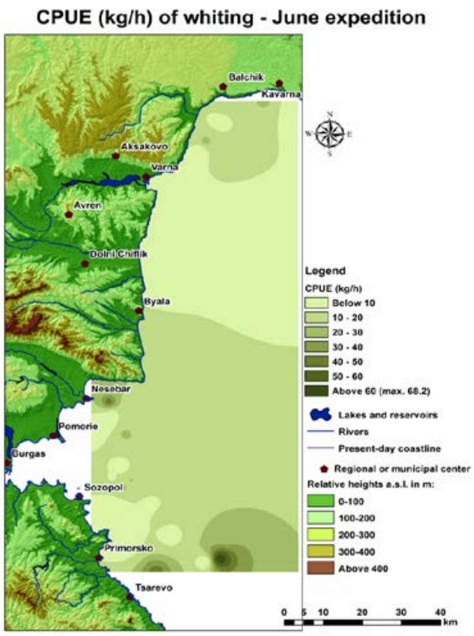

Fig. 7.4.2. Catch per unit effort (CPUE kg.h^{-1}) of whiting in June 2019

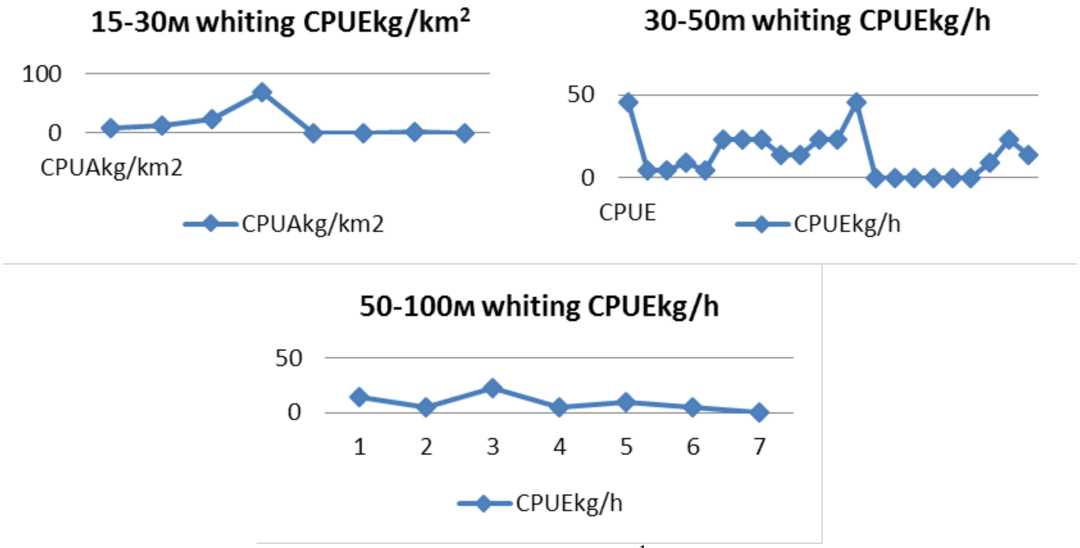

Fig. 7.4.3. Catch per unit effort (CPUE kg.h^{-1}) of whiting in June 2019

Catch per unit effort (CPUE) marked the highest values in the depth range of 50-100m (Fig.7.4.4).

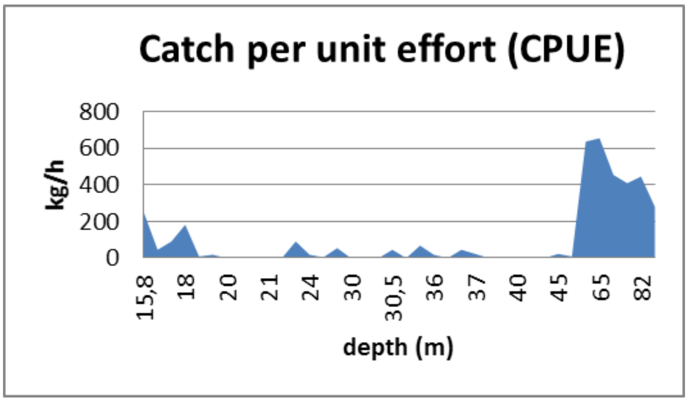

Fig. 7.4.4. Catch per unit effort (CPUE kg.h^{-1}) of whiting in October-November 2019

8. Horse mackerel (*Trachurus mediterraneus*)

8.1. Horse mackerel biomass from different depth layers

In October-November 2017 biomass indices in the depth layers 50-75m and 75-100 m varied between 4-107 t. In the 40-42 m range (October-November) CPUA varied between 873 kg.km^{-2} and 1628 kg.km^{-2}. The catch per unit area was 873 kg.km^{-2} at 35 m depth, and at other depths it did not exceed 280 kg.km^{-2}. In November - December, only at one station (15-30m) was recorded CPUA of 1048 kg.km^{-2}. In most stations no catches of horse mackerel were detected. The biomass of horse mackerel in the first stage of the study did not exceed 550t in the 30-50 m depth strip. In the second stage, an average of 1346 t were detected in the 50-75m strip (Fig. 8.1.1).

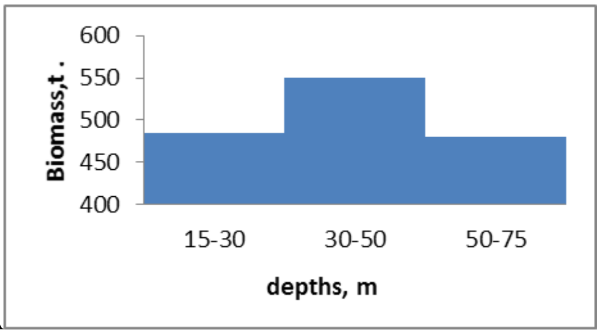

A

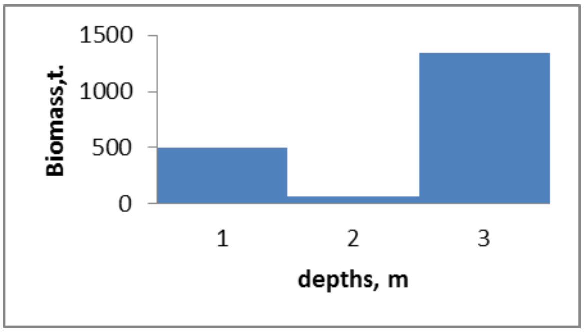

B

Fig. 8.1.1. Horse mackerel biomass from different depths in 2017 A. October-November, B. November-December

In November-December 2018, the species did not form dense clusters, being recorded in all layers examined with approximately the same (CPUA kg.km^{-2}) and biomass (t). In the stratum 50-75 m, CPUA = 460 kg.km^{-2} and biomass1266.9 t.

Comments on *Trachurus mediterraneus* biomass from different depth layers

The total biomass of horse mackerel throughout the Bulgarian Black Sea area in November and December 2018 was 2511.64 t, and 2965.407 t, respectively (Tables 8.1.1 and 8.1.2, Fig. 8.1.2). In the depth range 50-75 m, no clusters of this species were registered in December

2018 at 46 m depth CPUA was 1629 kg.km^{-2}. In the strata 15-30m and 30-50 m, biomass of the agglomerations was 1466t and 1500t, respectively. Like the sprat, the clusters in the 15-30 m layer prevailed (1612 t), followed by 925t (30-50 m) and 825t (50-75 m).

Table 8.1.1. Horse mackerel. Area method in November-December and December 2018 calculated average CPUA, biomass (kg), Ax - area and number of fields per area

Stratum	November-December 2018				December 2018			
	Area (Ax)	Number of fields	CPUA average	Biomass (kg)	Area (Ax)	Number of fields	CPUA average	Biomass (kg)
15-30	2065.14	33	309.6167	639.4019	2065.14	33	709.857	1465.954
30-50	1814.82	29	333.5253	605.2883	1814.82	29	826.227	1499.453
50-100	2753.52	44	460.1213	1266.953	0	44	0	0
Total	6633.48	106		2511.643	3879.96	106		2965. 407
Stratum	November-December 2018				December 2018			
	Area (Ax)	Number of fields	CPUA average	Biomass (kg)	Area (Ax)	Number of fields	CPUA average	Biomass (kg)
15-30	2065.14	33	309.6167	639.4019	2065.14	33	709.857	1465.954

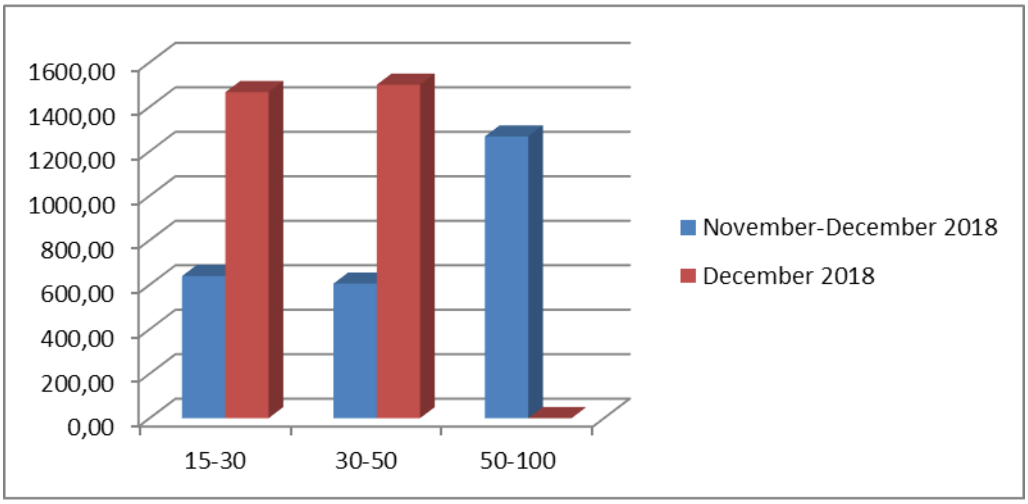

Fig. 8.1.2. Comparison of biomass (kg) of horse mackerel during the monitoring period

Table 8.1.2. Descriptive statistics on horse mackerel biomass indices (t) in November-December and December 2018

Parameters	**November-December 2018**			**December 2018**		
	15-30м	*30-50м*	*50-75м*	*15-30м*	*30-50м*	*50-75м*
Mean	13.22386	247.6469	234.2513	299.9	288	262.9
Standard Error	8.657051	81.79633	138.4441	67.7	44.5	154.7
Median	0	52.89545	105.7909	195. 1	349.1	34.9
Mode	0	0	52.89545	698.3	349.1	0
Standard Deviation	24.48584	383.6588	366.2886	234.5	208.9	435.6
Sample Variance	599.5562	147194.1	134167.4	54981.9	43629.5	189783.6
Kurtosis	-1.8E-15	0.69906	6.624525	-0.6	-0.7	0.3
Skewness	1.440165	1.492221	2.553935	0.8	0.1	1.4
Range	52.89545	1057.909	1005.014	698.3	723.2	1047.4
Minimum	0	0	52.89545	0	0	0
Maximum	52.89545	1057.909	1057.909	698.3	723.2	1047.4
Sum	105.7909	5448.232	1639.759	3598.7	6337	1840.5
Count	8	22	7	12	22	7
Largest(1)				698.3	723.2	1047.4
Smallest(1)				0	0	0
Conf. Level (95.0%)	20.47067	170.1048	338.7605	149	92.6	402.9

8.2. Catch per unit area

The densest passages from horse mackerel in the period October-November 2017 were registered in front of c. Emine and Sozopol, in the other regions they were scattered (Fig. 8.2.1).

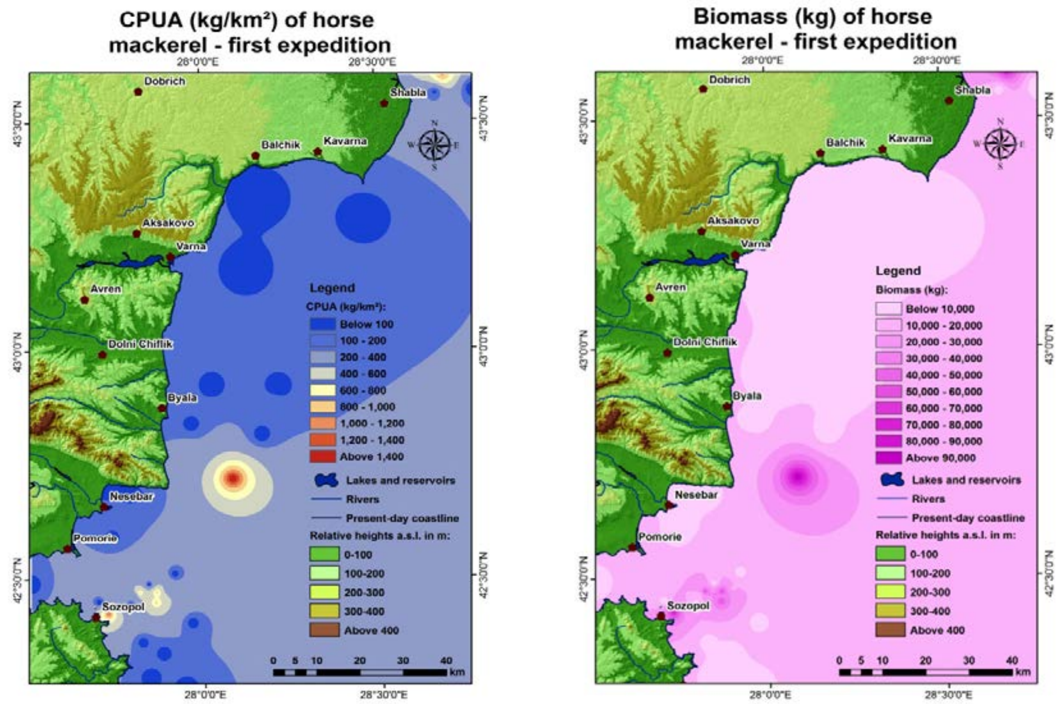

A **B**

Fig. 8.2.1. A. Catch per unit area (CPUA kg.km^{-2}), B. horse mackerel biomass October-November 2017

In front of Golden Sands and south of Balchik the densest accumulations of horse mackerel were registered in November-December 2017 (Fig. 8.2.2).

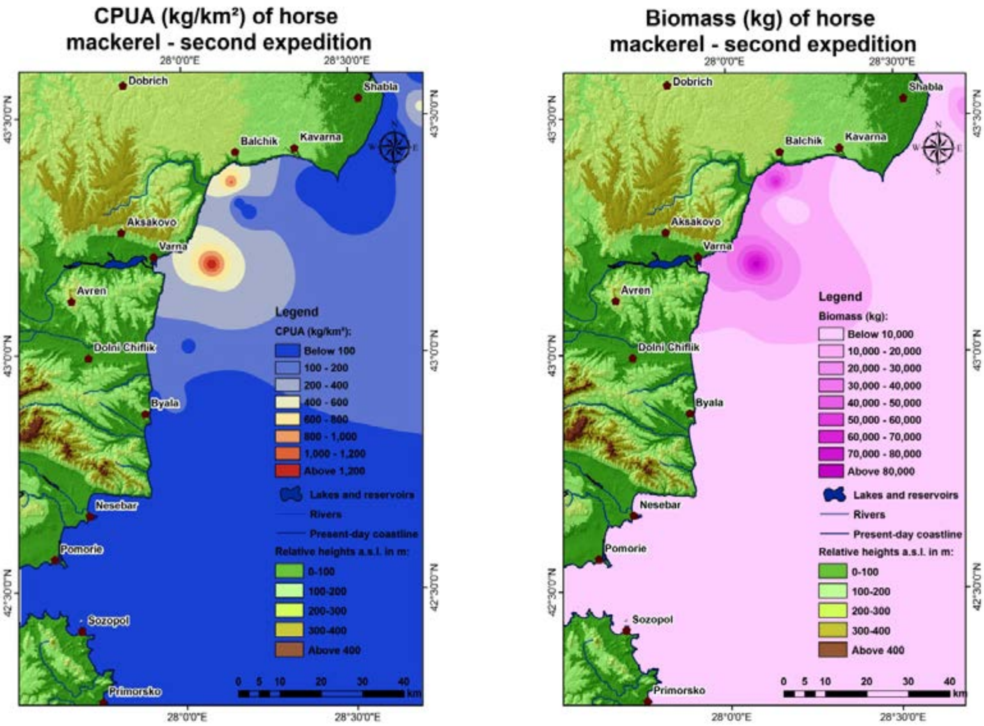

A **B**

Fig. 8.2.2. A. Catch per unit area (CPUA kg.km^{-2}), B. horse mackerel biomass November-December 2017

In November 2018, the species was not detected at 6 stations (on 3 stations at each depth layer). The lowest positive value of the CPUA (kg.km^{-2}) found in all layers was 17 kg.km^{-2} (Bourgas Bay), the highest - 1045 kg.km^{-2} discovered at 64 m depth, northeast of Byala. High CPUA values were also established in the area of Sozopol, east of Primorsko, in front of Golden Sands resort and south of Balchik. The densest aglomerations were found in front of Byala at depth of 50-75 m and in front of Primorsko (over 1000 kg.km^{-2}) (Fig. 8.2.3).

In December 2018, the species did not form dense clusters, being recorded in all depth layers examined with approximately the same CPUA (kg.km^{-2}) and biomass (t). The CPUA and biomass prevailed in the stratum 30-50 m (Fig. 28). At 50-75 m depth no aglomerations of the species were recorded, at 46 m depth CPUA = 1629 kg.km^{-2} (Fig. 8.2.4). In the other studied areas the clusters were insignificant and catches were not recorded in most areas. The same trend was observed in October-November 2019, as the species is thermophilic, and in a trawl only a few specimens were sporadically represented.

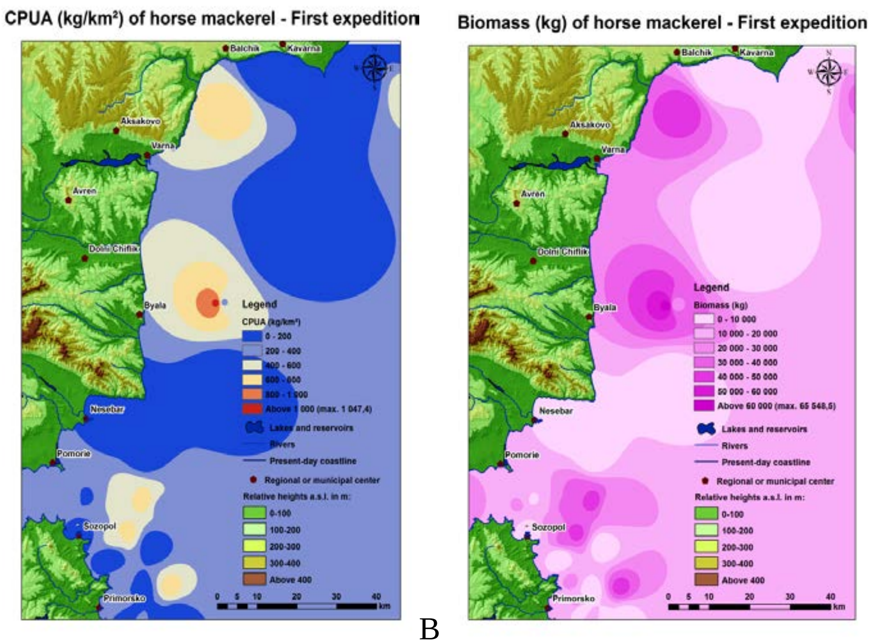

A B

Fig. 8.2.3. A Catch per unit area (CPUA kg.km^{-2}), B. horse mackerel biomass November 2018

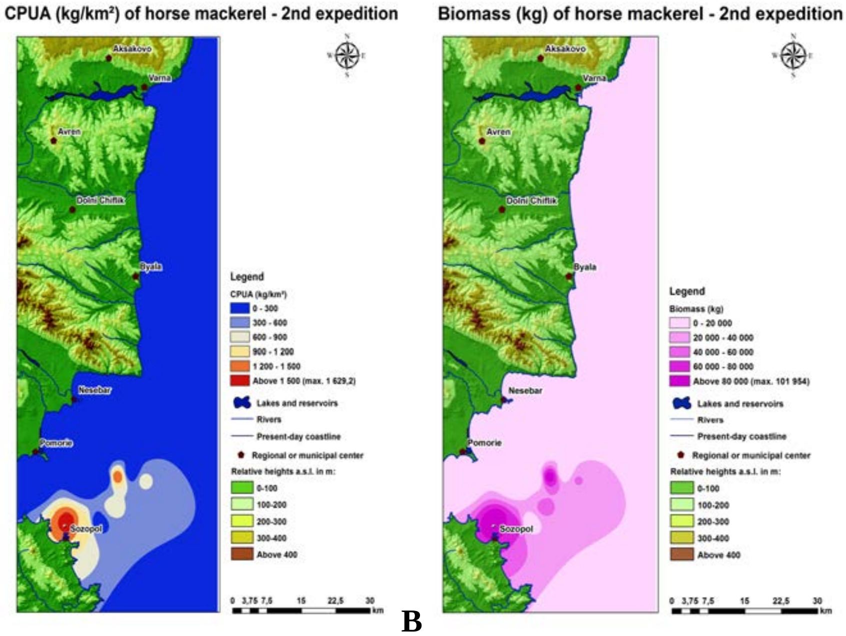

A B

Fig. 8.2.4. A. Catch per unit area (CPUA kg.km^{-2}), B. Horse mackerel biomass in Decmber 2018

8.3. Catch per unit effort (CPUE)

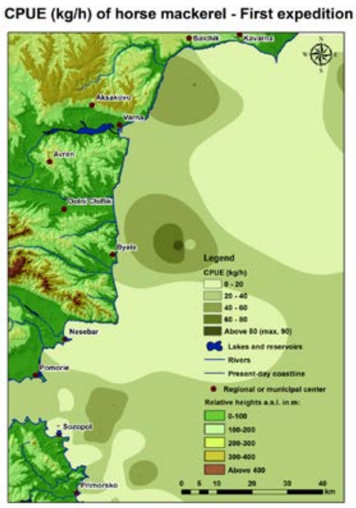

Fig. 8.3.1. Catch per unit effort (CPUE) for horse mackerel in November-December 2018

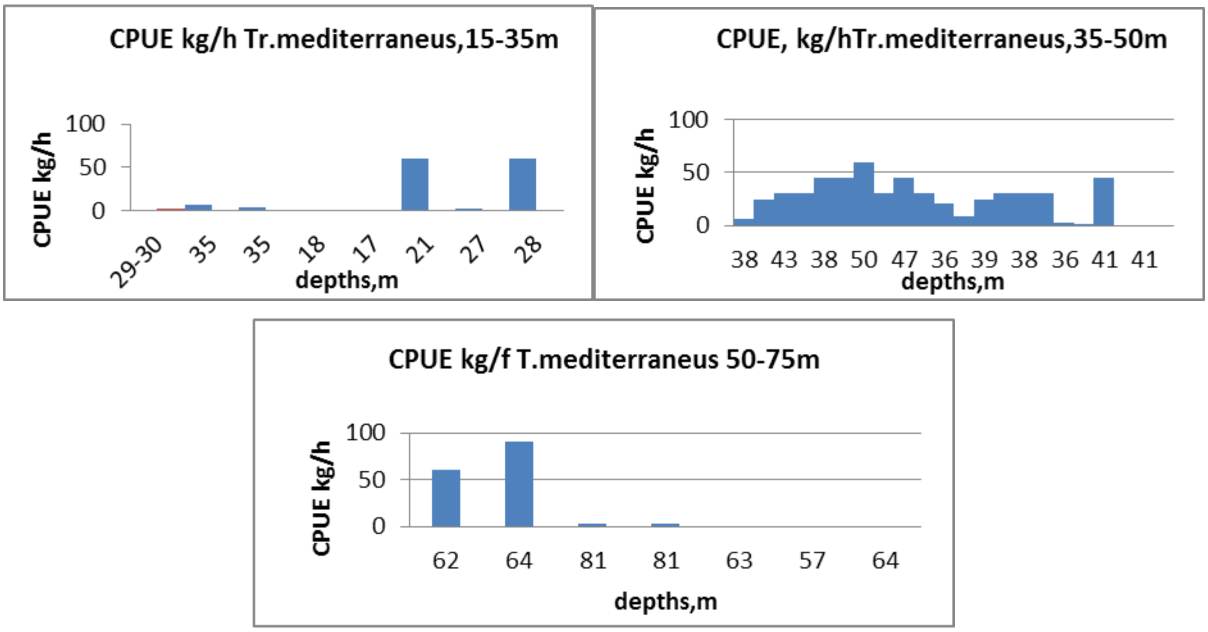

Fig. 8.3.2. Catch per unit effort (CPUE kg.h^{-1}) for horse mackerel in November-December 2018

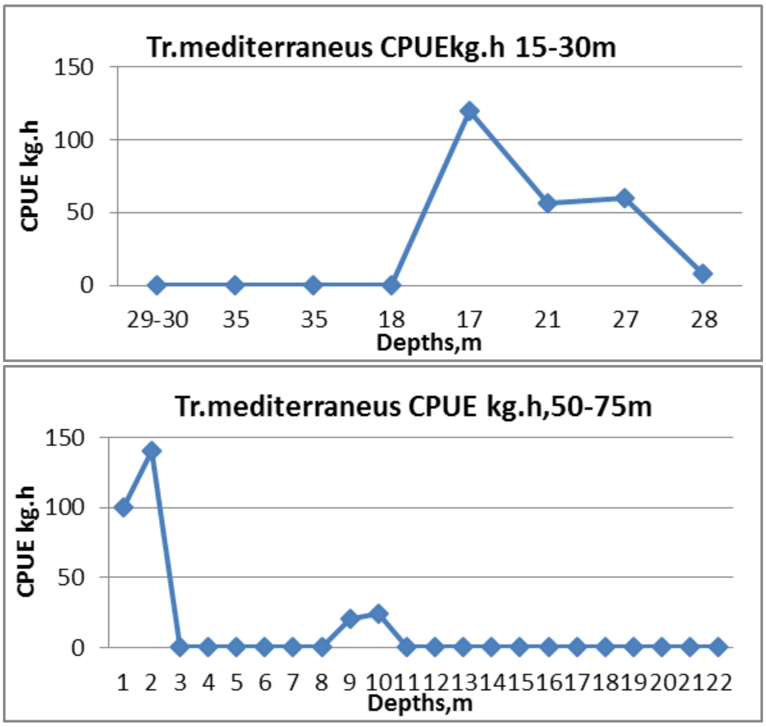

Fig. 8.3.3. Catch per unit effort (CPUE kg.h^{-1}) for horse mackerel in December 2018

9. Red Mullet (*Mullus barbatus*)

9.1. Distribution

In October-November 2017, at 15-30 m depth the average biomass index was 169 t. In the other depth layers, the index values were lower. In November-December at depths of 15-30m the biomass was very low - of the order of 24 t at the 15-30 m depth, and no catches of the species were recorded at 50-75m depth.

9.2. Biomass

The species had the highest recorded biomass and CPUA in the studied areas in November-December 2018. At stratum 15-30 m CPUA = 1102.9 kg.km^{-2} and biomasss = 2277.7 t. At depths of 30-50m and 50-75 m clusters were significantly lower, CPUA = 346.5 kg.km^{-2} and biomass = 930 t; CPUA = 396 kg.km^{-2} and biomass = 1090 t (Fig.9.2.1).

A
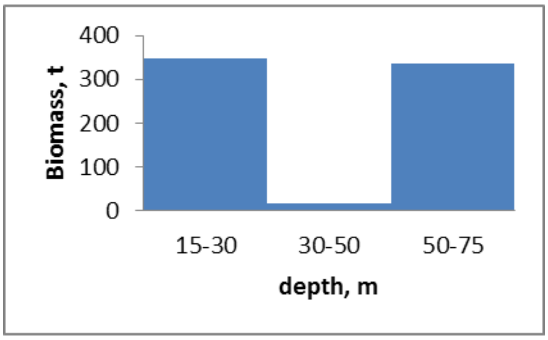

B
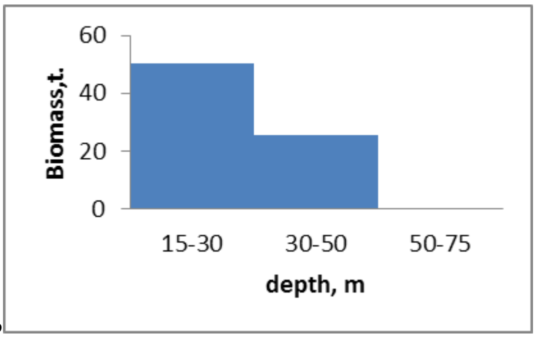

Fig. 9.2.1. Red mullet biomass in 2017 A. October-November B. November-December

In June 2019, the red mullet was represented with the lowest abundance in the shallow coastal zone (15-30 m) with CPUA = 52.9 kg.km^{-2} and biomass of 109.25 t. The highest CPUA values of 419 kg.km^{-2} were established in the 30-50m deep layer with biomass of 761 t, followed by 234.3 kg.km^{-2} values for CPUA and the highest biomass values of 968 t at depths of 50-100 m.

In October-November 2019, the red mullet was best represented in the shallow coastal zone

Project proposal № BG14MFOP001-3.003-0001 "Collection, management and use of data for the purposes of scientific analysis and implementation of the Common Fisheries Policy for the period 2017-2019", funded by the Maritime Affairs and Fisheries Program, co-financed by the European Union through the European Maritime and Fisheries Fund

(15-30 m) with CPUA = 1016 kg.km^{-2} and biomass of 2099 t. The lowest CPUA values of 331 kg.km^{-2} were detected at 50-100 m depths with 1366 t biomass, while the 914 kg.km^{-2} values for CPUA and 1658 t biomass values were recorded at 30-50 m depth.

Comments on the biomass of red mullet (*Mullus barbatus*) from different depth layers

The total studied area in November 2018 was 6633.48 km^2 and the registered total biomass of the red mullet was 3996.399 t. In the period October-November 2019 the studied area covered 8010.24 km^2 and the total biomass of red mullet was 1837.4 t, while in June 2019 the total biomass was 5122.056 t (Tables 9.2.1 and 9.2.2). The highest biomass during the autumn sampling in a depth band of 15-30 m was established, while in the summer it was at a greater depth (50-100 m) (Fig. 9.2.2).

Table 9.2.1. Red mullet. Area method in November-December 2018, June and October-November 2019, calculated average catch per unit area (CPUA, average), biomass weight in kg, Ah - area and number of fields per area

Stratum	November-December 2018				June 2019				October-November 2019	
	Area (Ax)	Number of fields	CPUA average	Biomass (kg)	Area (Ax)	Number of fields	CPUA average	Biomass (kg)	CPUA average	Biomass (kg)
15-30	2065.14	33	1102.924	2277.692	2065.14	33	52.9	109.2459	1016.1	2098.5
30-50	1814.82	29	346.356	628.5738	1814.82	29	419.095	760.5815	913.65	1656.1
50-100	2753.52	44	395.9054	1090.133	4130.28	66	234.251	967.5235	330.6	1365.5
Total	6633.48	106		3996.399	8010.24	128		1837.351		5122.056

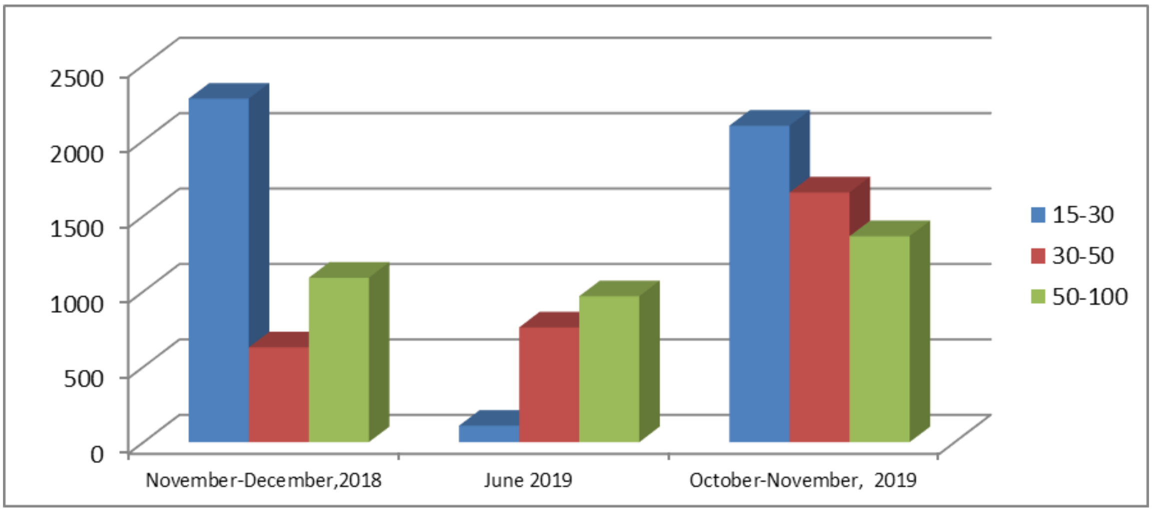

Fig. 9.2.2. Comparison of the red mullet biomass (kg) during the monitoring period

Table 9.2.2. Descriptive statistics on the red mullet biomass indices (t) in November-December 2018, June and October-November 2019

Parameters	November-December 2018			June, 2019			October-Novamber 2019		
	10-30м	*30-50м*	*50-75м*	*15-30м*	*30-50м*	*50-75м*	*15-30м*	*30-50м*	*50-75м*
Mean	275.7	314.9	226.2	13.22386	247.6469	234.2513	1016.1495	793.43182	340.04221
Standard Error	270.6	44.5	83.2	8.657051	81.79633	138.4441	324.17165	255.92377	73.780689
Median	0	349.1	349.1	0	52.89545	105.7909	528.95455	423.16364	317.37273
Mode	0	349.1	0	0	0	52.89545	264.47727	476.05909	105.79091
Standard Deviation	765.4	208.8	220.1	24.48584	383.6588	366.2886	1413.0314	886.54596	195.20535
Sample Variance	585803.7	43593.3	48430.6	599.5562	147194.1	134167.4	1996657.9	785963.73	38105.13
Kurtosis	8	-0.8	-2.1	-1.8E-15	0.69906	6.624525	12.259783	0.3783412	-1.835767
Skewness	2.8	0.2	0	1.440165	1.492221	2.553935	3.2938617	1.3948321	-0.0864083
Range	2169.7	698.3	523.7	52.89545	1057.909	1005.014	6294.5591	2591.8773	476.05909
Minimum	0	0	0	0	0	52.89545	52.895455	52.895455	105.79091
Maximum	2169.7	698.3	523.7	52.89545	1057.909	1057.909	6347.4546	2644.7727	581.85
Sum	2205.8	6927.1	1583.6	105.7909	5448.232	1639.759	19306.841	9521.1819	2380.2955
Count	8	22	7	8	22	7	19	12	7
Largest(1)	2169.7	698.3	523.7				6347.4546	2644.7727	581.85
Smallest(1)	0	0	0				52.895455	52.895455	105.79091
Conf. Level (95.0%)	639.9	9216	203.5	20.47067	170.1048	338.7605	681.05936	563.28443	180.53484

9.3. Catch per unit area

The densest clusters of red mullet were recorded south of c. Maslen Nos at relatively shallow depths in October-November 2017 (Fig. 9.3.1). In November-December 2017, the largest clusters of this species were recorded in the north of Byala and at greater depths near Nessebar.

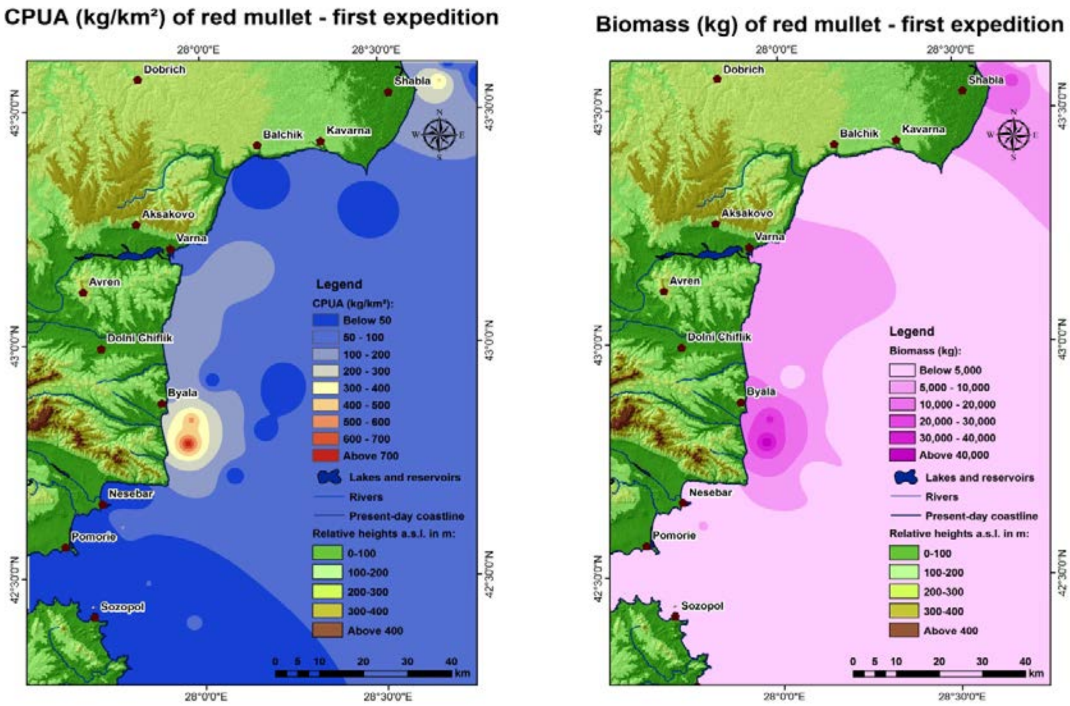

A **B**

Fig. 9.3.1. A. CPUA (kg.km^{-2}), B. Red mullet biomass in October-November 2017

In November-December 2018 in most of the studied areas the species was not detected in the depth range of 15-30 m. The highest concentrations were found at 27 m depth, at a station located southeast of Sozopol (CPUA = 2169, 7 kg.km^{-2}). In the other depth layers examined the index ranged from 36 kg.km^{-2} to 700 kg.km^{-2}. At 10 of the stations the species was not detected (Fig. 9.3.2).

Project proposal № BG14MFOP001-3.003-0001 "Collection, management and use of data for the purposes of scientific analysis and implementation of the Common Fisheries Policy for the period 2017-2019", funded by the Maritime Affairs and Fisheries Program, co-financed by the European Union through the European Maritime and Fisheries Fund

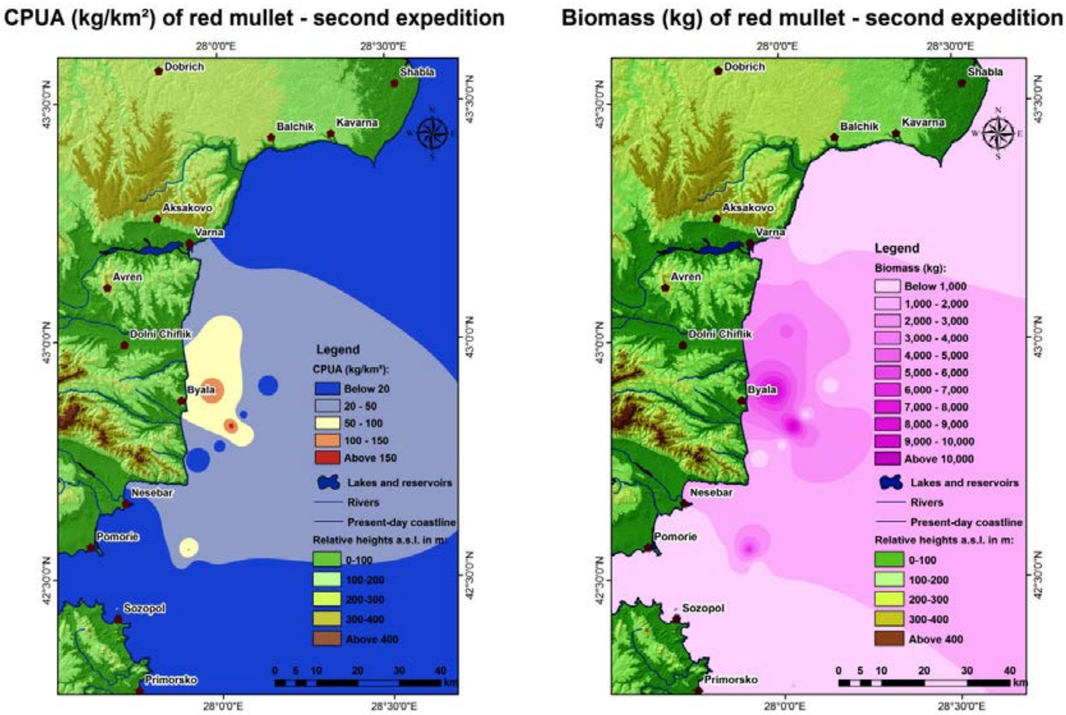

A **B**

Fig. 9.3.2. A. CPUA (kg.km^{-2}), B. Red mullet biomass in November-December 2017

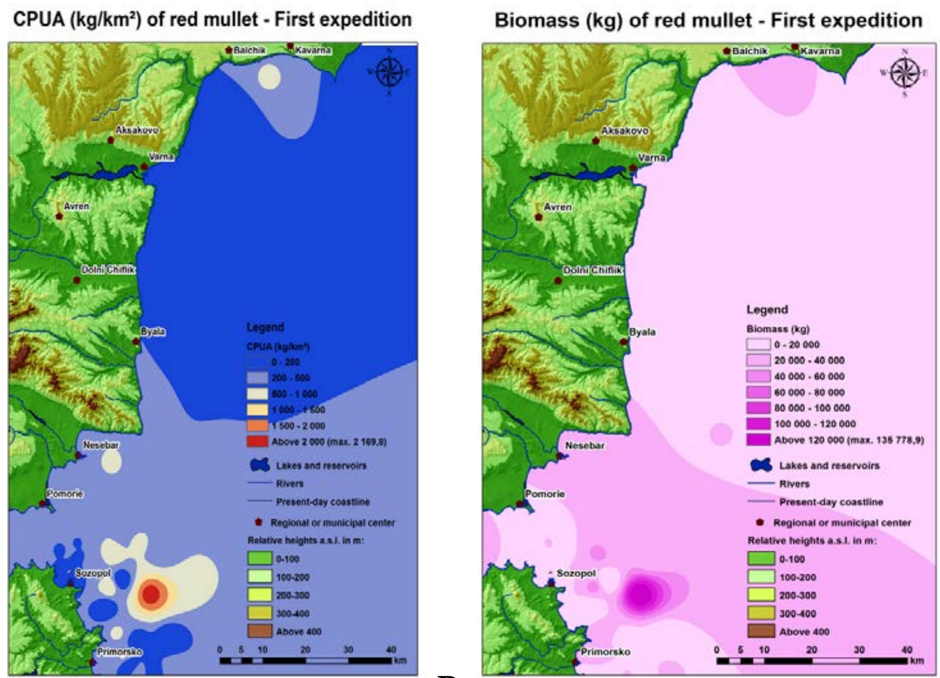

A **B**

Fig. 9.3.3. A. CPUA (kg.km^{-2}), B. Red mullet biomass in November-December 2018

The CPUA and CPUE of red mullet during June 2019 survey (Fig. 9.3.4) indicated that CPUA in most of the surveyed areas had values below 100 kg.km^{-2}. The exception was the area in front of Blachik and Kavarna, where CPUA of 1058 kg.km^{-2} was recorded at 30-50m depth.

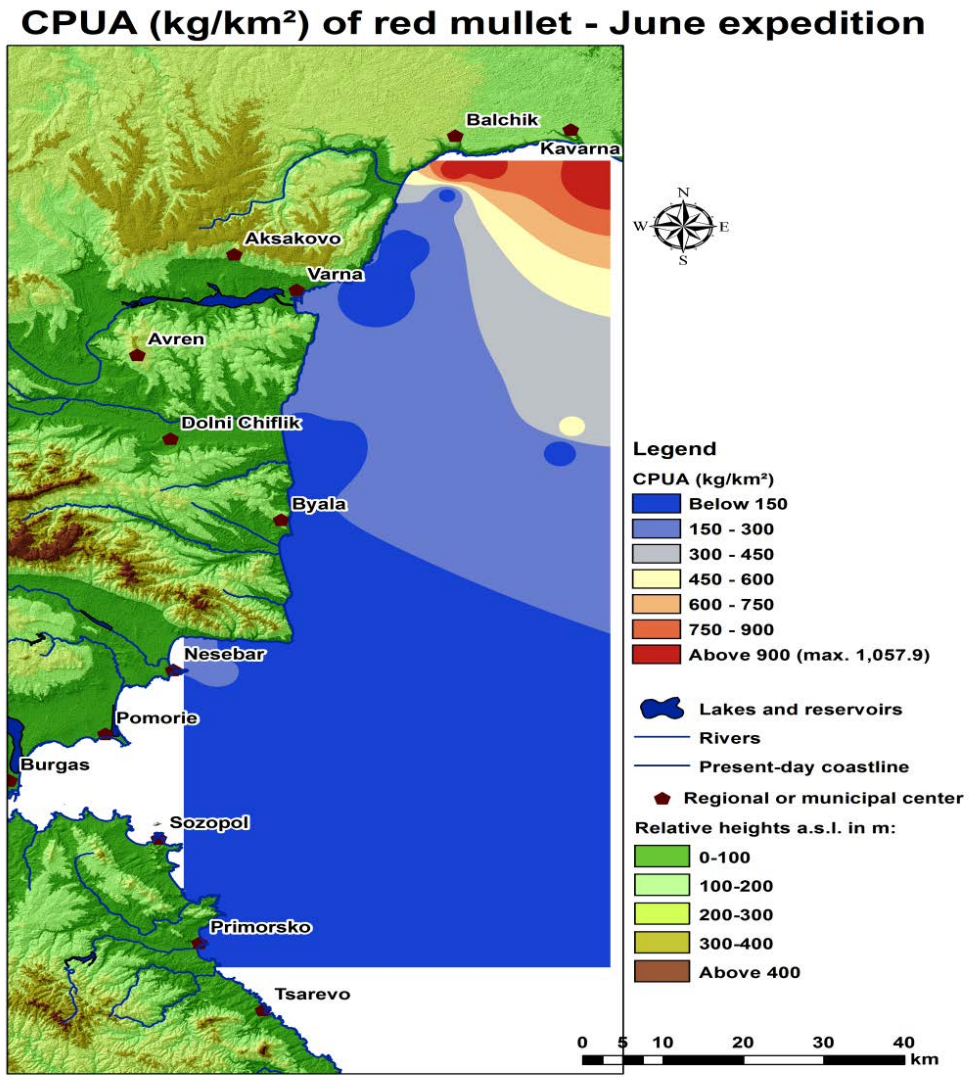

Fig. 9.3.4. CPUA (kg.km^{-2}) of the red mullet in June 2019

The CPUA and CPUE for the red mullet from the October - November 2019 survey (Fig. 9.3.5) indicated that CPUA at 15-30 m depth had the highest values (6348 kg.km^{-2}.) At greater depths of 50-100 m, the CPUA varied from 106 kg.km^{-2} to 476 kg.km^{-2}.

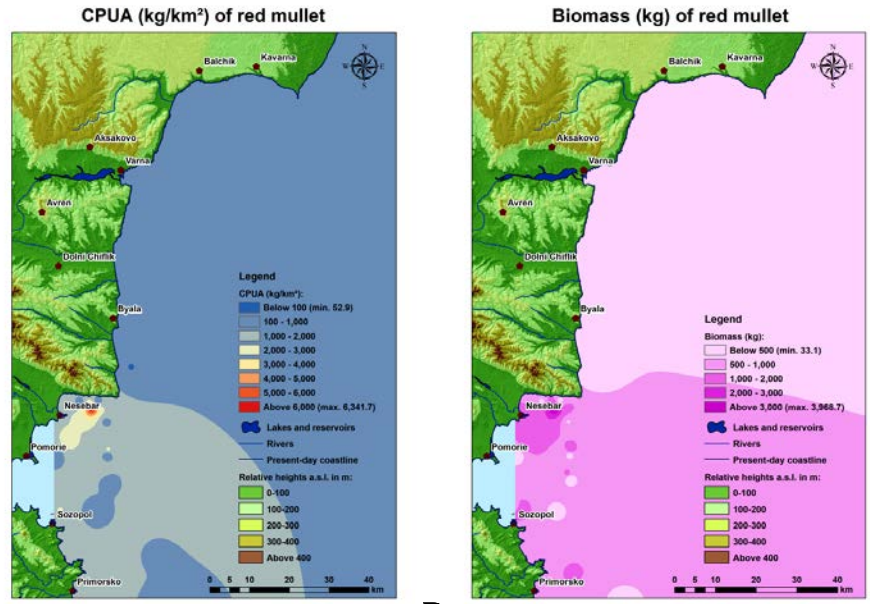

A **B**

Fig. 9.3.5. A. CPUA (kg.km^{-2}), B. Biomass (kg) of red mullet in October - November 2019

9.4. Catch per unit effort

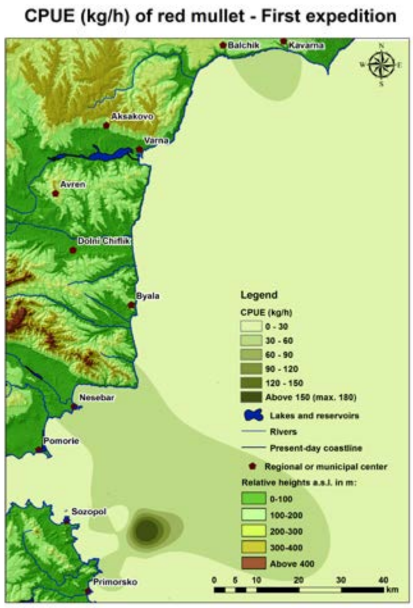

Fig. 9.4.1. Catch per unit effort (CPUE) of the red mullet in November-December 2018

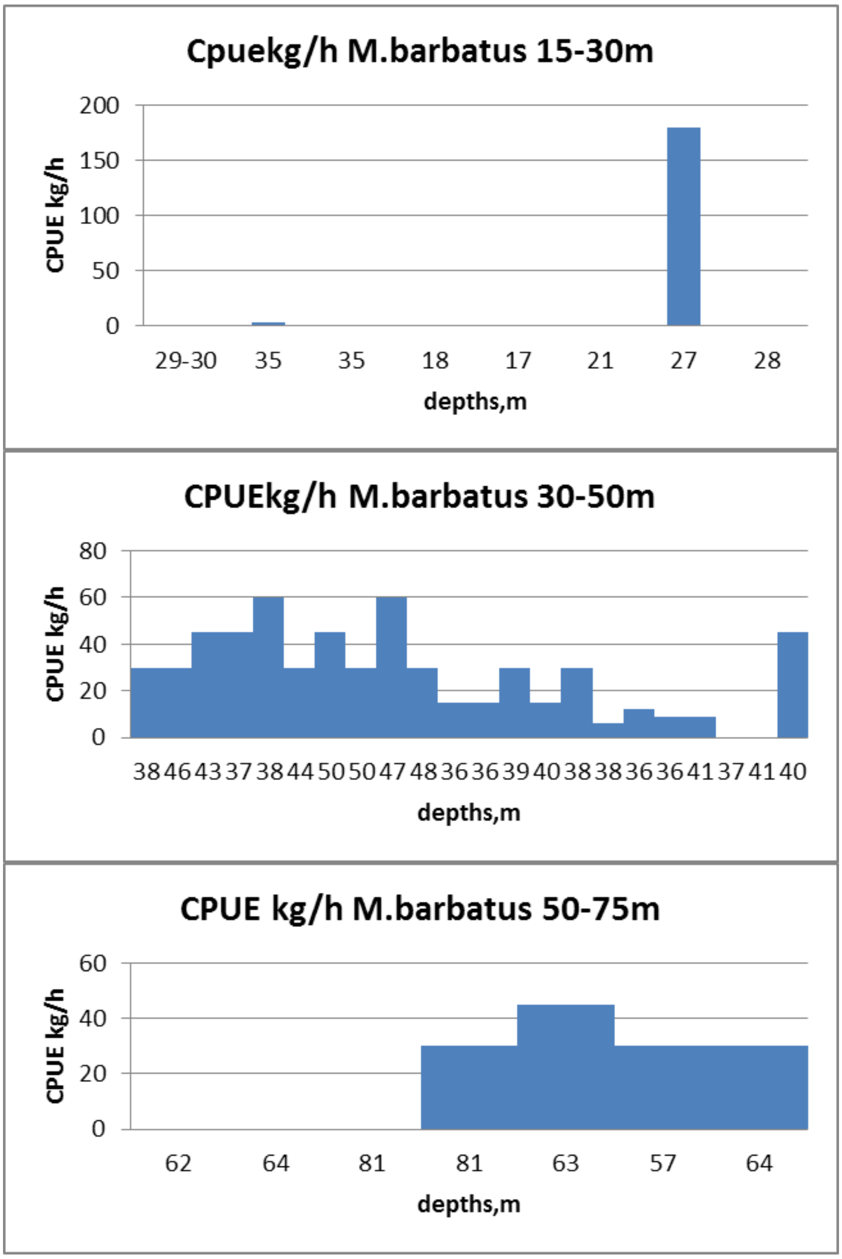

Fig. 9.4.2. Catch per unit effort (CPUE kg.h^{-1}) of the red mullet November-December 2018

CPUE (kg/h) of red mullet - First expedition

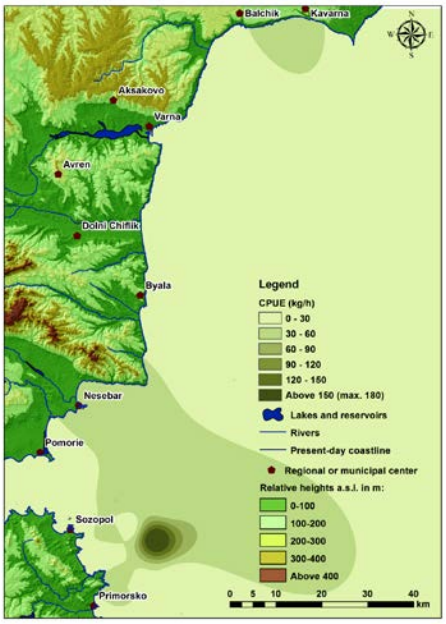

CPUE (kg/h) of red mullet - June expedition

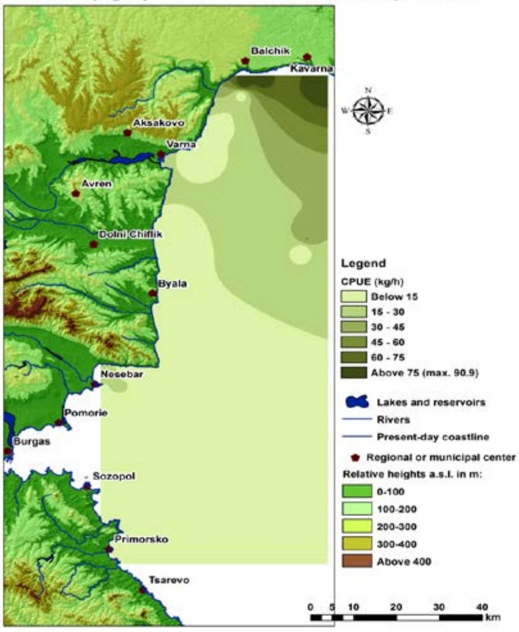

CPUE (kg/h) of red mullet - First expedition

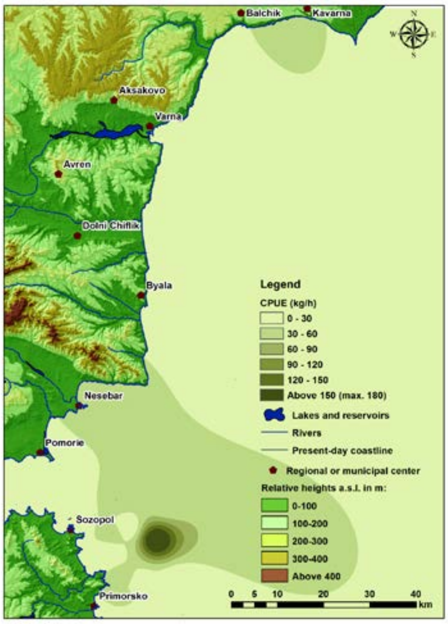

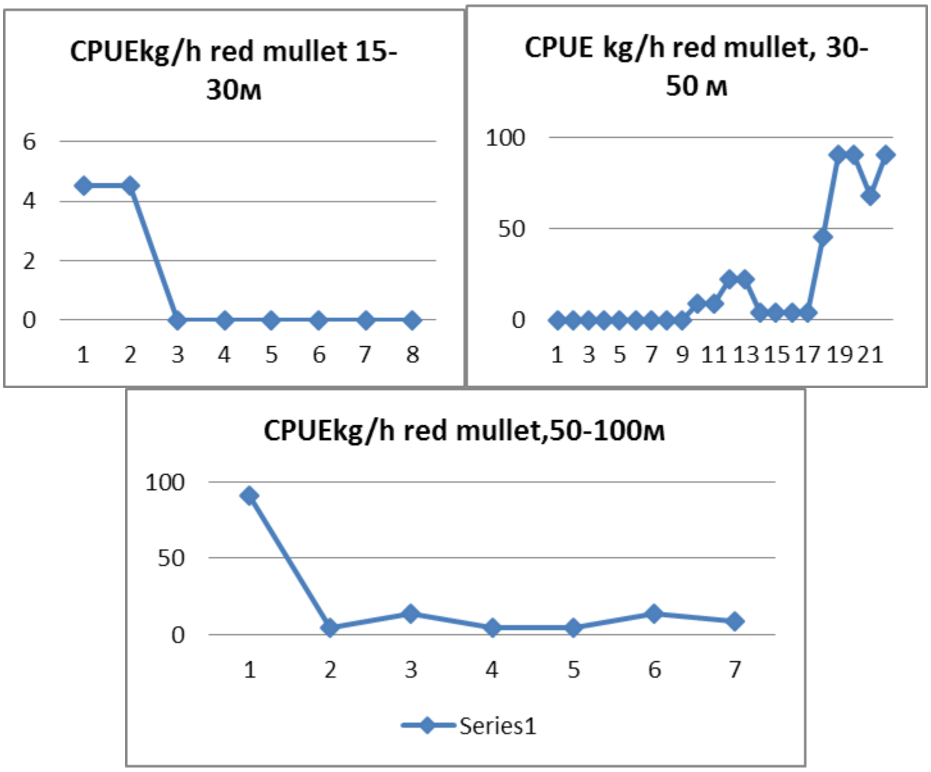

Fig. 9.4.3. Catch per unit effort (CPUE kg.h^{-1}) of the red mullet June 2019

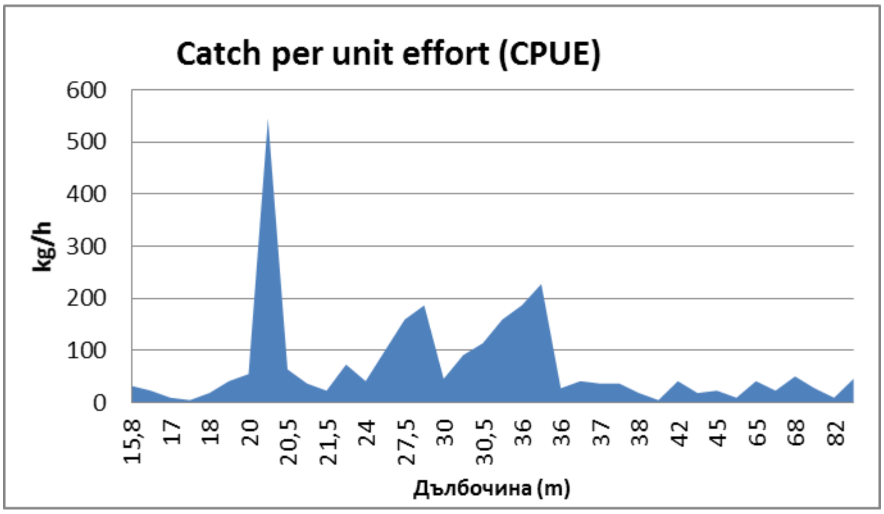

Fig. 9.4.4. Catch per unit effort (CPUE kg.h^{-1}) of the red mullet in October-November 2019

10. Bluefish (*Pomatomus satatrix*)

The October-November study showed that biomass indices in 30-50m and 50-75m depths varied within 90 t. Biomass indices were lower in the studied area. In November-December 2017, the bluefish was not presented in the catches.

In November-December 2018, the species did not form dense clusters, being recorded in all depth layers surveyed with approximately the same CPUA ($kg.km^{-2}$) and biomass (t): stratum 15-30 m CPUA = 279.3159 $kg.km^{-2}$, biomass = 576.8265 t; 30-50m CPUA = 327.1533 $kg.km^{-2}$, biomass = 593.7244 t; 50-75m CPUA = 142.77$kg.km^{-2}$, biomass = 393.1347 t).

In November-December 2018, in the northeast, between Primorsko and Sozopol, at a depth of more than 37-43 m, the highest concentrations of bluefish (699 kg. km^{-2}) were registered. Clusters of the species at 15-30 m and 50-75 m depths were almost absent (Fig. 10.1).

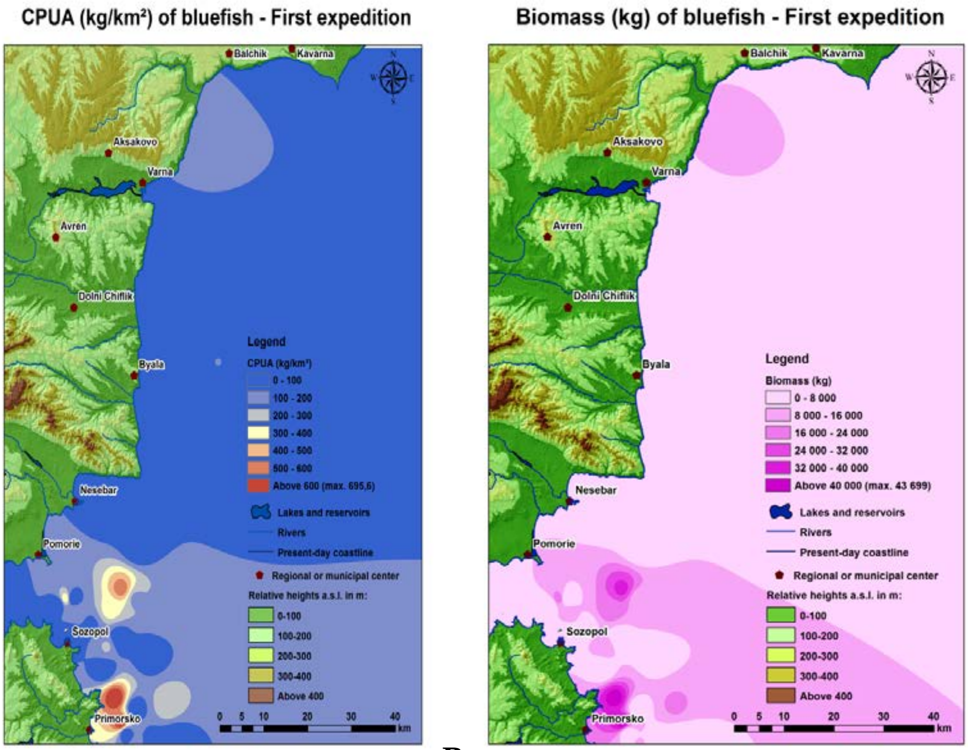

A B

Fig. 10.1. A. CPUA ($kg.km^{-2}$), B. Biomass of bluefish in November-December 2018

Comments on the bluefish (*P.satatrix*) biomass from different depth layers (Table 10.1,

Fig. 10.2).

Table 10.1. Bluefish. The Area method in November-December 2018, calculated average catch per unit area (CPUA, average), biomass- weight in kg., Ax - area and number of fields per area

CPUA average		Biomass(kg)	Ax (Area)	№ Fields
279.3159	15-30	576.8265	2065.14	33
327.1533	30-50	593.7244	1814.82	29
142.7753	50-75	393.1347	2753.52	44
		1563.686	6633.48	106

The total bluefish biomass in November-December 2018 was 1564 t in the Bulgarian Black Sea area.

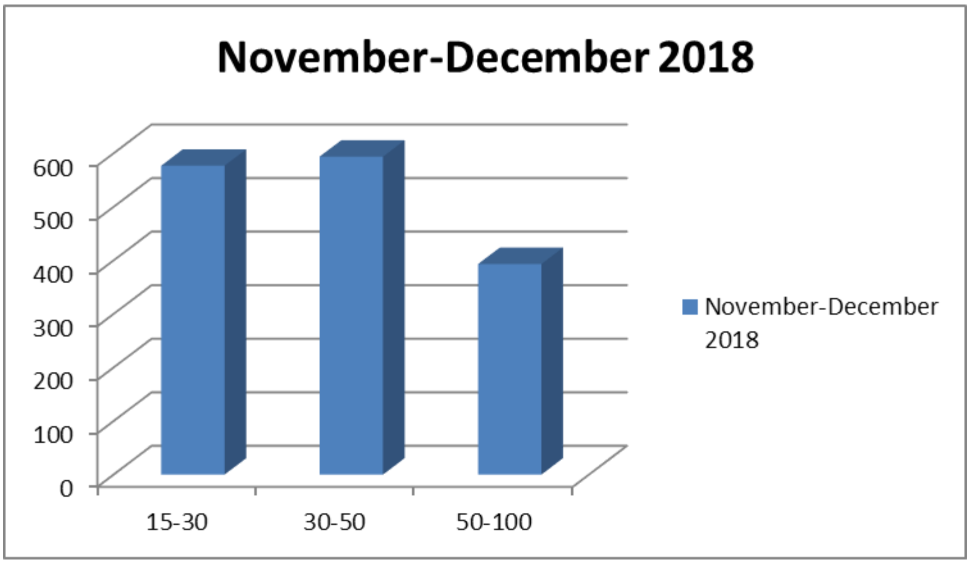

Fig. 10.2. Comparative representation of bluefish biomass (kg) during the monitoring period

Table 10.2. Descriptive statistics of the bluefish biomass index (t) in November - December 2018

Parameters	November-December 2018		
	10-30m	*30-50m*	*50-75m*
Mean	34.9	163.6	40.8
Standard Error	34.9	48.7	27.6
Median	0	34.9	0
Mode	0	0	0
Standard Deviation	98.8	228.4	73
Sample Variance	9752.2	2159.6	53355.7
Kurtosis	8	1.1	1.4
Skewness	2.8	1.4	1.6
Range	279.3	698.3	180.8
Minimum	0	0	0
Maximum	279.3	698.3	180.8
Sum	279.3	3598.7	285.6
Count	8	22	7
Largest(1)	279.3	698.3	180.8
Smallest(1)	0	0	0
Conf. Level (95.0%)	82.6	101.3	67.6

Round goby (*N.melanostomus*) The species is benthic and coastal. Only a few individuals were registered in the 2017-2018 trawls. Single specimens were recorded in June and October-November 2019.

Pontic shad (*A. immaculata*) Rarely presented, only a single number of catches were reported during the monitoring period.

Anchovy (*E. encrasicolus* L.) The species is migratory and pelagic. In November - December 2018, the catch was sporadic with the presence of individual specimens.

11. Length and weight

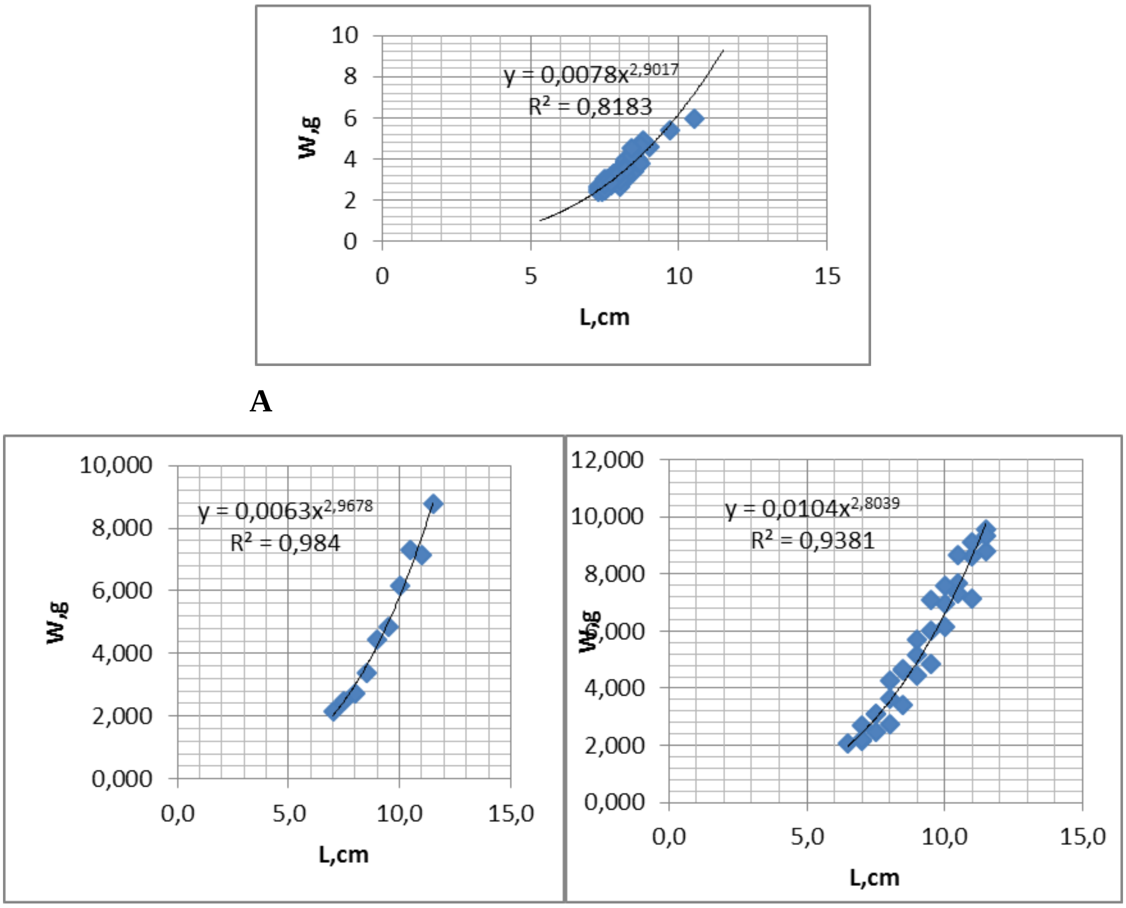

A

B C

Fig. 11.1. Relationship between linear size and weight of sprat: A- 2017, B- 2018, C - 2019

The size-weight relationship for the period 2017-2019 showed a similarity in the growth of sprat. In the three years, the sprat increased allometrically (negative n = 2.80-2.96, with a high coefficient of determination (R2 = 0.82 - 0.98) (Fig. 11.01).

The size structure of sprat is shown on Fig.11.2. In 2017, the minimum size group was 7.0 cm and the maximum 10.5 cm, the predominance was observed in the 9.0 cm size group, and peaks were also reported in the 8.0-8.5cm groups. The other groups were in a subordinate position. In the 2018 surveys, the minimum was 6.5 cm, the maximum was 11.5 cm, the minimum and maximum were shifted to the right (L = 9.0 - 9.5 cm). In 2019, high percentages were observed in size groups 7.0-7.5 -8.0 cm. The minimum size group was 5.5 cm and the maximum was 11.5 cm.

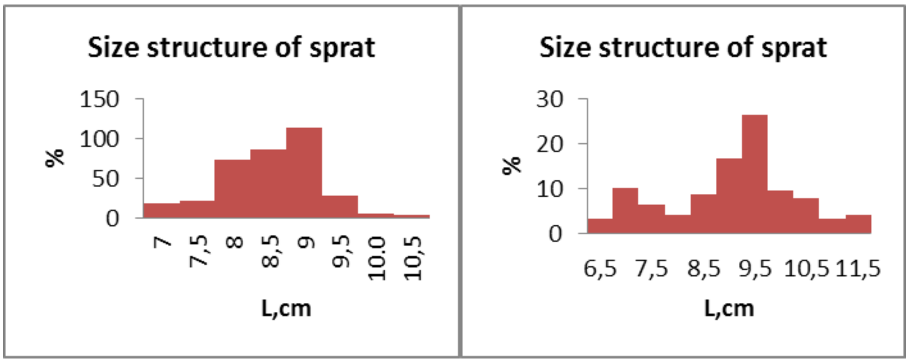

2017 2018

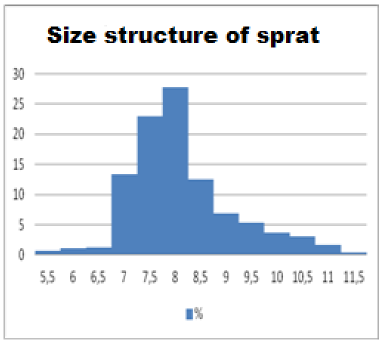

2019

Fig. 11.2. Size distribution of sprat 2017-2019

The somatic growth of horse mackerel from the first study in 2018 indicated that the average weight corresponding to the oldest age group was 39 g. The value corresponded to the size limit of the size class 16.8 cm observed in the samples of the trawl survey in the Bulgarian waters (Fig.11.3.).

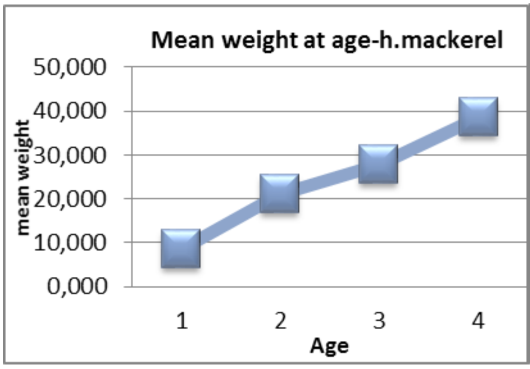

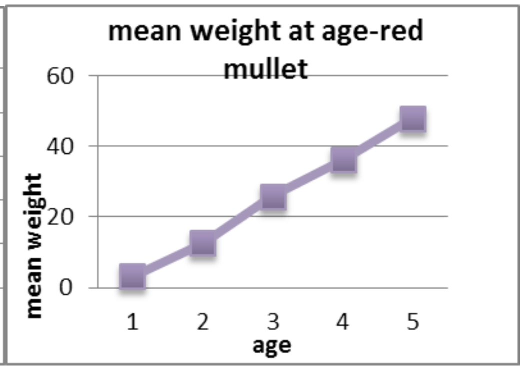

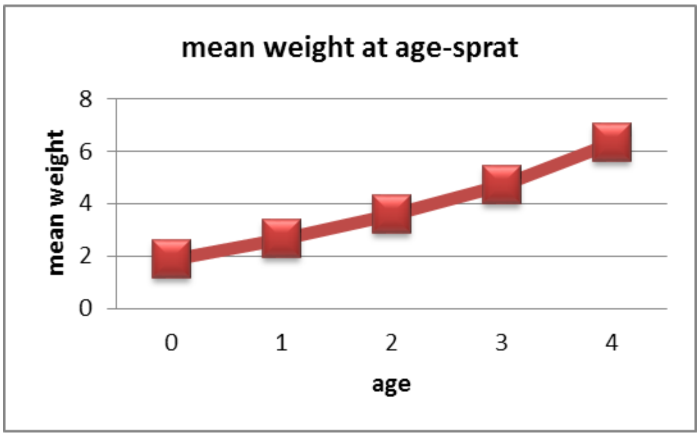

Fig. 11.3. Weight distribution of sprat 2017-2019

11.1. Size structure of sprat, whiting and red mullet in 2019

Frequency and average weights from different stations

The gap had a bimodal increase, with two peaks in the first 2019 survey (8-9.5cm; 11-12.5cm). In the second 2019 survey, we again observed bimodal distribution, with a slight shift to the right and a decrease in the percentage of 8.5-9.0 cm size groups. The size groups 13.5-17.5 cm were represented by a small percentage in 2019. Bimodal size distribution was again observed, with predominant size groups 11.0 - 12.0cm, followed by a decline to 12.5 - 13.0 cm and a sharp increase in the 13.5 cm group, with the highest catch in 2019. The other size groups had little presence in the catch.

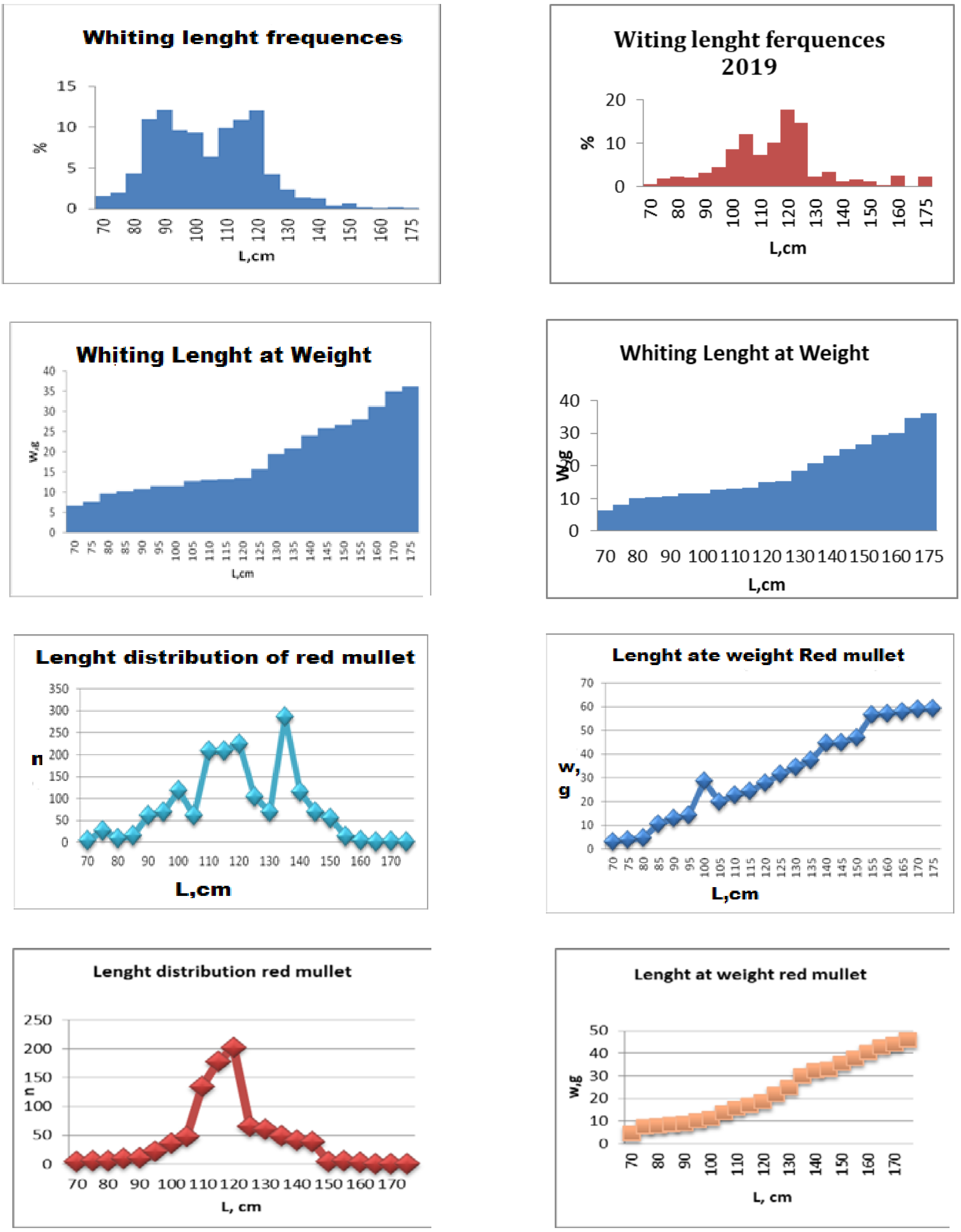

Fig. 11.1.1. Linear frequencies and mean weights in the sizes of whiting and red mullet

The red mullet during the autumn-winter period of 2019 showed one-modal size distribution (12.0cm), with all other size groups present with low catch numbers.

11.2. Survey December 2018

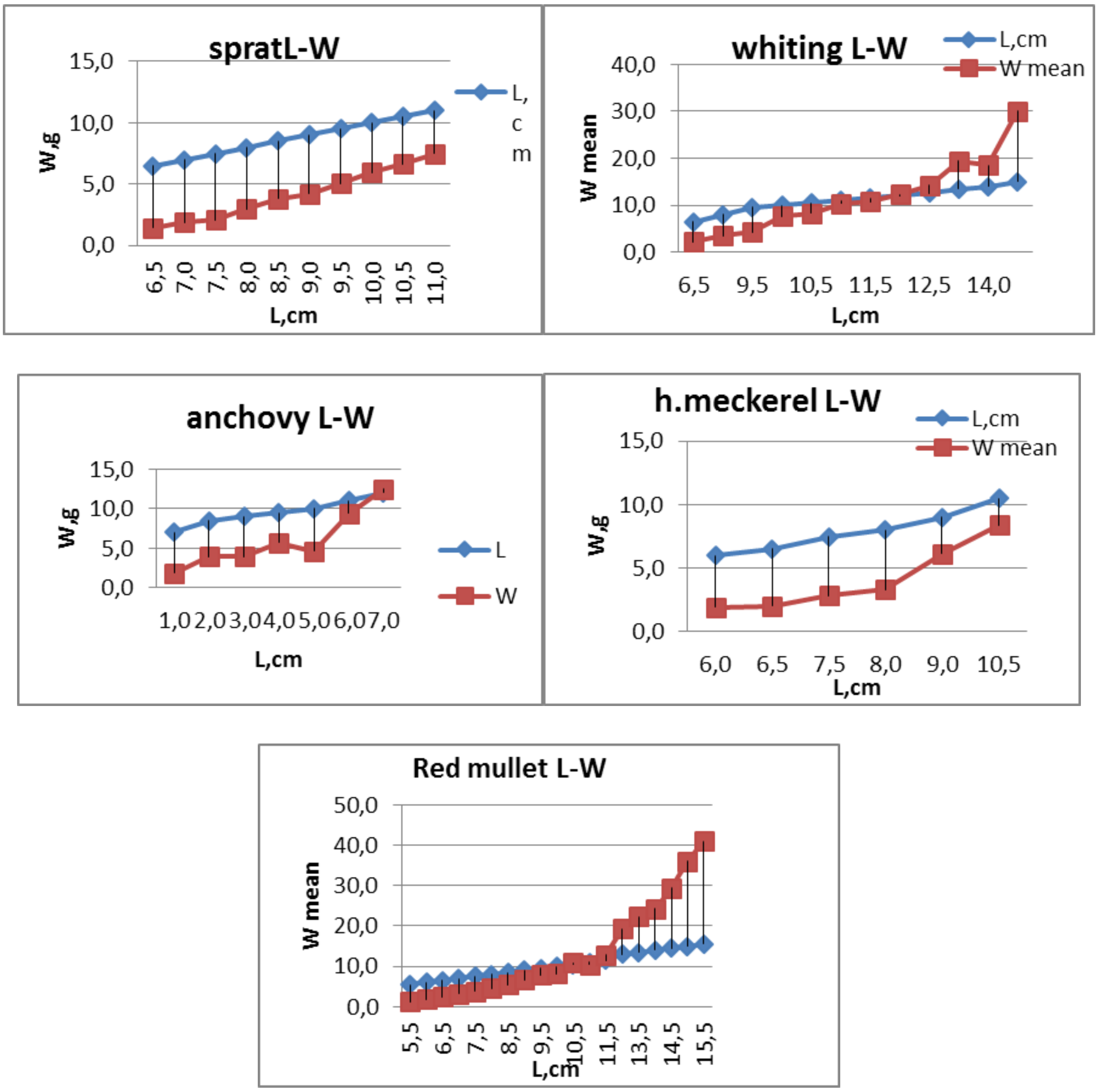

Fig. 11.1.2. Linear weight distribution of sprat, whiting, anchovy, horse mackrel and red mullet

Project proposal № BG14MFOP001-3.003-0001 "Collection, management and use of data for the purposes of scientific analysis and implementation of the Common Fisheries Policy for the period 2017-2019", funded by the Maritime Affairs and Fisheries Program, co-financed by the European Union through the European Maritime and Fisheries Fund

12. Age - 2017

The predominant age of sprat in 2017 surveys was 2-2 + (36%), followed by 1-1 + d (32%). Completion was represented by 3%. For horse mackerel, the age structure ranged from 0 to 4 + g with a prevalence of 40% being reported for 4-4 + g individuals, 30% for 3-3 +, 20% and 10% for 2- 2+ and 1-1 + y. The distribution of red mullet was similar, the difference with horse mackerel was that the recruitment was presented with a minimum percentage of 0.8%. The older age groups of whitings had a high percentage (33%, 6 y^{-1}; 27% - 5 y^{-1}; 20% -4 y^{-1}). One-year old specimens were 10% in the catches.

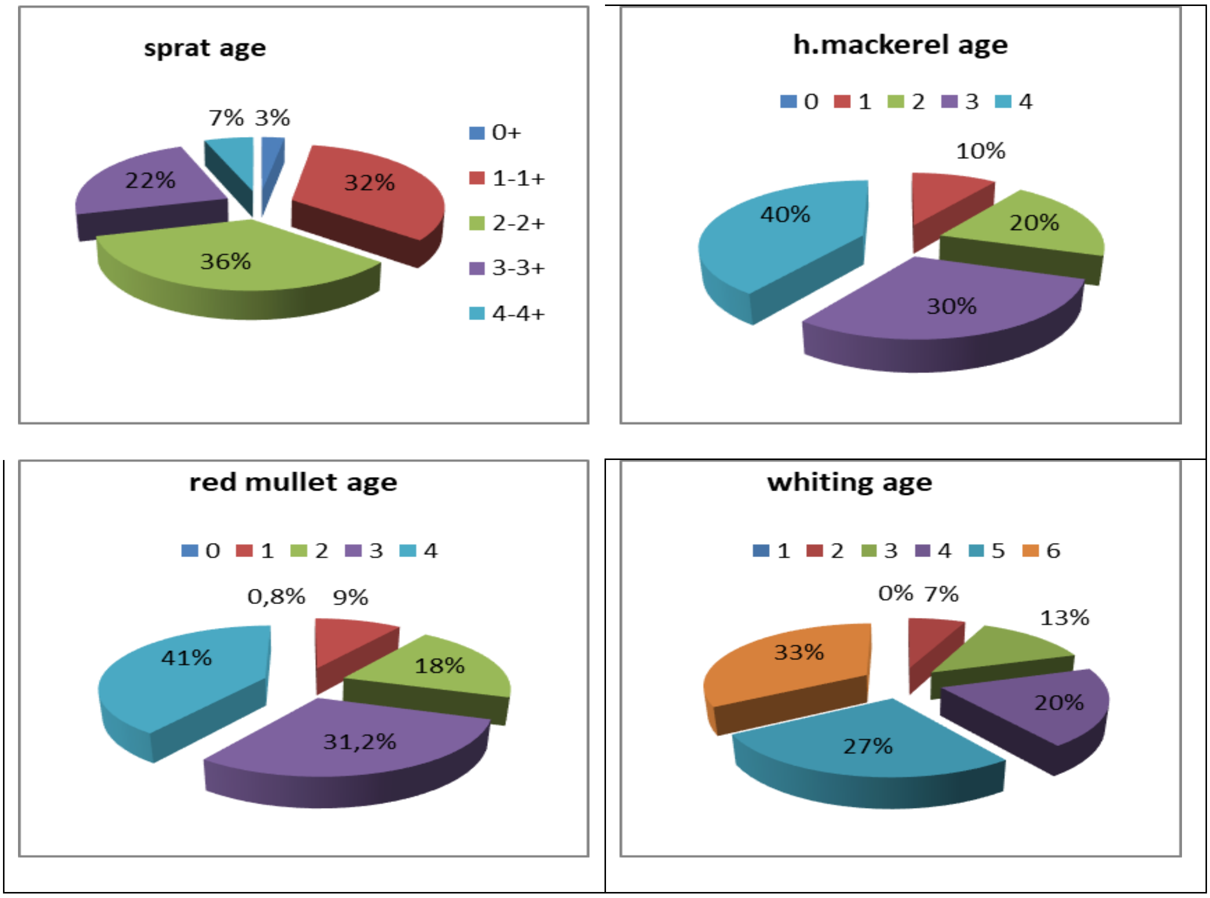

Fig. 12.1. Age of sprat, horse mackerel, red mullet and whiting in 2017

12.1. Age - 2018 (October-November)

The predominant age for horse mackerel was 2-2 + (63%), followed by ages 1-1 + (22%), 3-3 + (12%), 4-4 + (3%).

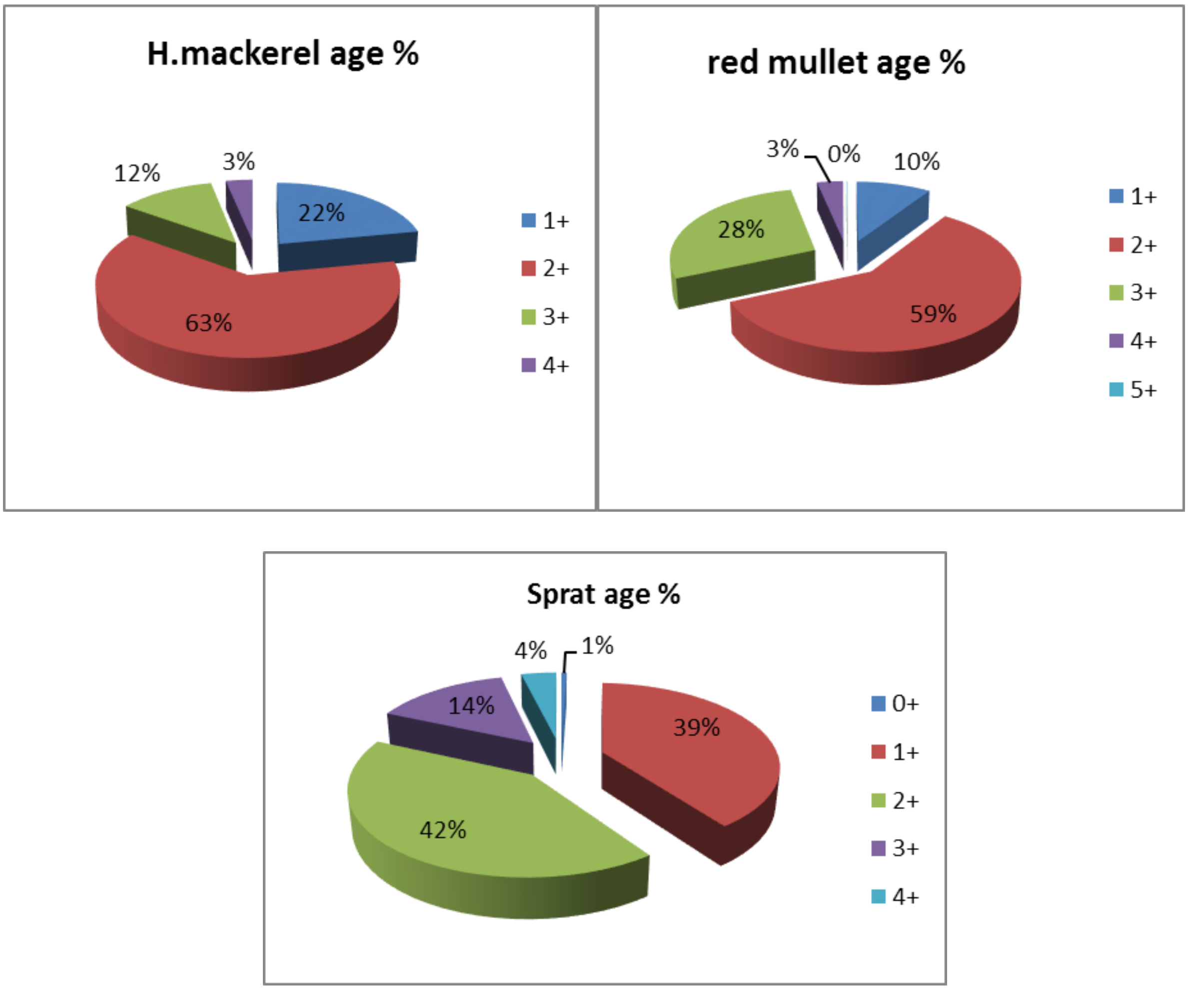

Fig. 12.1.1. Age structure of horse mackerel, red mullet and sprat in 2018

The predominant age of the red mullet was 2-2 + (59%), followed by age 1-1 + (28%), 3-3 + (10%), 4-4 + (3%), 5-5 + (0.5 The predominant age for sprat was 1-1 + (42%), followed by 1-1 + (39%).

12.2. Age - 2018 (December)

The age structure was determined on the basis of a direct reading of the binocular reflectors of the reflected light. The analysis showed that the percentage of two-year-olds was the highest in the present study (Fig.4.5.1.A, B.), with 1-1 + and 3-3 + g being equally present in the catches. For horse mackerel, 2-2 + g specimens prevailed by 63%, followed by 1-1 + g with almost 3 times fewer individuals.

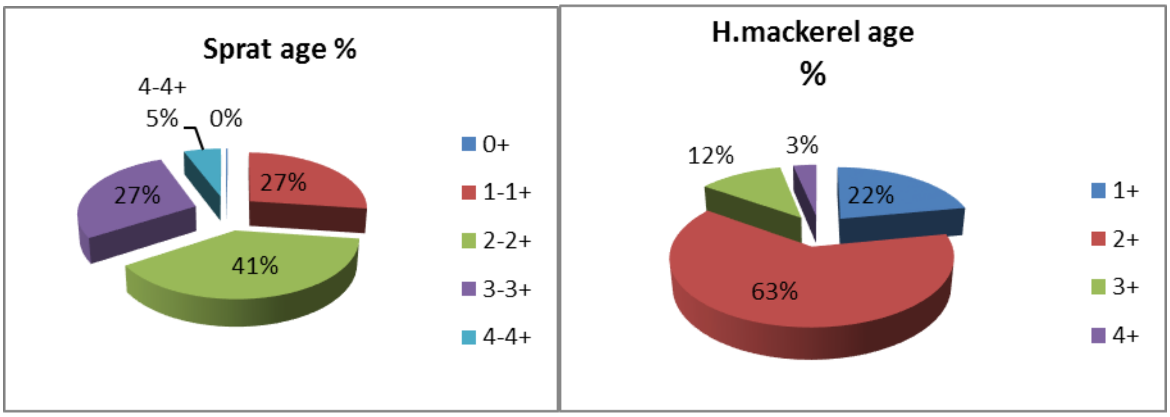

Fig. 12.2.1. Age distribution of sprat and horse mackerel in December 2018

2-2 + g of the red mullet were 59%, 3-3 + with 28%. The medium had 27% presence of 4-4 + g 20% - 3-3 + g.

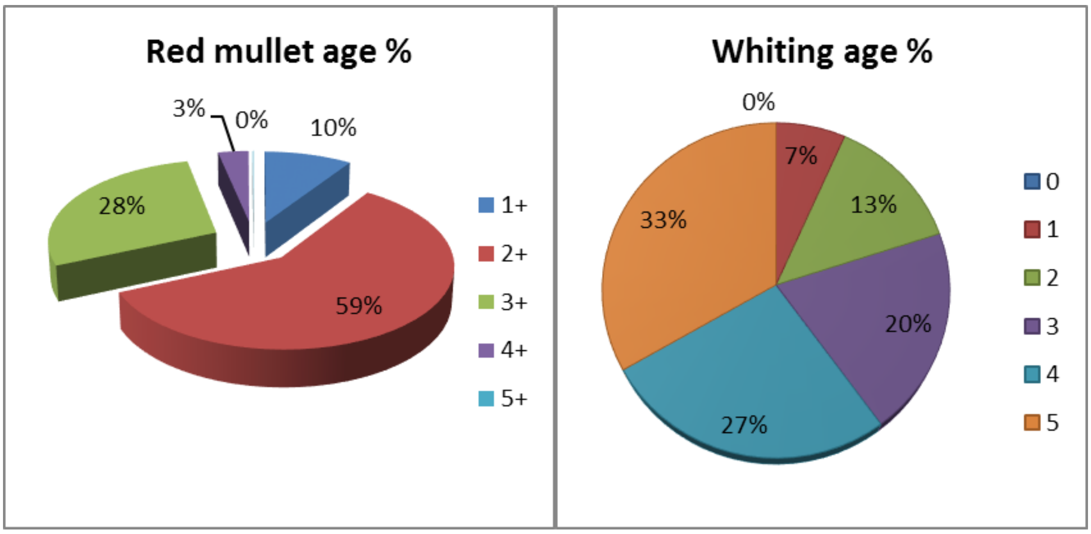

Fig. 12.2.2. Age distribution of the species in December 2018

12.3. Age - 2019 (June)

The majority of specimens caught belonged to age group 1-1+ (74%).

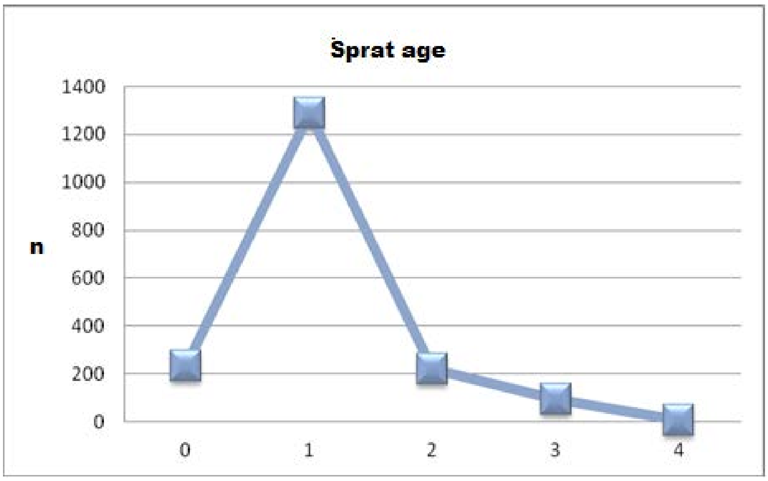

Fig. 12.3.1. Age distribution of sprat, June 2019

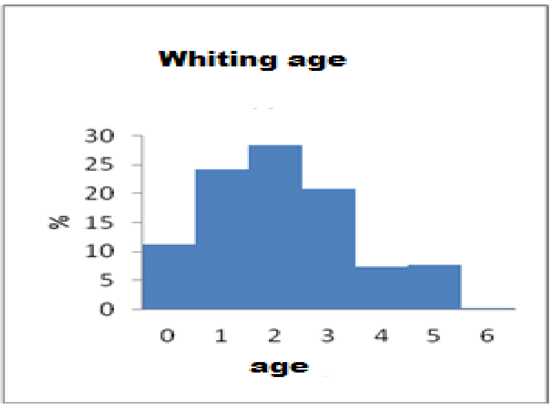

Fig. 12.3.2. Age of whiting from EEZ of Bulgaria

The predominant age of the whiting was 2-2 + (27%), followed by ages 1-1 + (24.7%), 3-3 + (20.5%), Senior age and juvenile forms were present with a low percentage.

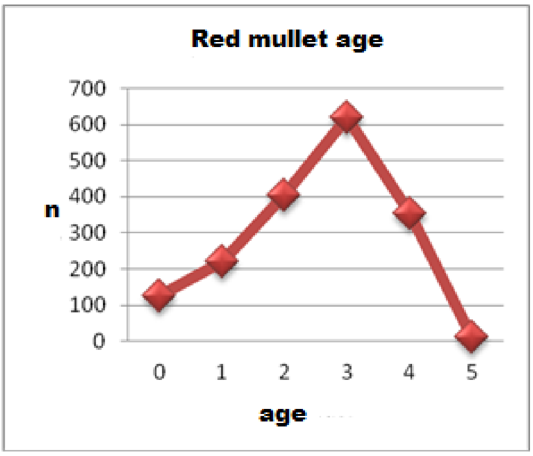

Fig. 12.3.3. Age of the red mullet from the Bulgarian Sea area

12.4. Age - 2019 (December)

The predominant age for sprat in this study was 1-1 + g (78%) (Fig. 3.7.1, Fig. 3.7.2).

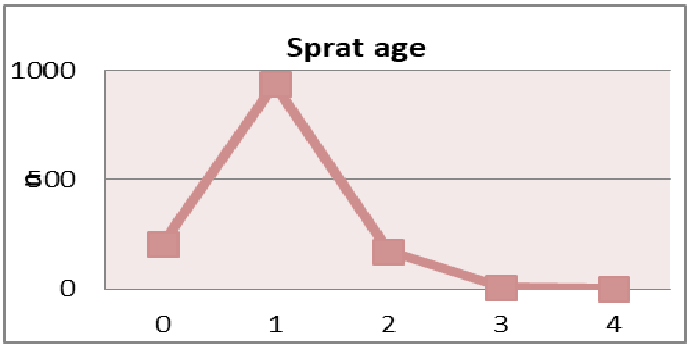

Fig. 12.4.1. Age distribution of sprat

The prevailing age for whiting in this study was 2-2 +, followed by ages 3-3 +. Missing were 0 + y.

Project proposal № BG14MFOP001-3.003-0001 "Collection, management and use of data for the purposes of scientific analysis and implementation of the Common Fisheries Policy for the period 2017-2019", funded by the Maritime Affairs and Fisheries Program, co-financed by the European Union through the European Maritime and Fisheries Fund

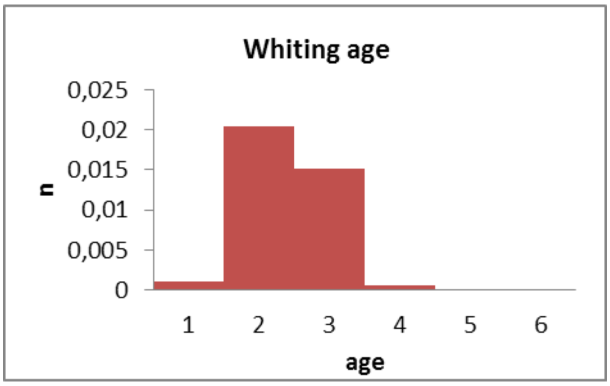

Fig. 12.4.2. Age of whiting from EEZ of Bulgaria

The predominant age of whiting was 2-2 + (46%),, 3-3 + (26.6%), The older age and juvenile forms were present with a low percentage (Fig. 3.7.3).

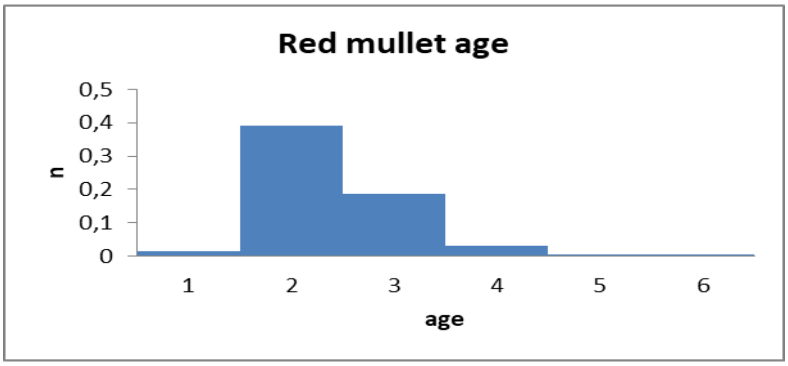

Fig. 12.4.3. Age of the red mullet from the Bulgarian marine area

Project proposal № BG14MFOP001-3.003-0001 "Collection, management and use of data for the purposes of scientific analysis and implementation of the Common Fisheries Policy for the period 2017-2019", funded by the Maritime Affairs and Fisheries Program, co-financed by the European Union through the European Maritime and Fisheries Fund

13. Growth

13.1. Growth - 2017

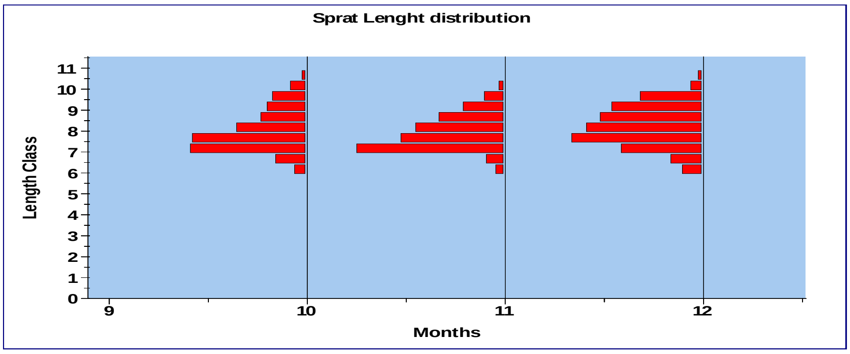

The increase in sprat, modeled after Von Bertalanffy's model (Fig. 13.1), showed an asymptotic length of 12.2 and a high rate of linear-weight growth. The whiting was characterized by a low growth rate, but a relatively high asymptotic length, similar to the red mullet of the current study (Table 13.1).

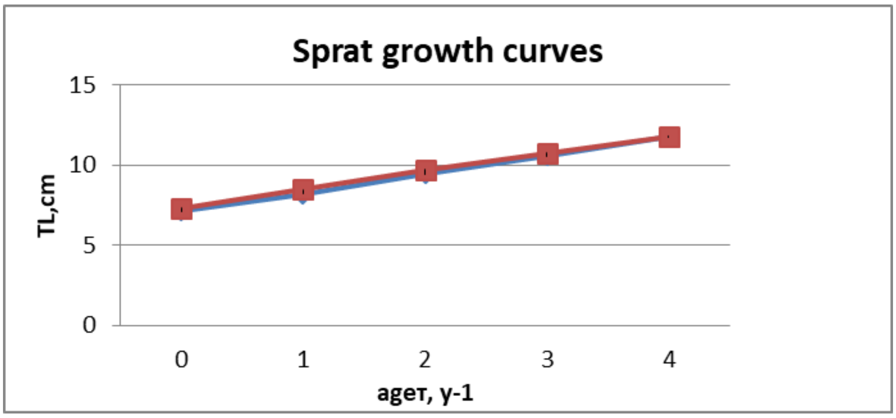

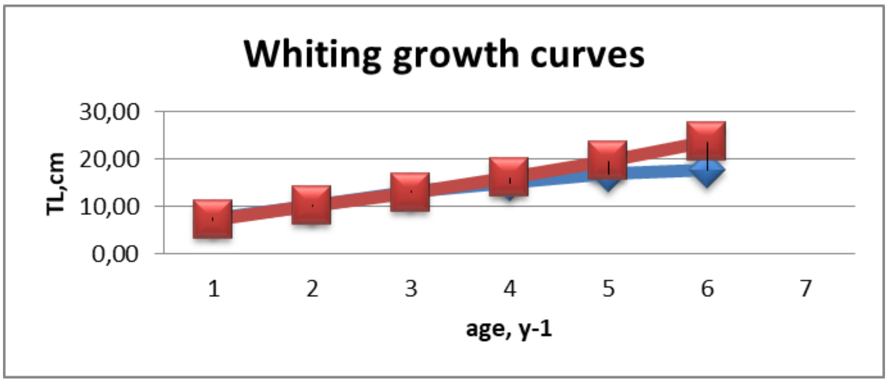

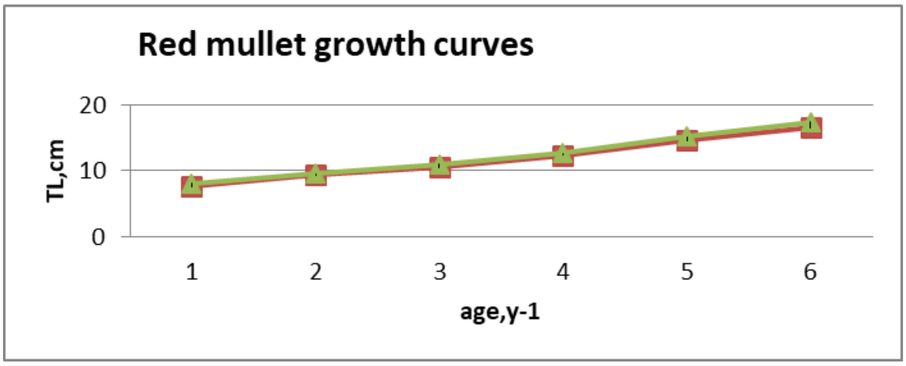

Fig. 13.1. Growth of sprat, whiting and red mullet (VBGF)

Table 13.1. VBGF for sprat, whiting and red mullet

L∞ = 12.2	L∞ = 27,66	L∞ = 19,33
k=0.44	к=0.25	к=0.24
t_0 = -1.115	t_0 = -2.0054	t_0 = -1.2111
q = 0.0008	q = 0.009	q = 0.009
n = 2.87	n = 3.002	n = 3.11

13.1.1. Somatic growth

The average weights of sprat, whiting and red mullet are expected to increase with age (Figs. 13.1.1.1 – 13.1.1.3).

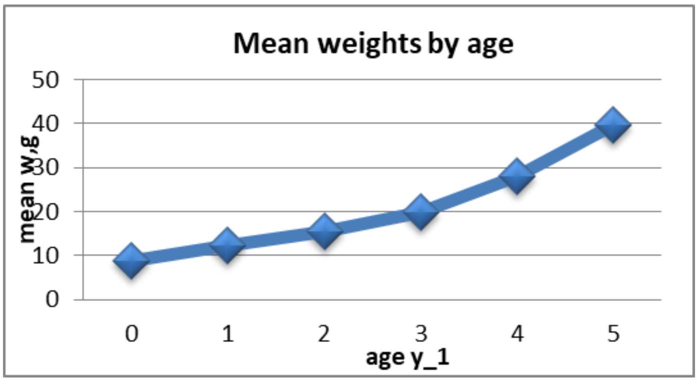

Fig. 13.1.1.1. Somatic growth of sprat

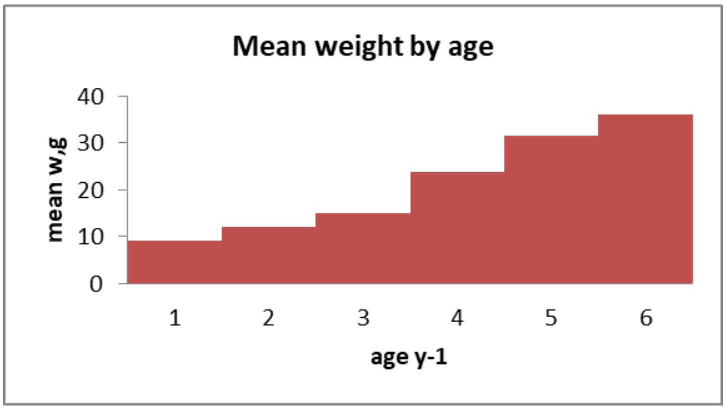

Fig. 13.1.1.2. Somatic growth of whiting

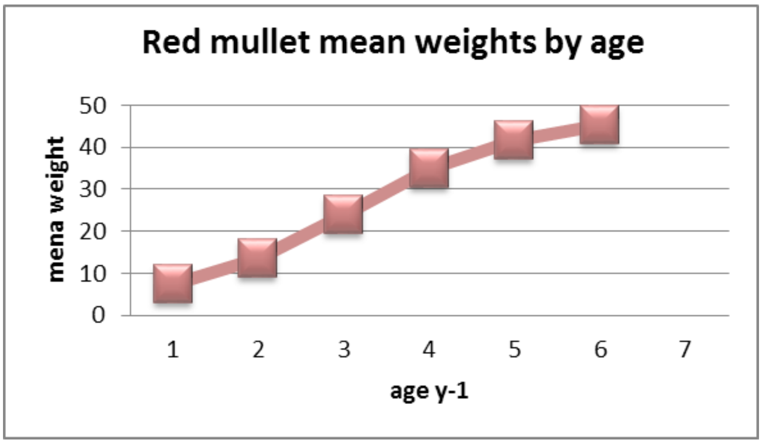

Fig. 13.1.1.3. Somatic growth of the red mullet

Project proposal № BG14MFOP001-3.003-0001 "Collection, management and use of data for the purposes of scientific analysis and implementation of the Common Fisheries Policy for the period 2017-2019", funded by the Maritime Affairs and Fisheries Program, co-financed by the European Union through the European Maritime and Fisheries Fund

To calculate the growth rate and growth parameters from the Bulgarian area, we used the Von Bertalanffy equation (VBGF). The estimation of asymptotic length, growth rate and related coefficients is presented on Table 13.1.1.1.

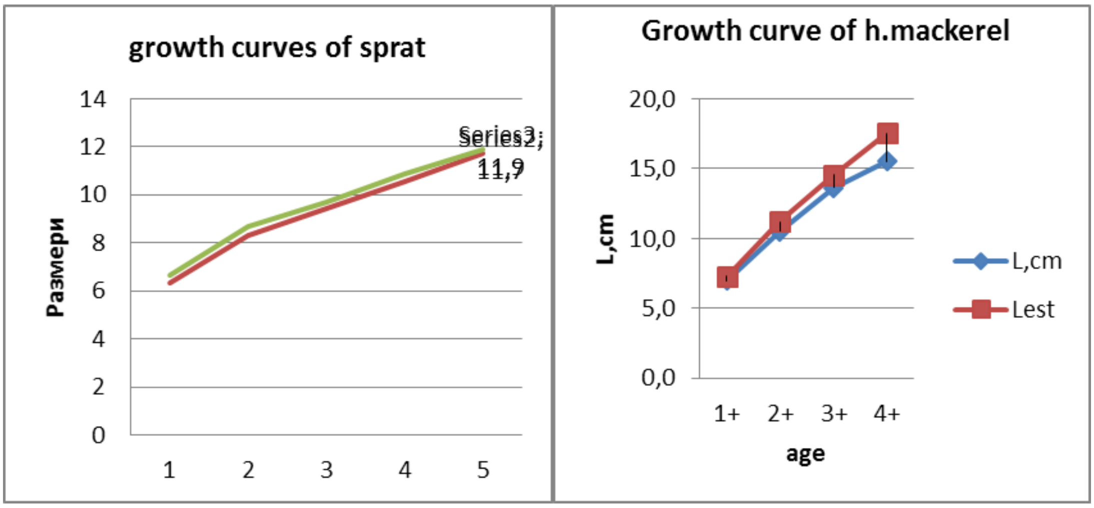

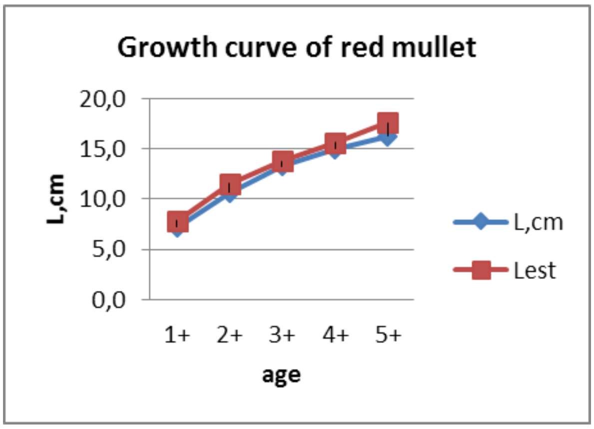

Fig. 13.1.1.4. L asymptotine for sprat, horse mackerel and red mullet

Table 13.1.1.1. Parameters in the VBGF model.

L∞ = 12.34
k=0.45
t_0 = -1.2355
q = 0.009
n = 2.76

Asymptotic length reached 12.34 cm; growth rate could be defined as relatively high 0.45 y^{-1}. The increase in sprat in this study was positive allometric (n = 2.76) (Fig.13.1.1.4). The most important note here is the fact that, due to the lack (or low proportion) of the largest age groups, the asymptotic size function shows a relatively low value. In this regard, the maximum or asymptotic length reaches this value, which may not be fully consistent with the literature data on species size and limiting levels of length and growth rate. Therefore, we can accept the analysis of growth as it is, which reflects in the current situation of absence (low presence) of large individuals.

13.2. Growth 2018 (October – November)

The growth of horse mackerel showed asymptotic values of L∞ = 18.8cm, at a growth rate of k = 0.35. For the red mullet, the maximum theoretical length was 19.24cm, k = 0.24. For sprat, the value of L∞ was 11.98 cm, with a high growth rate k = 0.55.

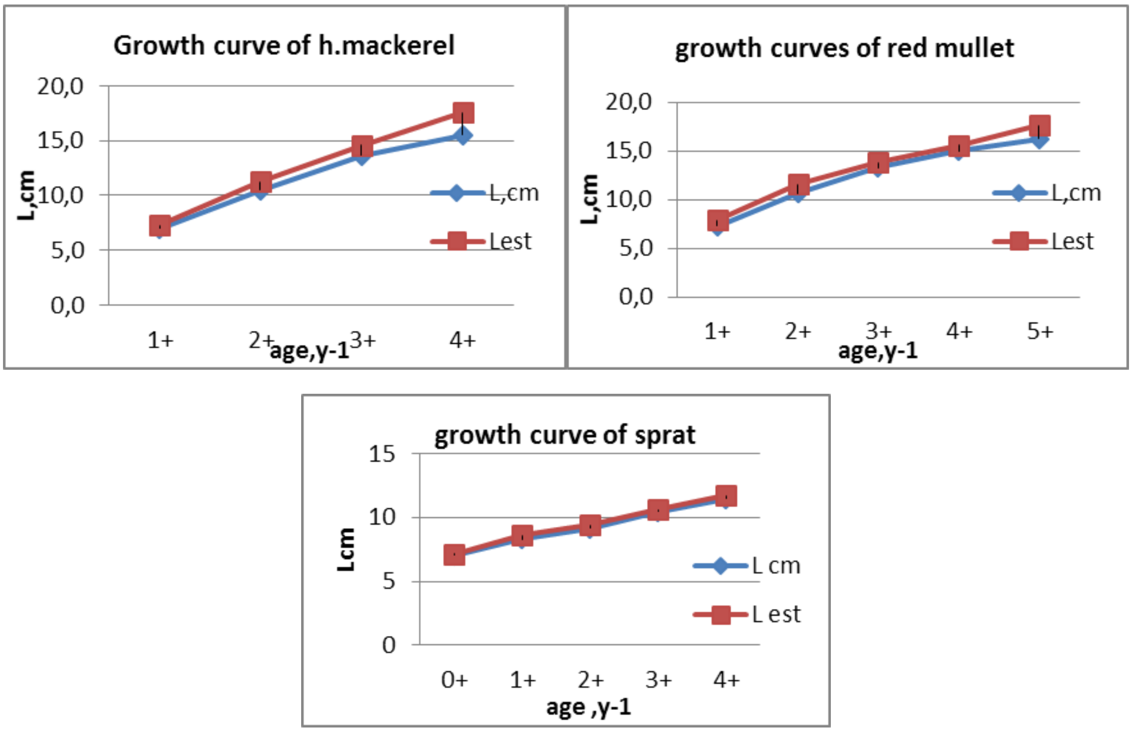

Fig. 13.2.1. Growth of horse mackerel red mullet and sprat (VBGF), 2018 Stage I

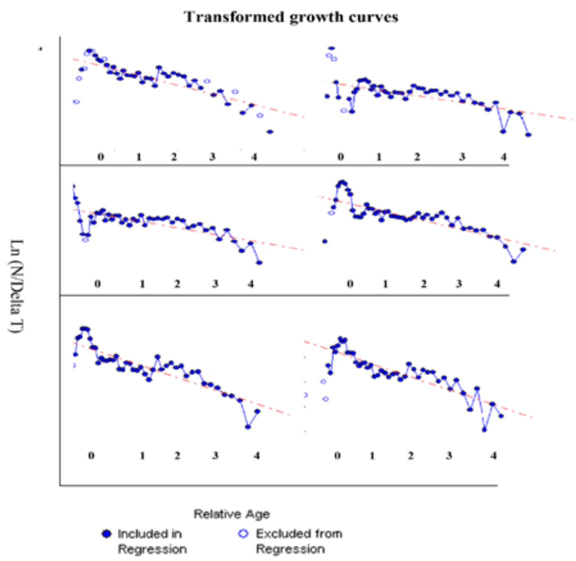

Fig. 13.2.2. Sprat expansion curves from December 2018

The composition of the size of the sprat consisted of the following size classes (TL, cm) from 6.5 cm to 11.5 cm in the samples from the Bulgarian marine area (Fig.13.2.2).

14. Catch numbers

It is obvious that the size classes 7.0 - 8.5 cm were dominant, the larger ones being represented by a low percentage. In October-November the size class 7.0 was very high, followed by L = 8.0 cm and 8.5 cm. The situation with the lack (or low share) of larger (oldest) individuals was the same in the period 2007-2015 (Raykov et al., 2007, 2008, 2009, 2010) (Fig14.1, Fig. 14.2).

The predominant size class in October-November was 12.5 cm, followed by L = 9 cm. In December, the lowest share of all classes was observed, with 11.5 cm prevailing.

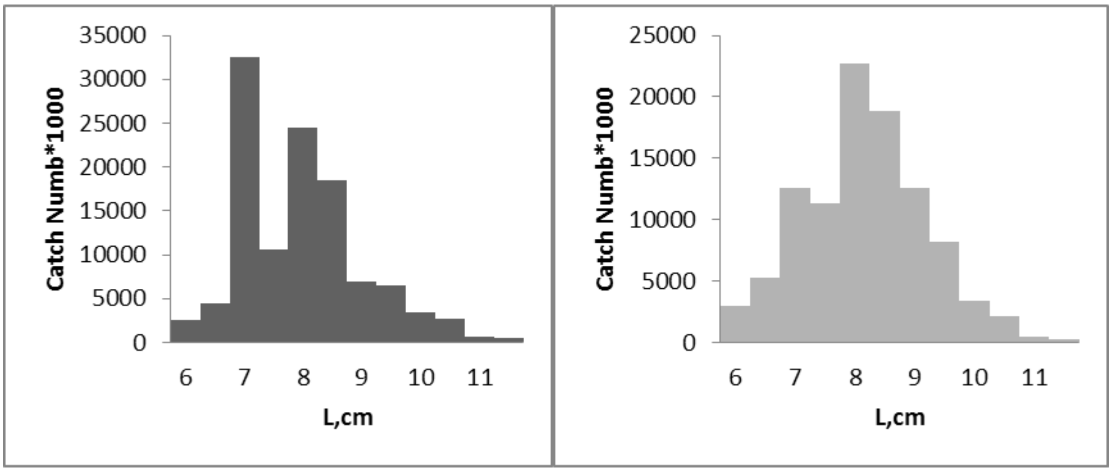

A Б

Fig. 14.1. Catch in numbers and size classes of sprat. A. October-November, B. November-December

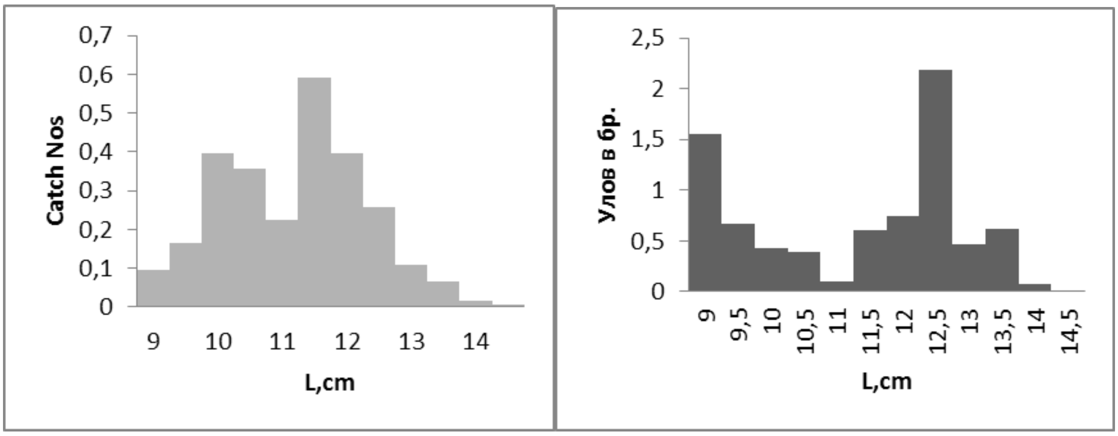

A B

Fig. 14.2. Catch in the numbers and size classes of the red mullet. A. October-November, B. November-December

Project proposal № BG14MFOP001-3.003-0001 "Collection, management and use of data for the purposes of scientific analysis and implementation of the Common Fisheries Policy for the period 2017-2019", funded by the Maritime Affairs and Fisheries Program, co-financed by the European Union through the European Maritime and Fisheries Fund

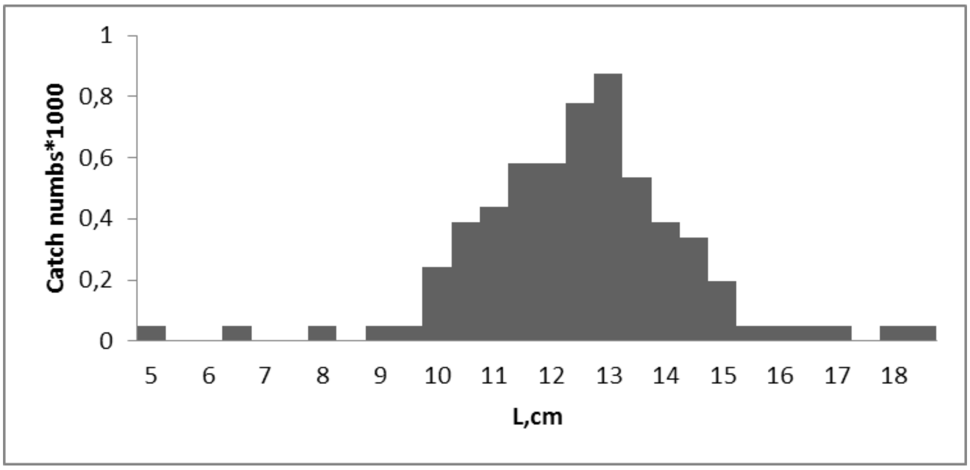

Fig. 14.3. Catch in numbers and size classes of whiting. A. November-December

In August, the proportion of 12.5 cm and 13 cm was the highest, despite the presence of all size classes.

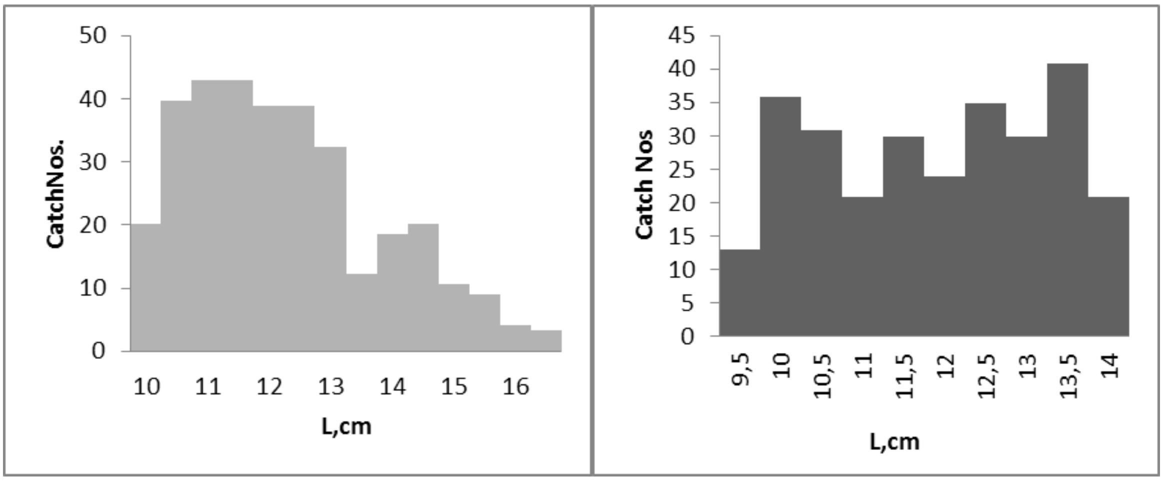

Fig. 14.4. Catch in numbers and size classes of horse mackerel. A. October-November, B. November-December

Project proposal № BG14MFOP001-3.003-0001 "Collection, management and use of data for the purposes of scientific analysis and implementation of the Common Fisheries Policy for the period 2017-2019", funded by the Maritime Affairs and Fisheries Program, co-financed by the European Union through the European Maritime and Fisheries Fund

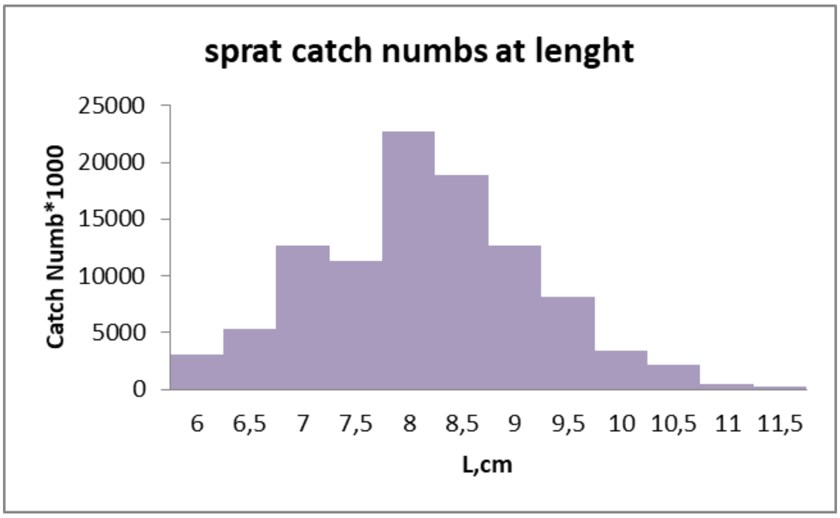

Fig. 14.5. Abundance by size classes of the size of the sprat from the Bulgarian marine area

It is obvious that the size classes 8 - 8.5 cm were dominant, with the larger classes represented by a low percentage. In December, size class 8 was very high, followed by L = 7.0,8.5 and 9 cm. The situation with missing (or low share) of larger (oldest) individuals was the same in the 2007-2018 period (Raykov et al., 2018).

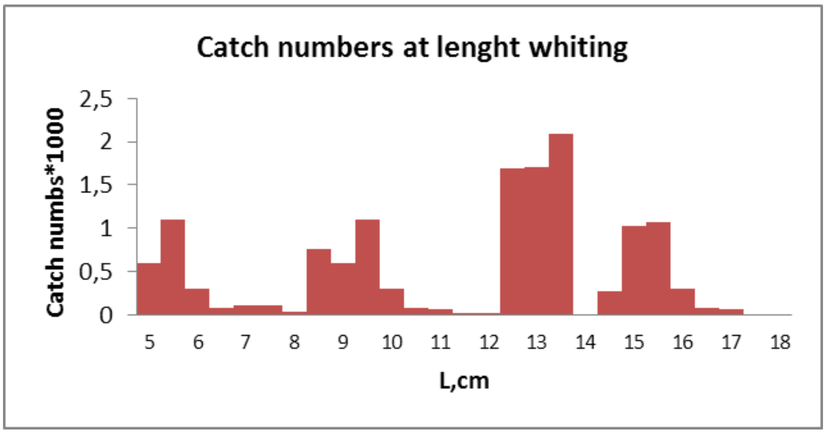

Fig. 14.6. Share of groups by size of whiting in the Bulgarian marine area

In December, the share of 12.5 cm and 13 cm was the highest, despite the presence of all size classes. Later in December, the share of all size classes increased, with 12.5, 13 and 13.5 classes increasing two times and more. The largest 15 cm and 15.5 cm classes increased significantly in December 2018.

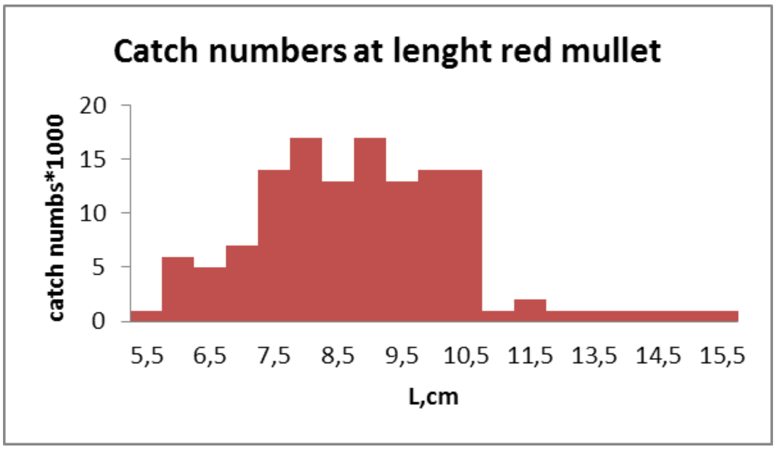

Fig. 14.7. Proportion of largemouth bass groups from the Bulgarian marine area

The composition of the size of the sprat consisted of the following size classes (TL, cm) from 6.5 cm to 11.5 cm in the samples from the Bulgarian marine area.

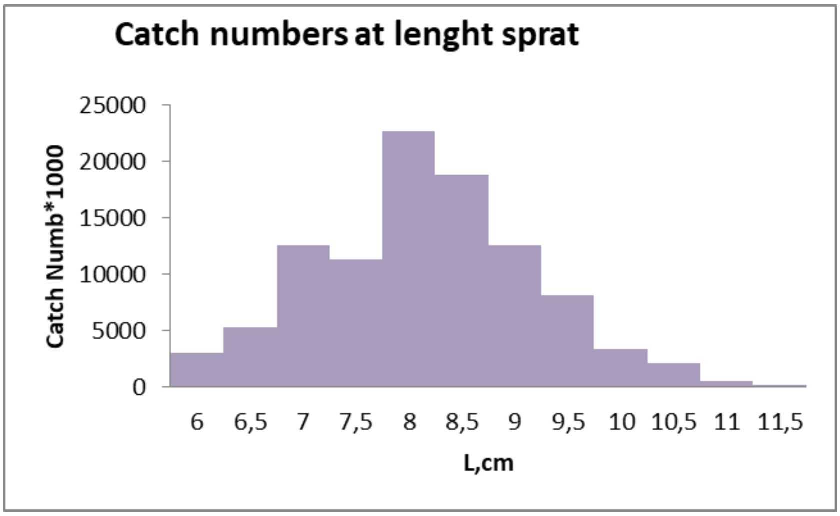

Fig. 14.8. Abundance by size classes of sprat from the Bulgarian marine area

It is obvious that the size classes 8 - 8.5 cm were dominant, with the larger classes represented by a low percentage. In December, size class 8 was very high, followed by L = 7.0,8.5 and 9 cm. The situation with the lack (or low share) of larger (oldest) individuals was the same in the period 2007-2018 (Raykov et al., 2018).

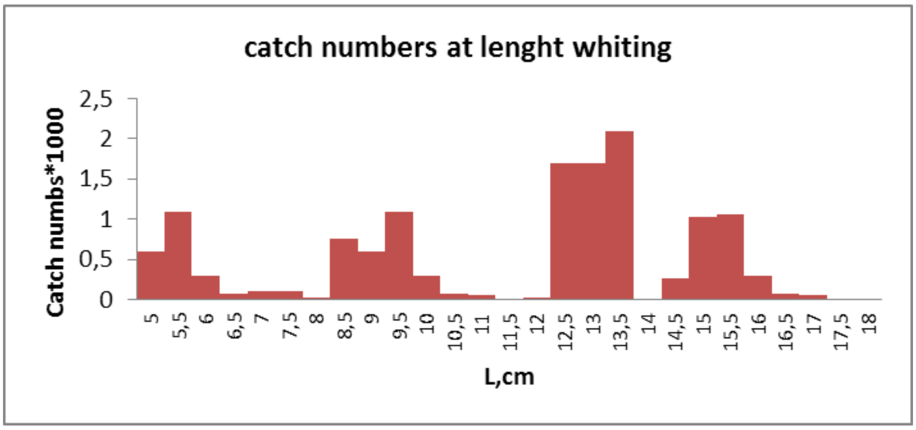

Fig. 14.9. Share of groups by size of whiting in the Bulgarian marine area

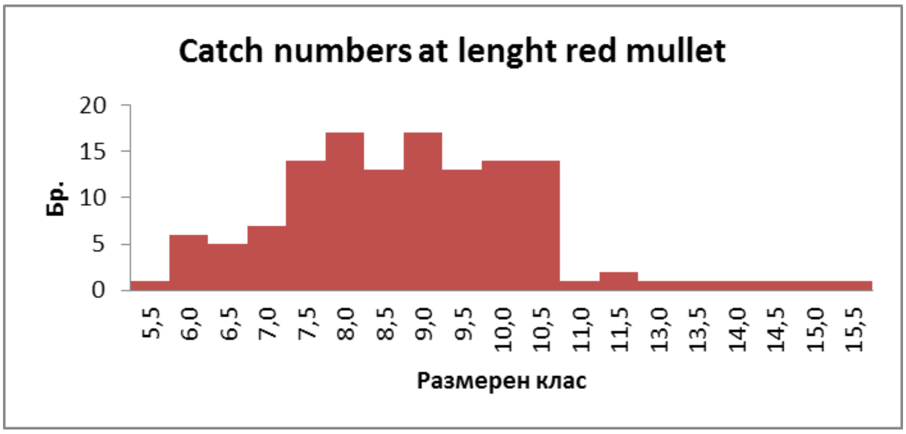

Fig. 14.10. Proportion of largemouth bass groups from the Bulgarian marine area

15. Growth 2018 (December)

To calculate the growth rate and growth parameters from the Bulgarian area, we used the Von Bertalanffy equation (VBGF). The estimated asymptotic length, growth rate and related coefficients are presented in Table 15.1.

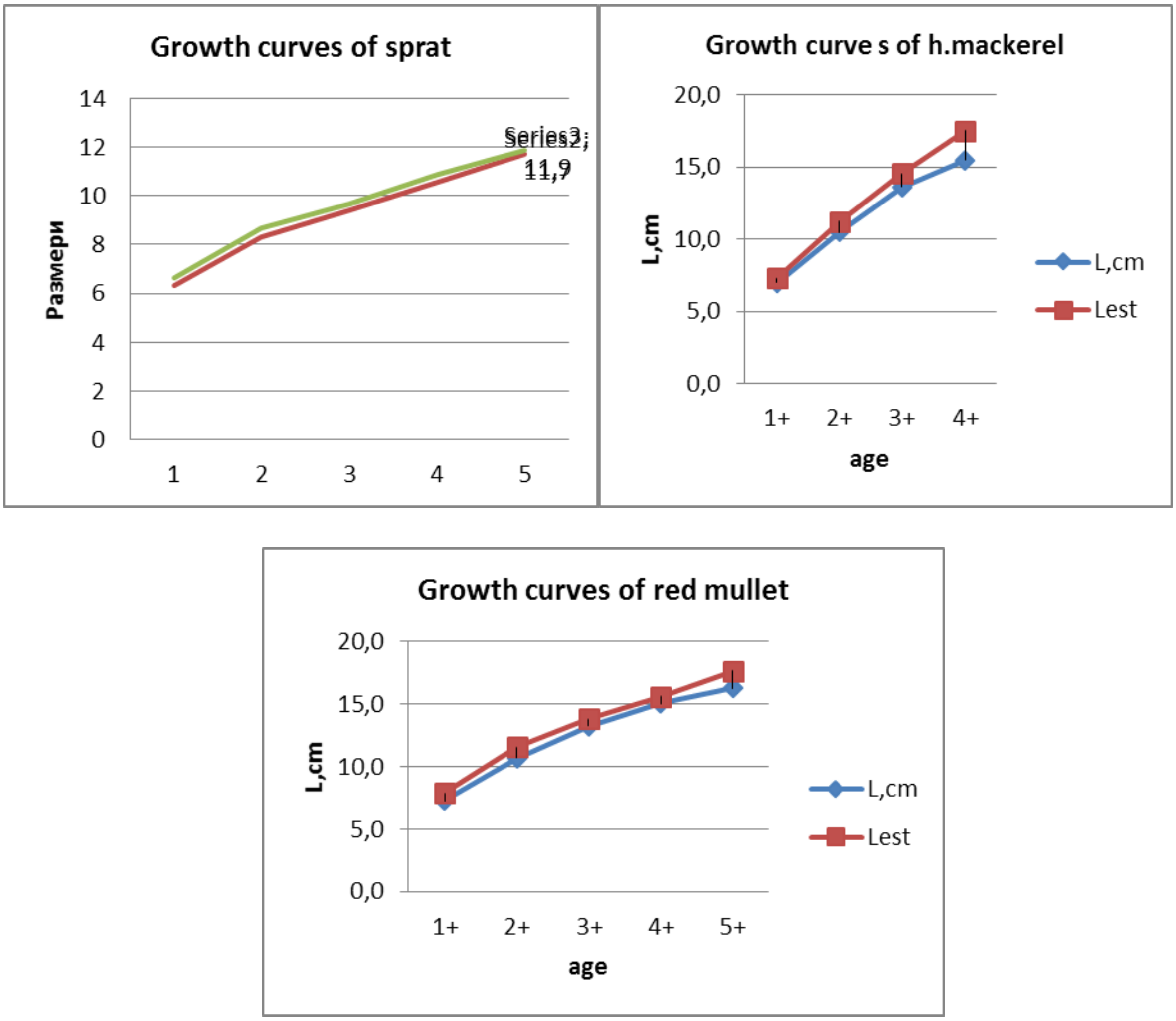

Fig. 15.1. L asymptotic for sprat, horse mackerel and red mullet

Table 15.1. Parameters in the VBGF equation

L∞ = 12.34
k=0.45
t_0 = -1.2355
q = 0.009
n = 2.76

Asymptotic length reached 12.34 cm; growth rate could be defined as relatively high 0.45 y^{-1}. The increase in sprat in this study was positive allometric (n = 2.76) (Fig.15.0.1).

The most important note here is the fact that, due to the lack (or low proportion) of the largest age groups, the asymptotic size function showed a relatively low value.

In this regard, the maximum or asymptotic length reaches this value, which is probably not completely consistent with the literature data on the size of the species and the limiting levels of length and growth rate. Therefore, we can accept the analysis of growth, so as it is, which reflects in the current situation of absence (low presence) of large individuals.

Somatic growth

The somatic growth of sprat from the present studies showed that the average weight, corresponding to the oldest age group, was 8.05 g. The value corresponded to the limit size of the dimension class 11.75 cm, observed in samples from the study of trawls in the Bulgarian waters (Fig.15.2.).

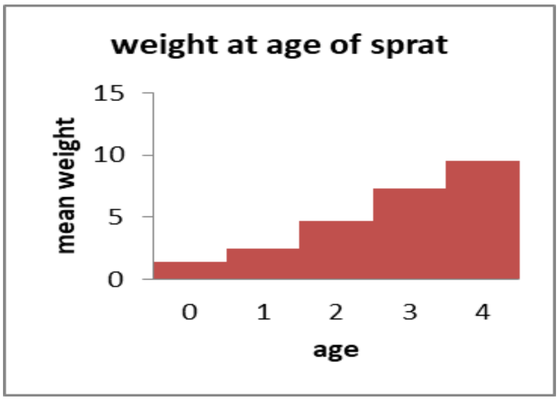

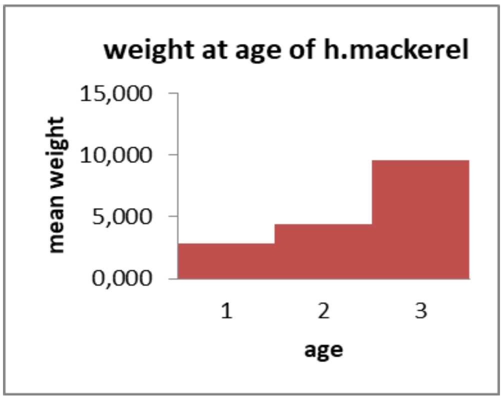

Project proposal № BG14MFOP001-3.003-0001 "Collection, management and use of data for the purposes of scientific analysis and implementation of the Common Fisheries Policy for the period 2017-2019", funded by the Maritime Affairs and Fisheries Program, co-financed by the European Union through the European Maritime and Fisheries Fund

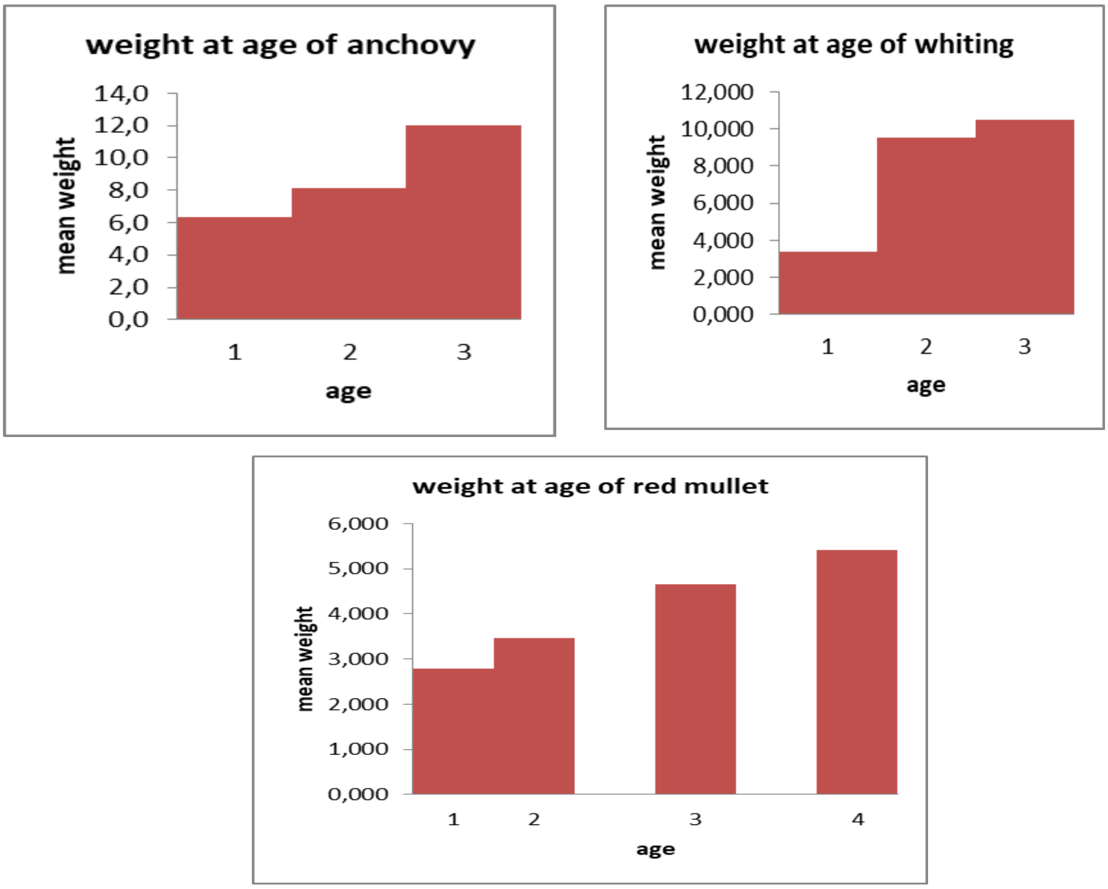

Fig. 15.2. Somatic growth of red mullet

The asymptotic weight reached 11.41 g. The weight was estimated to be relatively stable and high 0.44. This could be related to the fact that in December, the gonads had a high degree of maturity.

16. Growth 2019 (June)

To calculate the growth rate and growth parameters of the Bulgarian region, we used the Von Bertalanfi equation, VBGF. The estimated asymptotic length, growth rate and related coefficients are presented in Table 16.1.

Table.16.1. Growth parameters of sprat

L∞ = 12.03
k=0.45
t_0 = -2.0003
q = 0.009
n = 2.77

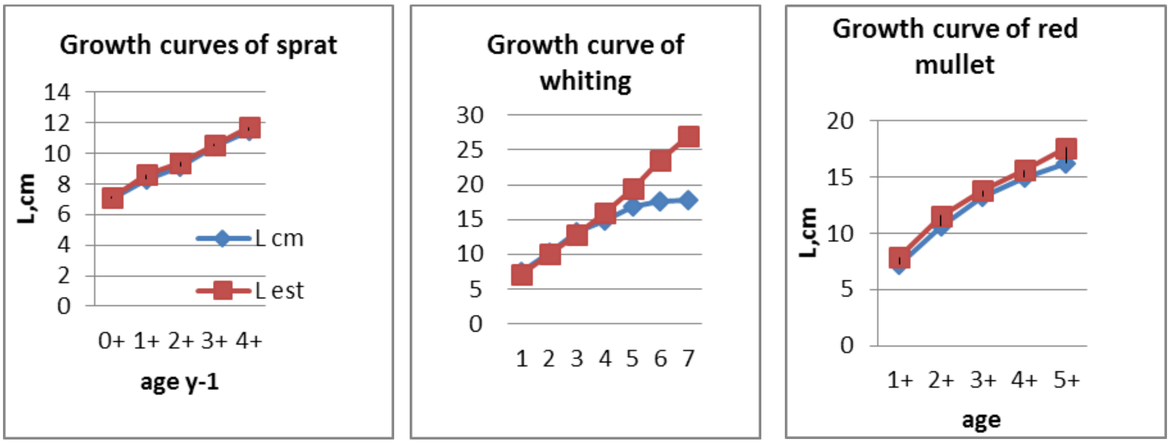

Fig. 16.1. Asymptotic length of sprat, whiting and red mullet, 2019 first stage

The asymptotic length was12.03 cm; the growth rate could be defined as relatively high 0.45 y^{-1}. The phlegm growth in this study was positive allometric (n = 2.77) (Fig.4.7.1) the most important note here was that, due to the lack (or low proportion) of the oldest large age groups, the asymptomatic size function showed a relatively low value. In this regard, the maximum or asymptotic length reaches this value, which is probably not fully compatible with the literature on species size and limiting length and growth rates. Therefore, we can accept the analysis of growth, so as it is, which reflects in the current situation of absence (low presence) of large individuals.

Somatic growth

The somatic growth of sprat from the present studies showed that the average weight, corresponding to the oldest age group, was 8.05 g. The value corresponded to the limit of 11.75 cm, measured in samples from the trawl surveys in the Bulgarian waters (Fig.16.2).

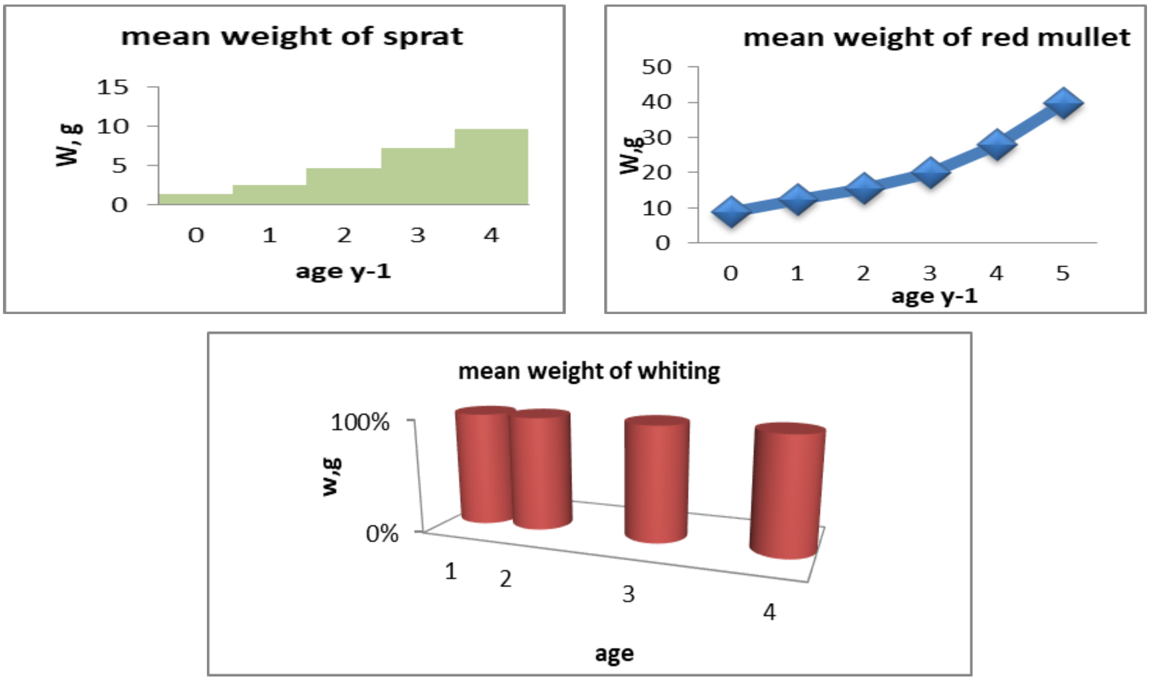

Fig.16.2. Asymptotic weight of sprat, red mullet and whiting, June 2019

17. Growth 2019 (October – November)

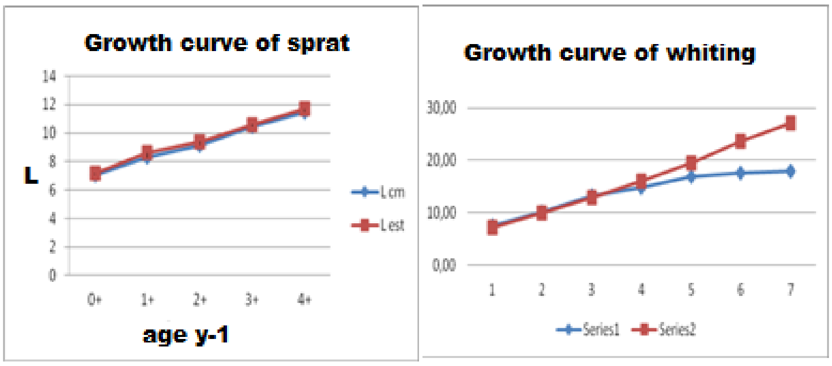

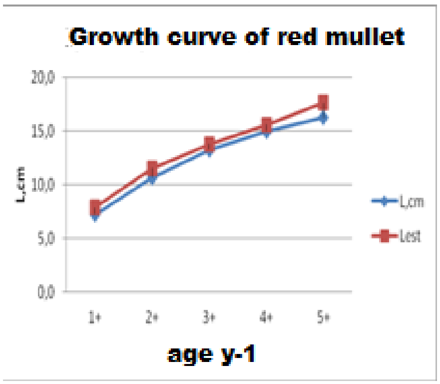

Fig. 17.1. Growth of sprat, whiting and red mullet (VBGF)

Somatic growth

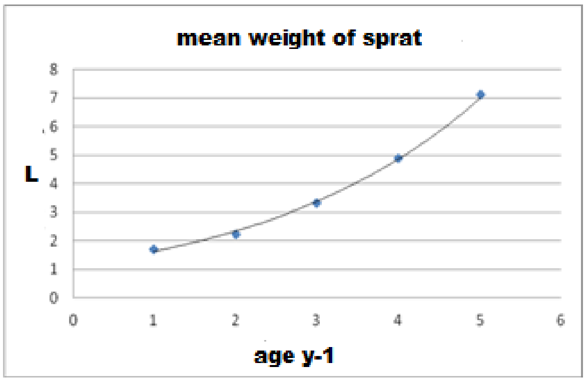

Fig. 17.2. Somatic growth of sprat

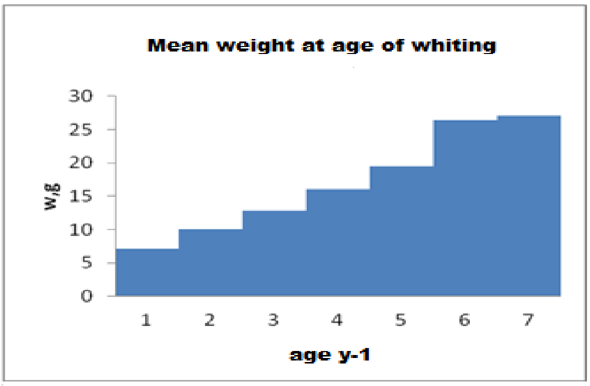

Fig.17.3. Somatic growth of whiting

Project proposal № BG14MFOP001-3.003-0001 "Collection, management and use of data for the purposes of scientific analysis and implementation of the Common Fisheries Policy for the period 2017-2019", funded by the Maritime Affairs and Fisheries Program, co-financed by the European Union through the European Maritime and Fisheries Fund

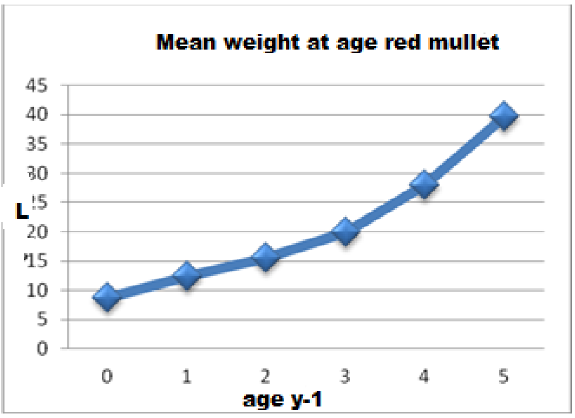

Fig. 17.4. Somatic growth of red mullet

The asymptotic weight reached 49mm. The weight was estimated to be relatively stable and high 0.44.

Physical growth

The somatic growth of sprat from the present studies showed that the average weight corresponding to the oldest age group was 8.05 g. The value corresponded to the limit size of the dimension class 11.75 cm, observed in the samples from the study of trawls in the Bulgarian waters (Fig.17.5.).

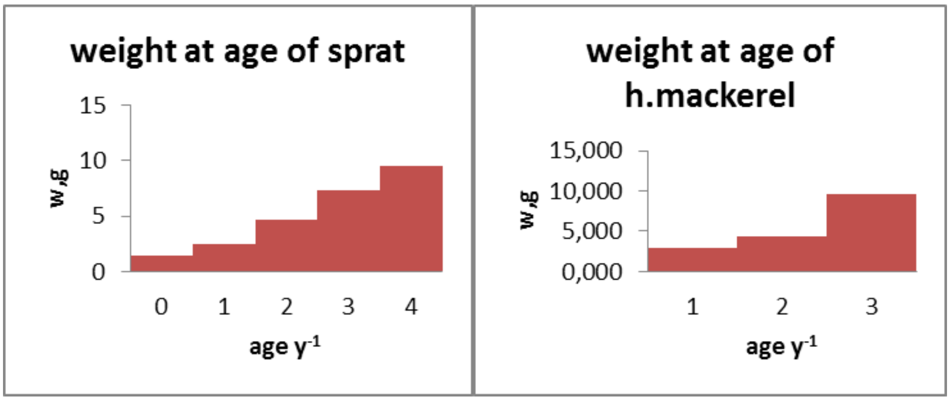

Project proposal № BG14MFOP001-3.003-0001 "Collection, management and use of data for the purposes of scientific analysis and implementation of the Common Fisheries Policy for the period 2017-2019", funded by the Maritime Affairs and Fisheries Program, co-financed by the European Union through the European Maritime and Fisheries Fund

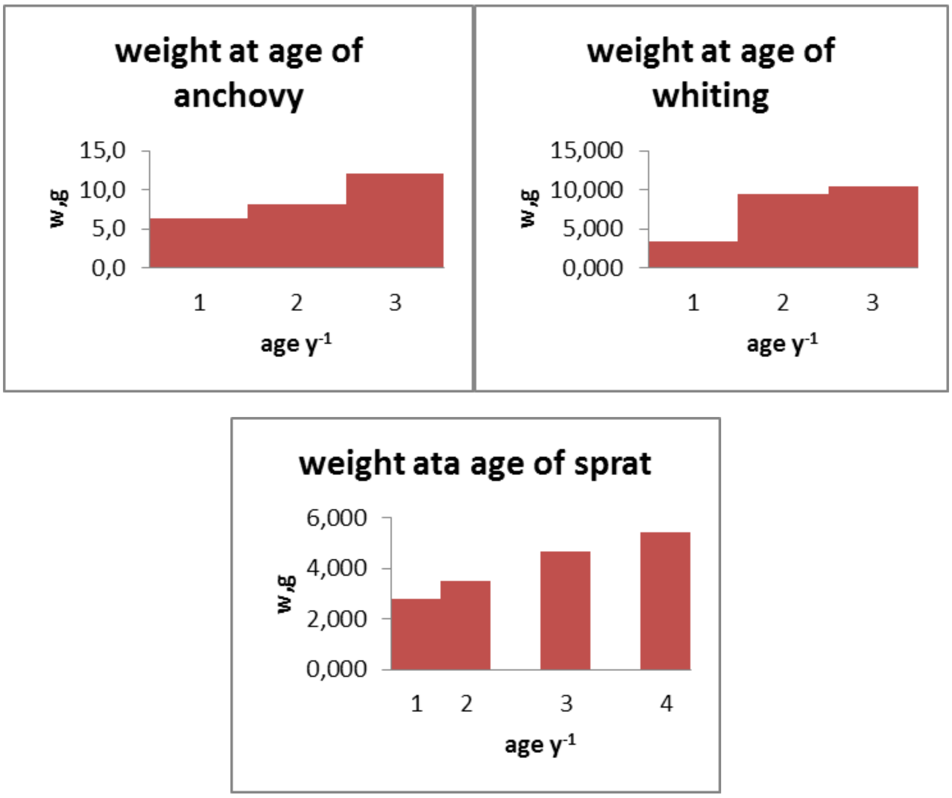

Fig. 17.5. Somatic growth of sprat

18. Sex ratio

In sprat, females predominated by 50%, followed by males (45%), and juveniles were represented by a low percentage (5%).

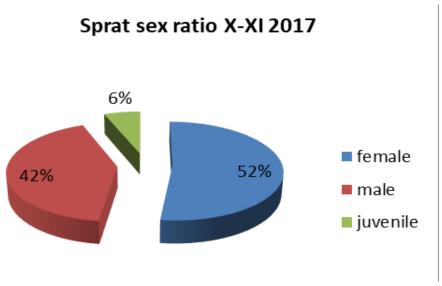

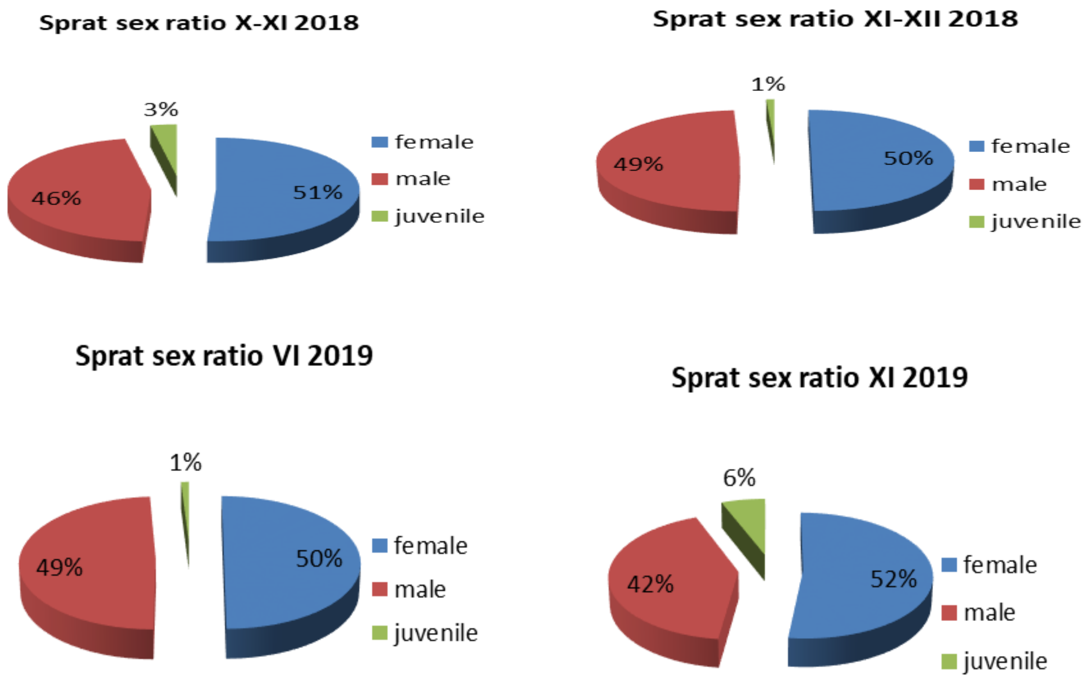

Fig.18.1. Sex ratio: 1 – juvenile, 2-male, 3-female

Females predominated by 49%, followed by males (48%), and juveniles represented a low percentage (3%) - 2018 (October-November).

In November 2019 , females predominatd by 51%, followed by males (45%). Juveniles were represented with a low percentage (4%). In whiting, females predominate by 50%, followed by males (45%). Juveniles were represented with a low percentage (5%). In the red mullet, females predominate by 49%, followed by males (44%). Juveniles were represented by 7% (Fig. 3.9.1.)

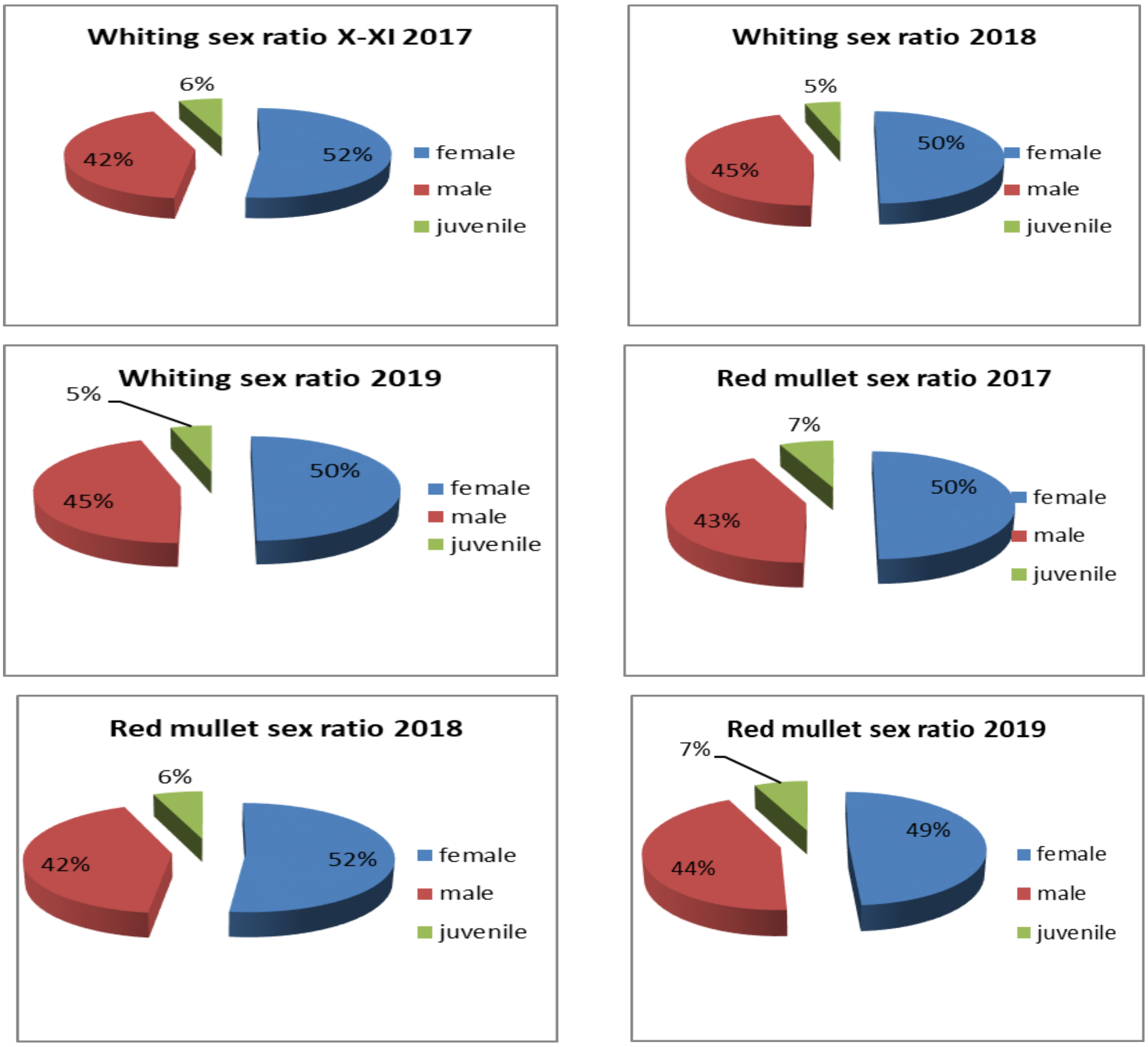

Fig.18.2. Sex ratio (male, female, juvenile)
A.2018, Novenber-Dcember; B.2019,June; C.2019, November.

18.1. Fecundity and Gonado-Somatic Index - 2017

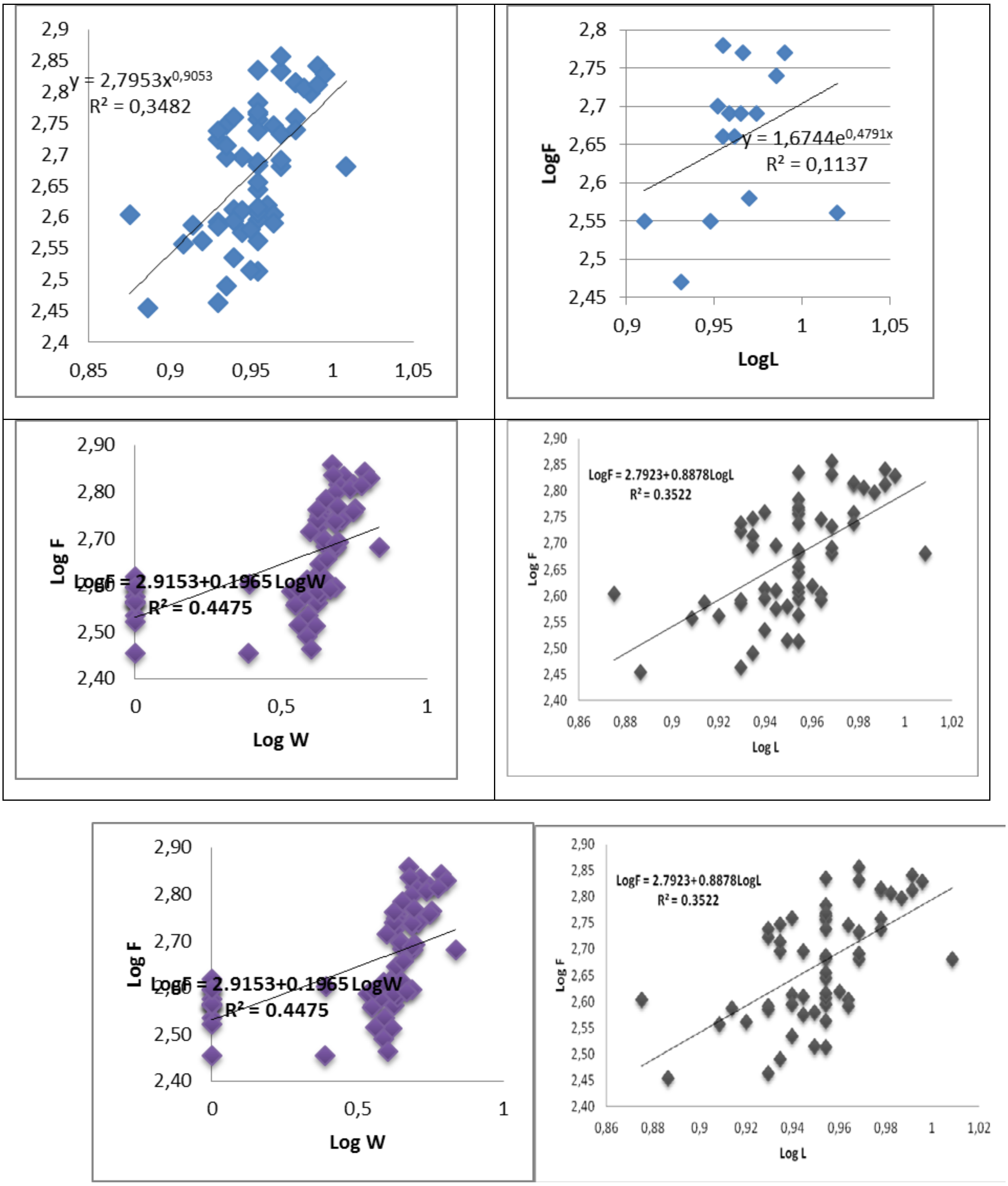

Fig.18.1.1 Fecundity - Portion (LogF) related to the sizes (LogL) of sprat from December 2017-2019 survey

Sprat fecundity correlated positively with its length (R^2 = 0.46), with large size classes corresponding to high fecundity.

18.2. Fecundity and Gonado-Somatic Index - 2018 (October-November)

Sprat fecundity correlates poorly with its length (R2 = 0.1137). Sprat (poorly represented in this study) was active in the spawning phase of the current investigation in December. Most of the individuals had stage III - IV glands. More detailed analysis should be made during the active spawning period of the species (October-February).

In the fall and winter of 2018, sprat was active in the spawning phase of that December investigation. Most of the individuals had stage III - IV glands. A more detailed analysis should be made in the active spawning period of the species (October-February).

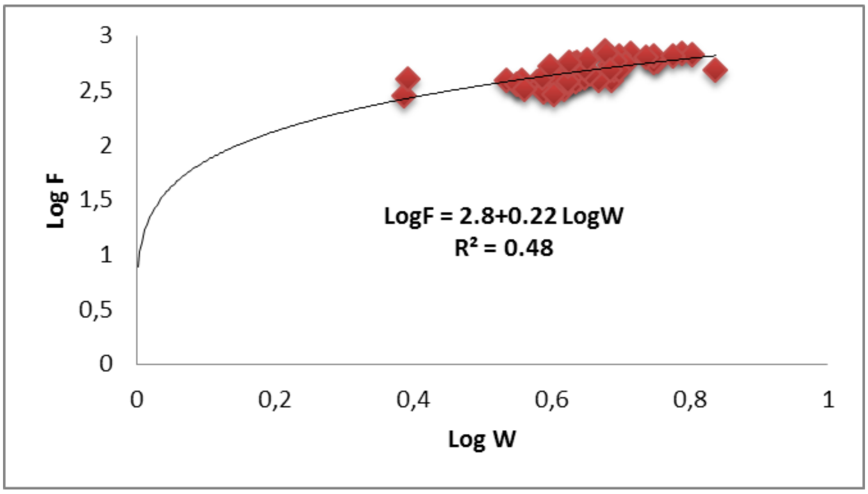

Fig.18.2.1. Fecundity - Portion (LogF) related to weight (LogW) of sprat in December, 2016

Fecundity-to-weight ratio of sprat is very well expressed (R^2 = 4.8; Fig. 18.2.2).

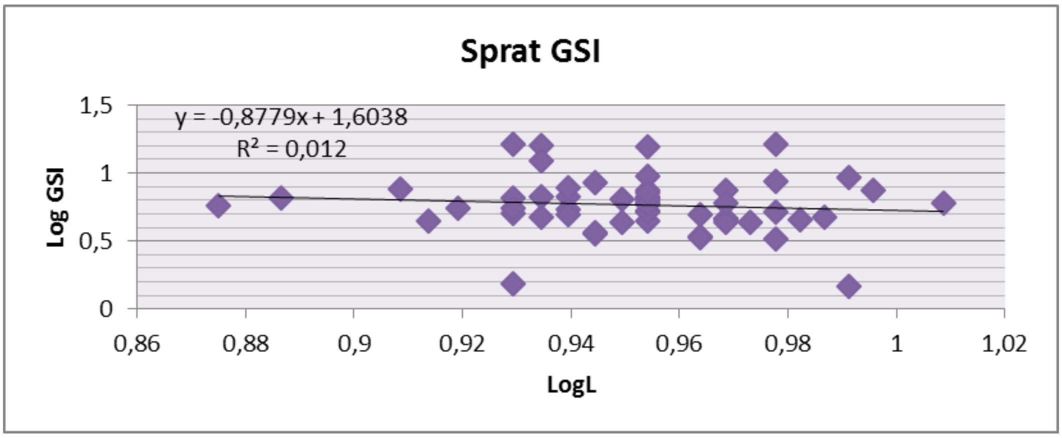

Fig.18.2.2. Gonadomatic sprat index of the present study (GSI,%)

The GSI (%) showed that over 50% of females were actively breeding. Very few specimens were in the early stages of maturation, so we could conclude that in December 2017, active reproduction began, even at relatively high water temperatures for the season.

18.3. Fecundity and Gonado-Somatic Index - 2018 (December)

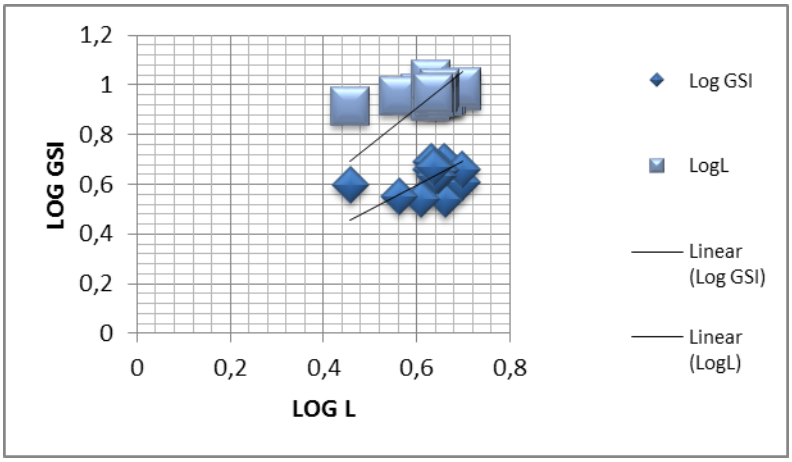

Fig.18.3.1. Gonadomatic sprat Index of the present study (GSI,%)

Project proposal № BG14MFOP001-3.003-0001 "Collection, management and use of data for the purposes of scientific analysis and implementation of the Common Fisheries Policy for the period 2017-2019", funded by the Maritime Affairs and Fisheries Program, co-financed by the European Union through the European Maritime and Fisheries Fund

The GSI (%) showed that over 50% of females were actively breeding. Very few specimens were in the early stages of maturation, so we could conclude that in November-December 2018, active reproduction began, even at relatively high water temperatures for the season.

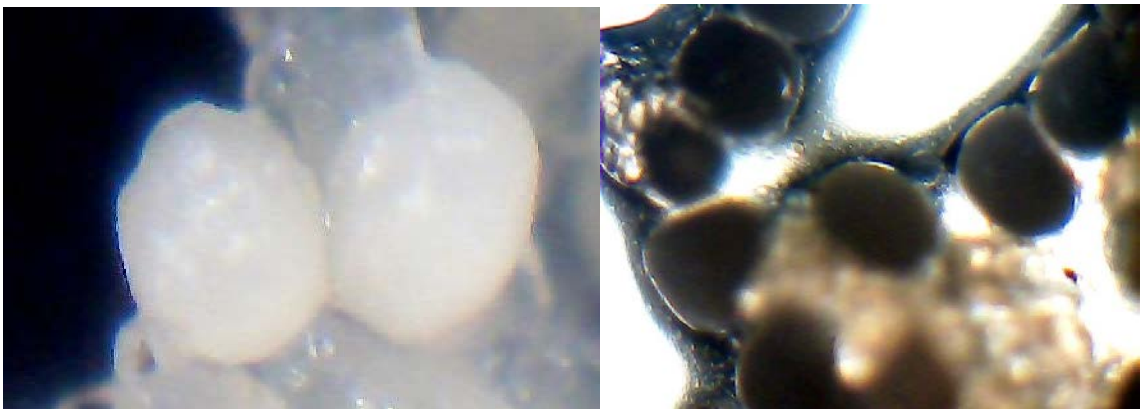

Photo 18.3.1. Sprat eggs

19. Natural mortality (2017- 2019)

We used asymptotic size values obtained from Pauly (1980) as average seawater temperature in the lower layers was 6.9 ° C.

From asymptotic length: **M = 0.7632**

From asymptotic weight: **M = 0.582**

In the present study, we used a natural mortality rate for sprat equal to 0.95 (Ivanov and Beverton, 1985; Prodanov et al., 1997).

20. Gonado somatic index

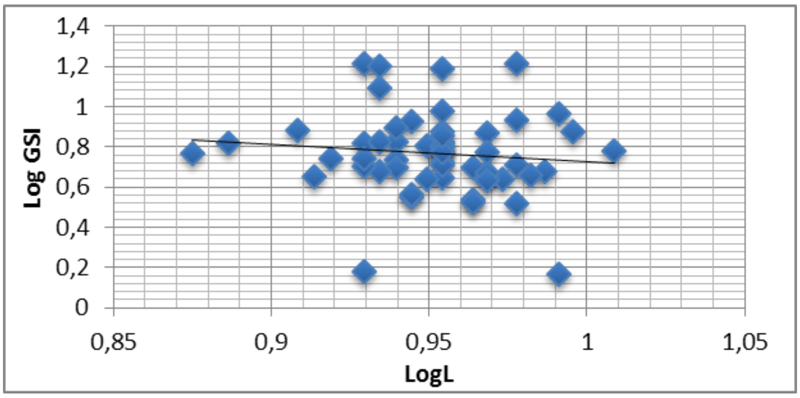

Fig. 20.1. Gonadomatic sprat Index of the present study (GSI,%)

The GSI (%) showed that over 50% of females were actively breeding. Very few specimens were in the early stages of maturation, so we could conclude that in December 2018, active reproduction began, even at relatively high water temperatures for the season.

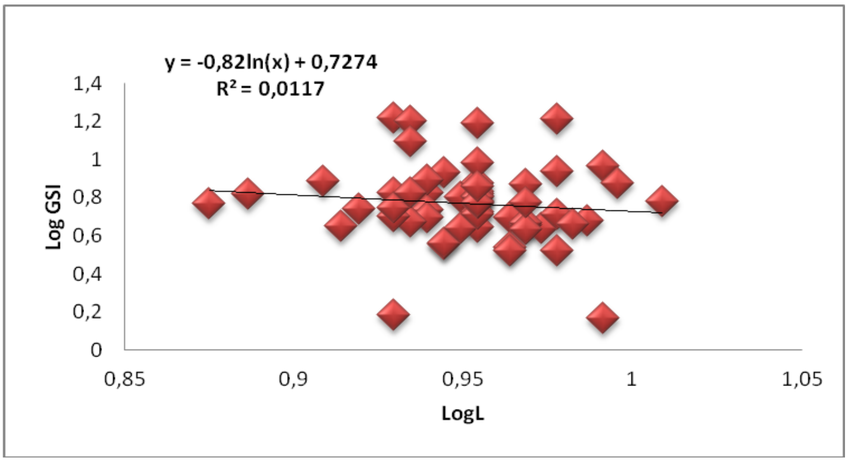

Fig. 20.2. Gonadomatic sprat Index, (GSI,%) 2019

20.1. Gonado somatic index 2019 (October-November)

In October-November study, sprat was not in the active spawning phase. Most of the individuals had stage-IV-V-II glands. The species did not show a high dependence of the partial ejection of the sexual products on the linear dimensions (Fig. 20.1.1).

The GSI (%) indicated that a small percentage of females were actively breeding. Most individuals were in the early stages of maturation, so we could conclude that in June 2019, active reproduction did not begin.

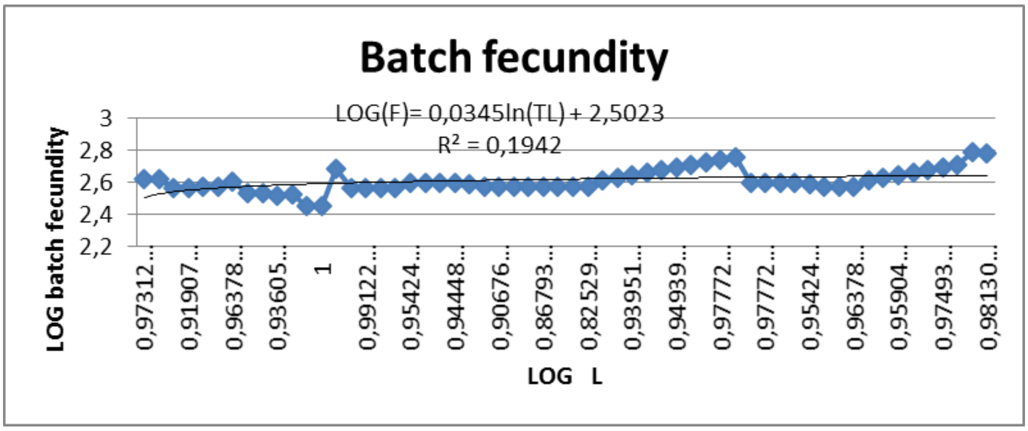

Fig. 20.1.1. Fecundity - portion (LogF) related to the sizes (LogL) of sprat from the October 2019 survey

Sprat fecundity correlated poorly with its length (R^2 = 0.19).

The relationship between fecundity and total size for whiting is linear, with a high degree of determination (R^2 = 0.7855) (Fig. 20.1.2).

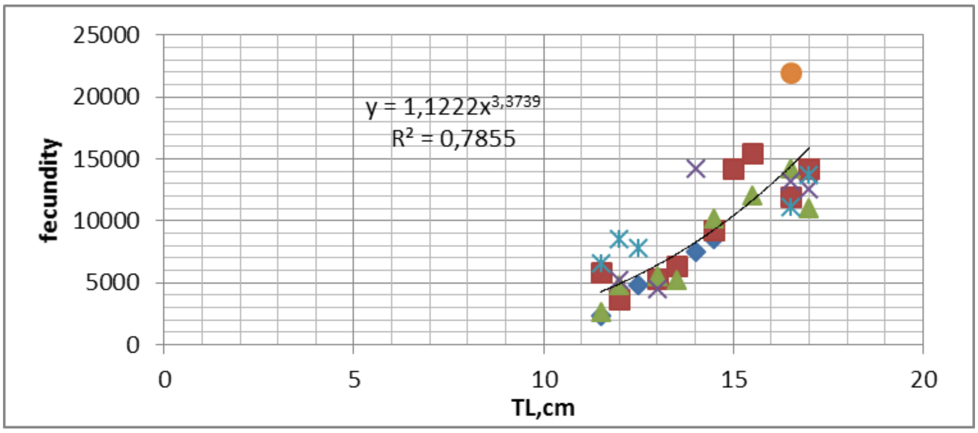

Fig. 20.1.2. Fecundity - portion (LogF) in relation to the size (LogL) of the whiting from the study in October-November 2019

The gonado somatic index of sprat varied widely in relation to individual weight, and to a greater extent its values indicated that the mass reproduction of the species began during the period under consideration (Fig. 20.1.3).

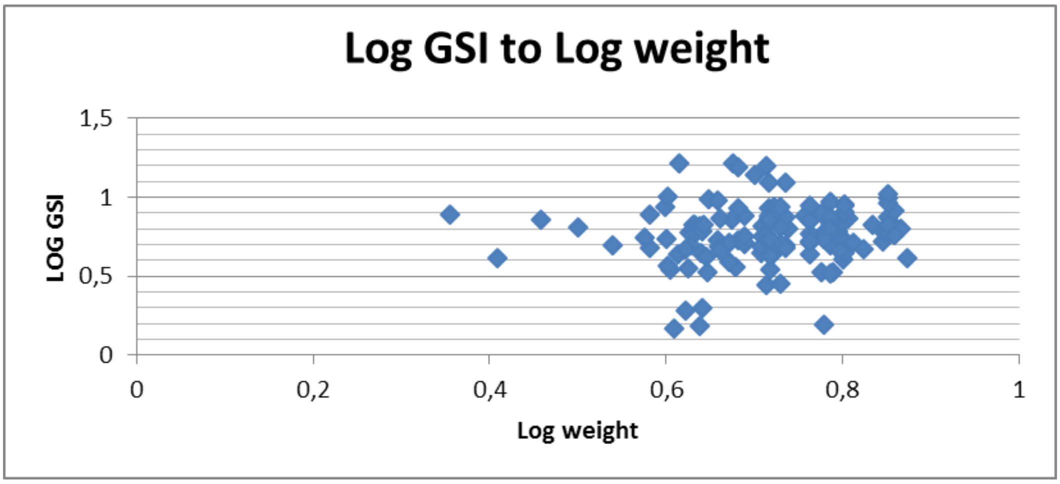

Fig. 20.1.3. Gonadomatic sprat Index of the present study (GSI,%)

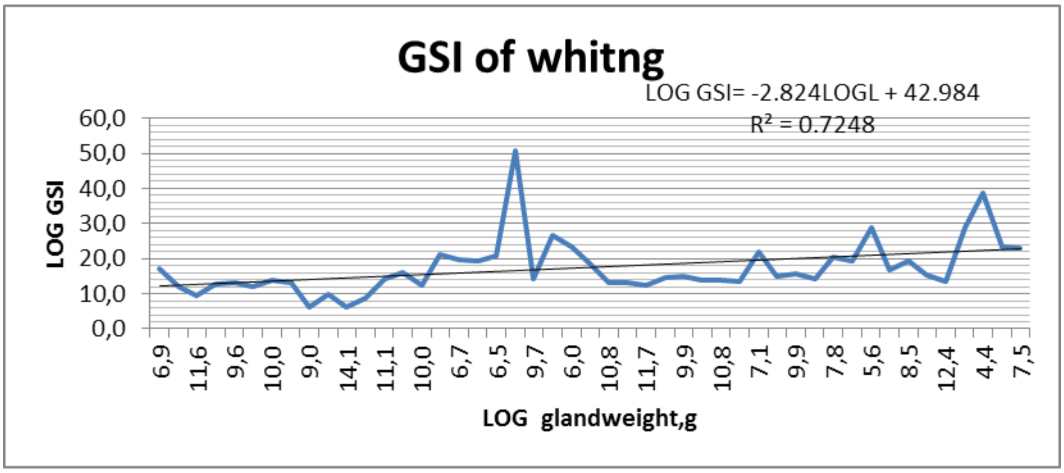

Fig. 20.1.4. Gonado-somatic index of the whiting of this study (GSI,%)

21. Feeding

21.1. Sprattus sprattus: weight - length dependence, Index of stomach fullness (ISF)

The mean absolute length of investigated sprat specimens reached 86.61 ± 0.65 (SD) mm, varying between 73 - 107 mm, correspondingly the mean weight was 4.29 ± 1.14 (SD) g, varying from 2.35 g to 8.43 g (Table 21.1.1, Fig. 21.1.1).

Project proposal № BG14MFOP001-3.003-0001 "Collection, management and use of data for the purposes of scientific analysis and implementation of the Common Fisheries Policy for the period 2017-2019", funded by the Maritime Affairs and Fisheries Program, co-financed by the European Union through the European Maritime and Fisheries Fund

Table 21.1.1. Summary statistics of length (L, cm) and weight (W, g) of sprat, analysed for stomach content composition in October-December 2017

	L, cm	W, g
Mean	8.66	4.29
Standard Error	0.07	0.13
Median	8.50	3.96
Mode	8.10	3.30
Standard Deviation	0.65	1.14
Sample Variance	0.42	1.30
Kurtosis	1.07	2.25
Skewness	0.98	1.39
Range	3.40	6.08
Minimum	7.30	2.35
Maximum	10.70	8.43

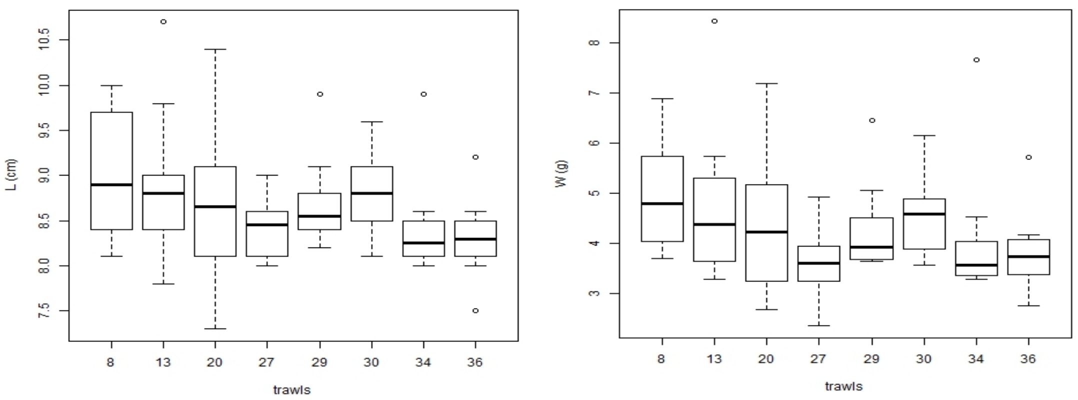

Fig. 21.1.1. Box plot: Distribution of length (cm) and weight (g) of sprat (included in stomach content composition analysis) per trawls (median values, 25 – 75 % hinge, minimal and maximal values) in October-December 2017

Table 21.1.1. Summary of Index of Somach Fullness - ISF (% of BW) in October-December 2017, October-November 2018, December 2018, June 2019, October-November 2019

	ISF, % BW
Mean	0.619
Standard Error	0.047
Median	0.513
Standard Deviation	0.417
Sample Variance	0.174
Kurtosis	17.04
Skewness	3.486
Range	3.019
Minimum	0.073
Maximum	3.091

	L, cm	W, g	ISF, % BW
Mean	10.593	8.05	1.05
Standard Error	0.137	0.32	0.16
Median	10.650	8.11	0.94
Mode	11.000	5.99	0.00
Standard Deviation	0.749	1.76	0.86
Sample Variance	0.561	3.08	0.74
Kurtosis	-0.267	-0.17	-0.61
Skewness	0.046	0.47	0.66
Range	2.900	7.20	2.88
Minimum	9.200	5.13	0.00
MaXImum	12.100	12.33	2.88
Sum	317.800	241.45	31.37
Count	30.000	30.00	30.00
Confidence Level (95.0%)	0.280	0.66	0.32

	L, cm	W, g	ISF, % BW
Mean	10.06	6.75	1.20
Standard Error	0.07	0.15	0.10
Median	10.00	6.58	0.87
Mode	10.00	#N/A	0.00
Standard Deviation	0.70	1.53	1.05
Sample Variance	0.49	2.34	1.11
Kurtosis	-0.39	0.54	-0.48
Skewness	0.34	0.66	0.69
Range	3.40	8.00	4.31
Minimum	8.50	3.61	0.00
Maximum	11.90	11.61	4.31
Sum	1107.10	742.66	128.13
Count	110.00	110.00	107.00
Confidence Level (95.0%)	0.13	0.29	0.20

	L, cm	W, g	ISF, % BW
Mean	10.593	8.05	1.05
Standard Error	0.137	0.32	0.16
Median	10.650	8.11	0.94
Mode	11.000	5.99	0.00
Standard Deviation	0.749	1.76	0.86
Sample Variance	0.561	3.08	0.74
Kurtosis	-0.267	-0.17	-0.61
Skewness	0.046	0.47	0.66
Range	2.900	7.20	2.88
Minimum	9.200	5.13	0.00
MaXImum	12.100	12.33	2.88
Sum	317.800	241.45	31.37
Count	30.000	30.00	30.00
Confidence Level (95.0%)	0.280	0.66	0.32

	L, cm	W, g	ISF, % BW
Mean	8.86	4.11	0.91
Standard Error	0.14	0.20	0.08
Median	8.75	3.80	0.78
Mode	8.50	#N/A	#N/A
Standard Deviation	0.98	1.39	0.60
Sample Variance	0.96	1.94	0.36
Kurtosis	1.00	1.44	-0.63
Skewness	0.66	1.07	0.53
Range	5.00	6.71	2.39
Minimum	7.00	2.09	0.12
Maximum	12.00	8.80	2.50
Sum	443.10	205.62	45.30
Count	50.00	50.00	50.00
Confidence Level (95.0%)	0.28	0.40	0.17

I. Survey 2017

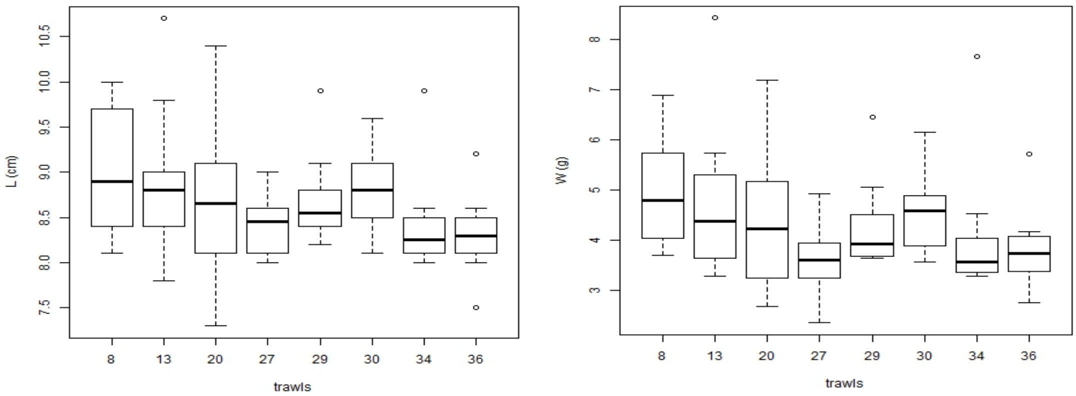

Fig. I.1. Box plot: Distribution of length (cm) and weight (g) of sprat (included in stomach content composition analysis) per trawls (median values, 25 – 75 % hinge, minimal and maximal values) during October-December 2017

The length-weight relationship of collected sprat specimens could be described by the following equation: logWW (g)=3.1504*log L (cm) - 2.331; (R2=0.89, p<0.05, Fig. I.2.).

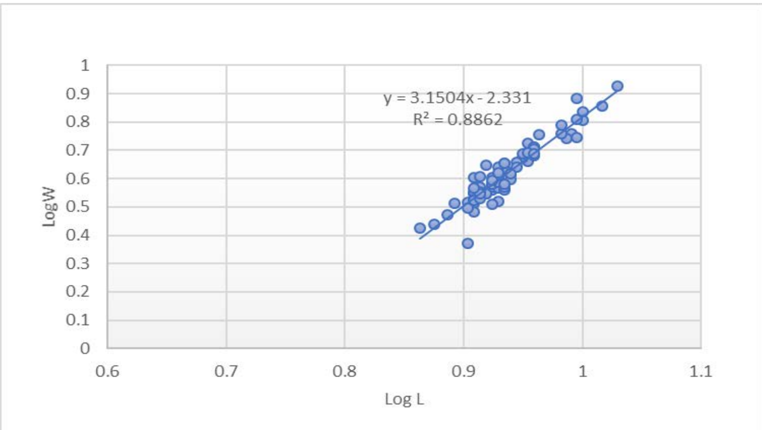

Fig. I.2. Length - weight relationship of sprat, collected in October-December 2017

In autumn 2017, the mean index of stomach fullness (ISF) reached 0.62 % ± 0.42 (SD) of sprat body weight (BW) (Table I.1) and exceeded with 17.54 % the multiannual average for 2007-2010 (0.52 %, Mihneva et al., 2015).

Table I.1. Summary statistics of data fn index of stomach fullness - ISF (% of BW) of sprat in October-December 2017

	ISF, % BW
Mean	0.619
Standard Error	0.047
Median	0.513
Standard Deviation	0.417
Sample Variance	0.174
Kurtosis	17.04
Skewness	3.486
Range	3.019
Minimum	0.073
Maximum	3.091

The highest average values of ISF > 0.7 % (Fig. I.3 and Fig. I.4) were registered in trawls 27, 20 and 13, located in the region Obzor - Tzarevo. The mean values of ISF decreased near to the shore line and increased in deep water (Fig. I.3).

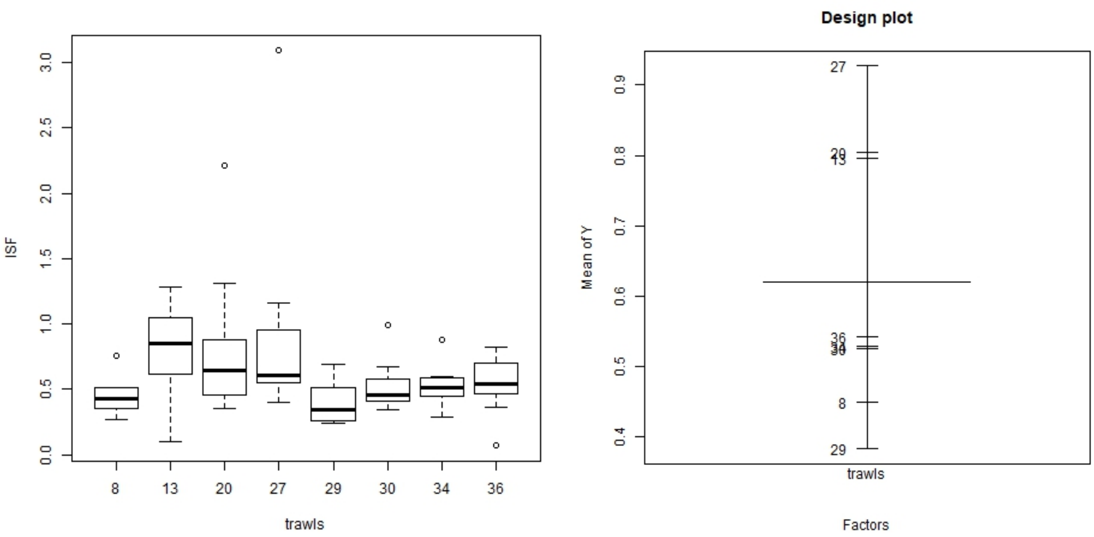

1. 2.

Fig. I.3. Box plot: Spatial distribution of ISF (1) per trawls in October-December 2017. Design plot (2): distribution of the mean ISF values per trawls

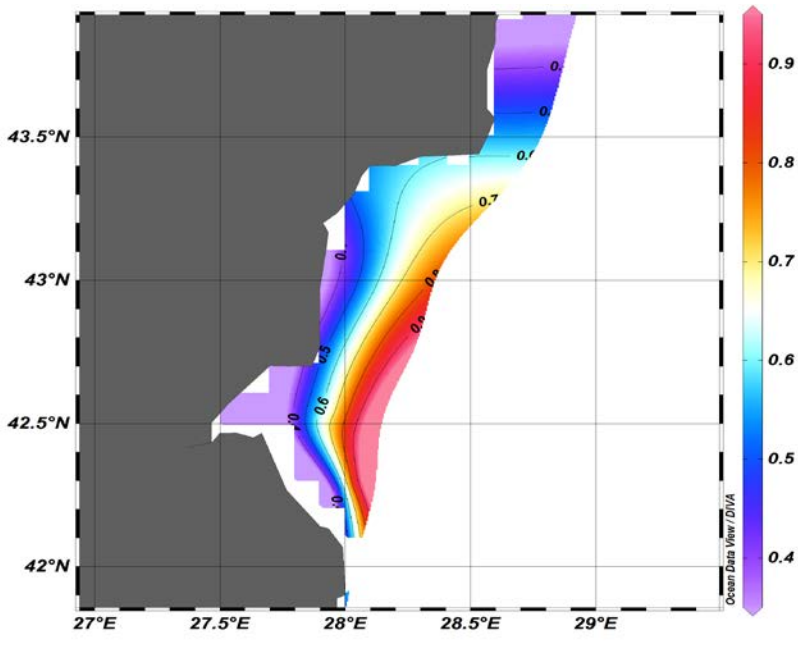

Fig. I.4. Spatial distribution of mean values of ISF per trawls in October-December 2017

Project proposal № BG14MFOP001-3.003-0001 "Collection, management and use of data for the purposes of scientific analysis and implementation of the Common Fisheries Policy for the period 2017-2019", funded by the Maritime Affairs and Fisheries Program, co-financed by the European Union through the European Maritime and Fisheries Fund

Statistically significant correlation could not be established among the ISF values and sprat weight within the limits of 2.34 - 8.43 g (Fig. I.5).

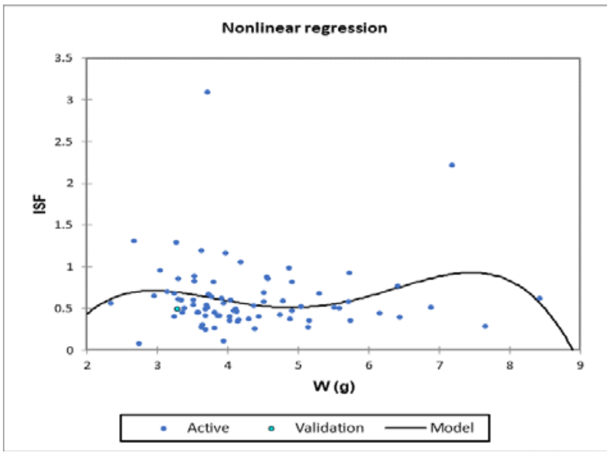

Fig. I.5. Scatterplot: relationship between sprat weight (W, g) and ISF in October-December 2017

Prey number (PN), species composition of sprat food and index of relative importance (IRI)

In the studied area, the mean number of prey items (PN) in sprat food attained 68 ind/stomach, comparable with the average PN, estimated during autumn months of 2007-2010 (64 ind/stomach). However, it remained with 4.8 folds lower than the mean PN, measured in autumn 2016 - 328 ind/stomach.

Over the studied period in 2017, spatial variability of the PN among samples was large and the highest values > 100 ind/stomach were detected in south direction and toward the 35 - meter isobath (Fig.I.1.1).

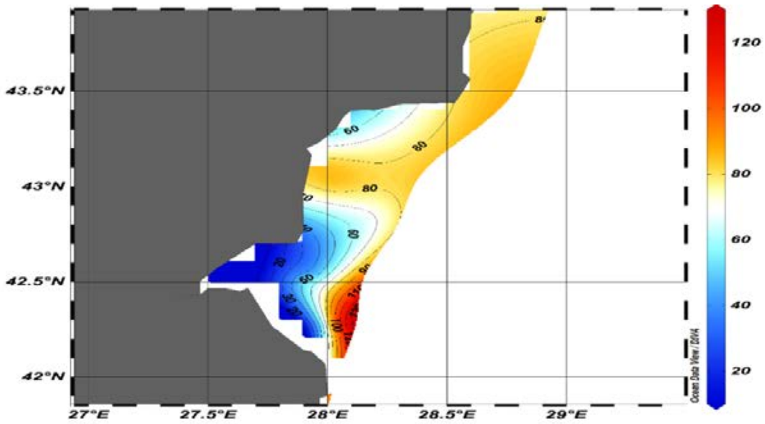

Fig. I.1.1. Spatial distribution of average prey number per station in October-December 2017

The maximal PN (253 ind/stomach) was registered in a sample from trawl 27, where the average value of PN attained 120 ind/stomach. Also, the maximal ISF was established in this sample, due to a high percent share of *Parasagitta setosa* in sprat diet, thus the combination of maximal values of both indexes, PN and ISF, could signify favourable feeding conditions.

The study of zooplankton diversity in marine environment allowed identification of 18 mesozooplankton species/groups over autumn season of 2017. From the latter, a total of 15 species/groups appeared as components of sprat diet. The copepods: *Calanus euxinus*, *Pseudocalanus elongates*, *Acartia clausi*, *Oithona* spp., *Paracalanus parvus*, *Copoepoda nauplii* and *Copepoda ova* were the most frequently identified objects in sprat diet; from the group of pelagic larvae of bottom species (meroplankton), four taxonomic subgroups were detected: *Lamellibranchia veliger*, *Cirripedia cypris*, *Decapoda mysis* and Polychaeta larvae; the planktonic Cladocera were represented by the species *Penilia avirostris*, and class Chaetognatha - by the species *Parasagitta setosa.* Presence of *Pisces ova* and larvae of Isopoda was also registered in the sprat food content.

The indices of relative importance (IRI) of the main components in sprat food spectrum are presented in Table I.1.1 (where IRI of different food items is based on the percent shares from total abundance and biomass, multiplied by the frequency of occurrence).

Project proposal № BG14MFOP001-3.003-0001 "Collection, management and use of data for the purposes of scientific analysis and implementation of the Common Fisheries Policy for the period 2017-2019", funded by the Maritime Affairs and Fisheries Program, co-financed by the European Union through the European Maritime and Fisheries Fund

Table I.1.1. The sprat food composition in October-December 2017

Sprat food composition	***N (%, from total abundance)***	***M (%, from total biomass)***	***FO (Frequency of occurrence)***	***IRI (Index of relative importance)***
Calanus euxinus	47.44	69.96	100	11740
Parasagitta setosa	7.92	28.99	55	2030
Pseudocalanus elongatus	18.84	0.802	86.25	1694
Copepoda ova	14.51	0.011	60	871
Paracalanus parvus	3.39	0.073	63.33	219
Lamellibranchia veliger	3.94	0.017	56.25	223
Oikopleura dioica	2.41	0.020	33.33	81
Others	1.55	0.122		
Total	100%	100%		

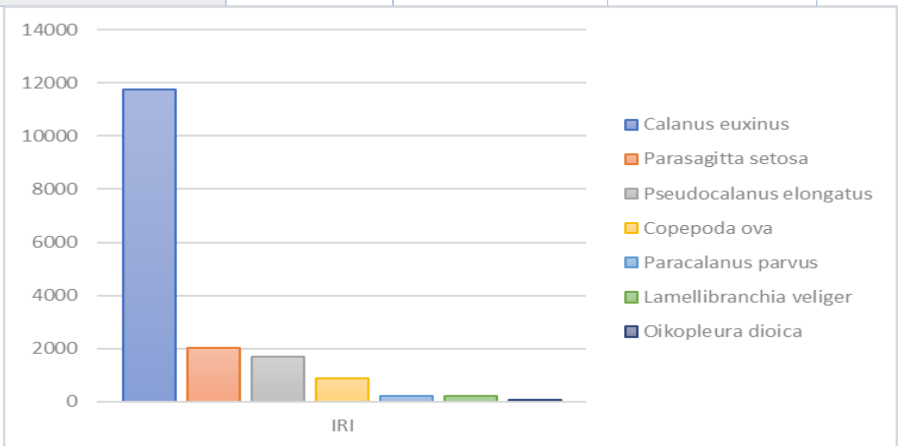

Fig. I.1.2. IRI of different zooplankton species in sprat food in October-December 2017

Data from all samples showed that sprat food was dominated by the copepod *Calanus euxinus*, followed by *Parasagitta setosa*, *Pseudocalanus elongatus*, *Copepoda ova*, *Paracalanus parvus* and *Lamellibranchia veliger* (Table I.1.1, Fig. I.1.2). The cold-water zooplankton species predominated by abundance and biomass in sprat food and showed high frequencies of occurrence.

Sprat food composition displayed some pronounced differences among the observed stations (Table I.1.1). In front of the southern costs, the sprat ration was dominated by *Calanus euxinus*, while *Parasagitta setosa* prevailed in feeding between Kamchia - Emine and the species *Pseudocalanus elongatus* was mostly detected in the sprat food along the northern coasts (Table I.1.2, Fig. I.1.3).

Table I.1.2. Distribution of IRI (%) of main mesozooplankton species in sprat food per observed stations in October-December 2017

Composition of sprat food	**13** **24 m**	**20** **54 m**	**8** **53 m**	**27** **35 m**	**29** **34 m**	**30** **34 m**	**34** **36 m**	**36** **30 m**
Calanus euxinus	94.41	8.91	81.68	71.67	71.26	91.48	47.37	44.63
Parasagitta setosa	0.69	73.21	3.35	0.07	5.37	0.89	20.93	24.45
Pseudocalanus elongatus	4.38	11.36	6.71	7.04	11.65	2.60	17.97	15.02
Copepoda ova	0.06	0.76	0.55	13.46	8.75	3.99	11.59	13.67
Paracalanus parvus	0.28	2.94	0.00	4.28	0.11	0.00	1.31	1.68
Lamellibranchia veliger	0.14	1.62	7.69	3.15	0.08	0.08	0.74	0.39
Oikopleura dioica	0.01	1.13	0.00	0.04	2.58	0.81	0.00	0.13
Others	0.03	0.07	0.02	0.29	0.2	0.15	0.09	0.03

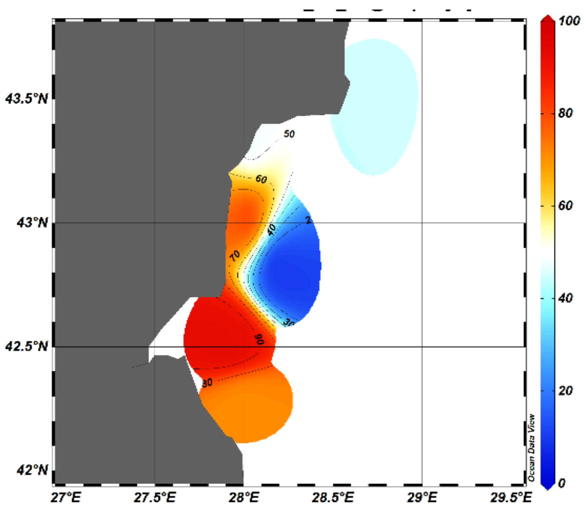

(1)

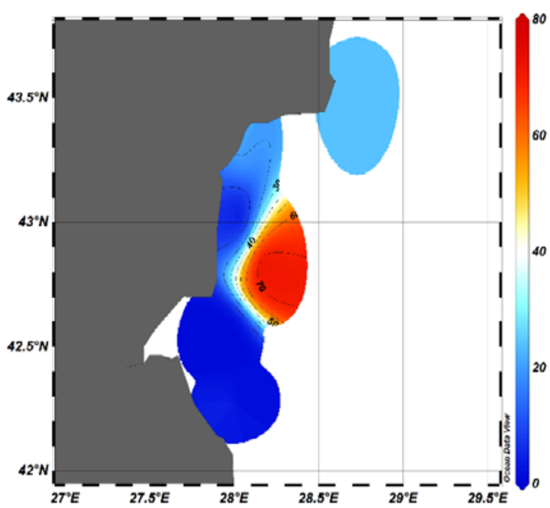

(2)

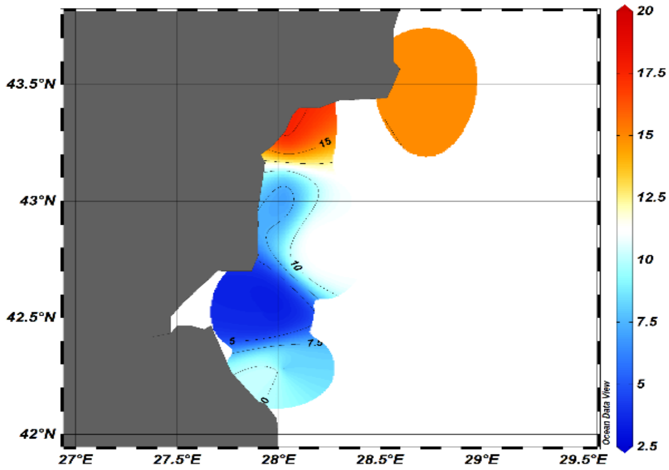

(3)

Fig. I.1.3. Spatial distribution of IRI (%) of some zooplankton species: (1) *C. euxinus*, (2) *Parasagittta setosa* and (3) *Pseudocalanus elongatus* in sprat food in autumn 2017

Trachurus mediteraneus: weight-length relationship, index of stomach fullness (ISF)

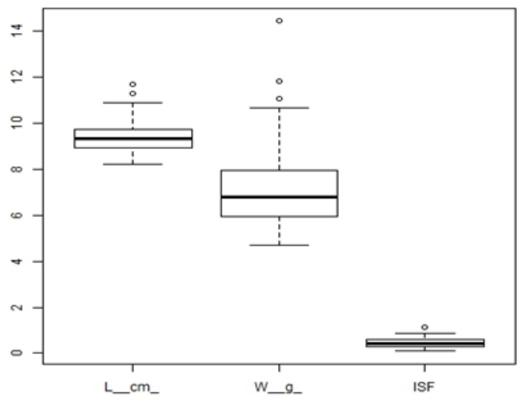

Fig. I.2.1. Boxplot: median values, 25 – 75 % hinge, minimal and maximal values for horse mackerel weight, size and index of stomach fullness (ISF) in 2016 (data extracted from the horse mackerel feeding study)

The weight-length relationship for horse mackerel could be described by the equation: logWW(g)=3.0232*log L(cm) – 2.0949; ($R2=0.92$, $p<0.001$, Fig. I.2.2).

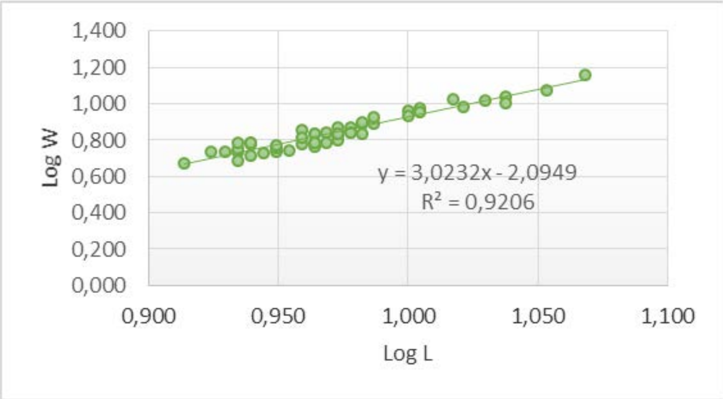

Fig. I.2.2. Weight-length relationship for horse mackerel, investigated in distribution of IRI (%) of main mesozooplankton species in sprat food per observed stations in October-December 2017

The mean value of ISF reached 0.46 % ± 0.22 (SD) of the horse mackerel body weight (BW). The highest mean values of ISF = 0.54 % BW were established in the coastal area in front of Emine - Sozopol and in the Bourgas Bay (Fig. I.2.3).

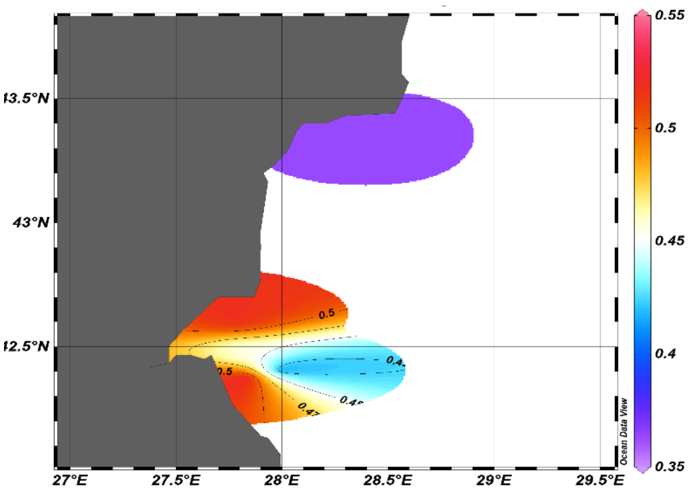

Fig. I.2.3. Spatial distribution of ISF of horse mackerel in October-December 2017

Statistically significant non-linear dependence was established among the ISF and horse mackerel body weight (within the limits of 3.02 g - 13.78 g) that explained 27 % of the observed variations by p<0.001 (Fig. I.2.4). The food amount, expressed as a percent of the sprat body mass, increased in small size groups of horse mackerel with weight < 6 g. The second, less expressed peak of ISF was found in the weight class 9 g (Fig. I.2.4). A large dataset, encompassing different size classes of horse mackerel, is required to achieve a complete model.

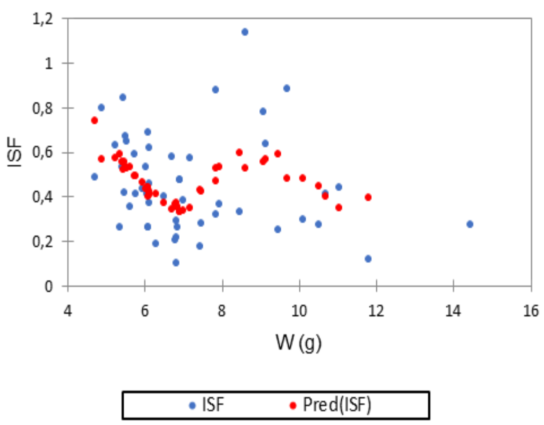

Formula: Y1 ~ 1 + s(W)

Parametric coefficients:

	Estimate	Std. Error	t value	Pr(>|t|)	
(Intercept)	0.45558	0.02826	16.12	<2e-16	***

Signif. codes: 0 '***' 0.001 '**' 0.01 '*' 0.05 '.' 0.1 ' ' 1

Approximate significance of smooth terms:

	edf	Ref.df	F	p-value	
s(W)	4.701	5.725	2.323	0.0512	.

Signif. codes: 0 '***' 0.001 '**' 0.01 '*' 0.05 '.' 0.1 ' ' 1

R-sq.(adj) = 0.19 Deviance explained = 26.7%

Fig. I.2.4. Contribution of the factor weight (W, g) to the fitted values of ISF. (Right: Statistical data for GAM model)

Species composition and index of relative importance (IRI) of different food items in the horse mackerel diet

The mean prey number in horse mackerel samples reached 383 ± 81.14 (SE) ind/stomach in the autumn of 2017. The maximal prey number of 1178 ind/stomach was identified in front of Sozopol (Fig. I.3.1), due to consumption of small food objects, namely meroplankton larvae of Lamellibranchia. Feeding on small size items is associated with low values of ISF and a negative correlation was established between these two indexes (although the dependence was not statistically significant).

Project proposal № BG14MFOP001-3.003-0001 "Collection, management and use of data for the purposes of scientific analysis and implementation of the Common Fisheries Policy for the period 2017-2019", funded by the Maritime Affairs and Fisheries Program, co-financed by the European Union through the European Maritime and Fisheries Fund

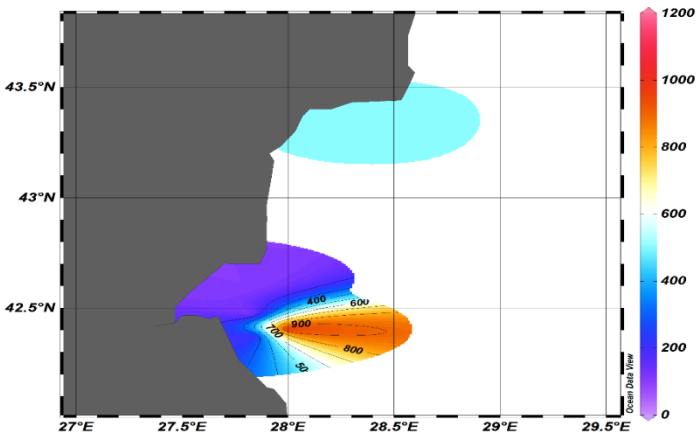

Fig. I.3.1. Spatial distribution of mean PN (ind/stomach) in samples of horse mackerel, collected in October-December 2017

A total of 15 zooplankton species/groups, as well as Mysidae, Isopods and fish remains were identified in the horse mackerel stomach content. From the group of meroplankton (pelagic larvae of benthic species), five taxonomic subgroups were identified in the horse mackerel food: *Lamellibranchia veliger*, *Decapoda mysis*, *Gastropoda veliger*, Polychaeta larvae, *Cirripedia cypris*; from crustacean copepods: *Acartia clausi*, *Paracalanus parvus*, *Pseudocalanus elongatus*, *Calanus euxinus*, *Centropages ponticus*, *Oithona similis* and *Oithona davisae*; the planktonic Cladocera were represented by *Penilia avirostris*; class Chaetognatha - from the species *Parasagitta setosa*. The food spectrum of horse mackerel included also Appendicularia, Izopoda larvae and *Paramysis* spp. The indices of relative importance (IRI) of the main food items and their percent shares from total abundance and biomass, and frequencies of occurrence are presented in Table I.3.1.

Table I.3.1. Horse mackerel food composition of in October-December 2017

Horse mackerel food composition	N (%, from total abundance)	M (%, from total biomass)	FO – Frequency of occurrence	IRI – Index of relative importance
Lamellibranchia veliger	85.25	27.16	84	9442
Acartia clausi	3.25	10.04	50	664
Parasagitta setosa	0.06	27.08	10	271
Paracalanus parvus	3.62	1.00	50	231
Paramysis spp.	1.04	19.10	8	161
Penilia avirostris	1.28	3.75	24	121
Decapoda mysis	0.72	5.03	12	69
Others	4.77	6.84		
Total	**100%**	**100%**		

The meroplankton larvae of Lamellibranchia had a leading position in the horse mackerel diet (Table I.3.2, Fig. I.3.2), while IRI of copepods *Acartia clausi*, *Paracalanus parvus*, as well as of Chaetognatha (*Parasagitta setosa*) and Decapoda larvae were relatively reduced.

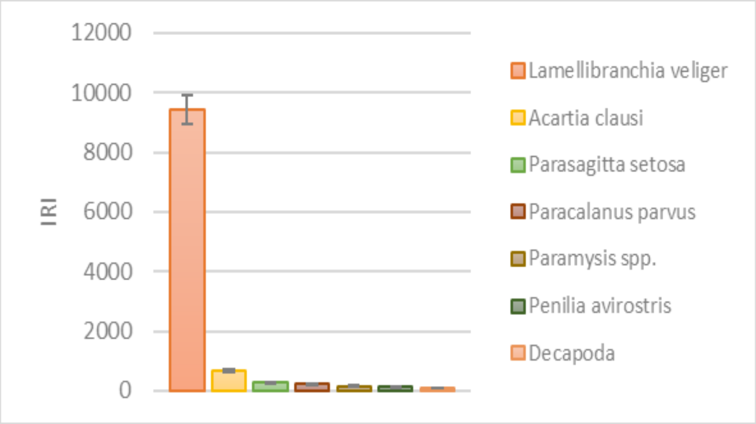

Fig. I.3.2. IRI of different mesozooplankton species in the horse mackerel diet during the period 28 August- 05 September 2016

At stations, located between 20-30 m isobaths, the horse mackerel diet was constituted predominantly by meroplankton larvae of Lamellibranchia (with IRI % - 80.1% - 93.06 %, Table I.3.2, Fig. I.3.3). The role of copepod *A. clausi* and mysidae *Paramysis* spp., as well as the share of Decapoda larvae increased in the deeper waters (around 34-36 m isobath, Table I.3.2, Fig. I.3.3).

Table I.3.2. Distribution of IRI (%) of main food items in the horse mackerel food, presented by sampling stations in October - December 2017

Composition of the diet of the horse mackerel	**2.1** **34m**	**5** **36m**	**18** **20m**	**2.2** **30m**	**3.2** **24m**
Lamellibranchia veliger	67.94	40.24	93.06	80.10	81.71
Acartia clausi	9.48	2.48	0.06	4.39	13.26
Decapoda	7.82	0.32	0.24	0.00	0.00
Centropages ponticus	6.35	0.35	0.00	0.00	0.00
Parasagitta setosa	0.00	0.00	5.82	13.18	0.34
Paramysis spp.	0.00	45.54	0.00	0.00	0.00
Penilia avirostris	5.12	0.28	0.00	0.08	0.53
Others	3.30	10.80	0.83	2.24	4.17

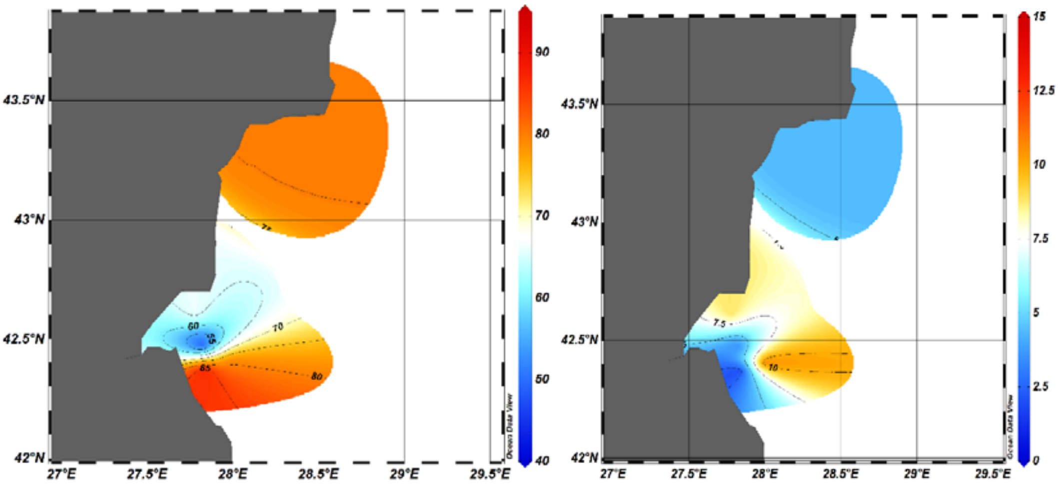

(1) (2)

Fig. I.3.3. Distribution of IRI (%) of some important zooplankton species in horse mackerel diet: (1) *L.veliger*, (2) *A.clausi* in autumn 2017

Zooplankton in marine environment: species composition and biomass

During the studied period, zooplankton diversity in the marine environment was formed by 18 species/groups (Table I.4.1). Persisting presence of warm-water zooplankton species *Penilia avirostris, Decapoda mysis* and meroplankton larvae was estimated till the middle of November, related to warm autumn and relatively high surface water temperatures.

Table I.4.1. Species diversity of zooplankton

	October-December 2017
1.	*Noctiluca scintillans*
2.	*Beroe ovata*
3.	*Pleurobrachia pileus*
4.	*Aurelia aurita*
5.	*Acartia clausi*
6.	*Pseudocalanus elongatus*
7.	*Calanus euxinus*
8.	*Paracalanus parvus*
9.	*Oithona davisae*
10.	*Oithona similis*
11.	*Penilia avirostris*
12.	*Cirripedia nauplii*
13.	*Lamellibranchia veliger*
14.	*Polychaeta larave*
15.	*Decapoda mysis*
16.	*Parasagitta setosa*
17.	*Oicopleura dioica*
18.	*Pisces ova*, larvae

Total zooplankton biomass was prevailed by gelatinous species (Fig. I.4.1 B, Table 25.0.2): *Noctiluca scintillans* (Protozoa) - 83.57 % and *Beroe ovata* - 8.80 %, while the percent share of fodder mesozooplankton was low - 7.33 %.

The Protozoa and Copepoda species dominated by abundance, forming 81.66 % and 13.16 % from the total zooplankton abundance (Fig. I.4.1.A).

A

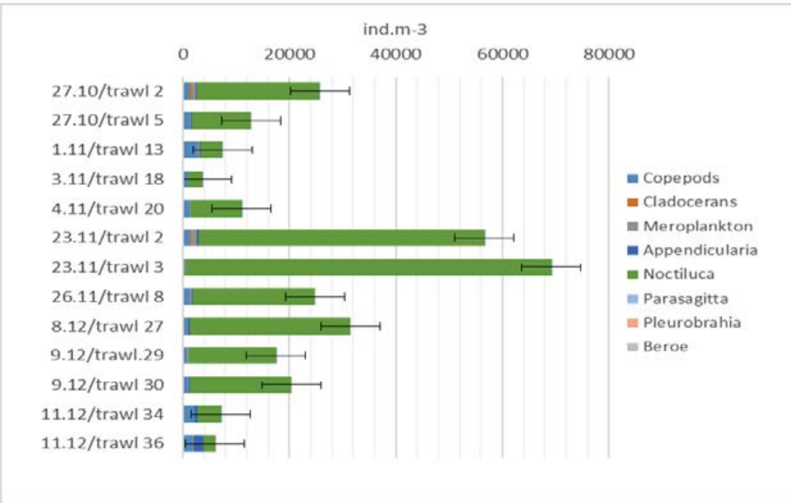

B

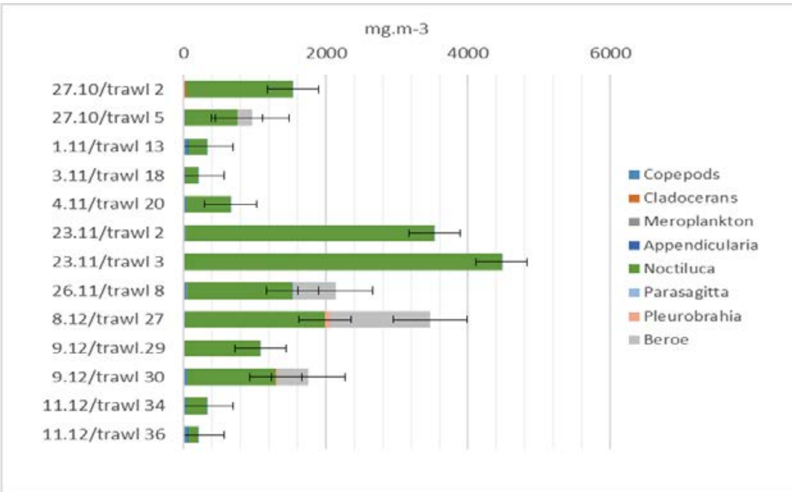

Fig. I.4.1. Distribution of abundance (A) and biomass (B) of the main zooplankton species/groups per trawls in October – December 2017

Table I.4.2. Percent shares (%, biomass) of the main zooplankton groups in October – December 2017

Trawl	Copepods	Cladocerans	Meroplankton	Appendicularia	Noctiluca	Parasagitta	Pleurobrahia	Total zooplankton biomass ($mg.m^{-3}$)
2.1	0.926	1.18	0.18	0.09	97.44	0.20	0	1539.7
5.1	2.840	0	0.05	0.11	74.99	0.20	0	961.9
13.1	17.057	0	0.22	0.51	81.66	0.56	0	327.9
18.1	9.036	0	0	0	86.52	4.44	0	209.1
20.1	5.432	0	0.10	0	94.45	0.02	0	660.1
2.2	0.529	0.26	0.10	0.08	99.01	0.02	0	3528.6
3.2	0.206	0	0.01	0	99.49	0.29	0	4486.9
8.2	1.969	0	0.11	0.05	69.64	0.42	0	2137.0
27.2	0.630	0	0.02	0.04	56.65	0.04	1.93	3465.5
29.2	1.106	0	0.07	0	98.79	0.03	0	1081.5
30.2	3.026	0	0.02	0.08	70.77	0.03	1.95	1753.5
34.2	11.365	0	0.06	1.00	87.54	0.04	0	330.8
36.2	23.729	0	0.25	6.33	69.44	0.26	0	205.7

Table I.4.3 shows summary statistical data about the total zooplankton biomass and its main components - the fodder mesozooplankton biomass, as well as the biomasses of Protozoa/Noctiluca and gelatinous zooplankton.

The total zooplankton biomass attained 1591.39 ± 396.43 (SE) $mg.m^{-3}$, as the biomass of Protozoa reached 1341.91 ± 365.55 (SE) $mg.m^{-3}$, and those of the fodder mesozooplankton - 38.85 ± 4.28 (SE) $mg.m^{-3}$. The fodder mesozooplankton biomass could be characterised as low for the season.

Analysis of spatial distribution of the mesozooplankton biomass showed a tendency of increasing values in the north direction (Fig. I.4.2) and formation of two well expressed blooms of *N. scintillans* - one in the region of c. Kalikara and the second - in front of Sozopol (Fig. I.4.2). The *N. scintillans* bloom, registered in the northern sector covered larger area and spread between Kaliakra - Kamchia, indicating water eutrophication.

Project proposal № BG14MFOP001-3.003-0001 "Collection, management and use of data for the purposes of scientific analysis and implementation of the Common Fisheries Policy for the period 2017-2019", funded by the Maritime Affairs and Fisheries Program, co-financed by the European Union through the European Maritime and Fisheries Fund

Table I.4.3. Summary statistics of zooplankton biomass by groups and total, October – December 2017

	Mesozooplankton	Protozoa	Jelly - plankton	Total zooplankton biomass
Mean	38.85	1341.91	210.63	1591.39
Standard Error	4.28	365.55	119.05	396.43
Median	36.65	1068.41	0.00	1081.46
Standard Deviation	15.44	1318.00	429.26	1429.33
Skewness	0.16	1.48	2.51	0.94
Range	49.79	4321.46	1477.07	4281.28
Minimum	13.06	142.81	0.00	205.65
Maximum	62.85	4464.27	1477.07	4486.93
Sum	505.07	17444.77	2738.23	20688.06

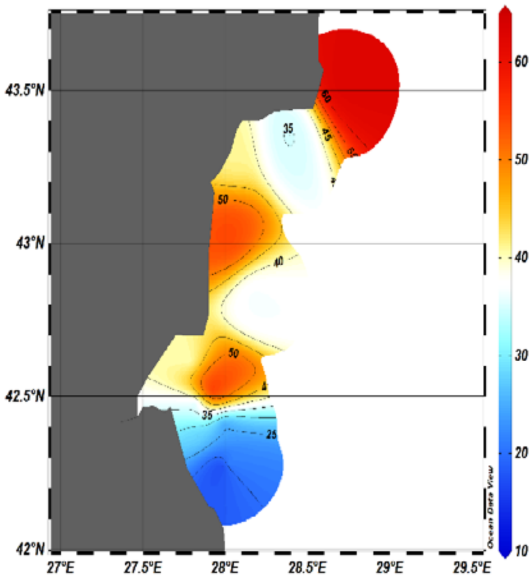

1.

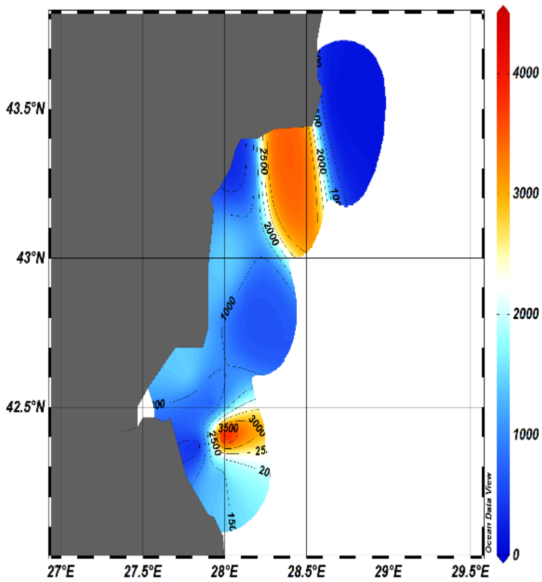

2.

Fig. I.4.2. Spatial distribution of the fodder mesozooplankton biomass (1, mg.m^{-3}) and *N. scintillans* biomass (2, mg.m^{-3}) in October – December 2017

II. 2018 – 1st Survey

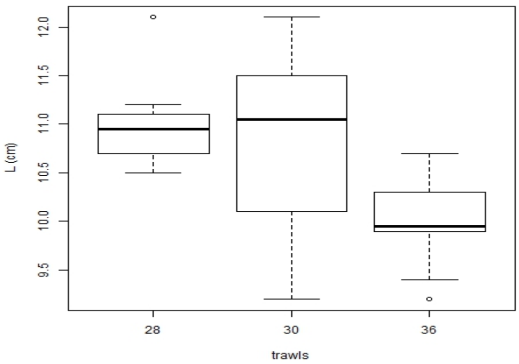

1.

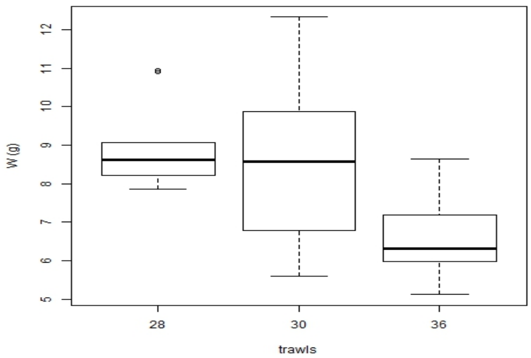

2.

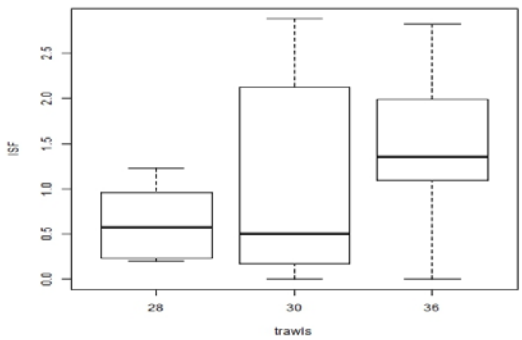

3.

Fig. II.1. Box plot: Distribution of sprat (1) length (cm), (2) weight (g), (3) ISF (% BW) per trawls (median values, 25 – 75 % hinge, minimal and maximal values) in October – December 2018

The highest average values of ISF = 1.45 % BW (Fig. II.2) were determined in a sample from trawl 36, located near to c. Emine, while minimal values of ISF were detected in front of c. Kalikara (Fig. II.2).

Project proposal № BG14MFOP001-3.003-0001 "Collection, management and use of data for the purposes of scientific analysis and implementation of the Common Fisheries Policy for the period 2017-2019", funded by the Maritime Affairs and Fisheries Program, co-financed by the European Union through the European Maritime and Fisheries Fund

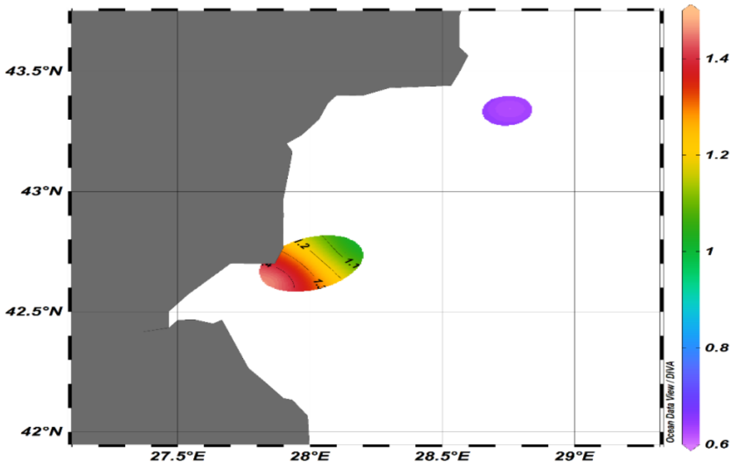

Fig. II.2. Spatial distribution of ISF (% BW) in December 2018

Statistically significant relationship was not detected between the ISF (% BW) and sprat weight within the limits 5.13 - 12.33 g.

Species composition, prey number (PN) and index of relative importance (IRI) of mesozooplankton in the sprat diet

In early December 2018, the average prey number (PN) in the sprat stomachs attained 94 ind/stomach, comparable by range with the mean PN through 2007-2010 - 64 ind/stomach, but 3.5 times lower than the mean PN in December 2016 - 328 ind/stomach.

The maximal number of prey items - 236 ind/stomach was established in a sample from station 36 (at 28-m depth, near to c. Emine). At the same station, the mean prey number (PN) attained 136 ind/stomach, by maximal ISF value and high consumption of the zooplankton species *Parasagitta setosa*. Spatially, the high average PN > 100 ind/stomach were detected in front of c. Emine (Fig. II.3).

Analysis of zooplankton samples, gathered from the marine environment in December 2018, showed a total diversity of 18 mesozooplankton species/groups, but only 8 species/groups were found in the sprat diet. In the sprat diet were identified several copepods: *Calanus euxinus*, *Pseudocalanus elongates*, *Paracalanus parvus*, *Acartia clausi*, Copepoda spp; the group of pelagic larvae of bottom species (meroplankton) was represented by Decapoda larvae; class Chaetognatha was represented by the species *Parasagitta setosa* and class Appendicularia – by *Oicopleura dioica*.

The indices of relative importance (IRI) of the main mesozooplankton representatives in sprat food spectrum (based on the percent shares from total abundance and biomass, and frequency of occurrence in samples) are presented in Table II.1.

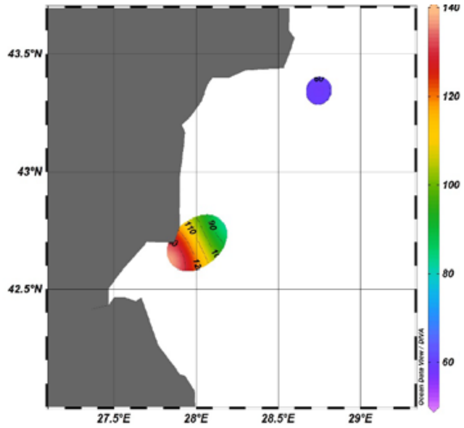

Fig. II.3. Spatial distribution of average prey number (PN) by trawls in Decemeber 2018

Table II.1. The sprat food composition of in December 2018

	N (% of total abundance)	*M (% of total biomass)*	*FO (Frequency of occurrence)*	*IRI (Index of relative importance)*
Calanus euxinus	56.74	66.78	90.00	11154.23
Parasagitta setosa	28.91	32.30	46.67	4733.40
Acartia clausi	10.20	0.81	30.00	658.57
Oicopleura dioica	3.12	0.03	20.00	156.53
Pseudocalanus elongatus	0.46	0.02	20.00	16.17
Decapoda larvae	0.25	0.06	10.00	5.55
Others	0.32	0.01		
Total	100%	100%		

The sprat food was dominated by copepod *Calanus euxIinus*, followed *by Parasagitta setosa*, *Acartia clausi*, *Oicopleura dioica*, *Ps. elongatus* and Decapoda larvae (Table II.2, Table II.4; Fig.II.5).

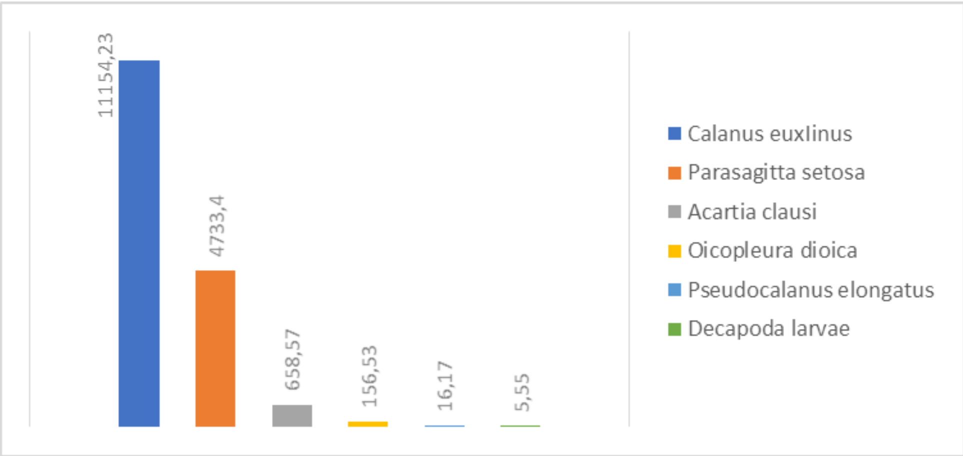

Fig. II.4. IRI of different mesozooplankton species in the sprat food in November – December 2018

Cold-water species predominated sprat food by abundance and biomass, and showed the highest frequency of occurrence (Table II.2).

Table II.2. Distribution of IRI (%) of main mesozooplankton species in sprat food per trawling stations

Sprat food composition	**Trawl 28, 81m**	**Trawl 30, 18m**	**Trawl 36, 28m**
Calanus euxInus	99.8	70.17	28.88
Parasagitta setosa	0.17	9.23	70.82
Acartia clausi		16.48	0.04
Pseudocalanus elongatus	0.01	0.01	0.25
Paracalanus parvus		0.06	0.004
Copepoda spp.	0.01		
Decapoda larvae	0.01	0.12	
Oikopleura dioica		3.93	0.004
	100	100	100

Parasitic nematodes were discovered in 10 % of a total of 30 sprat specimens.

Trachurus mediterraneus: weight structure, index of stomach fullness (ISF)

The mean absolute length of investigated horse mackerel specimens reached 9.86 cm ± 1.47 (SD) cm, varying between 7.7 – 15.8 cm, while the mean weight was 8.42 g ± 5.59 (SD), varying from 3.97 g to 33.96 g (Fig. II.5).

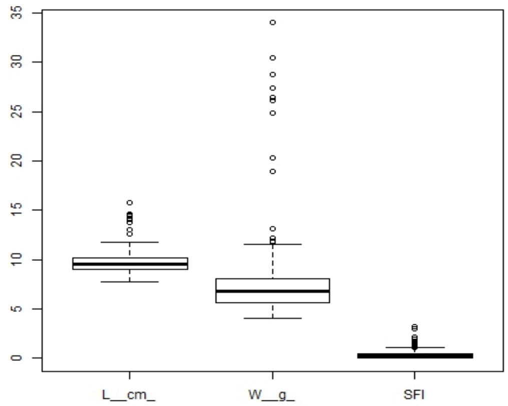

Fig. II.5. Boxplot: horse mackerel size (cm), weight (g) and index of stomach fullness (ISF, % BW) in December 2018

The mean value of stomach fullness index reached 0.40 % BW ± 0.56 (SD) during the studied period. The highest mean values of ISF (ISF = 0.7 - 1 % BW) were found in Bourgas Bay and in open sea along the central coast (Fig. II.6).

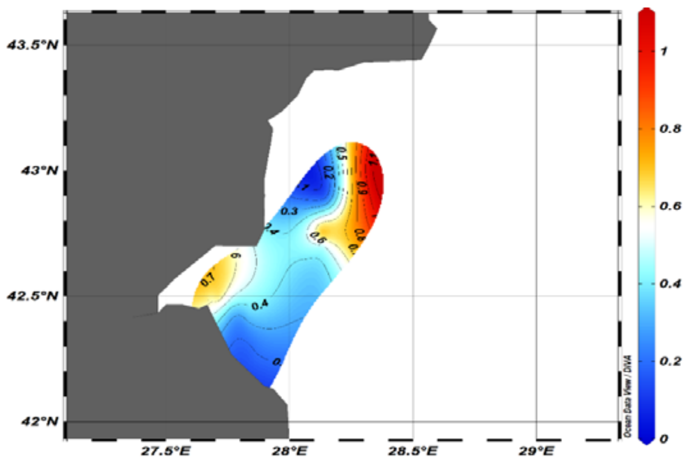

Fig. II.6. Spatial distribution of horse mackerel ISF (% BW) in November-December 2018

Between the ISF and horse mackerel body weight (within the span 3.97 - 33.96 g) was not established statistically significant dependence.

Species composition, PN and index of relative importance (IRI) of mesozooplankton in the horse mackerel diet

In November – December 2018, the average prey items number (PN) attained 11.94 ind/stomach ± 2.36 (SE). The maximal individual PN - 160 ind/stomach was found in specimens, collected in front of Byala (Fig. II.7), connected to high consumption of the copepod *Calanus euxinus.*

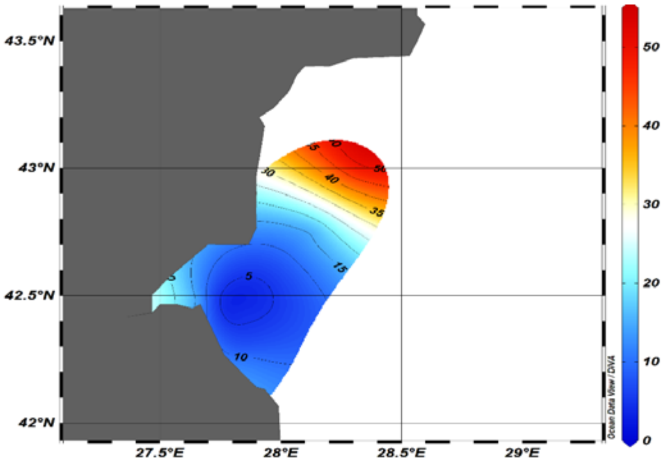

Fig. II.7. Spatial distribution of average prey number (PN per trawls) in horse mackerel ration in November-December 2018

In the horse mackerel stomach content, a total of 13 zooplankton species/groups and larvae of benthic Isopoda were identified. The meroplankton included: Cirripedia larvae, *Lamellibranchia veliger* and Decapoda larvae; from crustacean copepods, the following species were recorded: *Calanus euxinus*, *Paracalanus parvus*, *Acartia clausi*, *Pseudocalanus elongatus*, *Oithona davisae*, *Copepoda* spp; class Chaetognatha was represented by the species *Parasagitta setosa*. In horse mackerel food spectrum were discovered also Appendicularia, *Pleurobrachia pileus*, Izopoda larvae and youth stages of *Aurelia aurita*.

The indices of relative importance (IRI) of the main mesozooplankton species in the horse mackerel diet are presented in Table II.3.

Table II.3. Horse mackerel food composition in November- December 2018

Zooplankton	N (% of total abundance)	M (% of total biomass)	FO (Frequency of occurrence)	IRI (Index of relative importance)
Calanus euxinus	48.96	85.42	48.79	7453.34
Cirripedia cypris	8.02	0.43	23.61	381.19
Parasagitta setosa 5.5 - 11.4 mm	6.51	9.04	6.85	304.72
Pseudocalanus elongatus	9.18	1.38	15.68	240.92
Copepoda	9.91	1.35	3.33	74.27
Pleurobrachia pileus	0.38	1.91	1.67	45.96
Lamellibranchia veliger	2.63	0.06	10.19	39.94
Oikopleura dioica <2.5 mm	1.05	0.02	6.76	22.62
Paracalanus parvus	1.08	0.02	6.67	17.18
Acartia clausi	1.44	0.10	4.26	15.52
Others	10.84	0.28		
Total	100%	100%		

The cold-water copepod *C. euxinus* formed the highest proportion in the horse mackerel diet by IRI in November – December 2018, while other components, such as *Parasagitta setosa*, *Pseudocalanus elongates* and meroplanktonic Ciirripedia had lower importance as food sources.

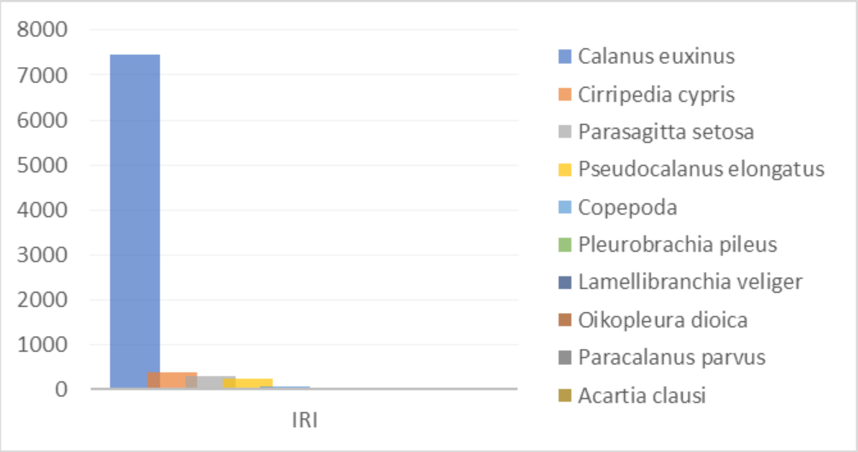

Fig. II.8. IRI of mesozooplankton species in the horse mackerel diet in November – December 2018

Project proposal № BG14MFOP001-3.003-0001 "Collection, management and use of data for the purposes of scientific analysis and implementation of the Common Fisheries Policy for the period 2017-2019", funded by the Maritime Affairs and Fisheries Program, co-financed by the European Union through the European Maritime and Fisheries Fund

The species *C. euxinus* formed between 64.29 % - 100 % of horse mackerel food content per stations and was detected almost in all samples (Table II.4). However, mostly in the Bourgas Bay region, the role of Cirripedia larvae was increased in the horse mackerel food , while the share of chaetognath *P. setosa* was maximal below c. Maslen Nos (Fig. II.9).

Table II.4. Distribution of IRI (%) of main mesozooplankton species in the horse mackerel diet per stations

Horse mackerel food composition	7 m	7 m	1 0 m	7 9 m	8 0 m	0 5 m	1 6 m	2 6 m	4 2 m	5 4 m	3 7 m	4 4 m
Calanus euxinus	2.44	9.98	7.66	2.63	4.29	5.30	7.76	9.22		8.93	00	9.94
Pseudocalanus elongatus	.21	.35	.57							.02		
Paracalanus parvus	.21		.64				.47	.03		.19		
Acartia clausi	.42	.16	.16							.60		
Oithona davisae	.20											
Copepoda spp.	.70	.64										
Cirripedia cypris	.62	.12	.18	5.83	6.31	4.70	.27	.03				.06
Lamellibranchia veliger	.60	.02	.77	.54	.19					.19		
Oikopleura dioica	.77	.34			.04			.03		.05		
Parasagitta setosa	2.73	.37	.03				.03	.49				
Pleurobrachia pileus	4.12											
Decapoda larave							.38	.16				
Isopoda larvae										.01		
Others					4.17		.09	.04		.01		

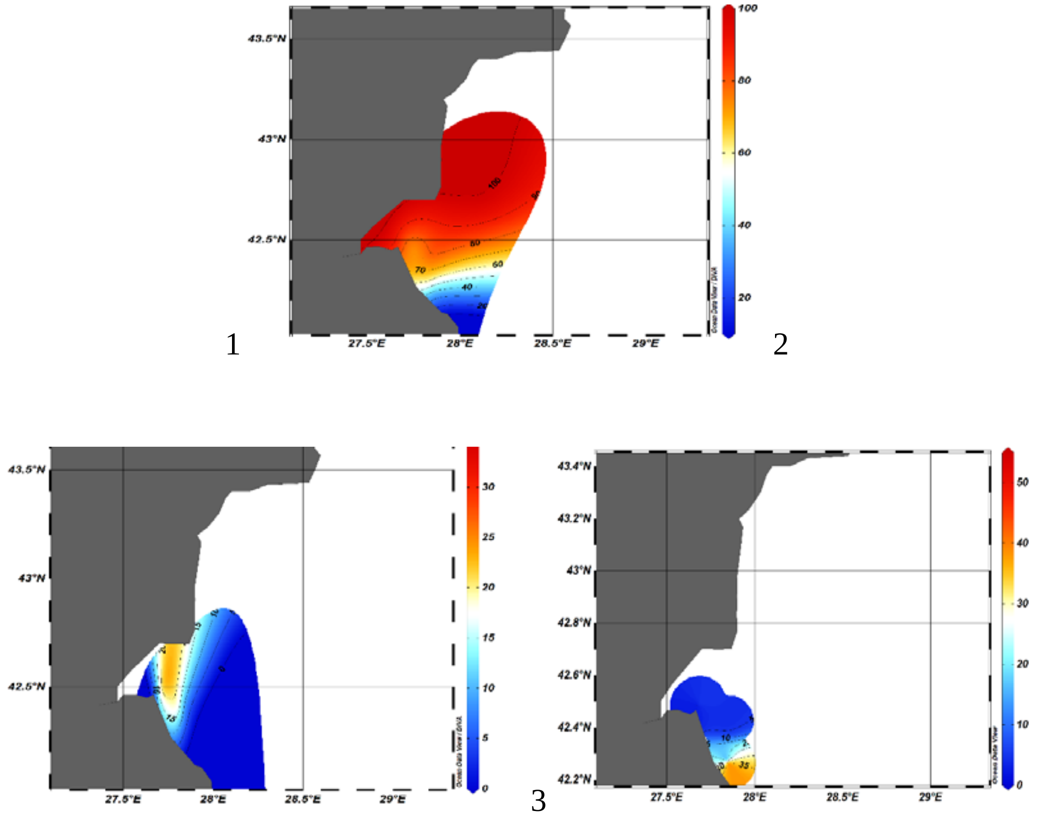

Fig. II.9. Distribution of IRI (%) of zooplankton species (1) *C. euxinus*, (2) *C. cypris* and (3) *Parasagitta setosa* in the horse mackerel food in November-Decembre 2018

Parasitic Nematoda were discovered in 26 % of the investigated horse mackerel specimens.

Mullus barbatus: length - weight parameters, index of stomach fullness (ISF)

The mean absolute length of investigated red mullet specimens reached 9.9 cm ± 0.99 (SD), varying between 8.50 – 11.70 cm, by mean weight - 9.27 g ± 2.99 (SD), varying from 5.11 g to 14.97 g. The mean value of the index of stomach fullness index reached 0.63 % BW ± 0.54 (SD) (Fig. II.10).

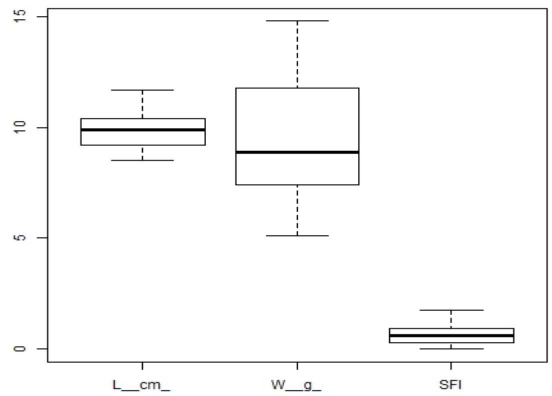

Fig. II.10. Boxplot: red mullet size (cm), weight (g) and Index of stomach fullness (ISF, % BW) in November 2018

Between the red mullet body weight (from 5.11 g to 14.97 g) and ISF was not found statistically significant relationship.

Species composition, PN and index of relative importance (IRI) of mesozooplankton in the red mullet diet

In December 2018, the average prey items number (PN) in stomachs of the investigated red mullet specimens attained 13.4 ind/stomach ± 5.51 (SE). The maximal individual PN - 55 ind/stomach was connected to consumption of polychaete *Nephthys* spp.

In the red mullet diet, a total of 7 benthic and plankton species/groups were detected. The meroplankton included *Lamellibranchia veliger*; from crustacean copepods were recorded *Harpacticoida* spp; class Gastropoda was presented by the species *Retusa variabilis*.

In the red mullet food spectrum were discovered also Terebelides, Nemertina and Amphipoda.

The indices of relative importance (IRI) of the main mesozooplankton species in the red mullet diet are presented in Table II.5.

Table II.5. The red mullet food composition in December 2018

Red mullet food composition	N (% of total abundance)	M (% of total biomass)	FO (Frequency of occurrence)	IRI (Index of relative importance)
Nephthys spp.	92.5	15.6	80.0	8653.0
Harpacticoida spp.	0.7	45.1	10.0	458.9
Lamellibranchia veliger	0.7	22.9	10.0	236.6
Amphypoda	1.5	1.4	20.0	57.6
Retusa variabilis	1.5	0.7	20.0	43.7
Nemertina	0.7	0.3	10.0	10.9
Terebelides	0.7	0.0	10.0	7.5
others	1.70	14.00		
Total	100%	100%		

The polychaete *Nephthys* spp. dominated in the red mullet food (Fig. II.11), by relatively low presence of *Harpacticoida* spp. and meroplanktonic Lamellibranchia in the ration.

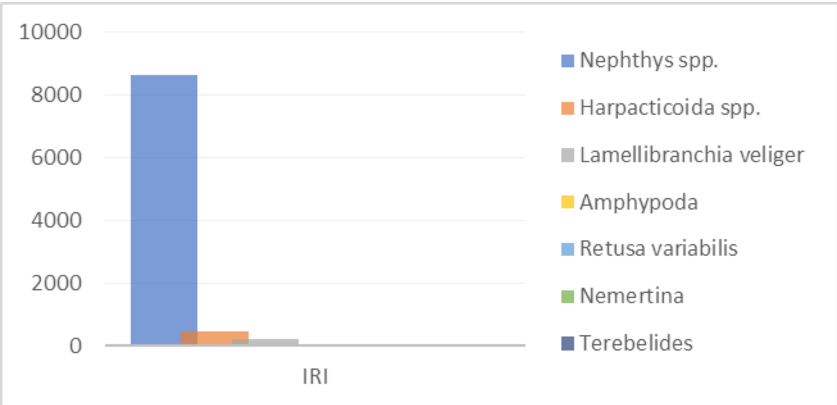

Fig. II.11. IRI of mesozooplankton species in the red mullet diet in November 2018

Parasitic Nematoda were discovered in 20 % of the investigated red mullet specimens.

Zooplankton in marine environment: species composition and biomass

During the studied period the zooplankton biodiversity was formed by 23 species – 22 species were identified in November and 18 species - in December 2018 (Table II.6). Presence of seasonal warmwater species *Penilia avirostris* and *Centropages ponticus* was detected in November 2018, corresponding to warm autumn and relatively high sea surface water temperatures.

Table II.6. Zooplankton species diversity

Zooplankton species composition	XI.2018	XII.2018
Noctiluca scintillans	+	+
Beroe ovata	+	
Pleurobrachia pileus		+
Aurelia aurita	+	+
Acartia clausi	+	+
Acartia tonsa	+	+
Calanus euxinus	+	+
Paracalanus parvus	+	+
Pseudocalanus elongatus	+	+
Centropages ponticus	+	
Oithona davisae	+	+
Oithona similis	+	+
Pleopis polyphemoides	+	
Penilia avirostris	+	
Cirripedia nauplii, cypris	+	+
Gastropoda veliger	+	+
Lamellibranchia veliger	+	+
Polychaeta larave	+	+
Isopoda larvae	+	+
Phoronis larvae	+	
Parasagitta setosa	+	+
Oicopleura dioica	+	+
Pisces ova, larvae	+	+
Total	22	18

Project proposal № BG14MFOP001-3.003-0001 "Collection, management and use of data for the purposes of scientific analysis and implementation of the Common Fisheries Policy for the period 2017-2019", funded by the Maritime Affairs and Fisheries Program, co-financed by the European Union through the European Maritime and Fisheries Fund

The jellyfish *Aurlia aurita* (Scyphozoa) had dominant position in the total zooplankton biomass formation with a share of 98.20 % (Fig. II.12, Table II.7), whereas the portion of mesozooplankton biomass was very low - 1.80 %. Copepods and Protozoa had leading position by abundance, generating 47.78 % and 26.68 % of the total zooplankton abundance during the studied period.

In November-December 2018, a significant increase of *Parasagitta setosa* (Chaetognatha) biomass was found in comparison with the previous years, so that the mean biomass of this species attained 18.73 mg.m^{-3}, i.e 1.6 times higher than the copepods biomass.

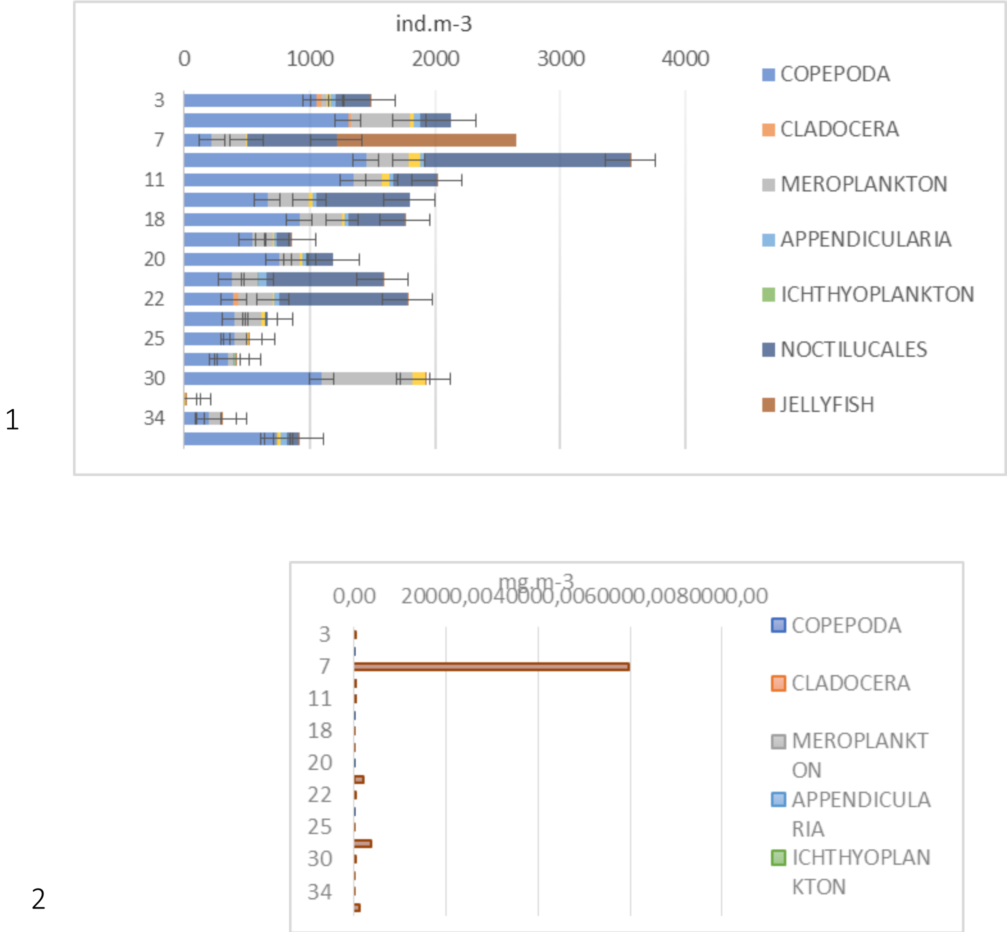

Fig. II.12. Distribution of abundance (1) biomass (2) of the main zooplankton groups per stations in November – December 2018

Table II.7. Percentage distribution (% of total biomass) of the main mesozooplankton groups per stations in November – December 2018

Trawl	Copepods	Cladocerans	Meroplankton	Appendicularia	Noctiluca	Parasagitta	Jellyfish	Total zooplankton biomass (mg.m^{-3})
	2.59	0.38	0.13	0.09	3.12	1.81	91.90	516.16
	44.78	2.81	5.96	0.91	31.21	14.33	0.00	46.14
	0.01	0.00	0.00	0.00	0.07	0.00	99.92	59759.26
	9.60	0.00	1.25	0.11	39.33	19.13	30.59	251.11
1	24.38	0.00	1.96	0.24	20.65	41.48	1.29	101.12
7	12.35	0.00	3.70	0.38	62.20	21.37	0.00	71.87
8	24.65	0.00	7.19	0.66	52.93	12.18	2.38	50.33
9	33.96	0.00	8.11	1.20	29.37	19.20	8.16	22.06
0	28.34	0.00	4.81	0.82	39.79	26.24	0.00	33.93
1	0.46	0.00	0.11	0.03	2.67	0.10	96.64	2085.48
2	6.79	1.32	1.88	0.32	51.95	3.06	34.69	118.51
4	23.84	0.00	3.20	0.00	2.49	70.47	0.00	45.95
5	19.60	0.00	2.25	0.00	0.00	48.00	30.15	50.94
8	0.13	0.00	0.01	0.00	0.00	0.04	99.82	3854.25
0	10.14	0.00	6.82	0.00	0.00	81.54	1.50	127.71
3	0.46	0.00	0.42	0.00	0.00	68.74	30.38	4.60
4	30.15	0.00	8.78	0.00	0.00	34.03	27.04	11.36
6	1.47	0.00	0.01	0.02	0.42	1.49	96.59	1406.10

Table II.9 shows general statistical data about the total zooplankton biomass variability in November-December 2018, including the three main groups: mesozooplankton, Protozoa and jellyfish.

The total zooplankton biomass attained 3808.72 mg.m^{-3} ± 3299.65 (SE), while only the jellyfish biomass reached 3753.2 mg.m^{-3} ± 3300.1 (SE), and that of the fodder mesozooplankton was low - 32.84 mg.m^{-3} ± 7.25 (SE). The quantity of fodder mesozooplankton could be characterized as alike to the previous year levels.

Table II.9. General statistical data on biomass (mg.m^{-3}) of the main zooplankton groups in autumn 2018

	Mesozooplankton	Protozoa	Jellyfish	Total zooplankton biomass
Mean	32.84	22.69	3753.2	3808.72
Standard Error	7.25	6.54	3300.1	3299.65
Median	24.10	13.89	7.2	86.49
Standard Deviation	30.75	27.74	14001.2	13999.21
Sample Variance	945.78	769.36	196033671.4	195977865.07
Kurtosis	4.07	1.92	17.8	17.78
Skewness	1.90	1.47	4.2	4.21
Range	122.60	98.76	59709.3	59754.66
Minimum	3.20	0.00	0.0	4.60
Maximum	125.80	98.76	59709.3	59759.26
Sum	591.15	408.48	67557.3	68556.89
Count	18.00	18.00	18.00	18.00
Confidence level(95.0%)	15.29	13.79	6962.6	6961.64

The mesoplankton biomass was maximal in north direction (Fig. II.13-1) as high quantities of *N. scintillans* were detected in Bourgas Bay and Primorsko (Fig. II.13-2). The species *Parasagitta setosa* formed high concentration along the central shore and up to c. Kaliakra (Fig.II.13-3), while the gelatinous zooplankton was most abundant on the south, in front of Sozopol and Primorsko (Fig. II.13-4).

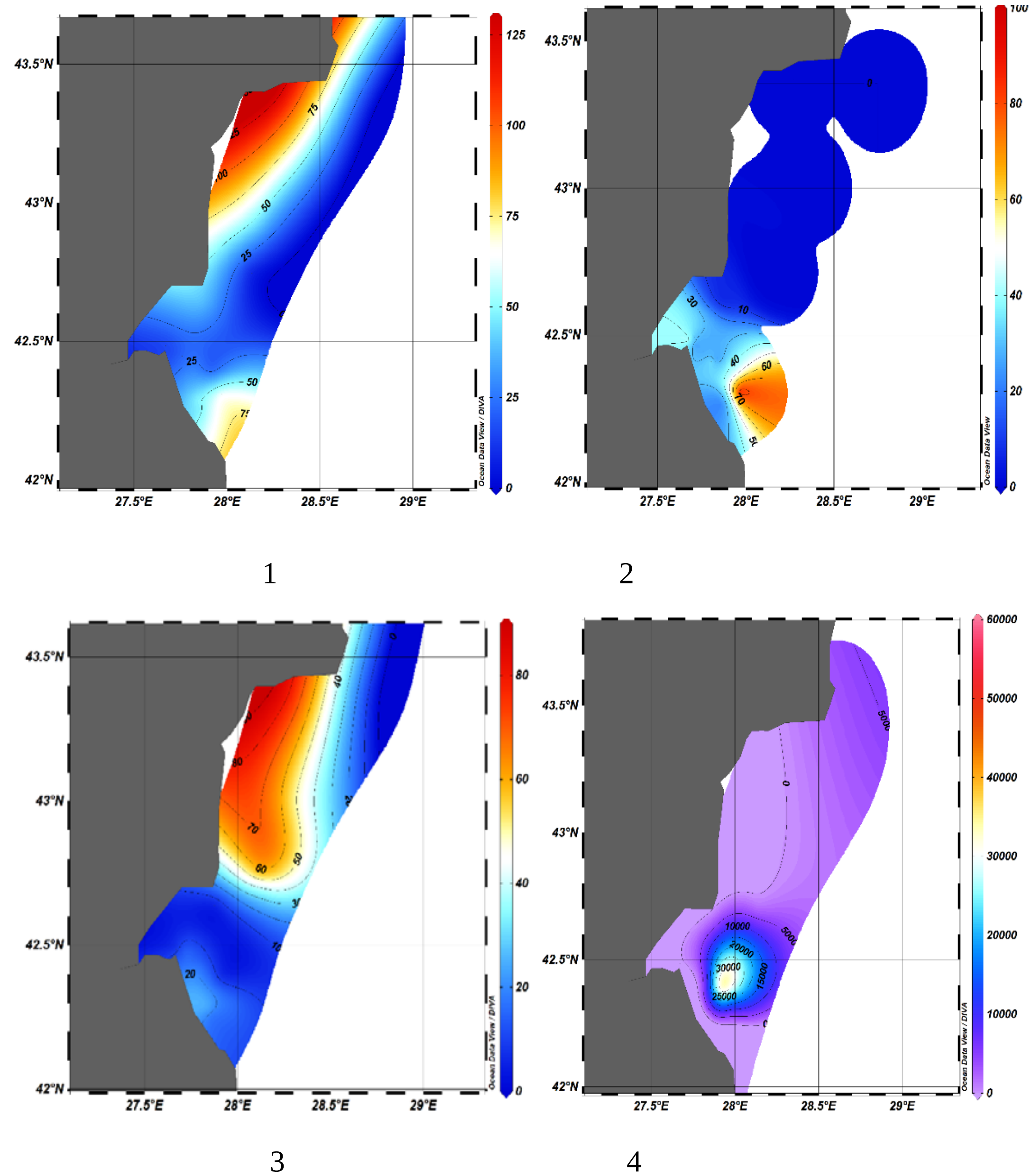

Fig. II.13. Spatial distribution of the fodder mesozooplankton biomass (mg.m^{-3}): (1) *N. scintillans* (Protozoa) (2) *Parasagitta setosa*, (3) Chaetognatha and (4) jellyfish in November-December 2018

Project proposal № BG14MFOP001-3.003-0001 "Collection, management and use of data for the purposes of scientific analysis and implementation of the Common Fisheries Policy for the period 2017-2019", funded by the Maritime Affairs and Fisheries Program, co-financed by the European Union through the European Maritime and Fisheries Fund

III. 2018 – 2nd Survey

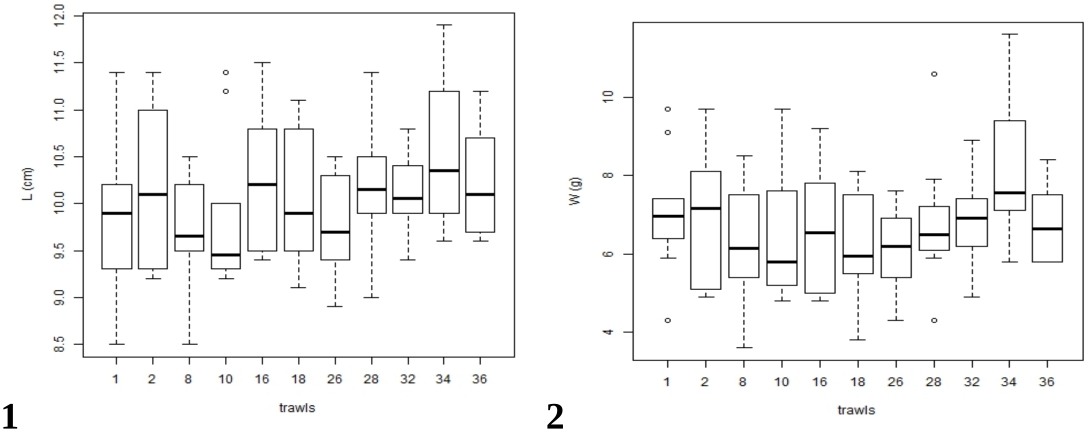

Fig. III.0.1. Boxplot (median values, 25 – 75 % hinge, minimal and maximal values) Distribution of sprat length (1, cm) and weight (2, g) per trawls in December 2018

The weight-length dependence for sprat could be described by the following equation: Log WW(g)=2.8631*Log L(cm) – 2.0495; (r^2=0.78, p<0.001 (Fig. II.0.2).

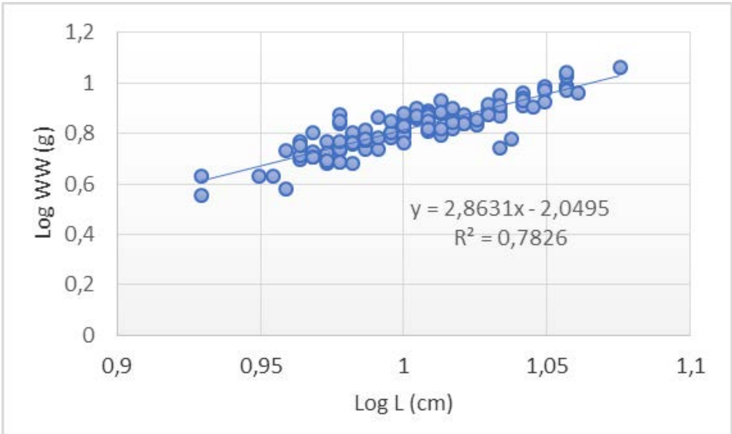

Fig. III.0.2. Weight-length relationship of sprat, investigated in December 2018

In the period from middle to late December 2018, the mean value of the index of stomach fullness (ISF) reached 1.20 % BW ± 1.05 (SD) (Table II.0.1). ISF in late December 2018 was with 63.74 % higher than the average level of ISF in 2017 (0.62 % BW). This index showed an increase with 18.87 % in comparison with the first stage of the study.

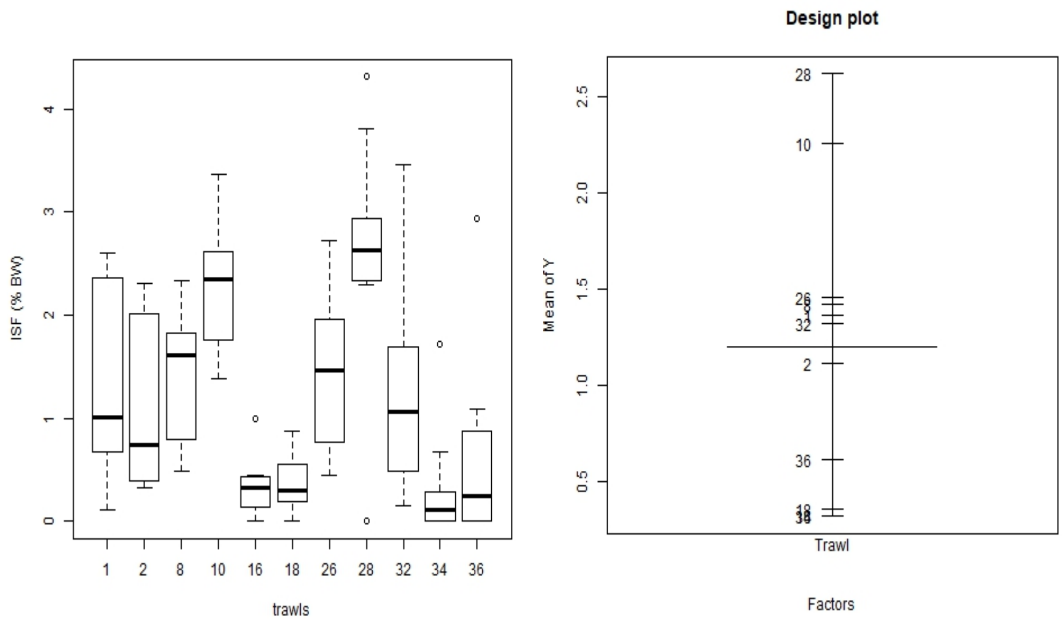

1 2

Fig. III.0.3. (1) Box plot: sprat index of stomach fullness (ISF, % BW) in late December 2018. (2) Design plot: distribution of mean ISF (% BW) by trawls

The highest mean values of ISF = 2.25 -2.61 % (Fig. III.0.4) were detected in trawls 28 and 10 in front of Sozopol and in Chernomorets, Varna region. ISF showed minimal levels in front of c. Emine and in the northern part of Bourgas Bay (Fig. III.0.4).

Project proposal № BG14MFOP001-3.003-0001 "Collection, management and use of data for the purposes of scientific analysis and implementation of the Common Fisheries Policy for the period 2017-2019", funded by the Maritime Affairs and Fisheries Program, co-financed by the European Union through the European Maritime and Fisheries Fund

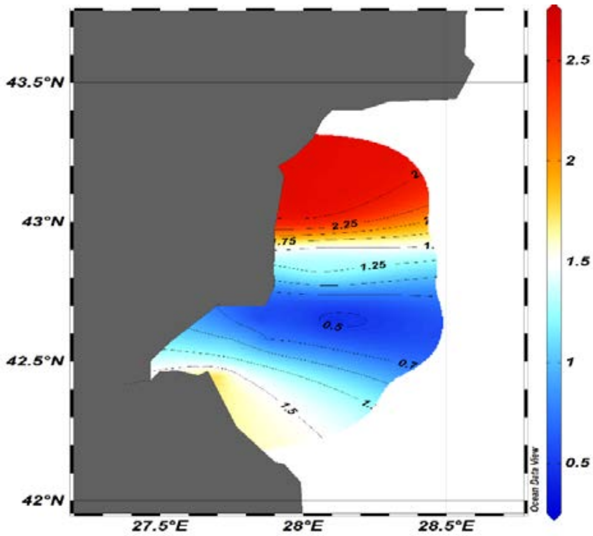

Fig. III.0.4. Spatial distribution of ISF (% BW) in December 2018

Between ISF and sprat weight within the limits of 3.61 - 11.61 g was not established statistically significant difference.

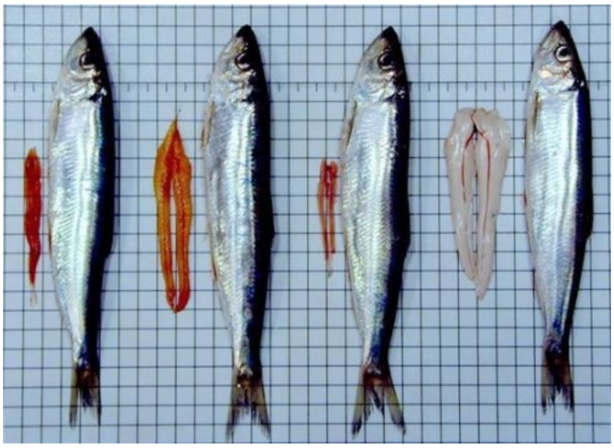

Photo III.0.1. Ovaries of clupeids (source: Internet)

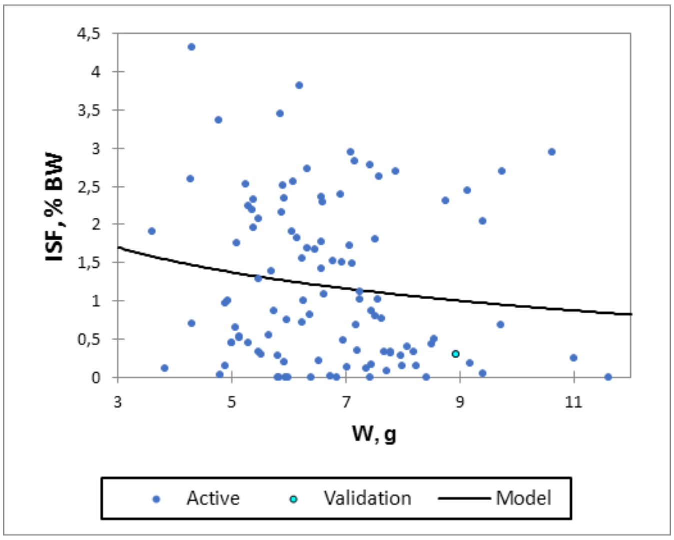

Fig. III.0.5. Scatterplot: Relationship between sprat weight (WW, g) and ISF (% BW)

Prey number, species composition and index of relative importance (IRI) of mesozooplankton species in the sprat diet

The average prey number (PN) in the sprat diet accounted to 100 ind/stomach ± 91.49 (SD), comparable with data from the first stage of the study. The maximal individual PN - 356 ind/stomach was found in front of Chernomorec (trawl 28, depth 22 m), by average PN - 233 ind/stomach and maximal ISF - 2.62 % BW, due to intensive consumption of *Calanus euxinus*. In spatial aspect, the highest PN > 150 ind/stomach were detected in north direction, above the town of Byala and near Varna region (Fig. III.0.6).

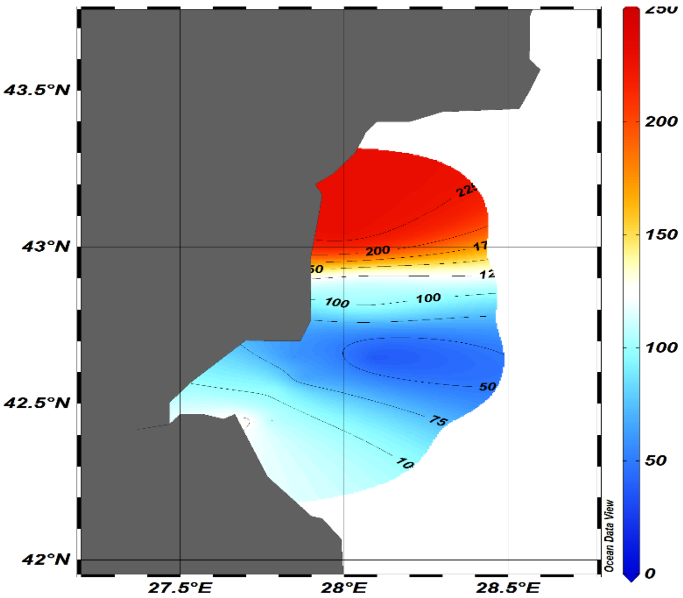

Fig. III.0.6. Spatial distribution of the average prey number (PN) per trawls in December 2018

Twenty mesozooplankton species/groups were identified in the marine environment during the studied period, but only 11 species/groups were detected in the sprat diet. In the sprat food, Copepods were represented by several species: *Calanus euxinus*, *Pseudocalanus elongatus*, *Acartia clausi*, *Oithona* spp., *Paracalanus parvus*, *Copepoda nauplii*, *Copepoda* spp.; three taxonomic groups were found from the pelagic larvae of bottom species (meroplankton) - *Lamellibranchia veliger*, *Cirripedia cypris* and Decapoda larvae; class Chaetognatha was represented by the species *Parasagitta setosa*, class Appendicularia - by *Oicopleura dioica*. The sprat food was more diverse in late December 2018 as compared with the first stage of the survey, but the structure of dominating species remained akin, including two main species - *Calanus euxinus* and *Parasagitta setosa*.

The indices of relative importance (IRI) of the zooplankton species in sprat food spectrum (based on the percent shares from total abundance, biomass and frequency of occurrence in the samples) are presented in Table III.0.1.

Project proposal № BG14MFOP001-3.003-0001 "Collection, management and use of data for the purposes of scientific analysis and implementation of the Common Fisheries Policy for the period 2017-2019", funded by the Maritime Affairs and Fisheries Program, co-financed by the European Union through the European Maritime and Fisheries Fund

Table III.0.1. Sprat food composition in December 2018

Sprat food components	N (% of total abundance)	M (% of total biomass)	FO (Frequency of occurrence)	IRI (Index of relative importance)
Calanus euxinus	68.81	76.31	94.86	13711.73
Parasagitta setosa	17.60	19.77	60.81	3455.89
Pseudocalanus elongatus	3.82	0.15	59.24	301.63
Paracalanus parvus	2.80	0.05	45.28	161.10
Acartia clausi	1.28	0.07	37.53	68.60
Oikopleura dioica	1.12	0.01	20.56	32.01
Copepoda	0.67	0.03	3.33	4.61
Lamellibranchia veliger	0.17	0.00	13.28	4.10
Cirripedia cypris	0.03	0.00	2.39	0.44
Others	3.44	3.61		
Total	100%	100%		

Sprat food was dominated by the copepod *Calanus euxinus*, followed by *Parasagitta setosa*, *Pseudocalanus elongatus*, *Paracalanus parvus* and *A. clausi* (Table III.0.1, Fig. III.0.7). The cold -water species predominated the sprat diet by abundance and biomass, and showed the highest frequency of occurrence.

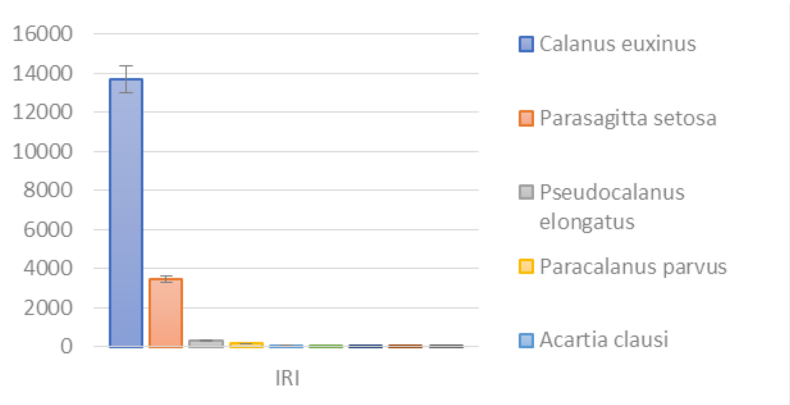

Fig. III.0.7. Mean IRI of mesozooplankton species in sprat food in December 2018

The species *C. euxinus* dominated almost all sprat food samples (with an exception of the samples from the southern Bourgas Bay, in front of Sozopol); the species *Parasagittta setosa* was detected in the sprat ration mostly in the large Bourgas Bay, while *Pseudocalanus elongatus* had an important role in the sprat food off the southern coasts, below Primorsko (Table III.0.2, Fig. III.0.8).

Table III.0.2. IRI (%) of mesozooplankton species in sprat food per trawls in December 2018

Sprat food components	1	2	8	10	16	18	26	28	32	34	36
Calanus euxinus	31.31	22.54	58.02	94.94	99.02	98.70	82.74	93.49	98.11	80.04	96.37
Parasagitta setose	55.36	74.29	30.92	1.61	0.00	0.95	3.97	4.48	0.85	15.83	0.42
Pseudocalanus elongatus	0.90	2.42	5.86	0.45	0.18	0.24	1.24	1.40	0.10	3.08	2.72
Paracalanus parvus	0.35	0.60	3.47	2.89	0.29	0.09	0.17	0.19	0.47	0.15	0.48
Acartia clausi	0.69	0.03	1.35	0.02	0.18	0.00	0.36	0.41	0.33	0.69	0.01
Oikopleura dioica	0.01	0.09	0.34	0.06	0.34	0.00	0.02	0.02	0.04	0.04	0.00
Lamellibranchia veliger	0.01	0.04	0.02	0.03	0.00	0.02	0.01	0.01	0.10	0.00	0.00
Others	11.36	0.01	0.02	0.00	0.00	0.00	11.50	0.00	0.00	0.17	0.00
Total	100	100	100	100	100	100	100	100	100	100	100

Project proposal № BG14MFOP001-3.003-0001 "Collection, management and use of data for the purposes of scientific analysis and implementation of the Common Fisheries Policy for the period 2017-2019", funded by the Maritime Affairs and Fisheries Program, co-financed by the European Union through the European Maritime and Fisheries Fund

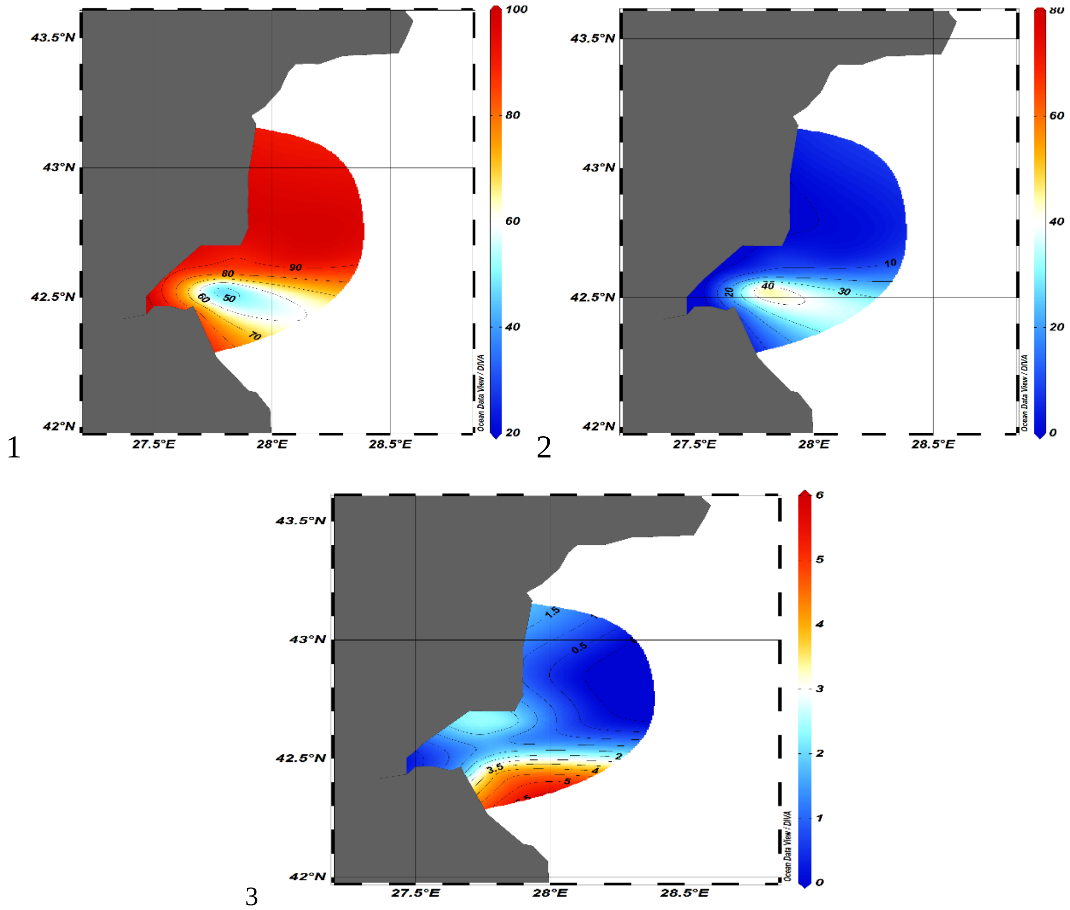

Fig. III.0.8. Spatial distribution of IRI (%) of mesoplankton species in sprat food: (1) *C. euxinus*, (2) *Parasagittta setosa* and (3) *Pseudocalanus elongatus* in December 2018

Parasitic Nematodes were discovered in 9 % of the total of 110 sprat specimens.

***Mullus barbatus*: length and weight parameters, index of stomach fullness (ISF)**

The mean absolute length of the investigated red mullet specimens reached 8.62 cm ± 0.90 (SD), varying between 7.4 - 10 cm, while the mean weight was 6.20 g ± 2.01 (SD), varying from 3.27 g to 10.72 g (Fig. III.0.9). The mean value of stomach fullness index reached 0.94 % BW ± 0.65 (SD) during the studied period (Fig. III.0.9), showing an increase with 39.49 % compared to the data from the first stage of the study in 2018.

Project proposal № BG14MFOP001-3.003-0001 "Collection, management and use of data for the purposes of scientific analysis and implementation of the Common Fisheries Policy for the period 2017-2019", funded by the Maritime Affairs and Fisheries Program, co-financed by the European Union through the European Maritime and Fisheries Fund

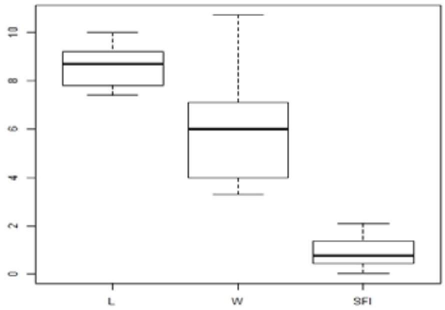

Fig. III.0.9. Boxplot: Red mullet size (L, cm), weight (W, g), and ISF (% BW) in 2018

Prey number, species composition and IRI of different mesozooplankton species in the red mullet diet

In the investigated samples, the mean prey number reached 11.8 ind/stomach ± 4.91 (SE), comparable with data from the first stage of the study. The maximal PN - 36 ind/stomach was found by high consumption of the polychaeta *Nephthys* spp.

In the red mullet stomach content, a total of 3 benthic groups - *Nephthys* spp., *Paramysis* spp. and Cumacea. The indices of relative importance (IRI) of the main food components in the red mullet diet are represented in Table III.0.3.

Table III.0.3. Red mullet food composition in December 2018

Red mullet food components	N (% of total abundance)	M (% of total biomass)	FO (Frequency of occurrence)	IRI (Index of relative importance)
Nephthys sp.	97.5	46.1	100.0	14361.9
Paramysis sp.	1.8	49.1	40.0	2036.0
Cumacea	0.7	4.8	30.0	164.4
Total	**100%**	**100%**		

The polychaeta *Nephthys* spp. dominated in the red mullet food in the studied area in late December 2018 (Table III.0.3, Fig. III.0.10).

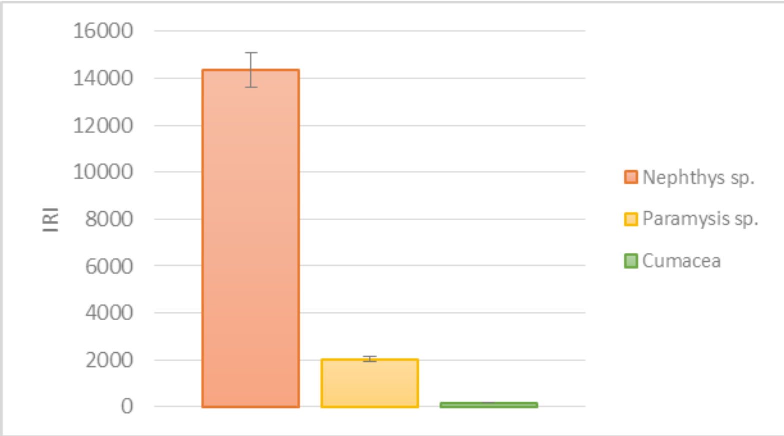

Fig. III.0.10. IRI of mesozooplankton species in the red mullet diet in late December 2018

Zooplankton in marine environment: species composition and biomass

During the studied period the zooplankton biodiversity was formed by 20 species (Table III.0.4).

Table III.0.4. Species diversity of zooplankton

	December 2018
1.	*Noctiluca scintillans*
2.	*Beroe ovata*
3.	*Pleurobrachia pileus*
4.	*Aurelia aurita*
5.	*Acartia clausi*
6.	*Acartia tonsa*
7.	*Pseudocalanus elongatus*
8.	*Calanus euxinus*
9.	*Paracalanus parvus*
10.	*Oithona davisae*
11.	*Oithona similis*
12.	*Harpacticoida* spp.
13.	*Cirripedia nauplii/cypris*
14.	*Lamellibranchia veliger*
15.	Polychaeta larave
16.	*Gastropoda veliger*
17.	Isopoda Larvae
18.	*Parasagitta setosa*
19.	*Oicopleura dioica*
20.	*Pisces ova*, larvae

The main component in the total zooplankton biomass (mg.m^{-3}) was the jellyfish species *Aurelia aurita* (Scyphozoa) - 93.06 %, by low percent share of the fodder mesozooplnakton - 3.73 % (Fig. III.0.11-1, Table III.0.5). Copepoda and meroplankton dominated by abundance, generating respectively 74.64 % and 16.86 % of the total zooplankton abundance (Fig. III.0.11-2).

1 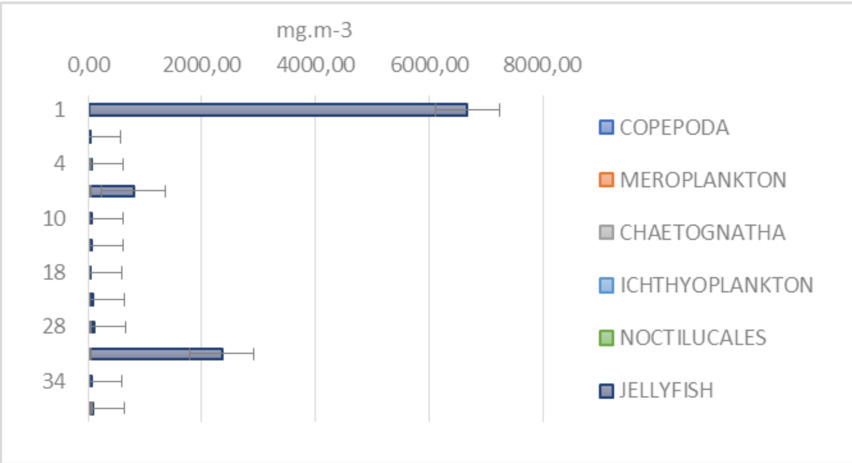

2 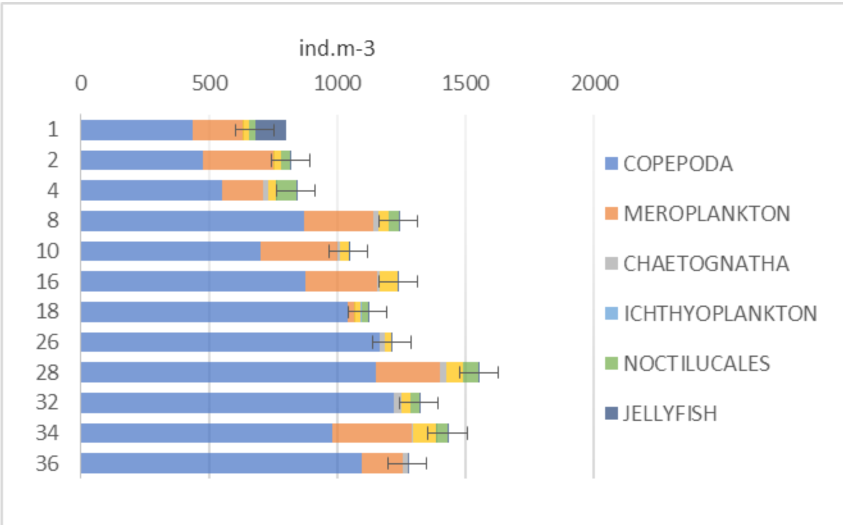

Fig. III.0.11. Distribution of biomass, mg.m^{-3}(1) and abundance, ind.m^{-3}(2) of the main zooplankton groups per stations in late December 2018

Table III.0.5. Percentage distribution (% of total biomass) of the main zooplankton groups per stations in late December 2018

Trawl	COPEPODA	MEROPLANKTON	CHAETOGNATHA	APPENDICULARIA	ICHTHYOPLANKTON	NOCTILUCALES	JELLYFISH	*Total zooplankton biomass (mg.m^{-3})*
1	0.12	0.03	0.00	0.00	0.00	0.02	99.83	6675.32
2	39.97	15.53	0.34	1.11	0.00	11.47	31.58	12.17
4	15.17	3.08	57.30	0.56	0.59	10.42	12.87	39.62
8	1.66	0.33	2.45	0.05	0.00	0.29	95.22	38.45
10	22.85	5.27	19.34	0.36	0.15	0.00	52.02	25.47
16	39.44	5.54	8.46	1.33	0.00	0.00	45.24	28.35
18	44.59	0.21	2.02	0.69	0.45	4.23	47.81	18.51
26	27.79	0.00	14.18	0.20	0.00	0.00	57.83	34.86
28	31.33	1.53	12.29	0.35	0.00	3.58	50.93	51.87
32	1.17	0.00	0.84	0.01	0.00	0.09	97.89	49.76
34	55.89	8.79	19.38	2.13	1.33	8.20	4.28	30.80
36	58.00	1.35	36.31	0.00	0.00	0.00	4.35	63.96

Table III.0.6 shows general statistical data about the total zooplankton biomass variability in late December 2018, including three main groups: mesozooplankton, Protozoa and jellyfish.

The total zooplankton biomass reached 860.66 mg.m^{-3}± 563.44 (SE), as the jellyfish component produced 826.87 mg.m^{-3}± 564.86 (SE), and the fodder mesozooplankton - 32.07 mg.m^{-3} ± 4.61 (SE). The monthly mesozooplankton biomass was close to the levels measured in the first stage of the study, while jelly- plankton biomass decreased with 128 % in comparison to November 2018.

Table III.0.6. General statistical data about biomasses (mg.m^{-3}) of the main zooplankton components in December 2018

	Meso-zooplankton	*Protozoa*	*Jellyfish*	*Total zooplankton biomass*
Mean	32.07	1.72	826.87	860.66
Standard Error	4.61	0.45	564.86	563.44
Median	31.60	1.77	25.51	59.98
Mode	#N/A	0.00	#N/A	#N/A
Standard Deviation	15.98	1.56	1956.72	1951.82
Sample Variance	255.24	2.44	3828764.52	3809584.96
Kurtosis	0.02	-0.41	8.54	8.47
Skewness	0.42	0.49	2.87	2.86
Range	53.84	4.74	6662.33	6657.54
Minimum	10.13	0.00	1.38	17.78
Maximum	63.96	4.74	6663.71	6675.32
Sum	384.79	20.64	9922.49	10327.93
Count	12.00	12.00	12.00	12.00
Confidence Level (95.0%)	10.15	0.99	1243.24	1240.12

During the study, the mesozooplankton biomass increased in north direction (Fig. III.0.12-1), while high quantities of Chaetognatha were registered in Bourgas Bay and in the Obzor - Byala area (Fig. III.0.12-2), where also was localised intensive development of gelatinous zooplankton (Fig.III.0.12-3).

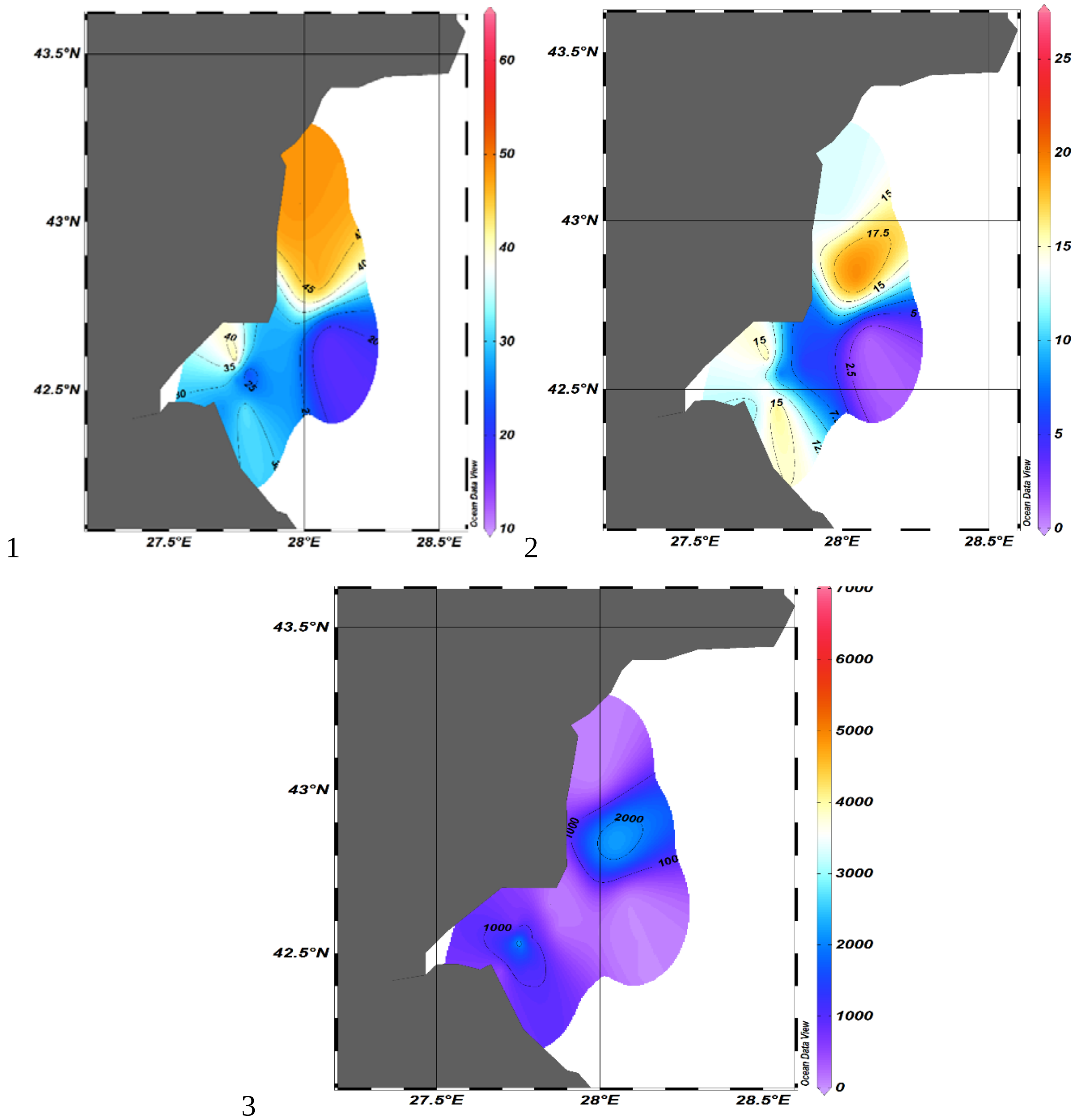

Fig. III.0.12. Spatial distribution of biomass (mg.m^{-3}) of fodder mesozooplankton (1) Chaetognatha (2) and jellyfish (3) in December 2018

IV. 2019 – 1st Survey

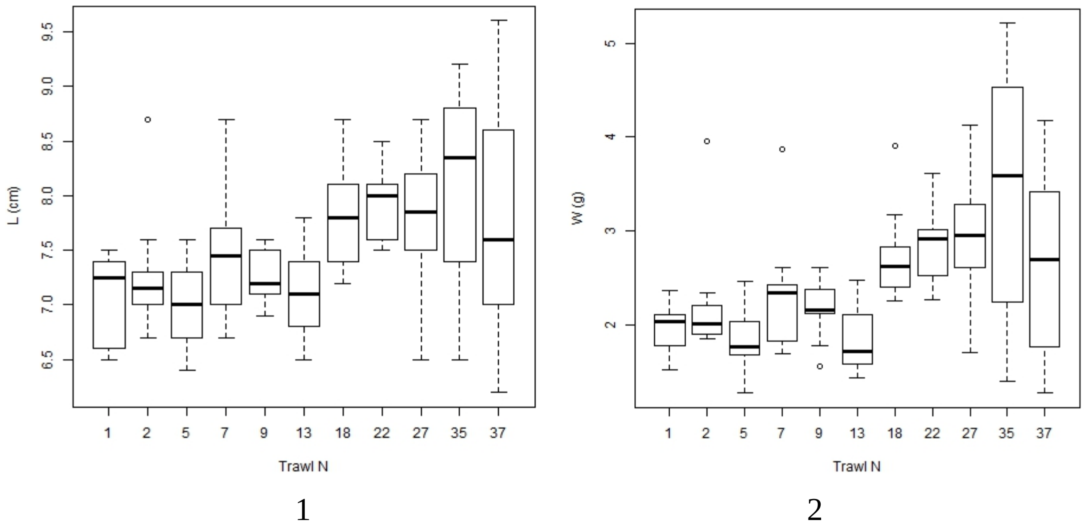

Fig. IV.0.1. Box plot (median values, 25 – 75 % hinge, minimal and maximal values): distribution of sprat length (1, cm) and weight (2, g) per trawls in June 2019

The weight-length dependence for sprat could be described by the following equation: Log WW(g)=3.2522*Log L(cm) - 2.4697; (R2=0.89, p<0.001(Fig. IV.0.2).

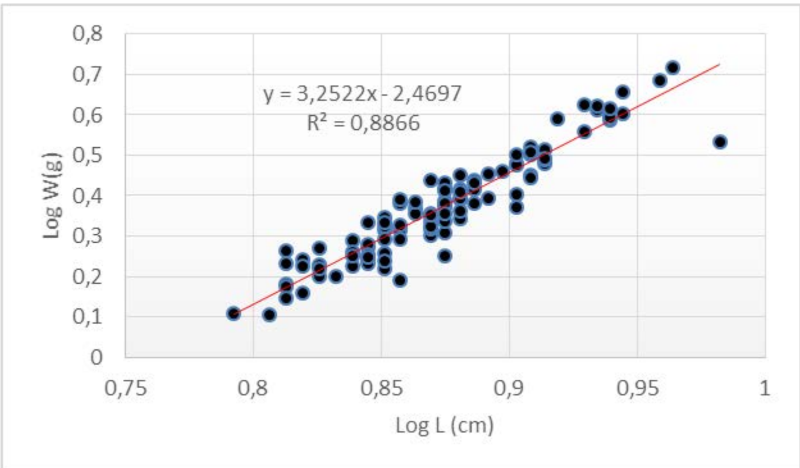

Fig. IV.0.2. Sprat weight-length relationship in June 2019

In June 2019, the average value of the index of stomach fullness reached 0.80% ± 0.53 (SD) of the sprat weight. ISF in June 2019 exceeded by 40.60% the average for springs 2007 - 2010 (0.53% BW).

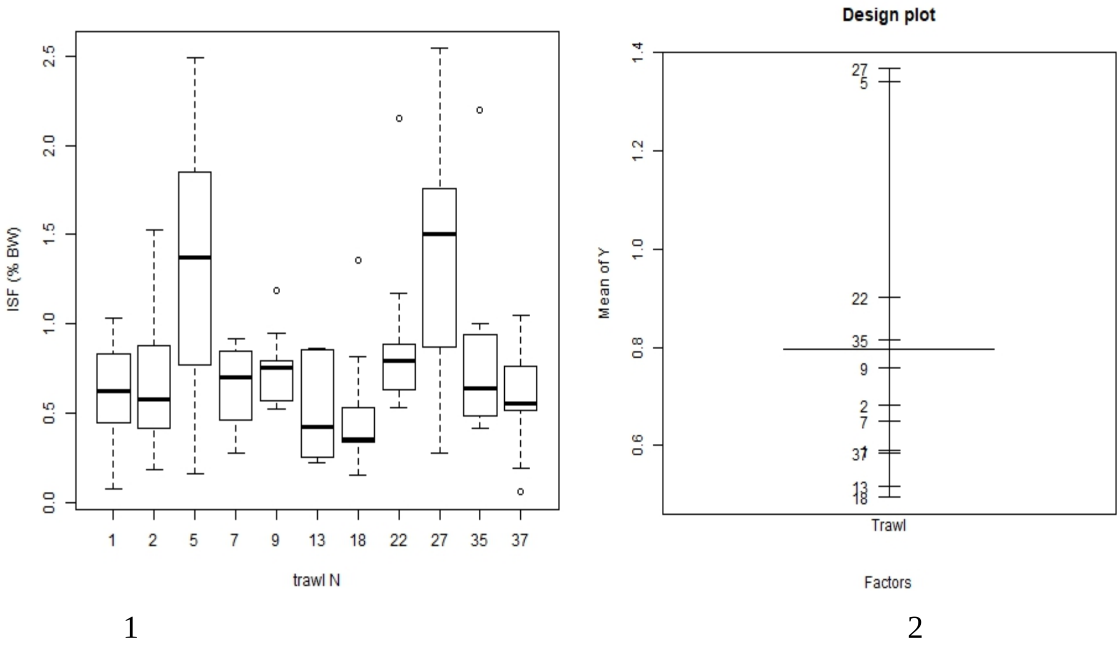

Fig. IV.0.3. (1) Boxplot: sprat index of stomach fullness (ISF, % BW) in June 2019. (2) Design plot: distribution of mean ISF (% BW) by trawls

The highest average index of stomach fullness (ISF) ~ 1.4% was detected in trawls 5 and 27, in front of Ahtopol and under c. Kalikara at depths of 60 m and 16 m. The average values of ISF were minimal (~ 0.5% BW) in the shallow coastal area between Varna and Sozopol Bays. (Fig. IV.0.4).

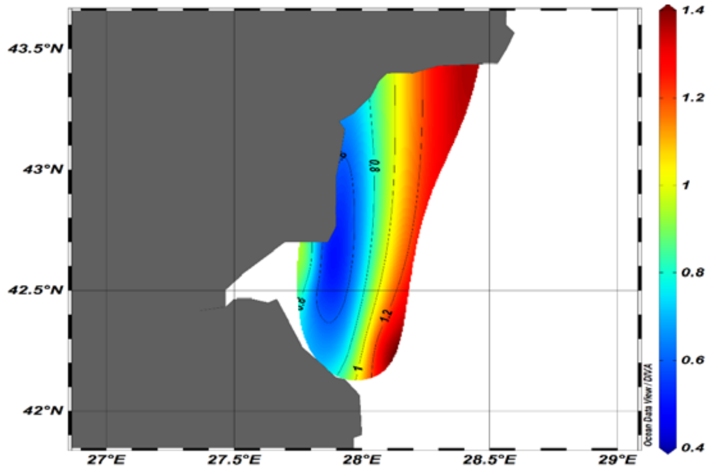

Fig. IV.0.4. Spatial distribution of ISF (% BW) in June 2019

Between ISF and sprat weight within the limits of 1.28 - 5.21 g was not established a statistically significant difference (Fig.IV.0.5).

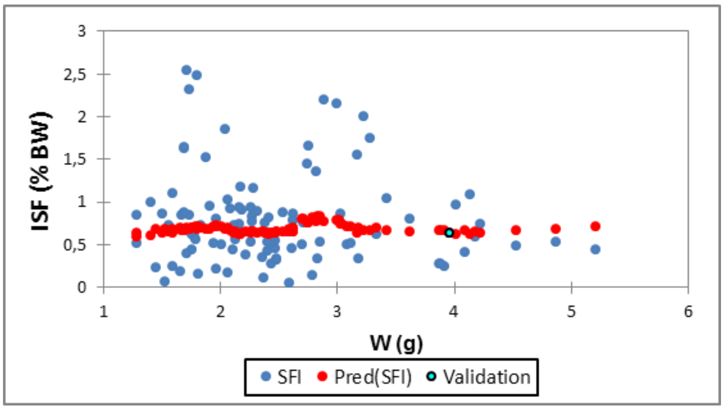

Fig. IV.0.5. Relationship between sprat weight (WW, g) and ISF (% BW)

Prey number, species composition and index of relative importance (IRI) of mesozooplankton species in the sprat diet

The average prey number in the sprat diet amounted to 205.35 ind/stomach 260.39 ± SD off the Bulgarian coast. The maximal individual number of food organisms (1055 ind/stomach) was established near c. Kalikara (trawl 27, depth 16 m) with average PN - 621 ind/stomach and maximal ISF - 1.34% BW, in connection with intensive consumption of *Acartia clausi*.

Significant average PN - 554 ind/stomach was also established near to c. Maslen Nos (trawl 9, depth 41 m), related to the consumption of *Lamellibranchia veliger* (Fig.IV.0.6).

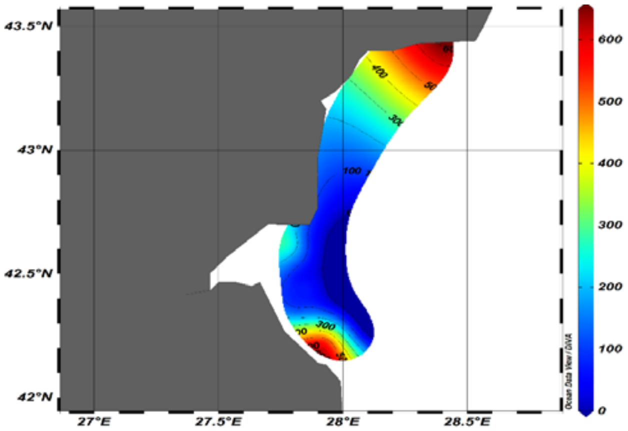

Fig. IV.0.6. Spatial distribution of the average prey number (PN) per trawls in June 2019

Twenty four zooplankton species/groups were identified in the marine environment and some of them (19 species/groups) were represented as food components in the sprat ration. The crustacean copepods were represented by several species: *Calanus euxinus*, *Pseudocalanus elongatus*, *Paracalanus parvus*, *Acartia clausi*, *Centropages ponticus*, *Oithona* spp., *Harpactiocoida* spp., *Copepoda* spp; five taxonomic groups of planktonic larvae of benthos organisms (meroplankton) were detected: *Lamellibranchia veliger*, *Gastropoda veliger*, Cirripedia larvae, Decapoda larvae, Polychaeta larvae; class Chaetognatha was represented by species *Parasagitta setosa*, class Appendicularia - by *Oicopleura dioica*. In the sprat food were established single specimens of *Pisces ova* and *Noctiluca scintillans*.

The indices of relative importance (IRI) of the zooplankton species in sprat food spectrum (based on the percent shares from total abundance, biomass, and frequency of occurrence in samples) are presented in Table IV.0.1.

Table IV.0.1. Sprat food composition in June 2019

Sprat food composition	N (% of total number)	M (% of total biomass)	FO (Frequency of occurrence)	IRI (Index of relative importance)
Acartia clausi	19.17	35.44	72.73	3971.29
Lamellibranchia veliger	24.17	9.05	53.18	1766.62
Paracalanus parvus	6.57	5.49	69.77	841.44
Calanus euxinus	7.58	19.95	20.45	563.24
Pleopis polyphemoides	11.86	13.60	21.14	538.09
Cirripedia larvae	4.97	3.14	46.14	374.32
Oithona spp.	6.77	1.76	37.50	319.81
Oikolpeura dioica	2.79	1.10	45.00	174.86
Centropages ponticus	5.16	1.40	25.68	168.49
Decapoda larvae	0.93	4.14	25.45	128.97
Pseudocalanus elongatus	1.00	0.93	27.27	52.63
Others	9.03	4.01		
Total	100%	100%		

The sprat food was dominated by *Acartia clausi*, followed by *Lamellibranchia veliger*, *Pseudocalanus elongatus*, *Paracalanus parvus* and *C. euxinus* (Tables IV.0.1, IV.0.2, Fig. IV.0.7). The eurytherm species predominated the sprat diet by abundance and biomass and showed the highest frequency of occurrence.

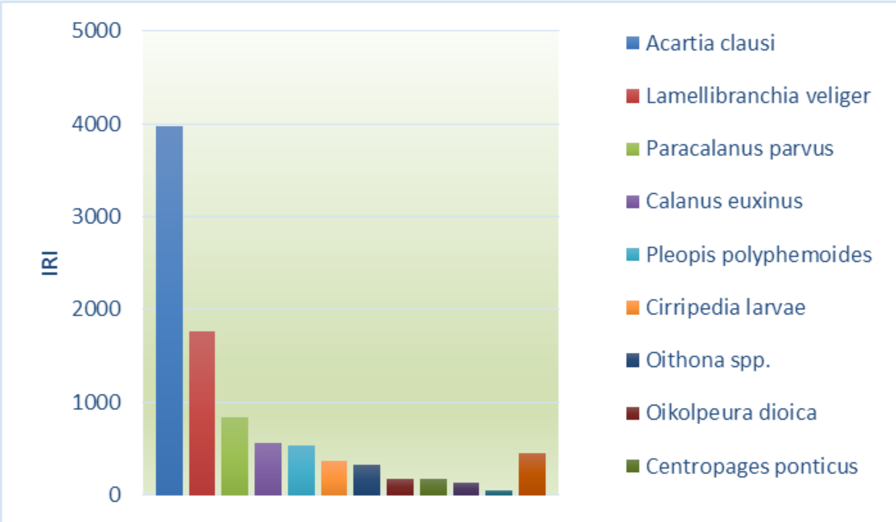

Fig. IV.0.7. Mean IRI of mesozooplankton species in the sprat food in June 2019

The species *A. clausi* was well represented in sprat food samples from the northern and central regions, the species *L.veliger* was detected in the area Sozopol – c. Maslen Nos; *Paracalanus parvus* was found in the sprat diet near to c. Emine, and the cold-water species *C. euxinus* was presented in open sea waters in the zone Kiten – c. Maslen Nos (Table IV.0.2, Fig. IV.0.8).

Table IV.0.2. IRI (%) of mesozooplankton species in sprat food per trawls in June 2019

Sprat diet components	1, 37 m	2, 39 m	5, 60 m	7, 42 m	9, 41 m	13, 36 m	18, 27 m	22, 31 m	27, 16 m	35, 21 m	37, 22 m
Acartia clausi	24.34	40.84	0.10	22.23	2.47	20.81	0.07	4.42	96.09	66.80	75.01
L. veliger	17.28	34.35	1.79	39.54	89.42	37.27	0.00	0.01	0.01	0.00	2.16
P. parvus	10.35	5.77	0.24	10.79	1.17	6.69	27.21	2.38	1.80	0.40	0.33
C. euxinus	1.53	14.90	94.46	14.13	1.50	0.00	0.17	0.00	0.00	0.00	0.59
P. polyphemoides	0.00	0.00	0.00	1.82	0.00	0.57	60.07	75.46	0.00	0.00	0.00
Cirripedia larvae	0.02	0.00	0.00	0.43	0.03	0.00	2.17	6.67	1.83	25.13	17.45
Oithona spp.	39.14	3.65	0.19	6.69	4.17	0.00	0.00	0.55	0.00	0.00	0.00
Oikolpeura dioica	6.39	0.05	0.02	1.86	0.43	4.18	4.15	3.50	0.00	0.00	0.01
C. ponticus	0.00	0.00	0.00	0.05	0.02	28.05	2.30	0.05	0.11	0.41	0.05
Decapoda larvae	0.00	0.00	0.00	0.00	0.00	0.00	2.76	6.21	0.15	7.07	3.51
Pseudocalanus elongatus	0.74	0.28	2.68	0.62	0.13	0.00	0.73	0.03	0.01	0.00	0.77
Others	0.22	0.16	0.52	1.84	0.65	2.45	0.38	0.73	0.01	0.19	0.11
	100	100	100	100	100	100	100	100	100	100	100

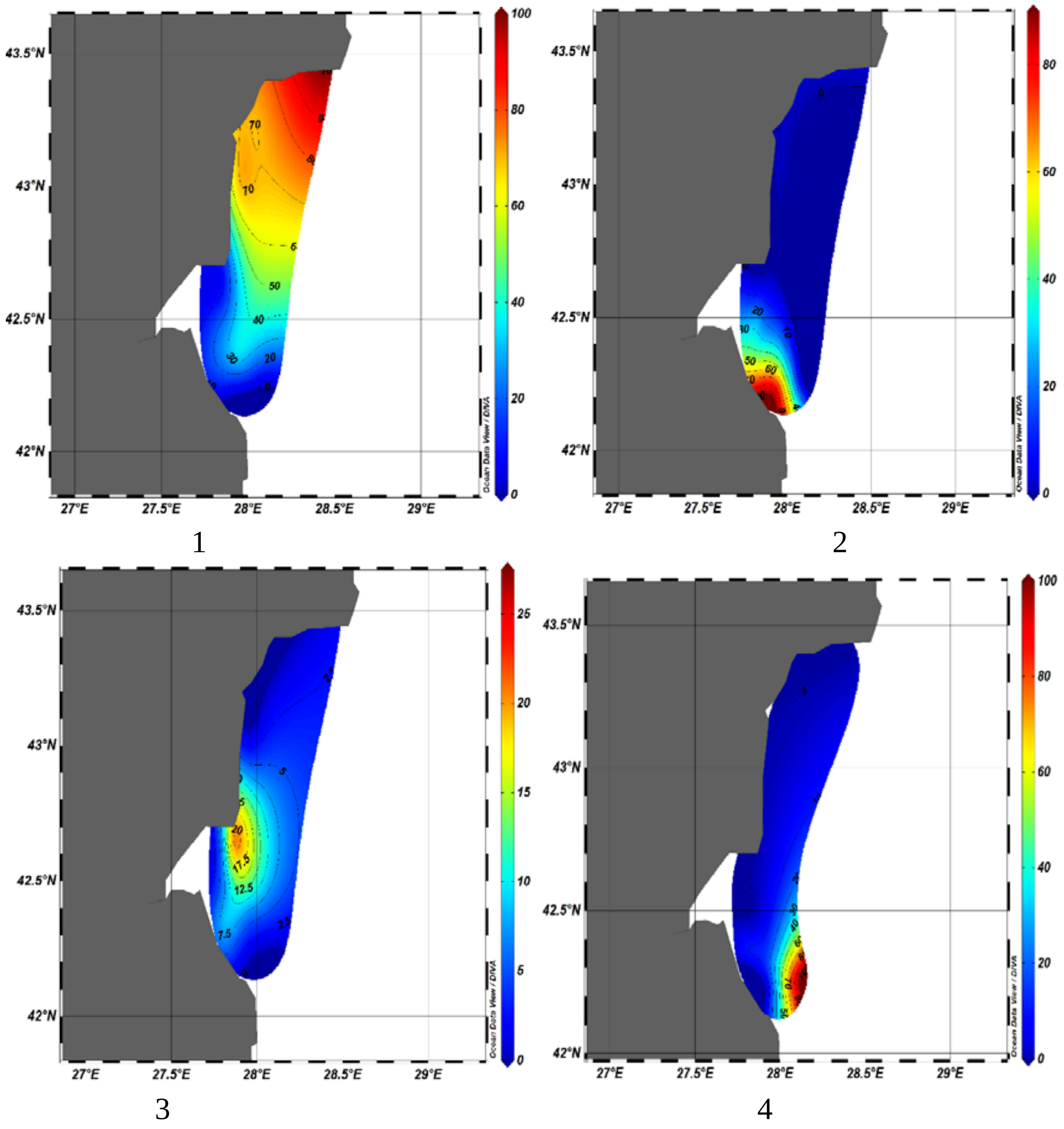

Fig. IV.0.8. Spatial distribution of IRI (%) of mesoplankton species in sprat food: (1) *A. clausi*, (2) *Paracalanus parvus* (3), *L.veliger*, (4) *Calanus euxinus* in June 2019

Zooplankton in marine environment: species composition and biomass

During the studied period, the zooplankton biodiversity was formed by 24 species (Table IV.0.3).

Table IV.0.3. Species diversity of zooplankton

	June 2019
21.	*Noctiluca scintillans*
22.	*Ctenophora larvae*
23.	*Pleurobrachia pileus*
24.	*Aurelia aurita*
25.	*Acartia clausi*
26.	*Acartia tonsa*
27.	*Pseudocalanus elongatus*
28.	*Calanus euxinus*
29.	*Paracalanus parvus*
30.	*Centropages ponticus*
31.	*Oithona davisae*
32.	*Oithona similis*
33.	*Harpacticoida* spp.
34.	*Pleopis polyphemoides*
35.	*Cirripedia nauplii/cypris*
36.	*Lamellibranchia veliger*
37.	Polychaeta larave
38.	*Gastropoda veliger*
39.	Nematoda Larvae
40.	Phoronis larvae
41.	*Decapoda zoea/mysis*
42.	*Parasagitta setosa*
43.	*Oicopleura dioica*
44.	*Pisces ova*, larvae

The species *Noctiluca scintillans* (Protozoa) played a dominant role in the total biomass formation - 83.10% (Fig. IV.0.9-1, Table IV.0.4), and the percentage of mesozooplankton (food zooplankton) reached 13.61%. The species *N. scintillans* and copepods predominated by abundance (Fig. IV.0.9-2) and formed 67.56% and 20.86% of the total zooplankton abundance, respectively.

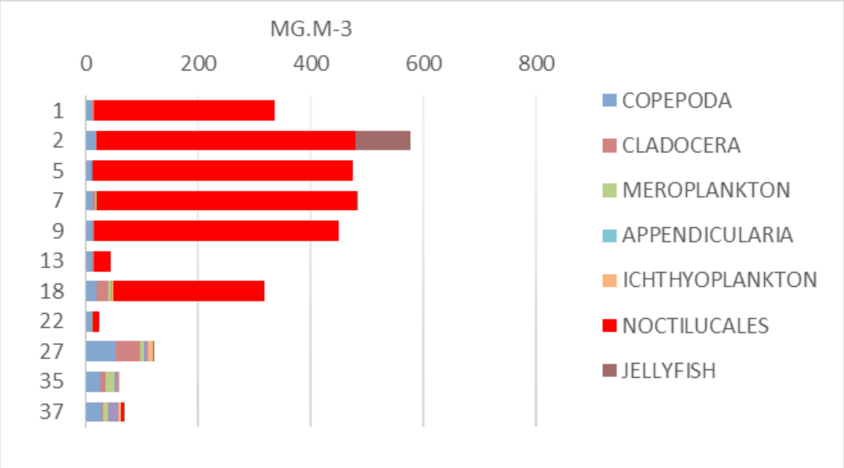

1.

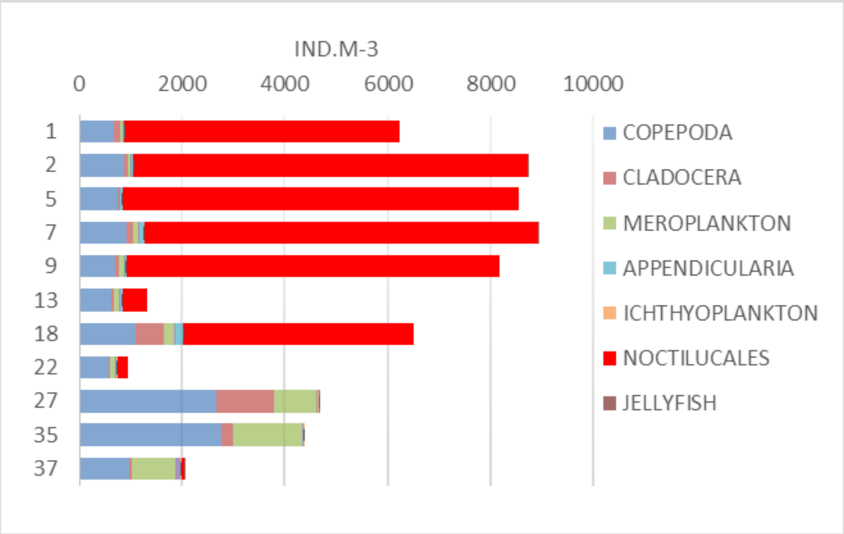

2.

Fig. IV.0.9. Distribution of the biomass (1, mg.m^{-3})) and abundance (2, ind.m^{-3}) of the main zooplankton groups (mg.m^{-3}) per stations in June 2019

Table IV.0.4. Percentage distribution (%, from total biomass) of main zooplankton groups per stations in June 2019

STATIONS	COPEPODA	CLADOCERA	MERO-PLANKTON	CHAETO-GNATHA	APPENDICULARIA	ICHTHYO-PLANKTON	NOCTILUCALES	JELLYFISH
1	2.76	1.31	0.07	0.09	0.05	0.00	95.73	0.00
2	2.77	0.58	0.01	0.05	0.06	0.05	79.85	16.62
5	2.12	0.20	0.00	0.07	0.13	0.06	97.42	0.00
7	2.44	1.12	0.33	0.16	0.12	0.05	95.53	0.25
9	2.17	0.61	0.18	0.03	0.04	0.06	96.90	0.00
13	23.80	3.59	3.02	2.37	0.52	1.31	65.38	0.00
18	6.19	6.64	0.84	0.32	0.29	1.06	84.66	0.00
22	37.09	5.33	3.14	2.06	0.77	3.38	48.22	0.00
27	44.48	36.88	4.79	4.78	0.00	8.80	0.00	0.27
35	43.02	13.91	27.98	10.71	0.00	4.38	0.00	0.00
37	41.69	3.89	15.43	24.84	0.00	8.31	5.83	0.01

Table IV.0.4 shows general statistical data about the total zooplankton biomass variability in June 2019, including three main groups – mesozooplankton, Protozoa, and jellyfish. The total biomass of zooplankton amounted to 268.36 mg.m^{-3} ± 63.13 (SE), with the biomass of the protozoan species *N. scintillans* reaching 223 mg.m^{-3} ± 64.46 (SE) and of the mesozooplankton biomass - 36.52 mg.m^{-3} ± 10.24 (SE). The total biomasses of food mesozooplankton and jelly species were assessed as relatively low for the season.

Table IV.0.5. Statistical data about biomasses (mg.m-3) of the main zooplankton groups in June 2019

	Meso-zooplankton	Protozoa	Jelly-plankton	Total zooplankton biomass
Mean	36.52	223.00	8.84	268.36
Standard Error	10.24	64.46	8.69	63.13
Median	20.29	268.26	0.00	316.85
Mode	#N/A	0.00	0.00	#N/A
Standard Deviation	33.96	213.79	28.82	209.37
Sample Variance	1153.50	45706.78	830.83	43834.31
Kurtosis	2.80	-2.19	11.00	-1.87
Skewness	1.70	0.02	3.32	0.11
Range	107.61	462.60	95.74	551.23
Minimum	12.23	0.00	0.00	24.76
Maximum	119.84	462.60	95.74	575.99
Sum	401.67	2452.98	97.27	2951.92
Count	11.00	11.00	11.00	11.00
Confidence Level (95.0%)	22.82	143.63	19.36	140.65

The mesozooplankton biomass showed an increase up to levels of 120 mg.m^{-3} in north direction (Fig. IV.0.10-1); the amount of *Noctiluca scintillans* increased to 460 mg.m^{-3} mostly along c. Emine – c. Maslen Nos (Fig. IV.0.10-2), and the species *Pleurobrachia pileus* was concentrated in front of Kiten – c. Maslen Nos (Fig. IV.0.10-3).

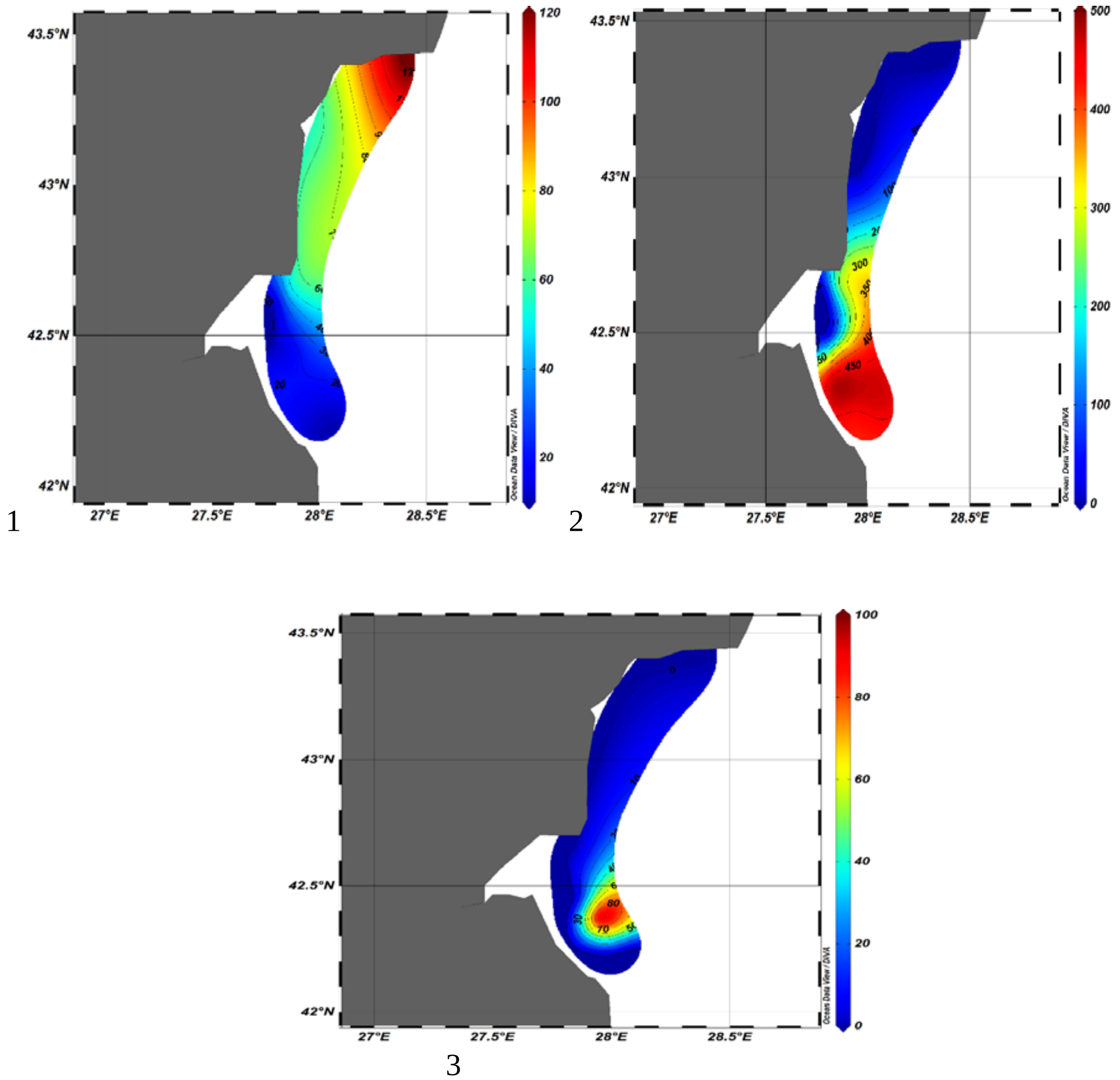

Fig. IV.0.10. Spatial distribution of biomass (mg.m^{-3}) of mesozooplankton (1) *Noctiluca scintillans* (2) and (3) jellyfish in June 2019

V. 2019 – 2nd Survey

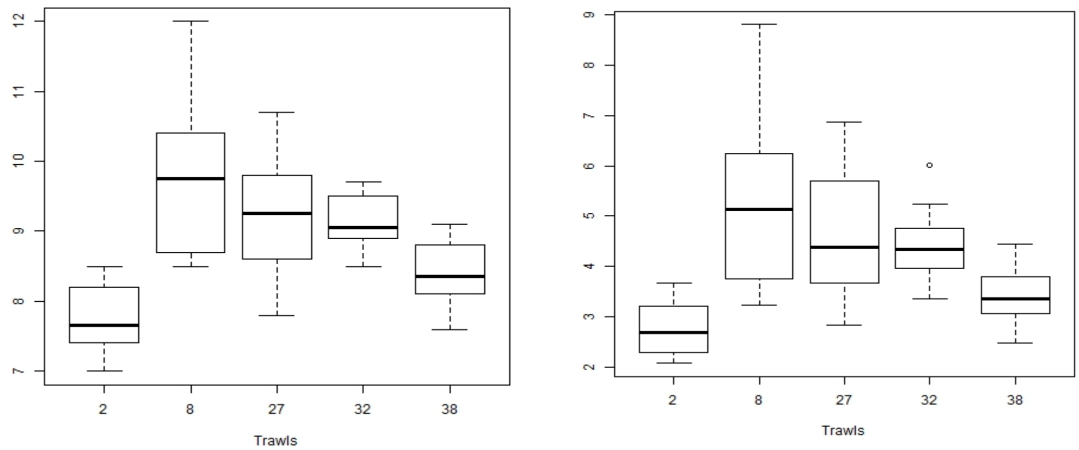

1 2

Fig. V.0.1. Box plot: sprat length (1, cm) and weight (2, g) per trawls during October-November 2019 (median values, 25 – 75 % hinge, minimal and maximal values)

The weight-length dependence of sprat could be described by the following equation: Log WW (g) = 2.9206*Log L (mm) – 5.0891; R2 = 0.96, p<0.001 (Fig. V.0.1).

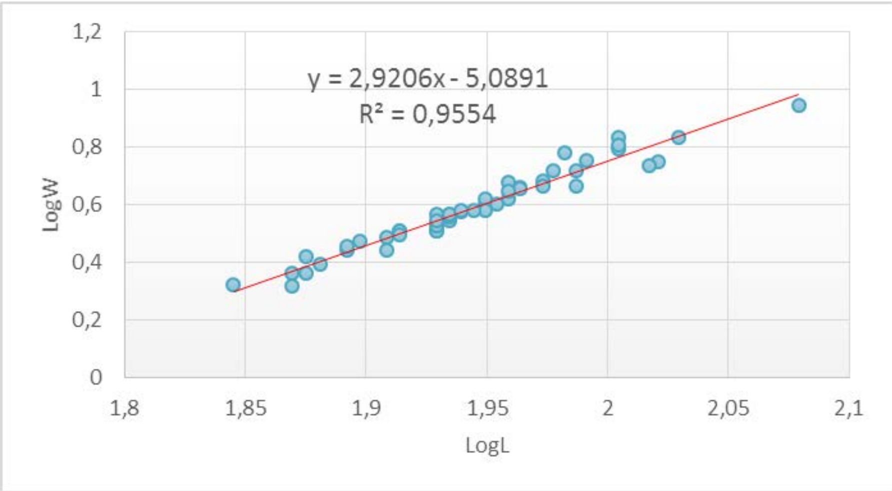

Fig. V.0.2. Sprat weight-length relationship in October-November 2019

In October - November 2019, the average index of stomach fullness (ISF) reached 0.91% ± 0.60 (SD) of the sprat weight (Fig. V.0.2). This value was with 13.75% higher than the level estimated during the spring season.

The highest average values of the ISF index 1.36 - 1.3 % were established in the Bay of Burgas and in front of Kamchia River mouth (trawls 38 and 2, Fig. V.0.3) at depths of 30 - 45 m (Fig. V.0.4). The average ISF values were minimal (~ 0.3% BW) in c. Maslen Nos region (Fig. V.0.4).

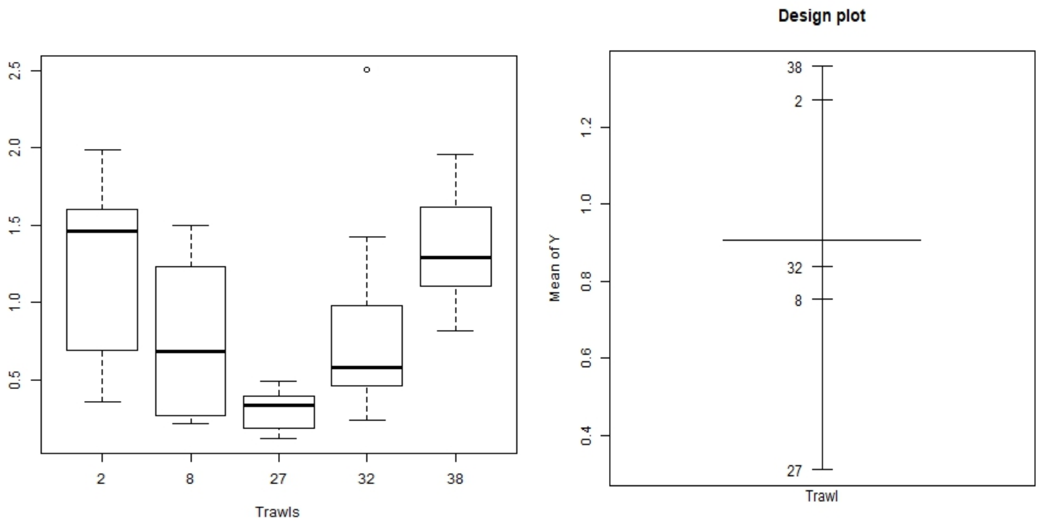

1 2

Fig. V.0.3. (1) Boxplot: sprat index of stomach fullness (ISF, % BW) in October-November 2019
(2) Design plot: distribution of mean ISF (% BW) by trawls

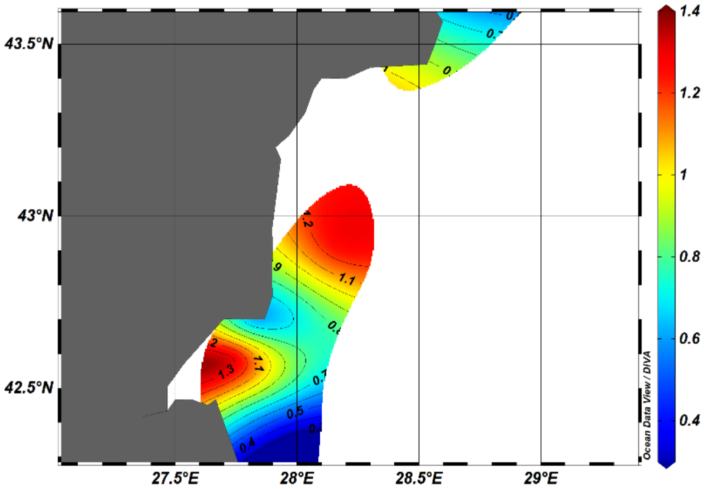

Fig. V.0.4. Spatial distribution of ISF (% BW) in October-November 2019

A statistically significant inverse correlation (R^2 = - 0.30, p <0.001, Fig. V.0.5) was found between the indices of stomach fullness and the sprat weight (ranging between 2.09 – 8.80 g) with a small percentage of explained variability - 34.4%.

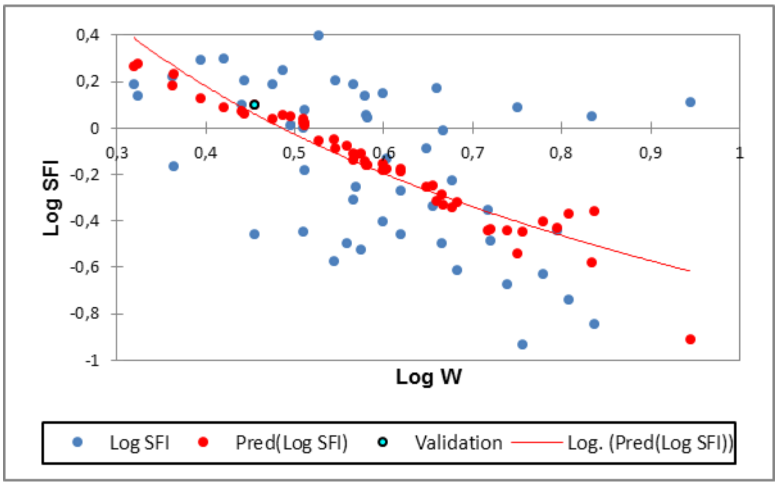

Fig. V.0.5. Relationship between the weights of sprat specimens (Log W, g) and stomach fullness index - Log ISF (% BW) in October-November 2019

Project proposal № BG14MFOP001-3.003-0001 "Collection, management and use of data for the purposes of scientific analysis and implementation of the Common Fisheries Policy for the period 2017-2019", funded by the Maritime Affairs and Fisheries Program, co-financed by the European Union through the European Maritime and Fisheries Fund

The most significant ISF was found in the small-sized sprat with a weight of ~ 2.5 g (Fig. V.0.5). Due to the relatively low level of explained variability, other factors influence the sprat diet, e.g. such factors might be the concentration and species composition of food zooplankton, the importance of intraspecies and interspecies competitive relationships, etc.

Prey number (PN), species composition and index of relative importance (IRI) of mesozooplankton species in the sprat diet

In the surveyed area off the Bulgarian coast, the average PN in the sprat food was 230 ind/stomach ± 321.64 (SD). The maximal individual number of food organisms - 1340 ind/stomach was established in Burgas Bay area (trawl 38, d = 30 m), where the average PN was 872 ind/stomach, corresponding to the maximal ISF index of 1.36% BW, due to intensive consumption of the zooplankton species *Paracalanus parvus* (Fig. V.0.6).

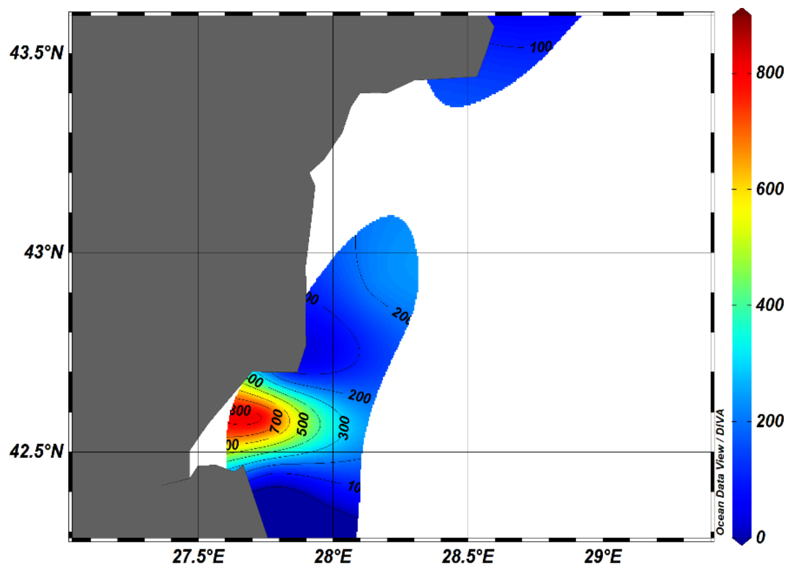

Fig. V.0.6. Spatial distribution of the average PN per trawls in October-November 2019

In the zooplankton samples from the marine environment, 27 species/groups were identified, of which 23 species/groups were presented as components in the sprat food. Copepoda were represented by *Calanus euxinus*, *Pseudocalanus elongatus*, *Paracalanus parvus*, *Acartia clausi*, *Centropages ponticus*, *Oithona similis*, *Oithona davisae* and *Harpactiocoida* spp., cladocerans included - *Pleopis polyphemoides*, *Penilia avirositis* and *Pseudoevadne tergestina*; five taxonomic groups were identified from the group of planktonic larvae of bottom organisms (meroplankton): *Lamellibranchia veliger*, *Gastropoda veliger*, Cirripedia larvae, Decapoda larvae, Polychaeta larvae; class Chaetognatha was represented by *Parasagitta setosa*, class Appendicularia - by *Oicopleura dioica*. Food objects were found in the stomachs of all studied sprat specimens with fluctuations between 1-15 zooplankton species in separate sprat specimens. The indices of relative importance (IRI) of the main zooplankton species in sprat food spectrum (based on the percent shares from total abundance, biomass, and frequency of occurrence in samples) are presented in Table V.0.1.

Table V.0.1. Sprat food composition and IRI values in October-November 2019

Sprat food composition	N (% of abundance)	M (% of biomass)	FO (frequency of occurrence)	IRI (Index of relative importance)
Calanus euxinus	12.02	62.18	84.0	6232.8
Pseudocalanus elongatus	6.21	1.33	62.0	467.48
Paracalanus parvus	40.17	20.39	62.0	3754.72
Acartia clausi	14.24	7.34	78.0	1683.24
Centropages ponticus	1.86	1.71	42.0	149.94
Pleopis polyphemoides	1.34	0.40	26	45.24
Lamellibranchia veliger	2.82	0.14	50	148
Decapoda larvae	1.91	2.95	26	126.36
Cirripedia nauplii, cypris	1.42	0.20	56	90.72
Parasagitta setosa	13.38	2.98	30	490.8
Oikopleura dioica	3.28	0.19	42	145.74
Other	1.35	0.19		
Total	100%	100%		

Data on the number of species in the sprat food and some species diversity indices based on IRI values per different trawls are presented in Table V.0.2.

Table V.0.2. Number of species and species diversity indices (d, species richness, J'-Pielou's evenness, Brillouin, Fisher, Shennon) based on zooplankton species IRI values per different trawls

Sample	S	d	J'	Brillouin	Fisher	H'(loge)	1-Lambda'
T2	15	2.60	0.45	1.14	3.65	1.23	0.54
T8	11	2.17	0.68	1.50	3.15	1.63	0.77
T27	11	4.42	0.85	1.26	****	2.03	0.93
T32	14	2.97	0.64	1.49	4.92	1.69	0.75
T38	15	2.07	0.09	0.22	2.57	0.24	0.08

Considering the representation of the different zooplankton species in the sprat food, we found relatively high species evenness in c. Maslen Nos region (trawl 27), but it corresponded to the lowest ISF value.

Dominant positions in the sprat food had the copepods: *Calanus euxinus*, *Paracalanus parvus*, *Acartia clausi*, *Pseudocalanus elongatus* and *Centropages ponticus*, as well as the chaetognath *Parasagitta setosa* (Tables V.0.1, V.0.2, Fig. V.0.4). The coldwater and eurytherm zooplankton species predominated in the sprat diet, both in frequency of occurrence and in numbers and biomass.

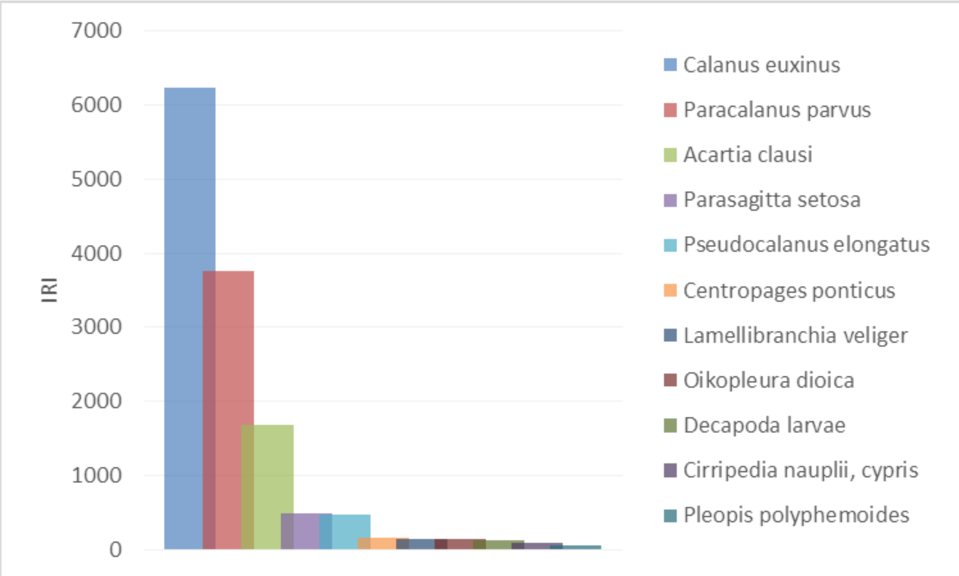

Fig. V.0.7. Mean IRI of mesozooplankton species in the sprat diet in October-November 2019

The species *A. clausi* was found in the sprat food almost at all studied regions, while the cold-water copepod *C. euxinus* was mostly presented in the sprat diet around c. Kaliakra and c. Maslen Nos, and the species *Paracalanus parvus* was found in the sprat diet in Bourgas Bay and off c. Emine; *P. setosa* was observed in the sprat food off the southern part of Burgas Bay and Sozopol (Table V.0.3, Fig. V.0.8).

Project proposal № BG14MFOP001-3.003-0001 "Collection, management and use of data for the purposes of scientific analysis and implementation of the Common Fisheries Policy for the period 2017-2019", funded by the Maritime Affairs and Fisheries Program, co-financed by the European Union through the European Maritime and Fisheries Fund

Table V.0.3. IRI(%) of different mesozooplankton species in sprat food per trawls in October-November 2019

Sprat food composition	T2	T8	T27	T32	T38
Calanus euxinus	28.23	83.11	52.60	47.20	4.49
Pseudocalanus elongatus	0.91	4.95	11.06	0.21	0.66
Paracalanus parvus	47.87	3.35	1.04	4.26	88.21
Acartia clausi	14.77	0.17	24.90	25.50	1.01
Centropages ponticus	0.16	0.00	2.36	0.56	3.37
Pleopis polyphemoides	0.06	0.00	0.47	1.79	0.00
Lamellibranchia veliger	4.62	2.13	0.00	0.08	0.05
Cirripedia nauplii/cypris	0.46	0.21	1.25	0.45	0.15
Decapoda larvae	0.00	0.00	1.87	1.87	1.98
Parasagitta setosa	2.74	6.03	0.00	16.33	0.01
Oikopleura dioica	0.15	0.01	4.45	1.74	0.06
Other	0.03	0.04	0.00	0.01	0.01
	100	100	100	100	100

Project proposal № BG14MFOP001-3.003-0001 "Collection, management and use of data for the purposes of scientific analysis and implementation of the Common Fisheries Policy for the period 2017-2019", funded by the Maritime Affairs and Fisheries Program, co-financed by the European Union through the European Maritime and Fisheries Fund

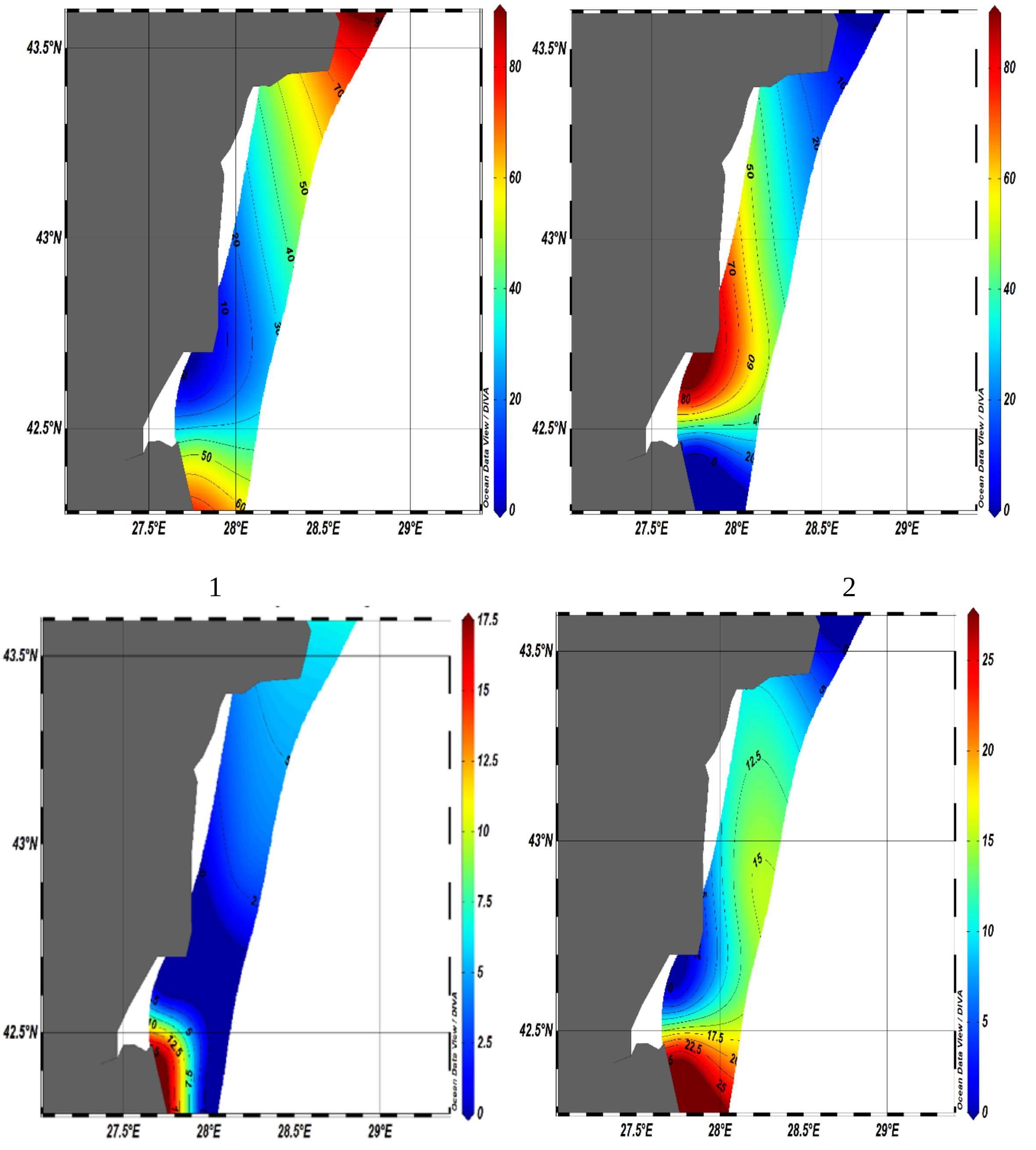

1 2

3 4

Fig. V.0.8. Spatial distribution of IRI (%) of zooplankton species in the sprat food: (1) *C. euxinus*, (2) *Parasagitta setosa*, (3) *Paracalanus parvus*, (4) *A. clausi* in October-November 2019

Horse mackerel: biological parameters and feeding

Ten specimens of horse mackerel were studied with an average absolute length of 9.22 cm ± 0.65 (SD) and an average weight of 6.60 g ± 1.61 (SD) (Table 5.1, Fig. 5.1.). The mean value of stomach fullness index of horse mackerel was 0.60% ± 0.27 (SD) of body weight (Table V.0.4, Fig. V.0.9).

Table V.0.4. Summary data on the size (L, cm), weight (W, g) and ISF (% BW) of the horse mackerel determined by the analysis of stomach contents in November 2019

	L, cm	W, g	ISF, % BW
Mean	9.22	6.60	0.60
Standard Error	0.21	0.51	0.09
Median	9.20	6.41	0.57
Mode	9.20	#N/A	#N/A
Standard Deviation	0.65	1.61	0.27
Sample Variance	0.43	2.58	0.07
Kurtosis	-1.24	3.38	-1.26
Skewness	-0.26	1.51	0.11
Range	1.80	5.78	0.81
Minimum	8.20	4.65	0.20
Maximum	10.00	10.43	1.01
Sum	92.20	66.00	5.98
Count	10.00	10.00	10.00
Confidence Level (95.0%)	0.47	1.15	0.19

The average prey number in horse mackerel food was 97.9 ind/stomach ± 57.21 (SD), and the maximal individual number of food organisms -178 ind/stomach.

Project proposal № BG14MFOP001-3.003-0001 "Collection, management and use of data for the purposes of scientific analysis and implementation of the Common Fisheries Policy for the period 2017-2019", funded by the Maritime Affairs and Fisheries Program, co-financed by the European Union through the European Maritime and Fisheries Fund

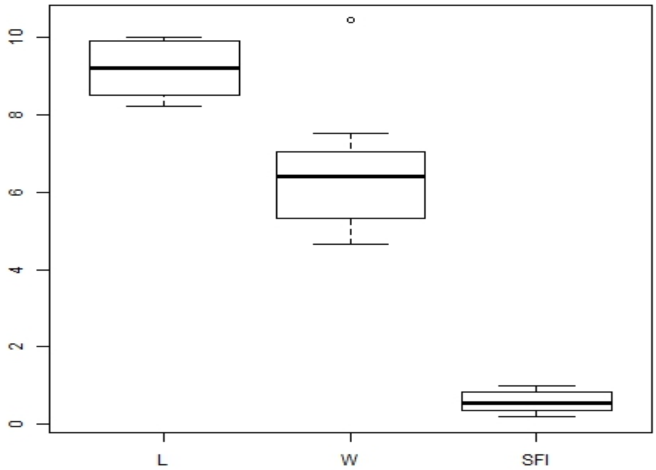

Fig. V.0.9. Size (L, cm), weight (W, g) and ISF index (% BW) of horse mackerel in November 2019

Nineteen mesozooplankton species were identified in the horse mackerel food. The identified copepods include *Calanus euxinus, Pseudocalanus elongatus, Paracalanus parvus, Acartia clausi, Centropages ponticus, Oithona davisae* and *Harpactiocoida* spp. Cladocera were represented by *Pleopis polyphemoides, Penilia avirositis, Pseudoevadne tergestina* and *Evadne spinifera*; four taxonomic groups were detected from the planktonic larvae of bottom organisms (meroplankton): *Lamellibranchia veliger, Gastropoda veliger,* Cirripedia larvae, Decapoda larvae; class Chaetognatha was presented by *Parasagitta setosa*, class Appendicularia - by *Oicopleura dioica*.

Food objects were found in all studied fish specimens, with an average number of zooplankton species consumed - 9 species, and fluctuations of 5-15 zooplankton species in the individually observed fish specimens. The indices of the relative importance of zooplankton organisms in the horse mackerel food, the percentages of abundance and biomass, as well as the frequency of occurrence among the studied horse mackerel specimens are presented in Table V.0.5.

Table V.0.5. Food composition of horse mackerel and IRI of main zooplankton species

Food composition of horse mackerel	N (% of abundance)	M (% of biomass)	FO (Frequency of occurrence)	IRI (Index of relative importance)
Acartia clausi	30.64	24.75	100.00	5539.25
Centropages ponticus	11.03	11.89	90.00	2063.35
Calanus euxinus	2.66	44.20	40.00	1874.20
Paracalanus parvus	21.55	5.00	70.00	1858.71
Cirripedia nauplii	6.33	1.43	100.00	776.47
Pleopis polyphemoides	6.54	4.33	70.00	760.77
Penilia avirostris	2.86	2.27	80.00	410.70
Oikopleura dioica	3.78	0.49	40.00	170.69
Lamellibranchia veliger	4.60	0.23	30.00	144.75
Decapoda larvae	0.61	1.73	50.00	116.92
Other	9.40	3.68		
Total	100%	100%		

The copepods *Acartia clausi*, *Centropages ponticus*, *Calanus euxinus* and *Paracalanus parvus* occupied leading position in the horse mackerel diet (Table V.0.5., Fig. V.0.10).

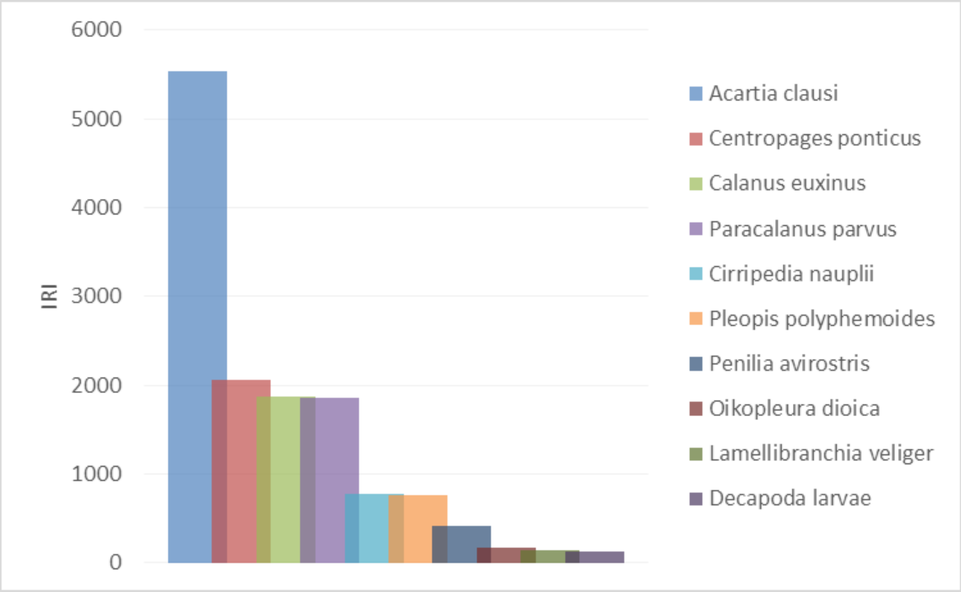

Fig. V.0.10. Average values of the relative importance indices (IRI) of the various mesozooplankton species/groups in the horse mackerel food off the Bulgarian coast in November 2019

Zooplankton in marine environment: species composition and biomass

Zooplankton biodiversity in marine environment was formed by 27 species/groups of organisms (Table V.0.6).

The groups of Copepoda (36.07 %), water fleas (Cladocera, 25.19 %) and jellyplankton (24.02 %) had dominating positions in the formation of the total zooplankton biomass (Fig. V.0.11.A, Table V.0.7). The representatives of crustaceans - Copepoda and Cladocera dominated in number (Fig. V.0.11.B) and formed significant proportions - 61.85 % and 14.54 % of the total zooplankton abundance.

Table V.0.6. Species diversity of zooplankton

	X-XI.2019
	Noctiluca scintillans
	Ctenophora larvae
	Pleurobrachia pileus
	Aurelia aurita
	Beroe ovata
	Favella spp.
	Acartia clausi
	Acartia tonsa
	Pseudocalanus elongatus
	Calanus euxinus
	Paracalanus parvus
	Centropages ponticus
	Oithona daX-XIsae
	Oithona similis
	Harpacticoida spp.
	Pleopis polyphemoides
	Penilia aX-XIrostris
	Pseudoevadne tergestina
	Cirripedia nauplii/cypris
	Lamellibranchia veliger
	Polychaeta larave
	Gastropoda veliger
	Bryozoa larvae
	Decapoda zoea/mysis
	Parasagitta setosa
	Oicopleura dioica
	Pisces ova

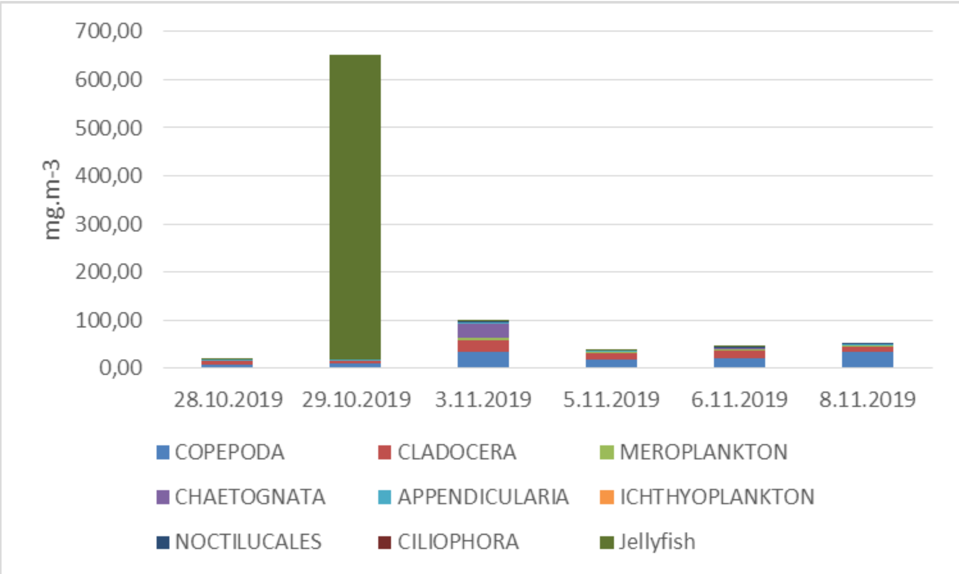

A

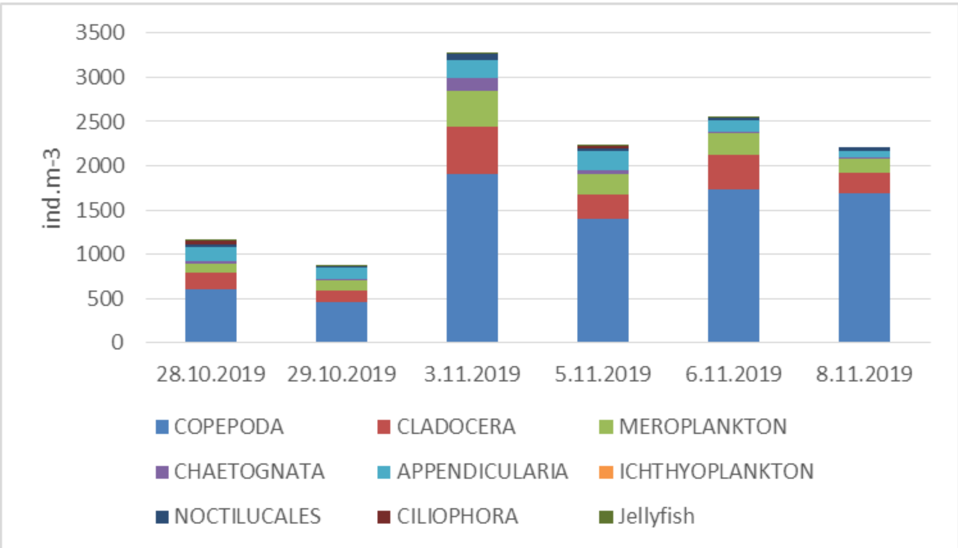

B

Fig. V.0.11. Distribution of the biomass (1. $mg.m^{-3}$) and abundance (2, $ind.m^{-3}$) of the main zooplankton groups ($mg.m^{-3}$) in October-N0vember 2019

Table V.0.7. Percentage distribution (% of total biomass) of the main zooplankton groups in Oct.-Nov. 2019

Date	COPEPODA	CLADOCERA	MERO-PLANKTON	CHAETO-GNATHA	APPENDICULARIA	ICHTHYO-PLANKTON	NOCTILUCALES	JELLYFISH
28.10.2019	28.89	40.20	3.18	2.25	4.40	0.00	9.23	11.54
29.10.2019	1.26	0.89	0.17	0.05	0.13	0.00	0.20	97.29
3.11.2019	32.95	25.42	4.69	31.01	1.48	0.27	4.16	0.02
5.11.2019	46.15	30.65	6.71	4.95	3.31	0.00	4.96	3.10
6.11.2019	41.75	34.93	7.33	5.51	1.48	0.00	5.09	3.91
8.11.2019	65.39	19.06	4.93	4.32	1.19	0.53	4.59	0.00
average	36.07	25.19	4.50	8.01	2.00	0.13	4.71	19.31

During the autumn survey, the total zooplankton biomass was 150 mg.m^{-3} ± 100.52 (SE), with the biomass of jellyplankton reaching 106.42 mg.m^{-3} ± 105.33 (SE), and that of mesozooplankton - 42.14 mg.m^{-3} ± 11.69 (SE). The biomass of food mesozooplankton was evaluated as relatively low for the season (Table V.0.8).

Table V.0.8**.** Statistical data about biomasses (mg.m^{-3}) of the main zooplankton groups in Oct.-Nov. 2019

	Mesozoo-plankton	*Protozoa*	*Jellyfish*	*Total zooplankton biomass*
Mean	42.14	2.32	106.42	150.88
Standard Error	11.69	0.38	105.33	100.52
Median	38.73	2.13	1.50	48.49
Mode	#N/A	1.92	#N/A	#N/A
Standard Deviation	28.63	0.94	258.02	246.21
Sample Variance	819.64	0.88	66572.65	60620.80
Kurtosis	2.19	3.29	6.00	5.77
Skewness	1.34	1.56	2.45	2.39
Range	77.67	2.76	633.09	629.92
Minimum	16.30	1.32	0.00	20.80
Maximum	93.97	4.08	633.09	650.71
Sum	252.83	13.92	638.51	905.26
Count	6.00	6.00	6.00	6.00
Confidence Level (95.0%)	30.04	0.99	270.77	258.38

The highest mesozooplankton biomass was found off c. Emine region - up to 93.97 mg.m^{-3} (Fig. V.0.12.A), while the jellyfish biomass increased to 650 mg.m^{-3} off the northern cost - in c. Kaliakra - Krapets strip (Fig. V.0.12.B).

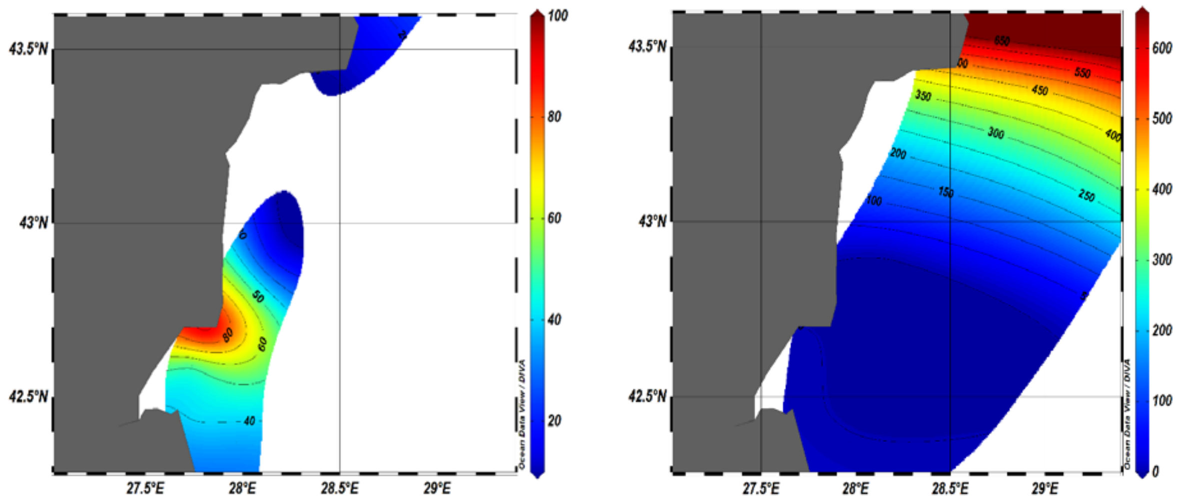

A B

Fig. 5.12. Spatial distribution of biomass (mg.m^{-3}) of (A) mesozooplankton and (B) jellyfish species in October-November 2019

The mean absolute length of the investigated sprat specimens reached 7.51 cm ± 0.67 (SD), varying between 6.20 - 9.60 cm, correspondingly the mean weight was 2.47 g ± 0.81 (SD), ranging from 1.28 g to 5.21 g (Table V.0.9, Fig. V.0.13).

Table V.0.9. Summary statistics of sprat length (L, cm), weight (W, g) and ISF (% BW), analysed for stomach content composition in June 2019

	L, cm	W, g	ISF, % BW
Mean	7.51	2.47	0.80
Standard Error	0.06	0.08	0.05
Median	7.50	2.32	0.72
Mode	7.50	1.68	0.75
Standard Deviation	0.67	0.81	0.53
Sample Variance	0.45	0.65	0.28
Kurtosis	0.24	1.13	2.09
Skewness	0.64	1.15	1.45
Range	3.40	3.93	2.48
Minimum	6.20	1.28	0.06
Maximum	9.60	5.21	2.54
Sum	825.70	271.60	84.37
Count	110.00	110.00	106.00
Confidence Level (95.0%)	0.13	0.15	0.10

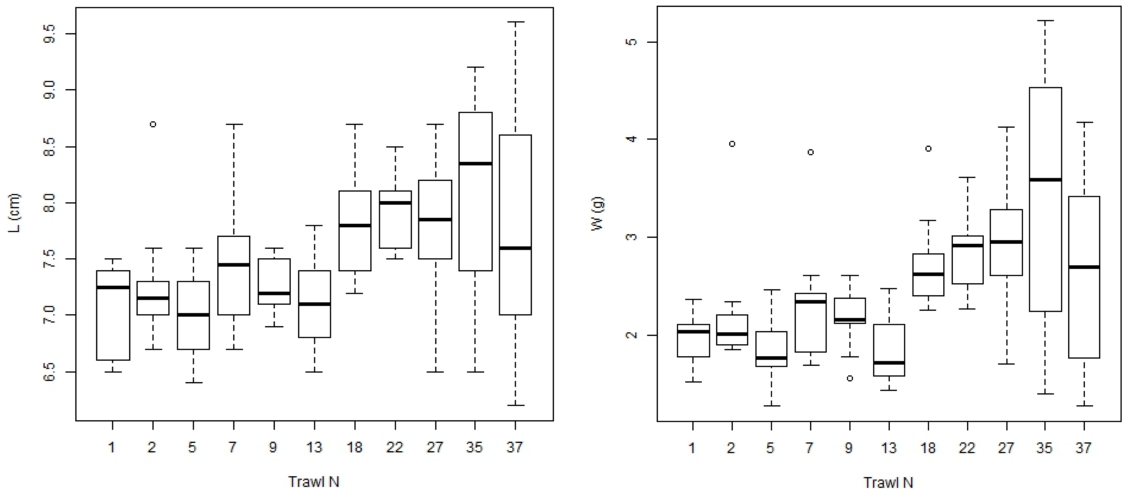

A B

Fig.V.0.13. Box plot (median values, 25–75 % hinge, minimal and maximal values): distribution of sprat length (1, cm) and weight (2, g) per trawls in June 2019

The weight-length dependence for sprat could be described by the following equation: Log WW(g)=3.2522*Log L(cm) - 2.4697; ($R2=0.89$, $p<0.001$, Fig. V.0.14).

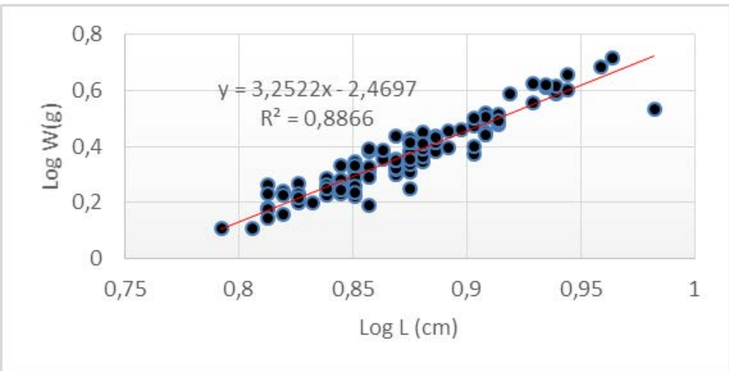

Fig. V.0.14. Sprat weight-length relationship in June 2019

In June 2019, the average value of the index of fullness reached 0.80% ± 0.53 (SD) of the sprat weight (Table V.0.9). ISF in June.2019 exceeded by 40.60% the average for springs 2007 - 2010 (0.53% BW) (Fig. V.0.15).

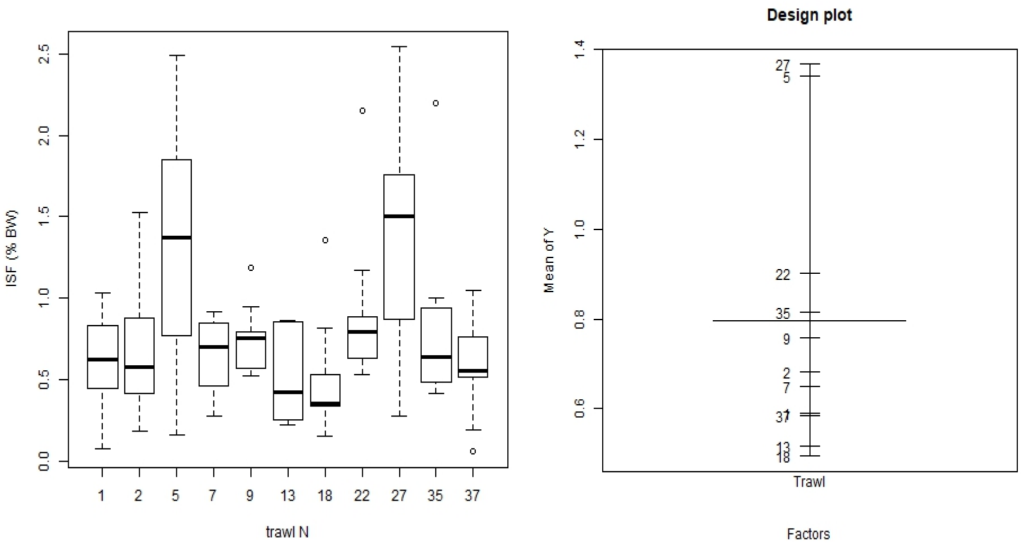

A B

Fig. V.0.15. (A) Boxplot: sprat index of stomach fullness (ISF, % BW) in June 2019. (B) Design plot: distribution of mean ISF (% BW) by trawls

The highest average index of fullness - ISF ~ 1.4% was detected in trawls 5 and 27 - in front of Ahtopol and under c. Kalikara, at depths of 60 m and 16 m. The average values of ISF were minimal (~ 0.5% BW) in the shallow coastal area between Varna and Sozopol Bays (Fig. V.0.16).

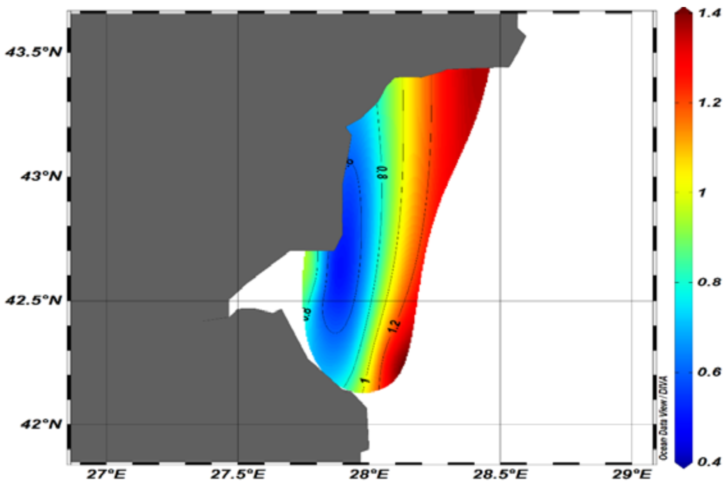

Fig. V.0.16. Spatial distribution of ISF (% BW) in June 2019

Between ISF and sprat weight within the limits of 1.28 - 5.21 g was not established a statistically significant difference (Fig. V.0.17).

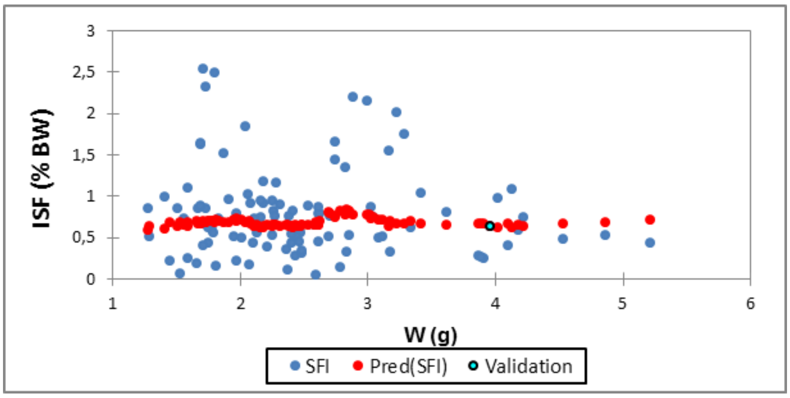

Fig. V.0.17. Relationship between sprat weight (WW, g) and ISF (% BW)

Prey number, species composition and index of relative importance (IRI) of mesozooplankton species in the sprat diet

The average prey number in the sprat diet amounted to 205.35 ind/stomach 260.39 ± SD off the Bulgarian coast. The maximal individual number of food organisms - 1055 ind/stomach was established near c. Kalikara (trawl 27, depth 16 m), with average PN - 621 ind/stomach and maximal ISF - 1.34% BW, in connection with intensive consumption of *Acartia clausi*. A significant average PN - 554 ind/stomach was also established near to c. Maslen Nos (trawl 9, depth 41 m), related to the consumption of *Lamellibranchia veliger* (Fig. V.0.18).

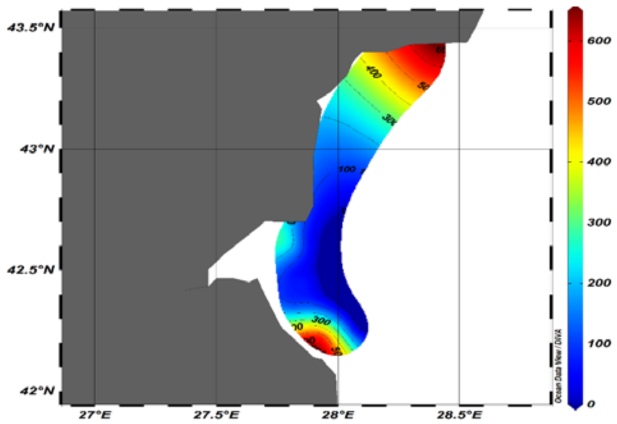

Fig. 5.18. Spatial distribution of the average prey number (PN) per trawls in June 2019

Twenty four zooplankton species/groups were identified in the marine environment, and some of them - 19 species/groups were represented as food components in the sprat ration. The crustacean copepods were represented by several species: *Calanus euxinus*, *Pseudocalanus elongatus*, *Paracalanus parvus*, *Acartia clausi*, *Centropages ponticus*, *Oithona* spp., *Harpactiocoida* spp., *Copepoda* spp; five taxonomic groups of planktonic larvae of benthos organisms (meroplankton) were detected: *Lamellibranchia veliger*, *Gastropoda veliger*, Cirripedia larvae, Decapoda larvae, Polychaeta larvae, class Chaetognatha was represented by species *Parasagitta setosa*, class Appendicularia - by *Oicopleura dioica*. In the sprat food were established single specimens of *Pisces ova* and *Noctiluca scintillans*. The indices of relative importance (IRI) of the zooplankton species in sprat food spectrum (based on the percent shares from total abundance, biomass, and frequency of occurrence in samples) are presented in Table V.0.10.

Table V.0.10. The sprat food composition in June 2019

Sprat food composition	N (% of total abundance)	M (% of total biomass)	FO (Frequency of occurrence)	IRI (Indices of relative importance)
Acartia clausi	19.17	35.44	72.73	3971.29
Lamellibranchia veliger	24.17	9.05	53.18	1766.62
Paracalanus parvus	6.57	5.49	69.77	841.44
Calanus euxinus	7.58	19.95	20.45	563.24
Pleopis polyphemoides	11.86	13.60	21.14	538.09
Cirripedia larvae	4.97	3.14	46.14	374.32
Oithona spp.	6.77	1.76	37.50	319.81
Oikolpeura dioica	2.79	1.10	45.00	174.86
Centropages ponticus	5.16	1.40	25.68	168.49
Decapoda larvae	0.93	4.14	25.45	128.97
Pseudocalanus elongatus	1.00	0.93	27.27	52.63
Others	9.03	4.01		
Total	100%	100%		

Project proposal № BG14MFOP001-3.003-0001 "Collection, management and use of data for the purposes of scientific analysis and implementation of the Common Fisheries Policy for the period 2017-2019", funded by the Maritime Affairs and Fisheries Program, co-financed by the European Union through the European Maritime and Fisheries Fund

The sprat food was dominated by *Acartia clausi*, followed by *Lamellibranchia veliger*, *Pseudocalanus elongatus*, *Paracalanus parvus* and *C. euxinus* (Tables V.0.10, V.0.11, Fig. V.0.19). The eurytherm species predominated the sprat diet by abundance and biomass and showed the highest frequency of occurrence.

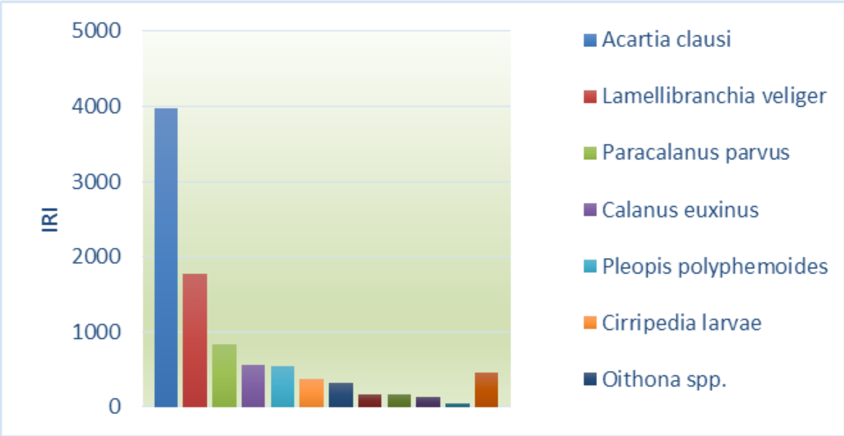

Fig. V.0.19. Mean IRI of mesozooplankton species in the sprat food in June 2019

The species *A. clausi* was well presented in sprat food samples from the northern and central regions, the species *L.veliger* was detected in the area Sozopol – c. Maslen Nos; *Paracalanus parvus* was found in the sprat diet near to c. Emine, and the cold-water species *C. euxinus* was presented in open sea waters in the zone Kiten – c. Maslen Nos (Table V.0.11, Fig. V.0.20).

Project proposal № BG14MFOP001-3.003-0001 "Collection, management and use of data for the purposes of scientific analysis and implementation of the Common Fisheries Policy for the period 2017-2019", funded by the Maritime Affairs and Fisheries Program, co-financed by the European Union through the European Maritime and Fisheries Fund

Table V.0.11. IRI (%) of mesozooplankton species in sprat food per trawls in June 2019

Sprat diet components	1, 37 m	2, 39 m	5, 60 m	7, 42 m	9, 41 m	13, 36 m	18, 27 m	22, 31 m	27, 16 m	35, 21 m	37, 22 m
Acartia clausi	24.34	40.84	0.10	22.23	2.47	20.81	0.07	4.42	96.09	66.80	75.01
L. veliger	17.28	34.35	1.79	39.54	89.42	37.27	0.00	0.01	0.01	0.00	2.16
P. parvus	10.35	5.77	0.24	10.79	1.17	6.69	27.21	2.38	1.80	0.40	0.33
C. euxinus	1.53	14.90	94.46	14.13	1.50	0.00	0.17	0.00	0.00	0.00	0.59
P. polyphemoides	0.00	0.00	0.00	1.82	0.00	0.57	60.07	75.46	0.00	0.00	0.00
Cirripedia larvae	0.02	0.00	0.00	0.43	0.03	0.00	2.17	6.67	1.83	25.13	17.45
Oithona spp.	39.14	3.65	0.19	6.69	4.17	0.00	0.00	0.55	0.00	0.00	0.00
Oikolpeura dioica	6.39	0.05	0.02	1.86	0.43	4.18	4.15	3.50	0.00	0.00	0.01
C. ponticus	0.00	0.00	0.00	0.05	0.02	28.05	2.30	0.05	0.11	0.41	0.05
Decapoda larvae	0.00	0.00	0.00	0.00	0.00	0.00	2.76	6.21	0.15	7.07	3.51
Pseudocalanus elongatus	0.74	0.28	2.68	0.62	0.13	0.00	0.73	0.03	0.01	0.00	0.77
Others	0.22	0.16	0.52	1.84	0.65	2.45	0.38	0.73	0.01	0.19	0.11
	100	100	100	100	100	100	100	100	100	100	100

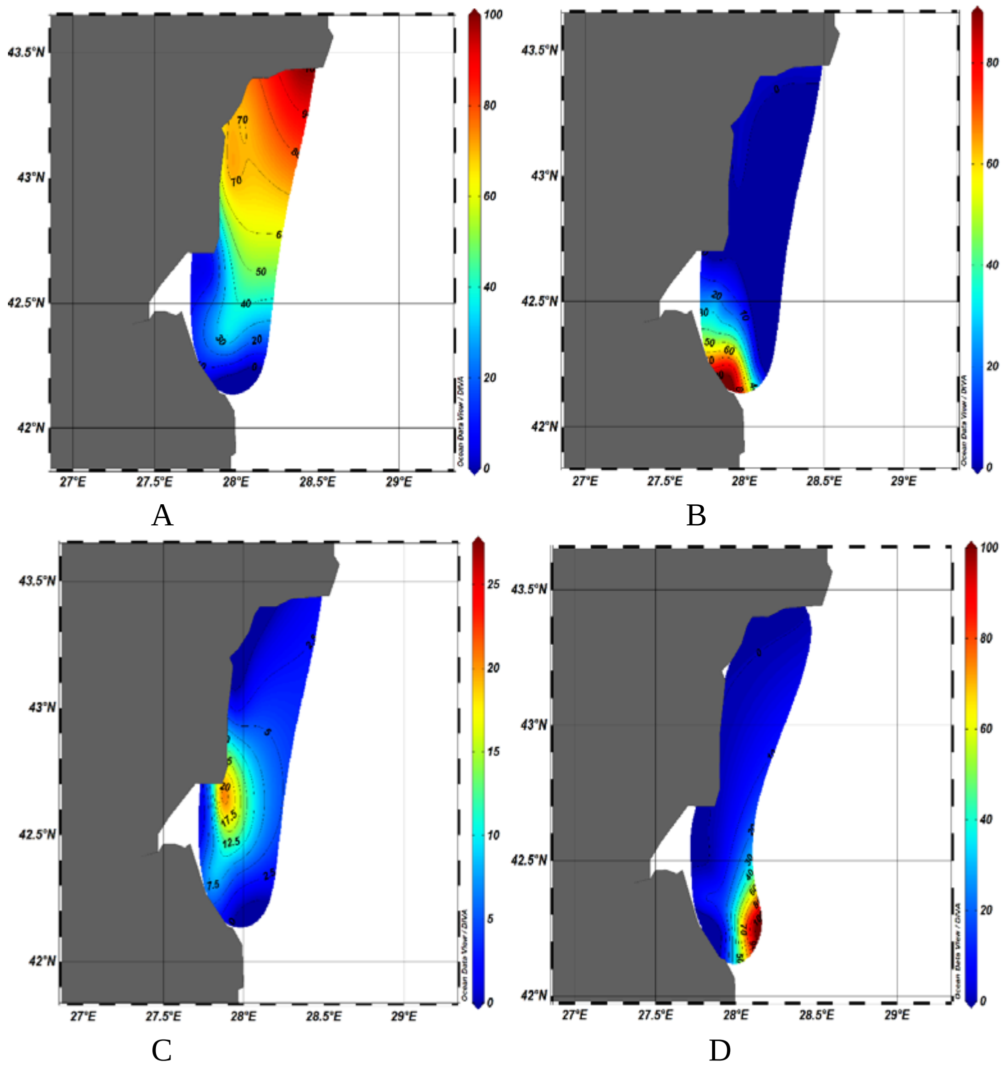

Fig. V.0.20. Spatial distribution of IRI (%) of mesoplankton species in sprat food (A) *A. clausi*, (B) *Paracalanus parvus*, (C) *L.veliger*, (D) *Calanus euxinus* in June 2019

Zooplankton in marine environment: species composition and biomass

During the studied period, the zooplankton biodiversity was formed by 24 species (Table V.0.12).

Table V.0.12. Species diversity of zooplankton

June 2019
Noctiluca scintillans
Ctenophora larvae
Pleurobrachia pileus
Aurelia aurita
Acartia clausi
Acartia tonsa
Pseudocalanus elongatus
Calanus euxinus
Paracalanus parvus
Centropages ponticus
Oithona davisae
Oithona similis
Harpacticoida spp.
Pleopis polyphemoides
Cirripedia nauplii/cypris
Lamellibranchia veliger
Polychaeta larave
Gastropoda veliger
Nematoda Larvae
Phoronis larvae
Decapoda zoea/mysis
Parasagitta setosa
Oicopleura dioica
Pisces ova, larvae

The species *Noctiluca scintillans* (Protozoa) played a dominant role in the total biomass formation - 83.10% (Fig. V.0.21.A, Table V.0.13), and the percentage of mesozooplankton (food zooplankton) reached 13.61%. The species *N. scintillans* and copepods predominated in abundance (Fig. V.0.21.B) and formed 67.56% and 20.86% of the total zooplankton abundance, respectively.

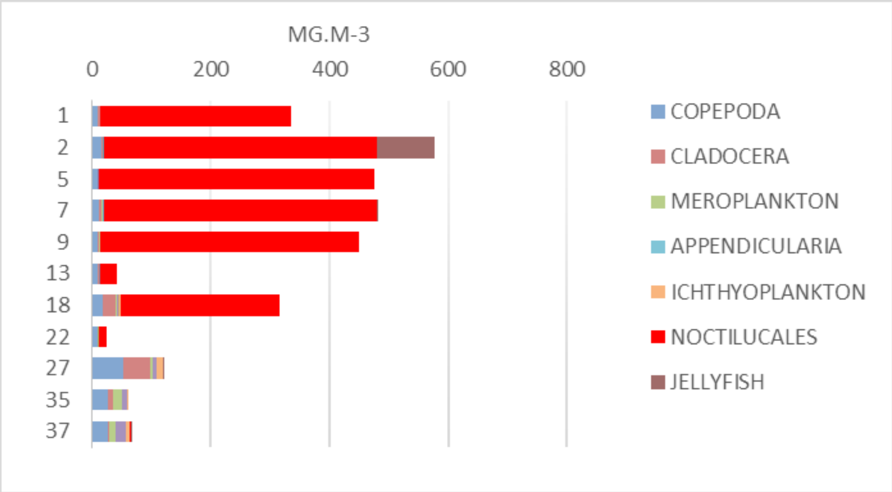

A

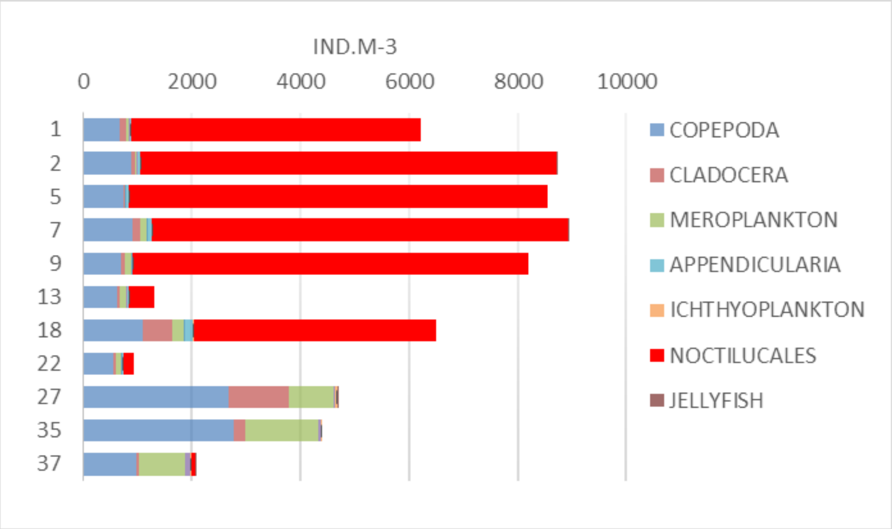

B

Fig. V.0.21. Distribution of the biomass (1. $mg.m^{-3}$) and abundance (2, $ind.m^{-3}$) of the main zooplankton groups ($mg.m^{-3}$) per stations in June 2019

Table V.0.13. Percentage distribution (%, from total biomass) of main zooplankton groups per stations in June 2019

STATIONS	COPEPODA	CLADOCERA	MERO-PLANKTON	CHAETO-GNATHA	APPENDICULARIA	ICHTHYO-PLANKTON	NOCTILUCALES	JELLYFISH
1	2.76	1.31	0.07	0.09	0.05	0.00	95.73	0.00
2	2.77	0.58	0.01	0.05	0.06	0.05	79.85	16.62
5	2.12	0.20	0.00	0.07	0.13	0.06	97.42	0.00
7	2.44	1.12	0.33	0.16	0.12	0.05	95.53	0.25
9	2.17	0.61	0.18	0.03	0.04	0.06	96.90	0.00
13	23.80	3.59	3.02	2.37	0.52	1.31	65.38	0.00
18	6.19	6.64	0.84	0.32	0.29	1.06	84.66	0.00
22	37.09	5.33	3.14	2.06	0.77	3.38	48.22	0.00
27	44.48	36.88	4.79	4.78	0.00	8.80	0.00	0.27
35	43.02	13.91	27.98	10.71	0.00	4.38	0.00	0.00
37	41.69	3.89	15.43	24.84	0.00	8.31	5.83	0.01

Table V.0.14 shows general statistical data about the total zooplankton biomass variability in June 2019, including three main groups – mesozooplankton, Protozoa, and jellyfish.

The total biomass of zooplankton amounted to 268.36 $mg.m^{-3}$ ± 63.13 (SE), with the biomass of the protozoan species *N. scintillans* reaching 223 $mg.m^{-3}$ ± 64.46 (SE) and of the mesozooplankton biomass - 36.52 $mg.m^{-3}$ ± 10.24 (SE). The total biomasses of food mesozooplankton and jelly species were assessed as relatively low for the season.

Table V.0.14. Statistical data about biomasses (mg.m^{-3}) of the main zooplankton groups in June 2019

	Meso-zooplankton	Protozoa	Jelly-plankton	Total zooplankton biomass
Mean	36.52	223.00	8.84	268.36
Standard Error	10.24	64.46	8.69	63.13
Median	20.29	268.26	0.00	316.85
Mode	#N/A	0.00	0.00	#N/A
Standard Deviation	33.96	213.79	28.82	209.37
Sample Variance	1153.50	45706.78	830.83	43834.31
Kurtosis	2.80	-2.19	11.00	-1.87
Skewness	1.70	0.02	3.32	0.11
Range	107.61	462.60	95.74	551.23
Minimum	12.23	0.00	0.00	24.76
Maximum	119.84	462.60	95.74	575.99
Sum	401.67	2452.98	97.27	2951.92
Count	11.00	11.00	11.00	11.00
Confidence Level (95.0%)	22.82	143.63	19.36	140.65

Mesozooplankton biomass showed an increase up to levels of 120 mg.m^{-3} in north direction (Fig. V.0.22.A); the amount of *Noctiluca scintillans* increased to 460 mg.m^{-3} mostly along c. Emine – c. Maslen Nos area (Fig. V.0.22.B), and the species *Pleurobrachia pileus* was concentrated in front of Kiten – c. Maslen Nos (Fig. V.0.22.C).

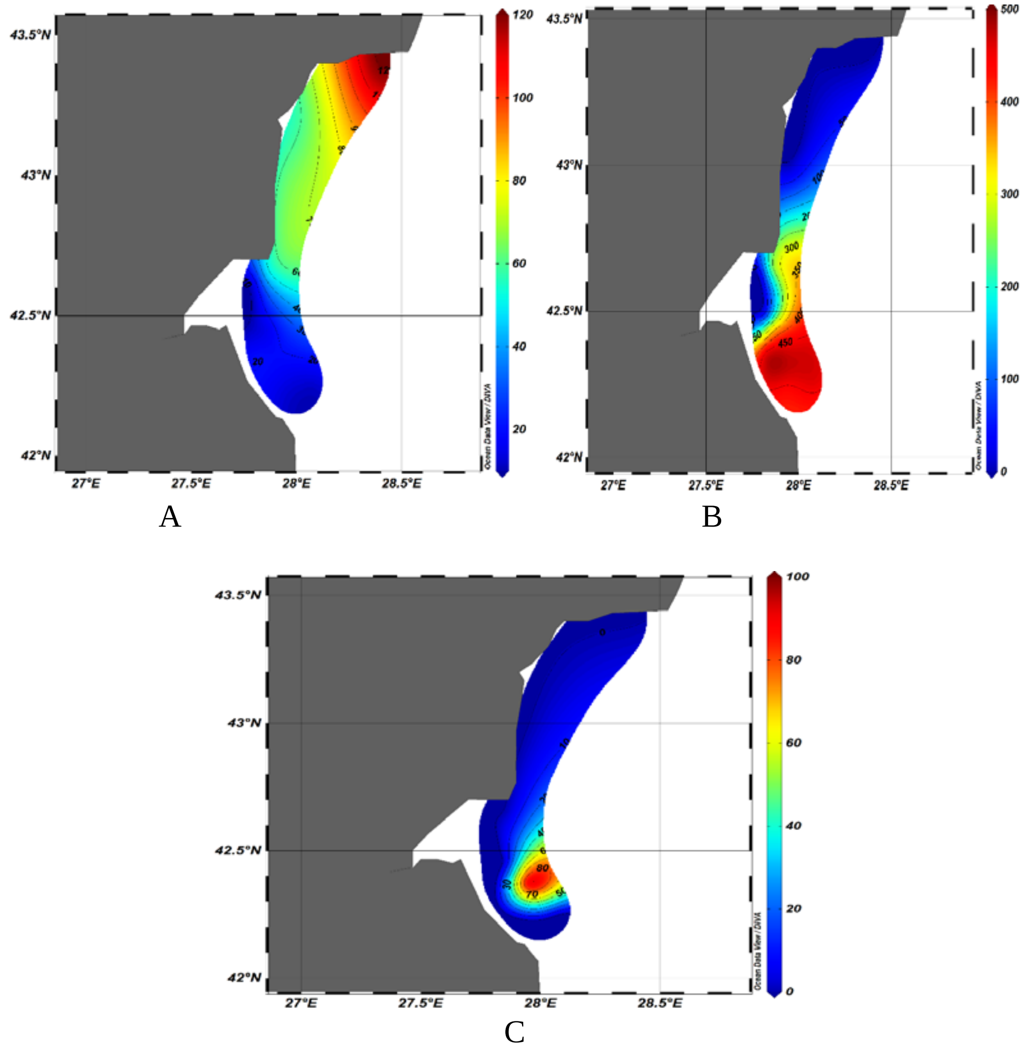

Fig. V.0.22. Spatial distribution of biomass (mg.m^{-3}) of mesozooplankton (A), *Noctiluca scintillans* (B) and jellyfish (C) in June 2019

VI. Forecasts and operational opportunities

Steady state of sprat stock

Equilibrium and the associated biomass of sprat from the Bulgarian Black Sea waters are presented graphically on Fig. VI.0.1. On the first graph, Equilibrium Yield with confidence intervals (showing very low Cimed and CI2.5%), Y / R with CI97.5% reaches its maximum and corresponds to fishing mortality at about 1.16 then follows the plateau and the determination of Fmax becomes impossible.

Obviously, levels above F = 0.8 will result in stock collapse. Sustained fishing mortality rates were around F = 0.5, which would correspond to the level of the catch of 12.5 thousand tons of sprat in the NW Black Sea.

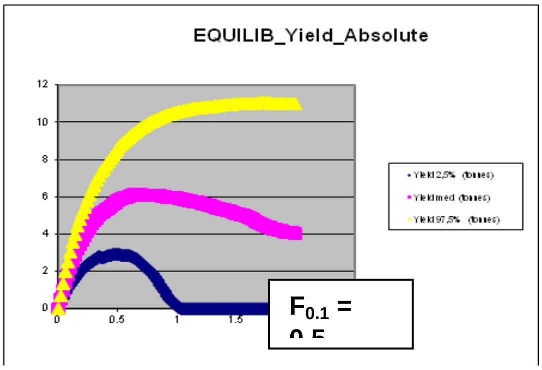

Fig. VI.0.1. Equilibrium level with CI. Optimal level of fishing mortality and corresponding catches of sprat from the Bulgarian waters

Biomass of the reproductive stock, vulnerable to fishing biomass and total biomass followed a similar downward trend since only CI values of 97.5% had relatively high levels of the lowest fishing mortality. Therefore, with increasing fishing mortality of all biomass tested (Fig. VI.0.2, Fig. VI.0.3, Fig. VI.0.4), a decreasing trend followed, following F = 0.8 (at CI2.5%) and after 1.16 (with Cimed), the stocks of sprat would fall below unsustainable levels (Fig. VI.0.1).

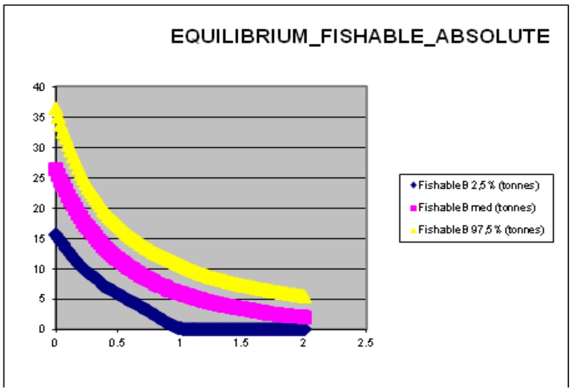

Fig. VI.0.2. Balance state of biomass vulnerable to fishing

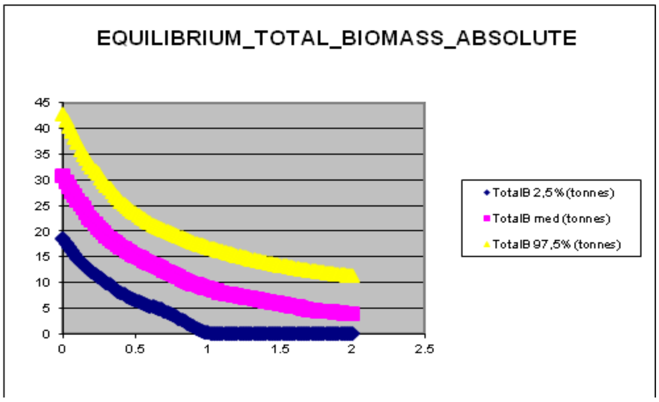

Fig. VI.0.3. Balanced state of total biomass

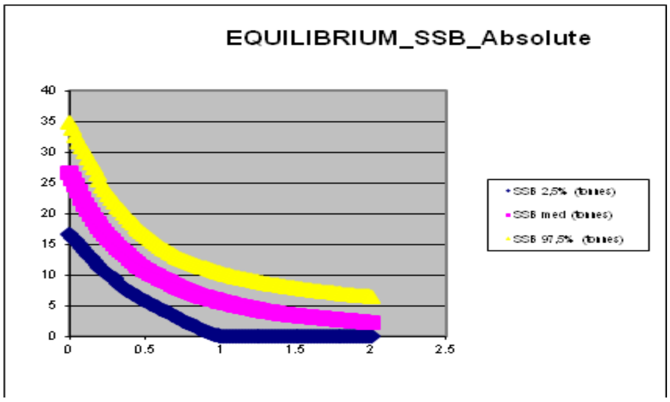

Fig. VI.0.4. Sustainable propagation biomass

Recruitment is heavily affected by fishing mortality and after F = 0.5 fell very steeply (Fig. VI.0.5).

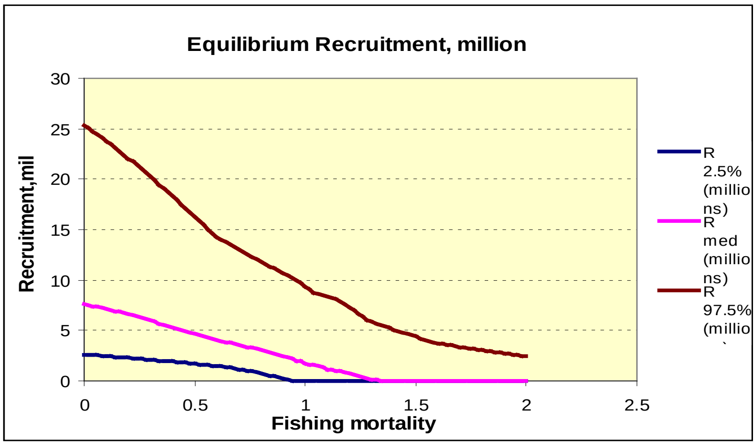

Fig. VI.0.5. Balance equilibrium

From Fig. VI.0.6 it is clear that the number of individuals in the catch in December marked a peak for 3-3+ year olds. From Fig. 6.6 it can be seen that the maximum (R^2= 0.5) of catch numbers belonged to individuals aged 1-1 + years. What is noteworthy is the high proportion of recruits, 2-2 + aged were significantly less and the older age groups were in a subordinate position. Estimated model of stock parameters is related to variation in fishing mortality over 10 years. Modeled catch parameters, parental biomass, replenishment and total biomass depend on long-term fishing mortality.

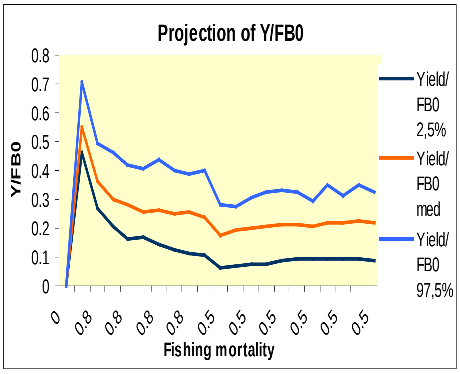

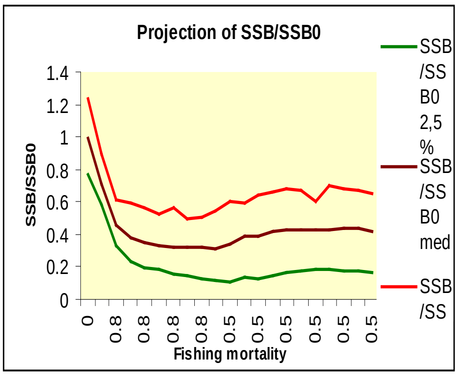

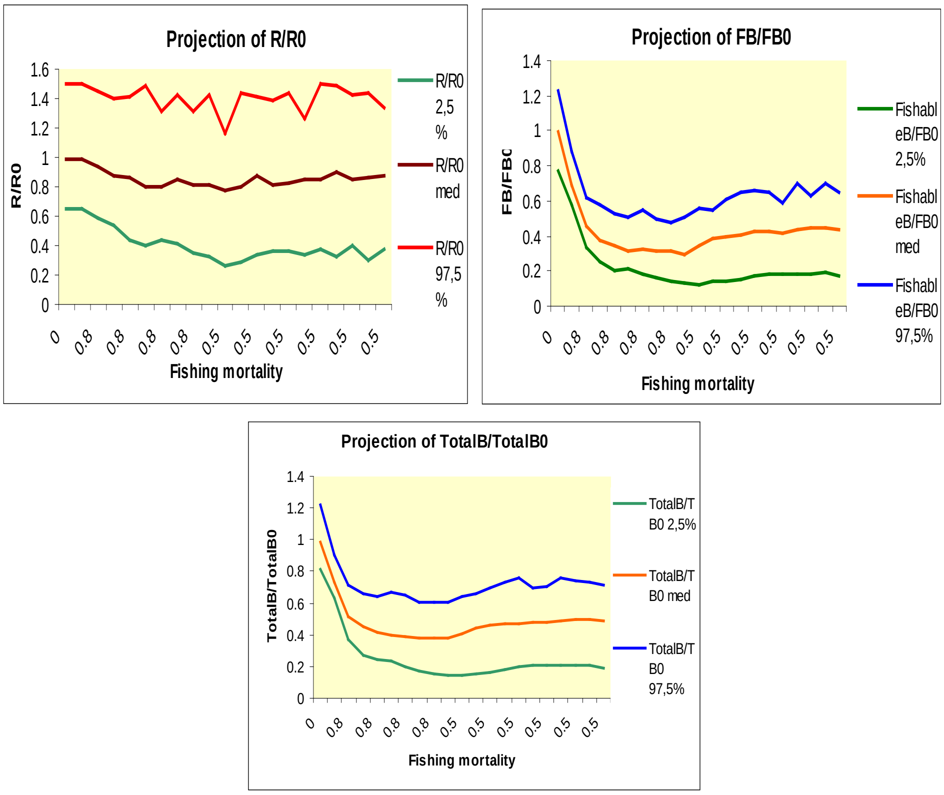

Fig. VI.0.6. Forecasts of the sprat stocks related to fishing mortality

(Unexploited state)

Relative catches (Y / F0) at very low fishing mortality rates were high during the first forecast year (Fig.VI.0.7. A). At F = 0.8, in the second year, the relative catch was expected to fall to levels of F = 0.5 (Fig. VI.0.7.A). After the fifth year it was expected that the Y / F0 connection plate would be observed at all tested confidence intervals. Similar to SSB / SSB0 (Fig. VI.0.7.B), and even a slight increase was observed of CI 97.5% and SSB / SSB0 of sprat after a change in fishing mortality (from F = 0.8 to F = 0.5). Recruitment (Fig. VI.0.7.C) was stable and was not affected by changes in fishing mortality. Biomass vulnerable by fishing and total biomass presented as a link with biomass when unused state, showed similar trends with those of the relative SSB (Fig. VI.0.7.D, E).

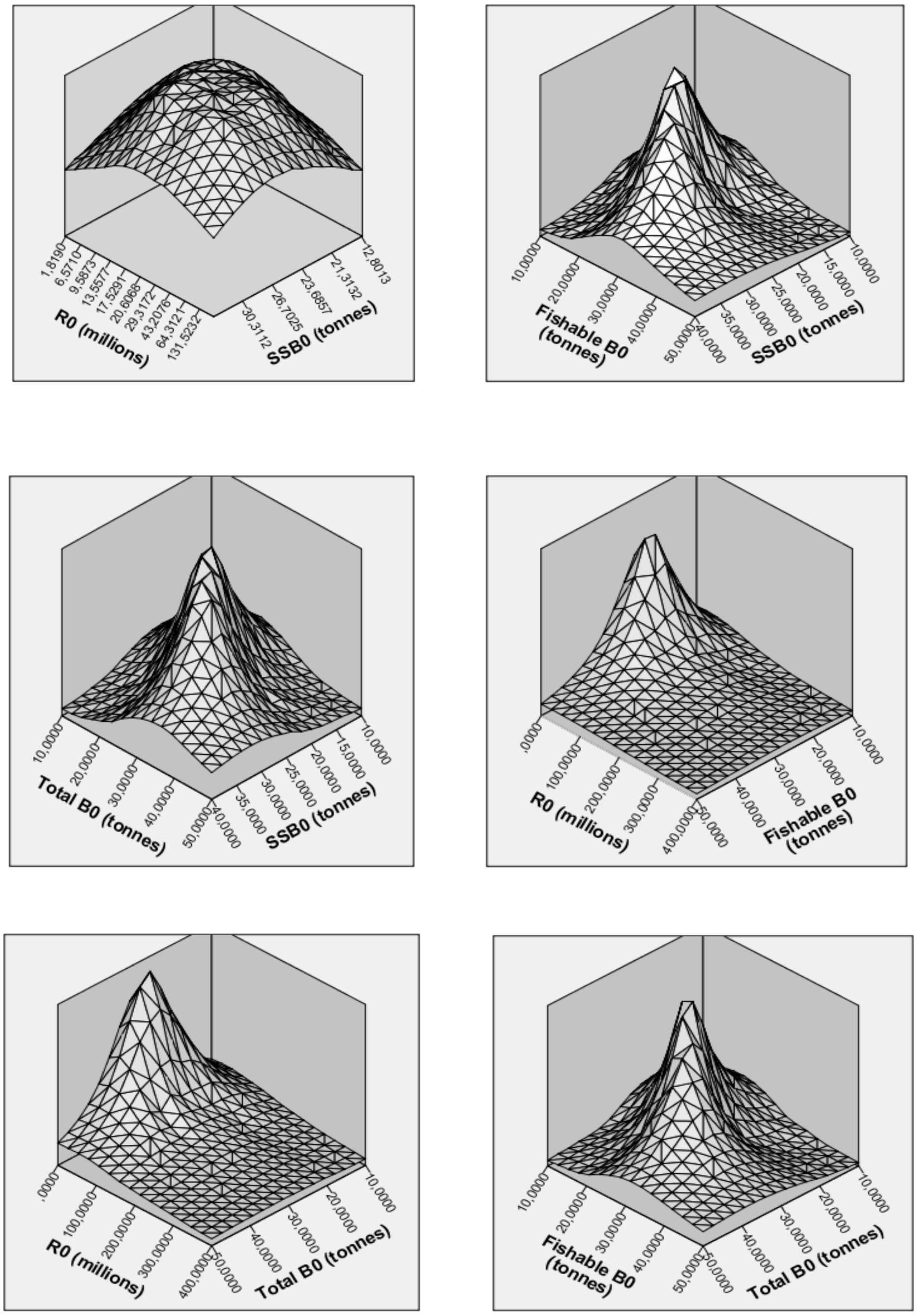

Fig. VI.0.7. Unused state

VII. Maximum sustainable yield

Maximum sustainable yield (MSY), in accordance with the mehod of Gulland (1970), was calculated for the exploited biomass from the studied area. In this study, we used the natural mortality rate M = 0.82, calculated by the method of Gislason et al., (2010). The results obtained are given in Table VII.0.1.

Table VII.0.1. Biomass (t) and MSY

Bulgaria	Biomass (t)	MSY (t) Gulland	MSY (t) BH steepness, $F_{0.1}$	2/3MSY
2017 – first exp.	1751	-	-	-
2017 – second exp.	1466			
2018 - first exp.	-	-	-	-
2018 – second exp.	10 898	5449		5500
2019 - first exp.	25 904	12 952	12500	8600
2019 - second exp.	46 081	18893	11750	7833

Expected MSYs are the maximum potential catches, including a quota-based catch, as well as false or unreported catches and by-catches in other fisheries. Calculated exploitation biomass and equilibrium levels (MSYs) should not be considered as an absolute value for possible future yields given the fact that the methods have some ambiguities and the share of IUU catches is still unknown. In such cases, special approaches are used, such as 2/3 MSY (Caddy and Mahon, 1995).

The recommended value of catches in the EEZ of the Republic of Bulgaria in the Black Sea, according to the current situation should be in the range of 5500 t for 2018 and 7833 - 8600 t for 2019.

VIII. Conclusions

2017

1. The total number of species identified was 11, of which 10 fish, 1 macrozooplankton.
2. The total studied Bulgarian marine area - 8135.40 km^2 and the total instantaneous biomass of sprat in October-November 2017 was 1751.313t and in November-December 2017 - 1466.422t. For the same period, the following biomass was found in horse mackerel – 1516.117 t and 1907.695 t, for the red mullet 704.7 t and 75.95 t respectively, and for whiting - 305.8 t.
3. The accumulation of all fish species studied was low, with passages scattered, which further complicated the determination of momentary biomass.
4. December was not the most suitable month for assessing the biomass of sprat because the species had a caviar disposal (cold-loving species). Much of the population was in the active phase of maturation, not actively feeding. Zooplankton during that period was dispersed, solar activity was low and SST - relatively high, i.e. all conditions were unfavorable for sprat agglomerations.
5. During the autumn-winter season no trend was established in the distribution of the species by strata, due to the unfavorable hydrometeorological conditions and the strong currents at that time of the year.
6. In the samples from the Bulgarian marine zone, the size composition of sprat varied from 6.5 cm to 11.75 cm.
7. The size classes of the 7.0-8.5 cm sprat were dominant with the larger classes represented by a low percentage. In October-November, the size class 7.0 had a very high percentage, followed by L = 8.0 and 8.5 cm.

8. For the red mullet, size class 12.5 cm prevailed during the winter period, followed by size class 9 cm. In December there was a low share of all classes.

9. In October-December, the size classes of horse mackerel ranged from L = 8 to 12.5 cm. In December, the classes with a length from 10.5cm to 14cm were presented with the peak being only 11, 11.5 and 12 cm size classes.

12. The asymptotic length reached 12.6 cm and the growth rate might be estimated to be relatively high, equal to 0.45 y^{-1}. The growth of the sprat from the present study was positive allometric (n = 2.66).

13. In the autumn of 2017, the average value of the stomach fullness index of sprat (ISF) reached 0.62% of body weight (BW) and exceeded by 17.54% the multiannual average value for the autumn months of 2007-2010. ISF was minimal near the coast and increased towards high seas. In the studied area off the Bulgarian coast, relatively high values of ISF (0.8-0.9% BW) were registered in the strip Obzor – Tsarevo.

14. No statistically significant correlation was found between the occupancy indices and the weight of sprat (within the range 2.34 - 8.43).

15. The average number of victims in the diet of sprat was 68 ind/stomach, comparable to the average number of casualties in the autumn months of 2007-2010 (64 ind/stomach) but 4.8 times lower than the average number of food organisms in autumn 2016 (328 ind/stomach). In spatial terms, a greater average number of casualties> 100 ind/stomach were established off the southern shores at the 35-meter isobath.

16. Fifteen zooplankton species/groups were identified in the food spectrum of sprat. Representatives of Copepoda included the species: *Calanus euxinus*, *Pseudocalanus elongates*, *Acartia clausi*, *Oithona* spp., *Paracalanus parvus*, *Copoepoda nauplii*, *Copepoda ova;* four taxonomic groups were identified from planktonic larvae of demersal organisms (meroplankton)*: Lamellibranchia veliger*, *Cirripedia cypris*, *Decapoda mysis*, Polychaeta larvae; the crustacean planktonic Cladocera were represented by *P. enilia avirostris*; Chaetognatha class - *Parasagitta setosa* species; fish and larvae of Ispodoa were also found.

17. The cold-loving species *Calanus euxinus* played a dominant role in the diet of sprat,

followed by *Parasagitta setosa*, *Pseudocalanus elongatus*, *Copepoda ova*, *Paracalanus parvus* and *Lamellibranchia veliger*. Cold-loving forms were prevalent both in frequency of occurrence and in numbers and biomass.

18. In the studied horse mackerel specimens, the average index of stomach fullness (ISF) reached 0.46% by weight (BW). The highest average values of ISF = 0.54% were established in the coastal region covering Emine - Sozopol and Burgas Bay.

19. The average number of casualties (PN) in gastric contents of horse mackerel was 383 ind/ stomach. The maximum average number of food organisms was registered in Sozopol due to the consumption of small food objects, mainly *Lamellibranchia veliger*. Despite the higher number of casualties, eating at small food establishments was associated with lower gastric filling (ISF), so there was an inverse correlation between these two parameters (not statistically significant) .

20. There were 15 zooplankton species in the food of horse mackerel, as well as mussids, isopods and fish remains. Five taxonomic groups were identified from the meroplankton group: *Lamellibranchia veliger*, *Decapoda mysis*, *Gastropoda veliger*, Polychaeta larvae, *Cirripedia cypris*; the group of copepods was represented by the species: *Paracalanus parvus*, *Acartia clausi*, *Calanus euxinus*, *Pseudocalanus elongatus*, *Centropages ponticus*, *Oithona similis* and *Oithona davisae*; Cladocera crustaceans were represented by *Penilia avirostris*; Chaetognatha class - by the species *Parasagitta setosa*. Appendicularia, Izopoda larvae and *Paramysis* spp . were also present in the anchovy's nutritional spectrum.

21.Meroplankton larvae *Lamellibranchia veliger* dominated the food of horse mackerel in the study area in October-December 2017. Comparatively well-nourishing components were also *Acartia clausi*, *Paracalanus parvus*, *Parasagitta setosa* and Decapoda larvae.

22. The total offshore zooplankton biomass amounted to 1591.39 $mg.m^{-3}$, with Protozoa biomass alone reaching 1341.91 $mg.m^{-3}$ and mesozooplankton-38.85 $mg.m^{-3}$. Nutritional mesozooplankton biomass could be characterized as being low in that season.

23. Two well-pronounced blooming of *N. scintillans* were established - in the area below c. Kaliakra and opposite Sozopol - Primorsko. Blooming off the northern shores covered a

larger area and spread in Kalikara - Kamchia area, indicating increased eutrophication of the water.

24. The feeding conditions of the red mullet were more favorable in the open sea and along Obzor and Tsarevo strip. Accordingly, for horse mackerel, the coastal region provided a better nutrient environment, mainly in Emine - Sozopol area and in Burgas Bay.

25. The relative catch (Y / F0) at very low fishing mortality rates was high during the first forecast year. At F = 0.8, in the second year the relative catch was expected to fall to the levels of F = 0.5.

26. Sprat is a fast-growing species with large variations in maternal biomass and replenishment and depends on anthropogenic impacts other than fishing, as well as on the dynamics of environmental factors. Therefore, when studying these dependencies of great importance is the continuous nature of the research.

2018 – 1st expedition

1. The total number of species found was 18, of which 14 fish, crustaceans - 1, molluscs - 1 and one macrozoo - planktonic species. In November 2018, the most common species in total trawl operations (in terms of presence/absence) were: *Tr.mediterraneus* (52.13%), *M.barbatus* (25, 66%), *E.encarsicolus* (8.11%) and *P. saltatrix* (14.1%). Other species such as *S.sprattus*, *M.merlangius*, *A. immaculata*, *N.melanostomus*, *G.niger*, *Mugil cephalus*, etc. had a negligible presence in the catches of November 2018.

2. During the study period, the largest number was of the *Aurelia aurita* jellyfish. The species had the highest recorded biomass and catch per unit area in the surveyed areas in November-December 2018.

3. Horse mackerel (*Trachurus mediterraneus*), during the studied period, did not form thick clusters and was recorded in all surveyed lanes with similarly equivalent CPUA kg.km^{-2} and biomass (t). The prevalence of catches per unit area and biomass was in a 50-75m stratum (CPUA = 460 kg. km^{-2}; 1266.9 t), where pelagic society dominated.

4. Bluefish (*Pomatomus saltatrix*), during the studied period, did not form thick clusters and

was recorded in all surveyed lanes with equally uniform CPUA kg. km^{-2} and biomass (t): stratum 15-30m, CPUA = 279.3159 kg. km^{-2}, 576.8265 t; stratum 30-50m, CPUA = 327.1533 kg. km^{-2}, 593.7244 t; stratum 50-75m, CPUA = 142.77kg. km^{-2}, 393.1347 t; *Aurelia aurita* - high levels of catch per unit area and biomass were recorded in all strata. The total biomass of the species was 3379 t; Sprat (*Sprattus sprattus L.*) - small pelagic species inhabiting the continental shelf area up to 100 - 120 m. In November 2018 survey, only single specimens were found in the catches. Hydrometeorological conditions, presence of large predators, strong underwater currents and large clusters of the *Aurelia aurita* jellyfish were probably factors that influenced the formation of schools.

5. Whiting (*Merlangius merlangus*) inhabits the bed near the bottom and feeds mainly on sprat. The species is a predator on sprat and is an important component of food for the biggest predators such as turbot and dolphins. In August it did not usually attend the catch. This may be related to the relatively high temperatures (SST) and these in the water column. The size of the catches of this species was small. In November - December, catches were sporadic, with individual specimens.

6. The instantaneous biomass in the test area was as follows: sprat: 3996.399 t; horse mackerel - 2511.643t; red mullet - 1563.686 t; *Aurelia aurita* – 3378.993t. The remaining species, as well as the target species, had a minor presence.

7. The predominant age for the horse mackerel was 2-2 + (63%), followed by age 1-1 + (22%), 3-3 + (12%), 4-4 + (3%).

8. The predominant age of the red mullet was 2-2 + (59%), followed by age 1-1 + (28%), 3-3 + (10%), 4-4 + (3%), 5-5 + (0.5%).

9. The somatic growth of horse mackerel in current studies showed that the mean weight corresponding to the oldest age group was 39 g. The value corresponded to the marginal size of the 16.8 cm size class observed in the samples of the trawl survey in the Bulgarian waters.

10. In the trawl bag of mesh size a = 8.00 mm, the probability is that 25% of the specimens retained in the bag should have a size of 6.2 cm (L25I. = 6.2 cm). With 50% probability (L50%), individuals with a size of 7.00 cm will be retained and the most likely to be retained

(L75%) will be individuals with a linear size of 7.8 cm.

11. According to the calculations made on the selectivity of the trawl bag of different mesh sizes, it can be seen that at a = 8mm, 50% of individuals with TL = 7cm have a chance to be trapped, while those with TL = 7.8 cm have a 75% retention capability. A further reduction in mesh size leads to a reduction in the selectivity of the trawl. In eye mesh a = 7.0cm, L50% = 6.2cm and L75% = 7cm. For nets with a mesh size of 6.5mm, the size of the trait-retained individuals droped to 5.7cm at L50%. As the mesh of the bag increases, the number of small individuals that escape from the trawl also increases.

12. Eight zooplankton species/groups were identified in the stomach content of the studied sprat specimens in November 2018 – copepods were represented by many species.

13. The sprat food spectrum was dominated by the cold-water copepod *Calanus euxinus*, followed by *Parasagitta setosa*, *Acartia clausi*, *Oicopleura dioica*, *Ps. elongatus* and Decapoda larvae.

14. The sprat mean index of stomach fullness was high in November 2018 - 1.05 % BW ± 0.86 (SD), surpassing with 51.50 % the mean value of 2017. The maximal ISF = 1.45 % BW was estimated near to c. Emine, while minimal values of this index were registered in front of c. Kalikara.

15. In the horse mackerel food were identified 13 zooplankton species/groups, as well as Isopoda larvae. The cold-water copepod *C. euxinus* dominated in the horse mackerel food during November-December 2018. Less represented in the diet were *Parasagitta setosa*, *Pseudocalanus elongatus* and meroplankton Ciirripedia. Parasitic nematodes were found in 26 % of all studied specimens.

16. The mean PN in stomach content of horse mackerel reached 11.94 ind/stomach ± 2.36 (SE). In front of Byala was obtained the maximal individual PN - 160 ind/stomach, due to intensive consumption of the copepod *Calanus euxinus*.

17. Horse mackerel reached 0.40 % BW ± 0.56 (SD) with the highest levels of the ISF = 0.7-1 % BW in Burgas Bay and in the open sea along the central coast.

18. The red mullet food consisted of seven benthic and plankton groups. In November 2018,

the average ISF of the red mullet attained 0.63 % BW ± 0.54 (SD), while the mean PN was 13.4 ind/stomach ± 5.51 (SE). Parasitic nematodes were established in 20 % of all studied red mullet specimens.

19. In marine environment, the total zooplankton biomass reached 3808.72 $mg.m^{-3}$ ± 3299.65 (SE), as jellyfish created high biomass - 3753.2 $mg.m^{-3}$ ± 3300.1(SE), by low level of fodder mesozooplankton - 32.84 $mg.m^{-3}$ ± 7.25 (SE). The fodder mesozooplankton biomass was close to the autumn levels in 2017. The fodder mesozooplankton biomass increased in north direction.

20. The nutritional conditions in the region off c. Emine were favourable for sprat feeding. Burgas Bay and the central coastal area presented relatively good conditions for horse mackerel feeding. We could not estimate the favourable feeding grounds for the red mullet due to limited number of samples.

2018 - 2nd expedition

1. A total of **36** trawlings in the Bulgarian water area were carried out on board the R/V *HaitHabu*. The total number of species found was 19, of which 15 fish, crustaceans - 2, molluscs - 1 and one macrozo - planktonic species.

2. The most common species in the total trawl operations (in terms of presence/absence) were (in descending order) in December 2018: single specimens of *Raja clavata* and *Dasyatis pastinaca*, *Scophthalmus maximus*. Most of the catch was sprat (21%), whiting (68%), horse mackerel 11%, other species were presented with single specimens.

3. The total biomass of the sprat in December 2018 was 10 898.18t for the Bulgarian Black Sea area. Catch predominance per unit area was 15-30m (1868 kg. km^{-2}).

4. The total biomass of horse mackerel in December 2018 is 2965.407 t for the Bulgarian Black Sea area. At a depth of 50-75m, agglomerations of the species were not recorded (CPUA = 1629 $kg.km^{-2}$.). In the strata 15-30 and 30-50m the biomass of the agglomerations was 1466t and 1500t, respectively.

5. Temporary biomass of whiting reported in December 2018 was 7277t. Similar to the sprat,

the clusters in the layer 15-30m had predominance of 1612t, followed by 925t and 825t at 30-50m and 50-75m, respectively.

6. The highest catch per unit of sprat was recorded at a depth of 50m southeast of Pomorie (CPUA = 5679 kg.km^{-2}). In Nesebar Bay at a depth of 29-30m, CPUA = 2560kg.km^{-2} and at a depth of 62m - CPUA = 1955kg.km^{-2} .

7. At a depth of 50-75 m, there were no accumulations of horse mackerel in December 2018. At a depth of 46 meters abundance was 1629 kg.km^{-2}. In the other surveyed areas, the clusters were insignificant and in most of the catch areas they were not registered.

8. In the 15-30m layer, the highest catch per unit of whiting was 2050kg.km^{-2}, average for the layer - 612kg.km^{-2}. In the 30-50m and 50-75m layers, CPUAs were close to 925 kg.km^{-2} and 825 kg.km^{-2}, respectively. Coastal zone biomass was 7277t. In all surveyed areas we recorded shoals of the species. The highest values of the highest catch per unit area and the biomass of the species were in front of c. Maslen Nos, Nesebar Bay and Pomorie.

9. The composition of the size of the sprat consisted of size classes (TL, cm) from 6.5 cm to 11.5 cm in the samples from the Bulgarian marine zone.

10. Size classes 8 - 8.5 cm were dominant, with older classes being represented with a low percentage. In December, size class 8 was very high, followed by L = 7.0, 8.5 and 9 cm. The situation with the lack (or low share) of larger (the most senior) individuals was the same in the period 2007-2018 (Raykov et al., 2018).

12. The age structure of the studied species did not show deviations from the norm in the long-term 2007 -2017.

13. Asymptotic length reached12.34 cm; the rate of growth could be determined as being relatively high 0.45 y^{-1}. The growth of sprat from the present study was positive allometric (n = 2.76).

14. The somatic growth of sprat from current studies showed that the mean weight corresponding to the oldest age group was 8.05 g. The value corresponded to the marginal size of 11.75 cm measured in the samples of the trawl survey in the Bulgarian waters.

15. The asymptotic weight reached 11.41g. The weight was assessed as relatively

stable and high 0.44 g. This fact could be related to the fact that in December, the species had a high degree of maturity.

16. The sprat was in an active spawning phase during the current investigation in December. Most of the individuals had III - IV stage of the gonads. A more detailed analysis should be made in the active period of spawning of the species (October-February).

17. The GSI (%) indicated that over 50% of females were actively breeding. Very few specimens were at an early stage of maturation, so we could conclude that in December 2018, active reproduction began, even with comparatively high water temperature for the season.

18. The fertility of the sprat correlated positively with its length (R2 = 0.45), with large size classes corresponding to high fertility.

19. The ratio between fertility and weight of sprat was very well expressed (R = 4.46)

20. In December 2018, the sprat food spectrum was constituted by 11 zooplankton species/groups, including several copepods.

21.The average sprat ISF reached 1.20 % BW ± 1.05 (SD), with 18.87 % increase in comparison with the first stage of the trawl studies in November 2018. High mean ISF = 2.25 - 2.61 % were found off Sozopol and Chernomorets, while minimal levels were detected in front of c. Emine and in the northern part of Burgas Bay.

22. During the survey, the total zooplankton biomass attained 860.66 $mg.m^{-3}$ ± 563.44 (SE), while the gelatinous zooplankton biomass was 826.87 $mg.m^{-3}$± 564.86 (SE), and the fodder mesozooplankton formed quantities of 32.07 $mg.m^{-3}$ ± 4.61 (SE). The fodder zooplankton biomass remained relatively low for the season. In December, the quantity of the jellyfish decreased with 128 % in compassion to November 2018.

24. The relative catch (Y/F0) at very low fishing mortality rates was high during the first forecast year. At F = 0.8, in the second year, the relative catch was expected to fall to F =0.5.

25. Sprat is a rapidly developing species with large variations in native biomass and recruitment, and is dependent on anthropogenic impacts other than fishing, as well as on the dynamics of environmental factors. Therefore, when studying these dependencies, the continuing nature of research is of great importance.

26. The momentary state of sprat biomass in December was 10 898t. According to the method of Gulland and BH steepness, F0.1, the limits of the yearly catch should be within 5 550t.

27. Calculated biomass and equilibrium levels (MSYs) should not be considered as an absolute value for future catches given the fact that the methods have some ambiguities and the share of IUU is still unknown. In such cases, special approaches are used, such as 2/3 MSY (Caddy and Mahon, 1995). The recommended value of the catches should not exceed 5500t of sprat for this year of exploitation in the Bulgarian waters of the Black Sea.

2019 – 1st expedition

1. The total number of identified species was 24, of which 16 fish (with 2 species more than the autumn survey in 2018), 2 crustaceans, 2 molluscs and 4 macrozooplankton species. The most common species in general trawl operations (in terms of presence/absence) were: *S. sprattus* (76.5%) *M. barbatus* (9.66%), and *M. merlangius* (4.86%). Other species such as *A. immaculata*, *N. melanostomus*, *G.niger*, etc. have a negligible presence in the catch in June 2019.

2. Sprat (*Sprattus sprattus*) had the highest recorded biomass and catch per unit area in the study areas in June 2019. At stratum 15-30m CPUA = 1867.7 kg.km^{-2} and biomass -12 497 t.

3. In June 2019, the red mullet was the least represented in the shallow coastal zone 15-30m with a CPUA = 52.9 kg.km^{-2} and biomass of 109.25 t. The highest CPUA values of 419 kg.km^{-2} were established in the 30-50m depth lane with biomass of 761 t.

4. In June 2019, the whiting was most strongly represented in the shallow coastal zone 15-30m with CPUA = 270 kg.km^{-2} and biomass of 557 t., followed by a depth strip of 30-50m with a catch per unit area of 218 kg.km^{-2} and biomass 396 t; 115 kg.km^{-2} for CPUA and 473 t biomass at depths of 50-100m.

5. The total biomass in June 2019 was 25 903.47t for the Bulgarian Black Sea area.

6. The total studied area of the Bulgarian part was 8010.24 km^{-2} and the total identified biomass of the red mullet - 1837.4t in June 2019.

7. The total area surveyed was 8010.24 km^{-2}. The total biomass of whiting in June 2019 was 1426.5t.

8. Sprat size frequencies indicated maxima in the distribution of classes 7.5-8 cm of whiting, with a pronounced bimodal distribution with peaks of 8-10 and 11-13 cm; peaks were also observed at 11-12 cm and 14 cm.

9. The prevalence of sprat in this study was 1-1 + (74%).

10. The prevailing age for whiting in this study was 2-2 $+y^{-1}$.

11. The predominant age of the red mullet was 2-2 + (27%), followed by ages 1-1 + (24.7%), 3-3 + (20.5%). Senior age and juvenile forms were present with a low percentage.

12. Sprat was not active in the spawning phase of this investigation in June. Most of the individuals had stage I-II, III glands. A more detailed analysis should be made in the active spawning period of the species (October-February).

13. GSI (%) indicated that a small percentage of females were actively breeding. Most individuals were in the early stages of maturation, so we could conclude that in June 2019, active reproduction did not begin.

14. In June 2019, the sprat food spectrum was composed of 19 zooplankton species/groups, including several copepods - *Calanus euxinus*, *Pseudocalanus elongatus*, *Paracalanus parvus*, *Acartia clausi*, *Centropages ponticus*, *Oithona* spp., *Harpactiocoida* spp., *Copepoda* spp; five taxonomic groups meroplankton - *Lamellibranchia veliger*, *Gastropoda veliger*, Cirripedia larvae, Decapoda larvae, Polychaeta larvae; class Chaetognatha was presented by *Parasagitta setosa*, class Appendicularia - by *Oicopleura dioica*. Single specimens of *Noctiluca scintillans* and *Pisces ova* were also found in the sprat ration.

15. The average ISF attained 0.80% BW ± 0.53 (SD), with an increase of 40.60% over the average value for 2007-2010 (0.53 % BW). High mean levels of ISF = 1.4% BW were registered in front of Ahtopol and below c. Kalikara, while minimal levels (~ 0.5% BW) were established in the shallow coastal zone between Varna and Sozopol Bays.

16. The mean PN attained 205.35 ind/stomach ± 260.39, as the highest average PN - 621 and/stomach was found in north direction, below c. Kalikara (16 m depth), connected with

the excessive consumption of *Acartia clausi*. A high average PN of 554 ind/stomach was established in front of c. Maslen Nos, (41 m depth), related to the consumption of *Lamellibranchia veliger*.

17. During the survey, the total zooplankton biomass attained 268.36 $mg.m^{-3}$ ± 63.13 (SE), while the protozoan *N. scintillans* biomass was 223 $mg.m^{-3}$ ± 64.46 (SE), the fodder mesozooplankton formed quantities of 36.52 $mg.m^{-3}$ ± 10.24 (SE), and the jellyfish biomass was 8.84 $mg.m^{-3}$ ± 8.69 (SE). The total biomasses of fodder zooplankton and jellyfish species were estimated as relatively low for the season.

18. An increase in the fodder mesozooplankton biomass up to 120 $mg.m^{-3}$ was established in the northern sector, and an increase in the amount of *Noctiluca scintillans* to 460 $mg.m^{-3}$ was recorded in c. Emine – c. Maslen Nos zone, while the species *Pleurobrachia pileus* was concentrated in front of Kiten – c. Maslen Nos. The northern shores presented relatively good conditions for sprat feeding, and a particular increase in the nutritional indices of sprat was also found in the Ahtopol – c. Maslen Nos zone.

19. An increase of the biomass of the food mesozooplankton in the northern coasts was established - up to 120 $mg.m^{-3}$; an increase in the amount of *Noctiluca scintillans* to 460 $mg.m^{-3}$ was recorded in c. Emine – c. Maslen Nos strip, while *Pleurobrachia pileus* species was concentrated in front of the strip Kiten – c. Maslen Nos. The northern shores offered relatively good conditions for feeding the sprat, and a certain increase in the nutritional indices of the sprat was also found in the Ahtopol – c. Maslen Nos zone.

20. The maximum sustainable yield (MSY), in accordance with the Gulland method (1970), was estimated at 12 952 t; BH steepness, F0.1 = 12500 t.

21. The calculated exploitation biomass and equilibrium levels (MSYs) should not be considered as an absolute value for possible future yields, given the fact that the methods have some uncertainties and the proportion of IUU catches is still unknown. In such cases, special approaches such as using 2/3 MSY are applied (Caddy and Mahon, 1995).

2019 - 2nd expedition

1. The total number of identified species was 34, of which 26 - fish, crustaceans - 2, molluscs - 2 and 4 macrozzooplankton species. The most common species in general trawl operations (in terms of presence/absence) were (in descending order): *S.sprattus* (82.99%). *M. merlangius* (9.44%), and *M.barbatus* - 6.54%). The other species were found in small quantities or as separate individuals in the catches.

2. Sprat (*Sprattus sprattus*) had the highest recorded biomass and catch per unit area in the study areas during the period October-November 2019. In the layer of 15-30m CPUA = 11 536 kg.km^{-2} and biomass 23 825 t., followed by 30-50 m layer with CPUA = 10 640 kg.km^{-2} and biomass 19 311 t, and 50-100m layer with CPUA = 7 130 kg.km^{-2} and 2945,2t biomass. In October-November 2019, the highest CPUA values of the red mullet of 1016.1 kg.km^{-2} were established in a stratum 15-30m, with biomass of 2098.5t, followed by 50-100m layer with CPUA of 496 kg.km^{-2} and biomass 1023.4 t, 172 kg.km^{-2} for CPUA and 312 t biomass at a depth of 30-50m.

3. The whiting was well presented in the 50-100m layer during the reported period with CPUA = 4 803,4.km^{-2} and biomass of 19 839t, followed by 30-50 m layer with CPUA of 218 kg.km^{-2} and biomass of 396 t, 115 kg.km^{-2} for CPUA and 473 t of biomass at a depth of 50-100m.

4. The total biomass of sprat in October-November 2019 was 46 081.4 t for the Bulgarian Black Sea zone.

5. The total area of the survey in the Bulgarian part was 8010.24 km^{-2} and the total identified biomass of the red mullet was 5122.056 t in October-November 2019.

6. The total surveyed area was 8010.24 km^{-2}. The total biomass of whiting in October-November 2019 was 21 174.59 t in the Bulgarian Black Sea area.

7. Sprat size frequencies indicated a maximum in the class distribution (7.5 cm), with a columnar decrease in the direction of the maximum established sample sizes.

8. The prevalence of sprat in this study was 1-1 + (78%).

Project proposal № BG14MFOP001-3.003-0001 "Collection, management and use of data for the purposes of scientific analysis and implementation of the Common Fisheries Policy for the period 2017-2019", funded by the Maritime Affairs and Fisheries Program, co-financed by the European Union through the European Maritime and Fisheries Fund

9. The predominant age of whiting in this study was 2-2 + (32%), 3-3 + (24%).

10. The predominant age of the red mullet was 2-2 + (46%), followed by the age of 3-3 + (26,6%).

11. Sprat was in the active phase of spawning in October-November. Most of the individuals had gonads in stage IV-V-II and an active reproduction had commenced.

12. GSI (%) indicated that a big percentage of females were actively breeding. Most individuals were in the late stages of maturation, so we could conclude that in October-November 2019, active reproduction begun.

13. During the autumn survey, the sprat food spectrum was constituted by 23 zooplankton species/groups, including several copepods - *Calanus euxinus*, *Pseudocalanus elongatus*, *Paracalanus parvus*, *Acartia clausi*, *Centropages ponticus*, *Oithona similis*, *Oithona davisae*, *Harpactiocoida* spp; cladocerans (water fleas) were presented by *Pleopis polyphemoides*, *Penilia avirositis* and *Pseudoevadne tergestina*; the group of planktonic larvae of bottom organisms included five taxonomic groups - *Lamellibranchia veliger*, *Gastropoda veliger*, Cirripedia larvae, Decapoda larvae and Polychaeta larvae; class Chaetognatha was represented by *Parasagitta setosa*, class Appendicularia - by *Oicopleura dioica*.

14.The average value of sprat ISF was 0.91% ± 0.60 (SD) (SD) or with 13.75% higher than the measured level during the spring survey. The highest average ISF = 1.36 - 1.3 % was established in Burgas Bay and in front of Kamchia River mouth at depths of 30 - 45 m, while the minimal ISF (~ 0.3% BW) was registered in the area of c. Maslen Nos.

15.The average prey number (PN) in the sprat diet was 230 ind/stomach ± 321.64 (SD). The maximal individual number of food organisms - 1340 ind/stomach was established in the open part of Burgas Bay (d = ~ 30 m), related to intensive consumption of the copepod *Paracalanus parvus*.

16.Nineteen mesozooplankton species were identified in the horse mackerel food: copepods - *Calanus euxinus*, *Pseudocalanus elongatus*, *Paracalanus parvus*, *Acartia clausi*, *Centropages ponticus*, *Oithona davisae* and *Harpactiocoida* spp., cladocerans - *Pleopis polyphemoides*, *Penilia avirositis*, *Pseudoevadne tergestina* and *Evadne spinifera*; four taxonomic groups were found from the meroplankton group: *Lamellibranchia veliger, Gastropoda veliger,* Cirripedia larvae and Decapoda larvae; class Chaetognatha was represented by *Parasagitta setosa*, class Appendicularia - by *Oicopleura dioica*.

17.The average stomach fullness index of horse mackerel was 0.60% BW ± 0.27 (SD) and the average PN - 98 ind/stomach ± 57.21 (SD), with the maximal individual number of food organisms - 178 ind/ stomach.

18.In October-November 2019, the total zooplankton biomass amounted to 150 $mg.m^{-3}$ ± 100.52 (SE), the biomass of jelly-plankton was 106.42 $mg.m^{-3}$ ± 105.33 (SE) and of mesozooplankton - 42.14 $mg.m^{-3}$ ± 11.69 (SE). Fodder mesozooplankton biomass was evaluated as low for the season.

19. The maximum sustainable yield (MSY), in accordance with the Gulland method (1970), was estimated at 18 893.38 t; BH steepness, F0.1 = 11 750 t.

20. The calculated exploitation biomass and equilibrium levels (MSYs) should not be considered as an absolute value for possible future yields, given the fact that the methods have some uncertainties and the proportion of IUU catches is still unknown. In such cases, special approaches such as using 2/3 MSY are applied (Caddy and Mahon, 1995).

21. The recommended value of catches in the Bulgarian Black Sea waters, according to the current situation, should not exceed 7333t.

IX. References

Alexandrov B. and Korshenko A., 2006. Manual for zooplankton sampling and analysis in the Black Sea Region.

Bertalanffy L. von, 1938. A quantitative theory of organic growth (Inquiries on growth laws. II). Human Biol. 10: 181-213.

Beverton, R.J. and S.J. Holt, 1957. On the dynamics of exploited fish populations. Fish. Invest. Ser. 2, Vol 19.

Caddy, J.F., and R. Mahon, 1995. Reference points for fisheries management Rome: Food and Agriculture Organization of the United Nations. ,Vol. 374.

Debes, P.V., F.E. Zachos and R. Hanel, 2008. Mitochondrial phylogeography of the European sprat (*Sprattus sprattus* L., Clupeidae) reveals isolated climatically vulnerable populations in the Mediterranean Sea and range expansion in the northeast Atlantic. Molecular Ecology 17: 3873-3888.

Dimov I., 1959. Improved quantitative method for zooplankton calculation. Rep. BAS, 12, 5, 427 429. (in Russian)

FAO, 1995. Precautionary approach to fisheries. FAO Fish. Tech. Paper N. 350 (1), 1995.

Foote, K.G., 1996. Quantitative fisheries research surveys, with special reference to computers. In: B.A. Megrey & E. Moksness. Computers in fisheries research. Chapman & Hall. 254 pp. 80-112.

Fryer, R.J., Shepherd, J.G., 1996. Models of codend size selection. Journal of Northwest Atlantic Fishery Science, 19, 51-58.

Gislason, H., Daan, N., Rice, J. C., Pope, J. G., 2010. Size, growth, temperature and the natural mortality of marine fish. Fish and Fisheries, 11(2), 149-158.

Godø, O. R., Pennington, M., Vølstad, J.H., 1990. Effect of tow duration on length composition of trawl catches. Fisheries Research, 9(2), 165-179.

Gulland J.A., 1966. Manual of sampling and statistical methods for fisheries biology. Part I: Sampling methods. FAO Manuals in Fisheries Science No. 3, Rome.

Gulland J.A., 1970. The fish resources of the ocean. FAO Fish. Techn. Pap. No. 97, 1-425, Rome.

Holden, C., 1971. "Fish flour: protein supplement has yet to fulfill expectations.": 410-412.

Hunter, J.R., Lo, N.C., Leong, R.J., 1985. Batch fecundity in multiple spawning fishes. NOAA Technical Report NMFS, 36, pp.67-77.

ICES, 2012. Report of the Workshop on Sexual Maturity Staging of Turbot and Brill (WKMSTB 2012), 5–9 March 2012, Ijmuiden, Netherlands. ICES 2012/ACOM: 56-48 pp

ICES, 2011. Report of the Workshop on Sexual Maturity Staging of Herring and Sprat (WKMSHS), 20-23 June 2011, Charlottenlund, Denmark. ICES CM 2011/ACOM:46. 143pp.

Jearld, A., 1983. Age determination. In In: Nielsen LA and Johnson DL (eds) Fisheries Techniques.

Kasapoglu, N., Duzgunes, E. 2014. Otolith Atlas for the Black Sea. Journal of Environmental Protection and Ecology 16, No 1, 133–144

Korshenko, A., Alexandrov B., 2012. Manual for mesozooplankton sampling and analysis in the Black Sea monitoring (Black Sea Zooplankton Manual) Online: http://bsc.ath.cx/documents/ExpertNetwork/default.asp?I=/Expert%20Network%20-%20 Zooplankton

Laevastu, T., 1965. Manual methods in fisheries biology. Observations on the chemical and physical environment. Chemical analysis of water FAO. Marine Physiological Sci., 6: 86-86.

Mihneva V., Raykov V., Grishin A., Stefanova K., 2015. Sprat feeding in front of the Bulgarian Black Sea Coast, MEDCOAST conference 2015, vol.1, 431- 44

Mordukhay-Boltovskoy, F.D. (Ed.). 1968. The identification book of the Black Sea and the Sea of Azov Fauna.- Kiev: Naukova Dumka Publ., T. 1 (Protozoa, Porifera, Coelenterata, Ctenophora, Nemertini, Nemathelminthes, Annelida, Tentaculata), 423 pp. (in Russian).

Mordukhay-Boltovskoy, F.D. (Ed.). 1969. The identification book of the Black Sea and the Sea of Azov Fauna.- Kiev: Naukova Dumka Publ., T. 2 (Artropoda: Cladocera, Calanoida, Cyclopoida, Monstrilloida, Harpacticoida, Ostracoda, Cirripedia, Malacostraca, Decapoda), 536 pp. (in Russian).

Mordukhay-Boltovskoy, F.D. (Ed.). 1972. The identification book of the Black Sea and the Sea of Azov Fauna.-Kiev: Naukova Dumka Publ., T. 3 (Arthropoda, Mollusca, Echinodermata, Chaetognatha, Chordata: Tunicata, Ascidiacea, Appendicularia), 340 pp. (in Russian).

Panfili, J., De Pontual, H., Troadec, H., Wrigh, P.J., 2002. Manual of fish sclerochronology.

Pinkas L., Oliver M.S, Iverson I.L.K., 1971. Food habits of albacore, bluefin tuna and bonito in Californian waters. California Fish Game 152:1-105.

Pısıl, Y., 2006. Karadeniz'de Yaşayan Çaça Balığı (Sprattus sprattus (L., 1758))'nda Kemiksi Yapıları ve Uzunluk-Frekans Metodu ile Yaş Tayini. 19 Mayıs Üniversitesi, Fen Bilimleri Enstitüsü, Y. Lisans Tezi, 32 s.

Polat, N., & Beamish, R. J., 1992. Annulus formation on anatomical structures of Siraz (Capoeta capoeta) in Altınkaya Dam Lake. Ondokuz Mayıs Uni J Sci, 4(1), 70-88.

Prodanov, K., Mikhailov K., Daskalov G., Maxim C., Chashchin A., Arkhipov A., Shlyakhov V., Ozdamar E., 1997. Environmental management of fish resources in the Black Sea and their rational exploitation. Studies and Reviews. GFCM. No. 68. FAO, Rome.

Raykov, V., 2007. Primary management objectives for sustainable Sprat (Sprattus sprattus L.) stock exploitation at the Bulgarian Black Sea coast - preliminary results J.Environmental Protection and Ecology, 8 (2),302-318.

Raykov V.S, V.V.Mihneva, G, Daskalov, 2007. Investigations on sprat (Sprattus sprattus L population dynamics related to its trophic base and climate change over the period 1996-2004 in Bulgarian waters of the Black Sea. J.Environmental Protection and Ecology, 8 (2), 319-332.

Raykov V., Panayotova M., Stefanova K., Stefanova E., Radu G., Maximov V., Anton E., 2011. Statement to the Deputy Minister of Ministry of environment and waters in order to annual workshop of Black Sea commission National Report to GFCM 35 - Annual

Assembly; Scientific report from international pelagic trawl survey in the Bulgarian and in the Romanian Black Sea area, June 2010 to National Agencies of Fisheries and Aquaculture of Bulgaria and Romania in relation to National Data Collection programs for 2010, 71 pp.

Simon, K.D., Y. Bakar, A.G. Mazlan, C.C. Zaidi and A. Samat et al., 2012. Aspects of the reproductive biology of two archer fishes Toxotes chatareus, (Hamilton, 1822) and Toxotes jaculatrix (Pallas, 1767). Environ. Biol. Fish., 93: 491-503.

Somerton, D. A., Otto, R. S., Syrjala, S. E., 2002. Can changes in tow duration on bottom trawl surveys lead to changes in CPUE and mean size?. Fisheries Research, 55(1-3), 63-70.

Sparre, P., Venema, S.C., 1998. Introduction to tropical fish stock assessment, Vol. 1. FAO Fisheries Technical Paper, Rome.

Treschev, AI (1974). Scientific bases of selective fisheries. M .: Pisht prom, 443, 3 (in Russian)

Wassenberg, T.J., Dews,G., and Cook, S.D., 2002. The impact of fish trawls on megabenthos (sponges) on the north-west shelf of Australia. Fisheries Research, 58(2), 141-151.

Annex I

2017

CPUE kg.h^{-1} и CPUAkg.km^{-2} в in the Bulgarian part of the Black Sea: sprat, h.mackerel,whiting, red mullet

CPUEkg/h	CPUAkg/	CPUAkg/k	Biomass	CPUAkg/k	Biomass	CPUEkg/h	CPUAkg/k
0	0	17,45725	1092,474	0	0	6,0006	69,82898
0	0	0	0	0	0	9,0009	108,4843
0	0	180,8072	11314,91	0	0	21,0021	253,1301
0	0	488,8029	30589,28	0	0	7,50075	87,28623
0	0	0	0	0	0	75,0075	872,8623
0	0	0	0	1047,435	65548,47	0	0
0	0	0	0	1396,58	87397,96	42,0042	488,8029
18,0018	216,969	0	0	209,487	13109,69	0	0
12,0012	144,646	108,4843	6788,948	72,32288	4525,966	0	0
0	0	349,1449	21849,49	0	0	0	0
0	0	0	0	0	0	75,0075	872,8623
75,0075	872,862	0	0	139,658	8739,796	0	0
1,50015	17,4572	698,2898	43698,98	17,45725	1092,474	0	0
120,012	1396,58	0	0	0	0	0	0
24,0024	289,292	433,9373	27155,79	0	0	0	0
15,0015	174,572	418,9739	26219,39	0	0	24,0024	279,3159
0	0	174,5725	10924,74	0	0	12,0012	139,658
1,50015	18,0807	0	0	0	0	0	0
42,0042	506,26	180,8072	11314,91	0	0	0	0
0	0	506,2601	31681,76	0	0	0	0
21,0021	253,13	253,1301	15840,88	0	0	0	0
0	0	0	0	0	0	75,0075	872,8623
0	0	349,1449	21849,49	0	0	90,009	1047,435
0	0	723,2288	45259,66	0	0	135,0135	1627,265
0	0	1745,725	109247,4	0	0	105,0105	1222,007
0	0	0	0	0	0	0	0
0	0	872,8623	54623,72	0	0	0	0
0	0	0	0	0	0	0	0
120,012	1446,46	180,8072	11314,91	0	0	0	0
0	0	361,6144	22629,83	0	0	0	0
0	0	108,4843	6788,948	0	0	0	0
105,0105	1265,65	0	0	0	0	0	0
6,0006	69,829	0	0	36,16144	2262,983	0	0
3,0003	36,1614	723,2288	45259,66	0	0	0	0
0	0	0	0	0	0	0	0
0		0	0	488,8029	30589,28	15,0015	174,5725

sprat h.mackerel

CPUEkg/h	CPUAkg/k
36,0036	418,9739
9,0009	108,4843
66,0066	795,5516
1,50015	17,45725
0	0
1,050105	12,22007
0	0
0	0
6,0006	72,32288
6,0006	69,82898
0	0
0	0
0	0
0	0
0	0
0	0
0	0
0	0
0	0
0	0
0	0
0	0
0	0
0	0
0	0
0	0
0	0
0	0
6,0006	72,32288
0	0
0	0
0	0
12,0012	139,658
0	0
45,0045	542,4216
15,0015	174,5725

CPUAkg/k	Biomass
0	0
0	0
0	0
10,47435	655,4847
0	0
0	0
34,91449	2184,949
72,32288	4525,966
0	0
0	0
174,5725	10924,74
0	0
0	0
0	0
0	0
174,5725	10924,74
0	0
0	0
0	0
0	0
0	0
0	0
0	0
0	0
0	0
0	0
17,45725	1092,474
104,7435	6554,847
0	0
0	0
0	0
0	0
0	0
0	0
0	0
0	0

red mullet

Project proposal № BG14MFOP001-3.003-0001 "Collection, management and use of data for the purposes of scientific analysis and implementation of the Common Fisheries Policy for the period 2017-2019", funded by the Maritime Affairs and Fisheries Program, co-financed by the European Union through the European Maritime and Fisheries Fund

Annex II

Видов състав в Българската част на Ч. Море, октомври -ноември

Species	1	2	3	4	5	6	7	8	9	10	11	12	13	14	15	16	17	18	19	20	21	22	23	24	25	26	27	28	29	30	31	32	33	34	35	36
Sq.acanthias																																				
R.clavata																																				
D.pastinaca																																				
A.immaculata																																				
S.sprattus																																				
M.merlangus																																				
E.encrasicolus																																				
Tr.mediterraneus																																				
M.barbatus																																				
P.maxima																																				
N.melanostomus																																				
G.niger																																				
Polybius vernalis																																				
M. galloprovincialis																																				
R.venosa																																				
A.aurita																																				

ноември-декември

Species	1	2	3	4	5	6	7	8	9	10	11	12	13	14	15	16	17	18	19	20	21	22	23	24	25	26	27	28	29	30	31	32	33	34	35	36
Sq.acanthias																																				
R.clavata																																				
D.pastinaca																																				
A.immaculata																																				
S.sprattus																																				
M.merlangus																																				
E.encrasicolus																																				
Tr.mediterraneus																																				
M.barbatus																																				
P.maxima																																				
N.melanostomus																																				
G.niger																																				
Polybius vernalis																																				
M. galloprovincialis																																				
R.venosa																																				
A.aurita																																				

Annex III

Surveys indicator targets and results in 2017(Bulgarian part of the Black Sea)

Black Sea	Length @age	market, discards, surveys	2,50%	Survey: **7250** 1250
Black Sea	Weight @length	market, discards, surveys	2,50%	Survey: **7250** 5000
Black Sea	Weight @age	market, discards, surveys	2,50%	Discard: - Survey: **7250** 1250
Black Sea	Maturity @length	surveys	2,50%	5000 **140**
Black Sea	Maturity @age	surveys	2,50%	250 **140**
Black Sea	Sex-ratio @length	market, surveys	2,50%	Market: **250** Survey: **250** 125
Black Sea	Sex-ratio @age	market, surveys	2,50%	Market: **250** Survey: **250** 500

CPUE kg.h^{-1} и CPUAkg.km^{-2} in the Bulgarian part of the Black Sea: (a) horse mackerel; (b) red mullet

CPUEkg/h	CPUAkg/km
0	0
6,0006001	72,322876
3,0003	36,161438
0	0
0	0
60,006001	723,22876
1,50015	18,080719
60,006001	698,28983
6,0006001	72,322876
24,0024	279,31593
30,003	349,14492
30,003	349,14492
45,0045	523,71738
45,0045	542,42157
60,006001	723,22876
30,003	349,14492
45,0045	523,71738
30,003	349,14492
21,0021	244,40144
9,0009001	104,74348
24,0024	289,2915
30,003	349,14492
30,003	349,14492
30,003	361,61438
3,0003	36,161438
1,50015	17,457246
45,0045	523,71738
0	0
0	0
0	0
60,006001	723,22876
90,009001	1047,4348
3,0003	34,914492
3,0003	34,914492
0	0
0	0
0	0

a)

CPUEkg/h	CPUAkg/km
0	0
3,0003	36,161438
0	0
0	0
0	0
0	0
180,018	2169,6863
0	0
30,003	361,61438
30,003	349,14492
45,0045	523,71738
45,0045	523,71738
60,006001	698,28983
30,003	361,61438
45,0045	542,42157
30,003	349,14492
60,006001	698,28983
30,003	349,14492
15,0015	174,57246
15,0015	174,57246
30,003	361,61438
15,0015	174,57246
30,003	349,14492
6,0006001	72,322876
12,0012	144,64575
9,0009001	104,74348
9,0009001	104,74348
0	0
0	0
45,0045	509,0884
0	0
0	0
0	0
30,003	349,14492
45,0045	523,71738
30,003	349,14492
30,003	361,61438

b)

Annex IV Species composition in the Bulgarian part of the Black Sea (November-December 2018)

вид	1	2	3	4	5	6	7	8	9	10	11	12	13	14	15	16	17	18	19	20	21	22	23	24	25	26	27	28	29	30	31	32	33	34	35	36
S.sprattus																																				
Tr.mediterr																																				
M.barbatus																																				
A.immaculata																																				
M.merlangius																																				
E.encrasicolus																																				
G.niger																																				
M.batrachocephalus																																				
S.porcus																																				
N.melanostomus																																				
Crenialabrus sp.																																				
S.aurata																																				
P.saltatrix																																				
Tr.draco																																				
D.pastinaca																																				
R.clavata																																				
Sq.acanthias																																				
S.maximus																																				

Project proposal № BG14MFOP001-3.003-0001 "Collection, management and use of data for the purposes of scientific analysis and implementation of the Common Fisheries Policy for the period 2017-2019", funded by the Maritime Affairs and Fisheries Program, co-financed by the European Union through the European Maritime and Fisheries Fund

Annex V Surveys indicator targets and results in November-December 2018 (Bulgarian part of the Black Sea)

Black Sea	Length @age	market, discards, surveys	2,50%	Survey: **2500** 1250
Black Sea	Weight @length	market, discards, surveys	2,50%	Survey: **2500** 5000
Black Sea	Weight @age	market, discards, surveys	2,50%	Market: Discard: - Survey: **2500** 1250
Black Sea	Maturity @length	surveys	2,50%	5000 **140**
Black Sea	Maturity @age	surveys	2,50%	5000 **140**
Black Sea	Sex-ratio @length	market, surveys	2,50%	Market: **250** Survey: **250** 125
Black Sea	Sex-ratio @age	market, surveys	2,50%	Market: Survey: **250** **250**

2018 October-December

CPUE kg.h^{-1} and CPUAkg.km^{-2} sprat

CPUEkg/h	CPUAkg/km2
220	2560.14002
400	4654.80003
120	1396.44001
60	698.220004
44	512.028003
100	1163.70001
200	2327.40001
140	1629.18001
240	2792.88002
88	1024.05601
112	1303.34401
152	1768.82401
100	1163.70001
180	2094.66001
488	5678.85604
132	1536.08401
160	1861.92001
240	2792.88002
84	977.508006
88	1024.05601
120	1396.44001
80	930.960006
56	651.672004
200	2327.40001
132	1536.08401
40	465.480003
120	1396.44001
160	1861.92001
200	2327.40001
100	1163.70001
168	1955.01601
128	1489.53601
80	930.960006
48	558.576004
200	2327.40001
132	1536.08401
96	1117.15201

Annex VI Species composition in the Bulgarian part of the Black sea

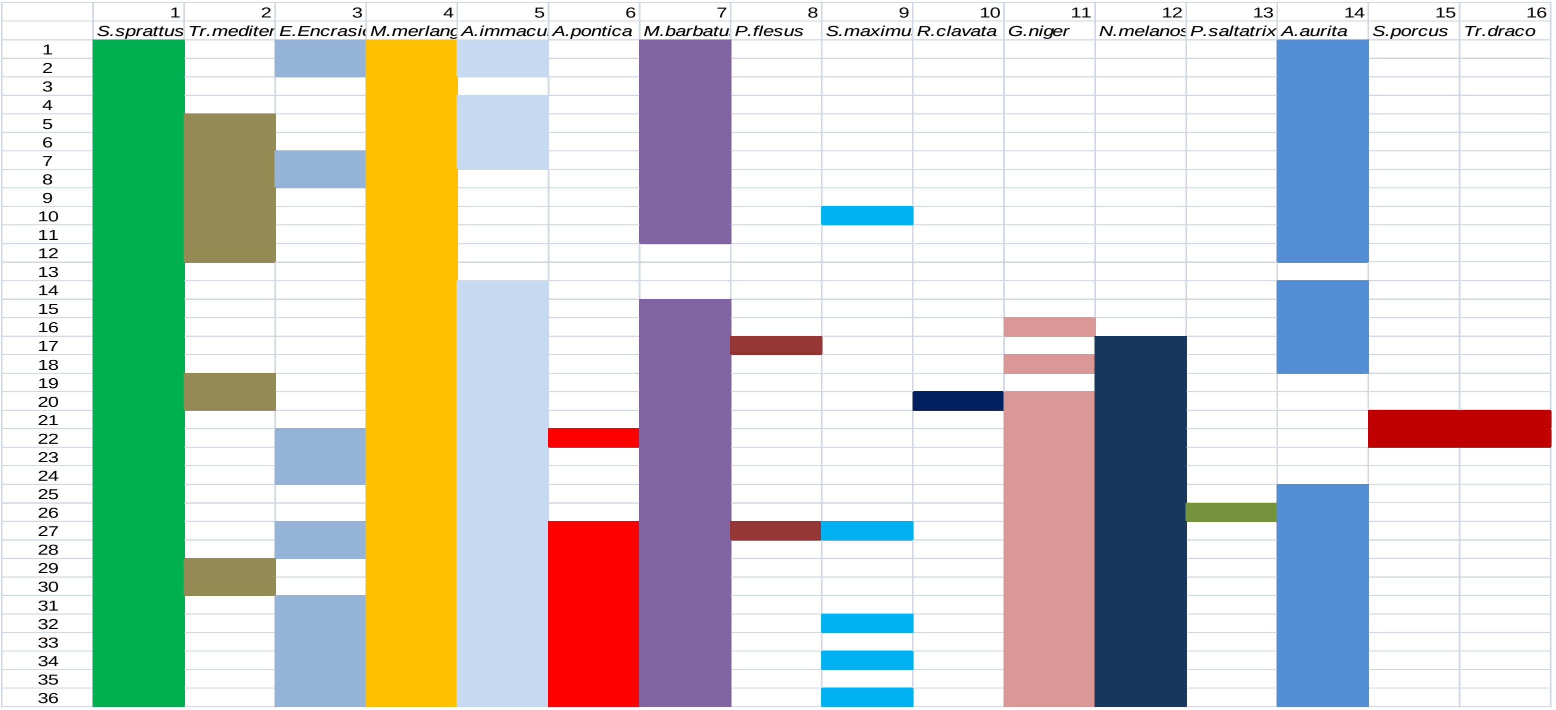

Black Sea	Length @age	market, discards, surveys	2,50%	Survey: **12 427** 1250
Black Sea	Weight @length	market, discards, surveys	2,50%	Survey: **12 427** 5000
Black Sea	Weight @age	market, discards, surveys	2,50%	Market: **2026** Discard: - Survey: **12 427** 1250
Black Sea	Maturity @length	surveys	2,50%	5000 **140**
Black Sea	Maturity @age	surveys	2,50%	5000 **140**
Black Sea	Sex-ratio @length	market, surveys	2,50%	Market: **250** Survey: **250** 125
Black Sea	Sex-ratio @age	market, surveys	2,50%	Market: **250 250 survey**

Project proposal № BG14MFOP001-3.003-0001 "Collection, management and use of data for the purposes of scientific analysis and implementation of the Common Fisheries Policy for the period 2017-2019", funded by the Maritime Affairs and Fisheries Program, co-financed by the European Union through the European Maritime and Fisheries Fund

CPUE kg.h^{-1} and CPUAkg.km^{-2} in the Bulgarian part of the Black Sea: sprat, whiting and red mullet (2019, June)

CPUEkg/h	CPUAkg/k
1636,364	19042,36
818,1818	9521,182
227,2727	2644,773
909,0909	10579,09
1363,636	15868,64
909,0909	10579,09
1363,636	15868,64
1363,636	15868,64
1818,182	21158,18
681,8182	7934,318
1090,909	12694,91
454,5455	5289,545
681,8182	7934,318
545,4545	6347,455
590,9091	6876,409
227,2727	2644,773
681,8182	7934,318
909,0909	10579,09
636,3636	7405,364
727,2727	8463,273
409,0909	4760,591
500	5818,5
636,3636	7405,364
818,1818	9521,182
150	1745,55
181,8182	2115,818
909,0909	10579,09
636,3636	7405,364
636,3636	7405,364
363,6364	4231,636
409,0909	4760,591
909,0909	10579,09
454,5455	5289,545
0	0
227,2727	2644,773
136,3636	1586,864
0	0

a)

CPUEkg/h	CPUAkg/k
9,090909	105,7909
13,63636	158,6864
22,72727	264,4773
68,18182	793,4318
0	0
0	0
2,272727	26,44773
0	0
45,45455	528,9545
4,545455	52,89545
4,545455	52,89545
9,090909	105,7909
4,545455	52,89545
22,72727	264,4773
22,72727	264,4773
22,72727	264,4773
13,63636	158,6864
13,63636	158,6864
22,72727	264,4773
22,72727	264,4773
45,45455	528,9545
0	0
0	0
0	0
0	0
0	0
0	0
9,090909	105,7909
22,72727	264,4773
13,63636	158,6864
13,63636	158,6864
4,545455	52,89545
22,72727	264,4773
4,545455	52,89545
9,090909	105,7909
4,545455	52,89545
0	0

b)

CPUEkg/h	CPUAkg/k
4,545455	52,89545
4,545455	52,89545
0	0
0	0
0	0
0	0
0	0
0	0
0	0
0	0
0	0
0	0
0	0
0	0
0	0
0	0
0	0
9,090909	105,7909
9,090909	105,7909
22,72727	264,4773
22,72727	264,4773
4,545455	52,89545
4,545455	52,89545
4,545455	52,89545
4,545455	52,89545
45,45455	528,9545
90,90909	1057,909
90,90909	1057,909
68,18182	793,4318
90,90909	1057,909
90,90909	1057,909
4,545455	52,89545
13,63636	158,6864
4,545455	52,89545
4,545455	52,89545
13,63636	158,6864
9,090909	105,7909

c)

Project proposal № BG14MFOP001-3.003-0001 "Collection, management and use of data for the purposes of scientific analysis and implementation of the Common Fisheries Policy for the period 2017-2019", funded by the Maritime Affairs and Fisheries Program, co-financed by the European Union through the European Maritime and Fisheries Fund

Annex VII

Date	Trawls	Start N	Start E	End N	End E	Description of trawls	№, plankton	№, stomach	depth, m	№, DNA
08.06.2019	1	42.458388	27.829595	42.449619	27.858528	*360 kg S.sprattus, 15 бр. M.merlangus, 1 бр. M.barbatus*	2	1	37	
08.06.2019	2	42.389953	27.924186	42.371801	27.945546	*180 kg S.sprattus, 20 бр. M.merlangus, 1 бр. M. barbatus*	3	4	39	
08.06.2019	3	42.313893	28.104401	42.318671	28.142564	*10 kg A.aurita*			67-75	
08.06.2019	4	42.265748	28.171686	42.261012	28.130405	*200 kg S.sprattus, 5 kg M.merlangus, 3 kg A.aurita*			81	
08.06.2019	5	42.254808	28.111101	42.252977	28.081764	*300 kg S.sprattus, 15 kg M.merlangus, 5 kg A.aurita, D.delphis - 20 бр.*	5	6	60	5-S.maximus
09.06.2019	6	42.418577	27.795370	42.391944	27.806546	*200 kg S.sprattus*			38	
09.06.2019	7	42.385003	27.808578	42.358501	27.818090	*300 kg S.sprattus*	7	9	42	
09.06.2019	8	42.338717	27.814046	42.300659	27.835064	*300 kg S.sprattus, 5 бр. M.merlangus*			50-52	
09.06.2019	9	42.254321	27.895999	42.231004	27.930733	*400 kg S.sprattus, D.delphis - 15 бр.*	8	10	41	
09.06.2019	10	42.291884	28.006395	42.319416	27.977566	*150 kg S.sprattus, 10 kg M.merlangus, 1 бр. P.flesus*			51-49	11-P.flesus
09.06.2019	11	42.375979	27.942515	42.389112	27.915019	*240 kg S.sprattus*			41-39	
11.06.2019	12	42.434899	27.770478	42.463454	27.799338	*100 kg S.sprattus, 10 kg A.aurita*			35	
11.06.2019	13	42.468698	27.804672	42.489822	27.825500	*150 kg S.sprattus, 15 kg A.aurita, D.delphis - 15 бр.*	11	`12	36	
11.06.2019	14	42.473905	27.886203	42.455591	27.856802	*120 kg S.sprattus, 5 бр. M.merlangus, 4 бр. Gobiidae, D.delphis - 15 бр.*			37	
11.06.2019	15	42.452590	27.851214	42.439847	27.831276	*130 kg S.sprattus, 7 бр. M.merlangus, 6 бр. Gobiidae, D.delphis - 15 бр.*			36	
12.06.2019	16	42.545857	27.864756	42.571139	27.841242	*20 kg A.aurita*			37	
12.06.2019	17	42.585774	27.854196	42.611589	27.843443	*150 kg S.sprattus, 15 бр. M.merlangus, 10 бр. M. barbatus, 10 kg A.aurita*			32	
12.06.2019	18	42.619065	27.844205	42.648905	27.855974	*200 kg S.sprattus, 15 бр. M.merlangus, 10 бр. M. barbatus, 10 kg A.aurita*	14	13	27	
12.06.2019	19	42.688405	27.844863	42.692831	27.808492	*140 kg S.sprattus, 5 kg M.merlangus, 5 kg M.barbatus*			20	
12.06.2019	20	42.692831	27.801253	42.689479	27.754313	*160 kg S.sprattus, 5 kg M.merlangus, 5 kg M.barbatus, A.stellatus, P.flesus, S.maximus, D.delphis-4 бр.*			19	18, 19, 20
13.06.2019	21	42.680526	27.780544	42.652097	27.790041	*90 kg S.sprattus, 3 kg M.merlangus, 1 kg M.barbatus*			23	

Annex VIII

Black Sea	Length @age	market, discards, surveys	2,50%	Survey: **2565** 1250
Black Sea	Weight @length	market, discards, surveys	2,50%	Survey: **2565** 5000
Black Sea	Weight @age	market, discards, surveys	2,50%	Market: Discard: - Survey: **2565** 1250
Black Sea	Maturity @length	surveys	2,50%	5000 **140**
Black Sea	Maturity @age	surveys	2,50%	5000 **140**
Black Sea	Sex-ratio @length	market, surveys	2,50%	Market: **250** Survey: **250** 125
Black Sea	Sex-ratio @age	market, surveys	2,50%	Market: Survey: **250** **250**

2019 October-November

CPUE kg.h^{-1} and CPUAkg.km^{-2} : sprat (a) whiting (b) и red mullet (c)

a)

CPUEkg/h	CPUAkg/k
909,0909	10579,09
681,8182	7934,318
336,3636	3914,264
1136,364	13223,86
1818,182	21158,18
2500	29092,5
681,8182	7934,318
1818,182	21158,18
636,3636	7405,364
772,7273	8992,227
1136,364	13223,86
409,0909	4760,591
1000	11637
681,8182	7934,318
909,0909	10579,09
181,8182	2115,818
818,1818	9521,182
1136,364	13223,86
1272,727	14810,73
1363,636	15868,64
1159,091	13488,34
1818,182	21158,18
1000	11637
909,0909	10579,09
227,2727	2644,773
681,8182	7934,318
818,1818	9521,182
904,5455	10526,2
1136,364	13223,86
454,5455	5289,545
500	5818,5
1136,364	13223,86
909,0909	10579,09
654,5455	7616,946
454,5455	5289,545
409,0909	4760,591
445,4545	5183,755
280,2735	3261,543

b)

CPUEkg/h	CPUAkg/k
31,81818	370,2682
22,72727	264,4773
9,090909	105,7909
4,545455	52,89545
18,18182	211,5818
40,90909	476,0591
54,54545	634,7455
545,4545	6347,455
63,63636	740,5364
36,36364	423,1636
22,72727	264,4773
72,72727	846,3273
40,90909	476,0591
100	1163,7
159,0909	1851,341
186,3636	2168,714
45,45455	528,9545
90,90909	1057,909
113,6364	1322,386
159,0909	1851,341
186,3636	2168,714
227,2727	2644,773
27,27273	317,3727
40,90909	476,0591
36,36364	423,1636
36,36364	423,1636
18,18182	211,5818
4,545455	52,89545
40,90909	476,0591
18,18182	211,5818
22,72727	264,4773
9,090909	105,7909
40,90909	476,0591
22,72727	264,4773
50	581,85
27,27273	317,3727
9,090909	105,7909
45,45455	528,9545

c)

CPUEkg/h	CPUAkg/k
250	2909,25
45,45455	528,9545
90,90909	1057,909
181,8182	2115,818
9,090909	105,7909
18,18182	211,5818
0	0
0	0
0	0
0	0
0	0
90,90909	1057,909
18,18182	211,5818
4,545455	52,89545
54,54545	634,7455
0	0
0	0
0	0
45,45455	528,9545
0	0
68,18182	793,4318
18,18182	211,5818
0	0
45,45455	528,9545
22,72727	264,4773
0	0
0	0
0	0
0	0
0	0
22,72727	264,4773
9,090909	105,7909
636,3636	7405,364
654,5455	7616,946
454,5455	5289,545
409,0909	4760,591
445,4545	5183,755
280,2735	3261,543

Annex IX

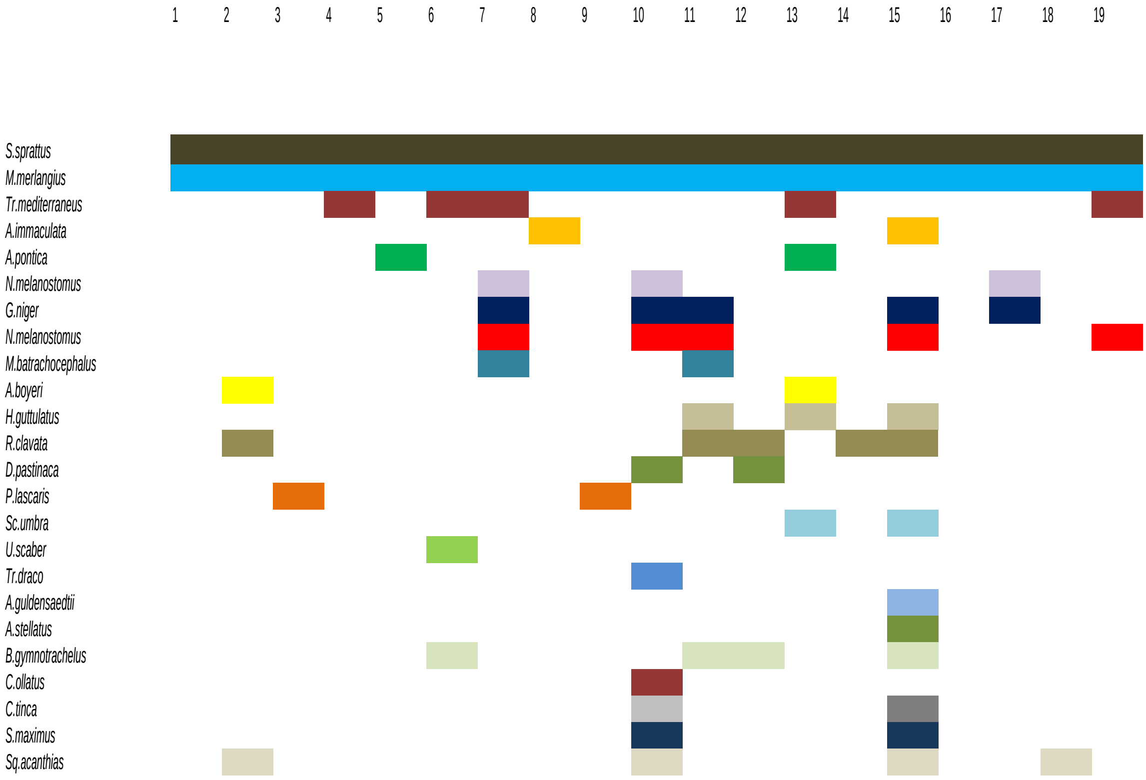
1 2 3 4 5 6 7 8 9 10 11 12 13 14 15 16 17 18 19
S.sprattus
M.merlangius
Tr.mediterraneus
A.immaculata
A.pontica
N.melanostomus
G.niger
N.melanostomus
M.batrachocephalus
A.boyeri
H.guttulatus
R.clavata
D.pastinaca
P.lascaris
Sc.umbra
U.scaber
Tr.draco
A.guldensaedtii
A.stellatus
B.gymnotrachelus
C.ollatus
C.tinca
S.maximus
Sq.acanthias

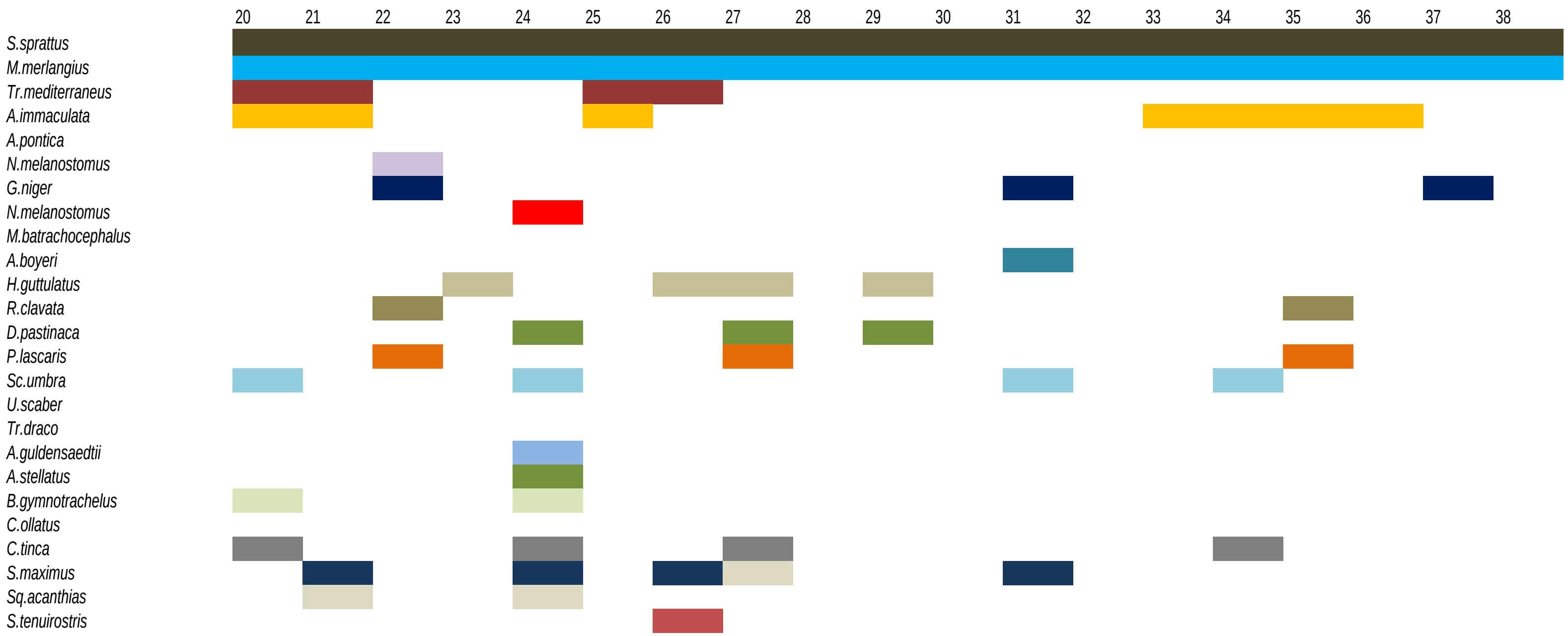
20
21
22
23
24
25
26
27
28
29
30
31
32
33
34
35
36
37
38
S.sprattus
M.merlangius
Tr.mediterraneus
A.immaculata
A.pontica
N.melanostomus
G.niger
N.melanostomus
M.batrachocephalus
A.boyeri
H.guttulatus
R.clavata
D.pastinaca
P.lascaris
Sc.umbra
U.scaber
Tr.draco
A.guldensaedtii
A.stellatus
B.gymnotrachelus
C.ollatus
C.tinca
S.maximus
Sq.acanthias
S.tenuirostris

Annex X

Black Sea	Length @age	market, discards, surveys	2,50%	Survey: **1326** 1250
Black Sea	Weight @length	market, discards, surveys	2,50%	Survey: **1326** 5000
Black Sea	Weight @age	market, discards, surveys	2,50%	Market: Discard: - Survey: **1326** 1250
Black Sea	Maturity @length	survey	2,50%	5000 **140**
Black Sea	Maturity @age	survey	2,50%	5000 **140**
Black Sea	Sex-ratio @length	market, survey	2,50%	market: **250** survey: **250** 125
Black Sea	Sex-ratio @age	market, survey	2,50%	market: survey: **250** **250**

Annex XI Navigation, bathymetry and hydroacoustics

Expeditions 2017-2019

For more sensitivity interpretation of the results of trawl picture was used navigation software **OpenCPN 4.8.0** [1] and **GPS "HOLLUX"** (Fig. 1 - 6)

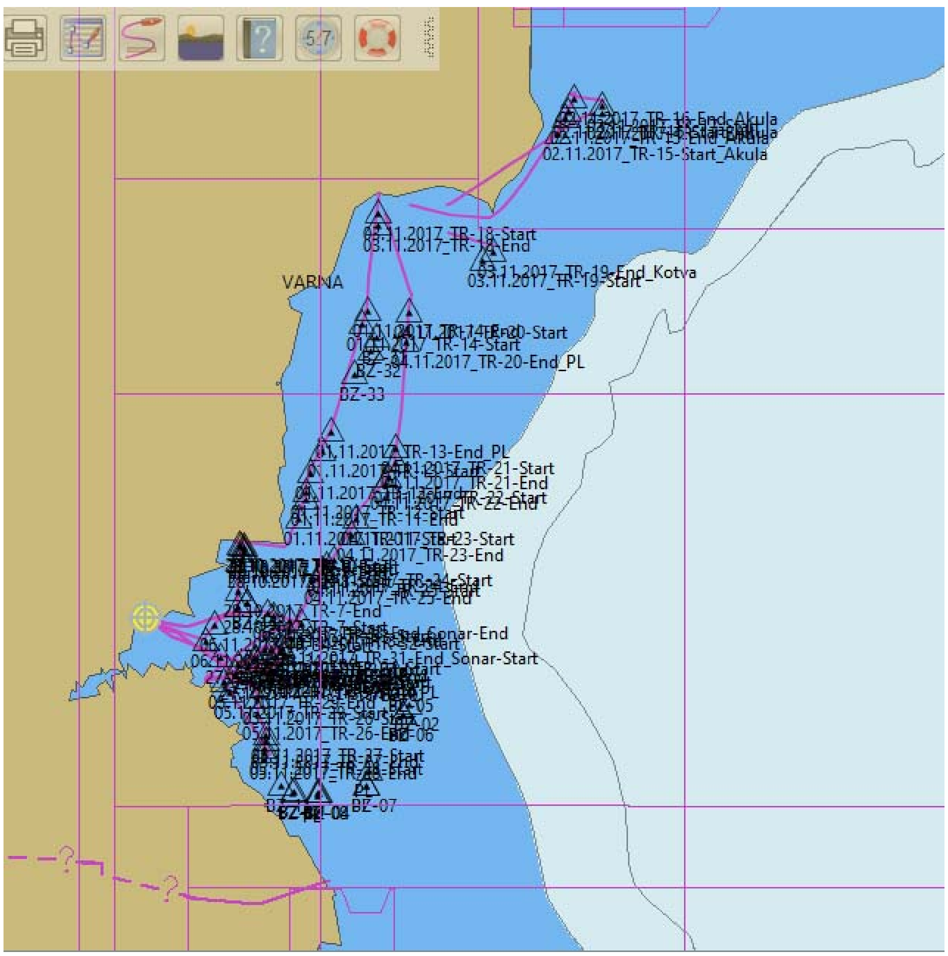

Fig. 1. Navigation map of the first expedition 2017 (OpenCPN 4.8.0.) [1]

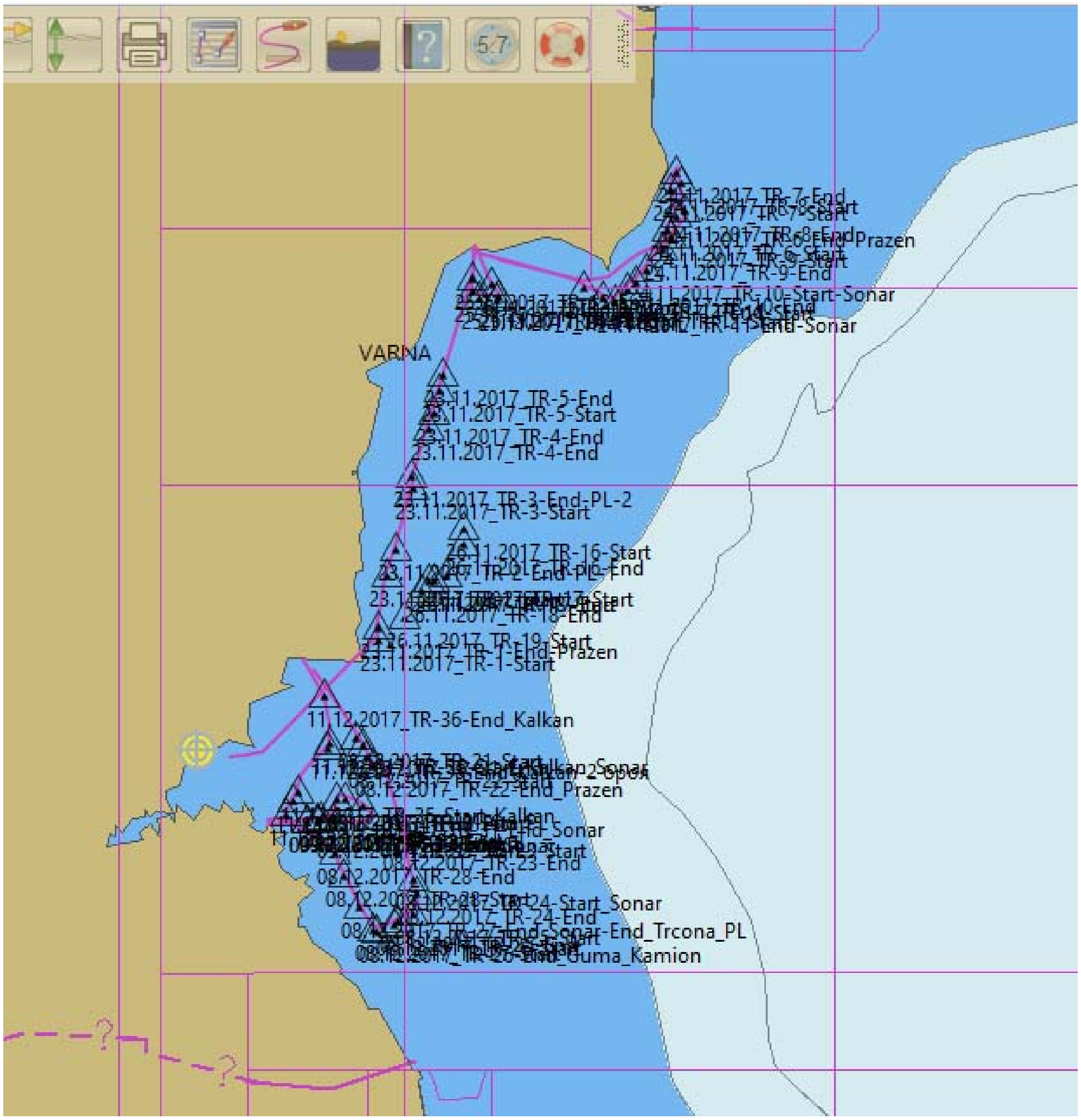

Fig. 2. Navigation map of the second expedition 2017 (OpenCPN 4.8.0.) [1]

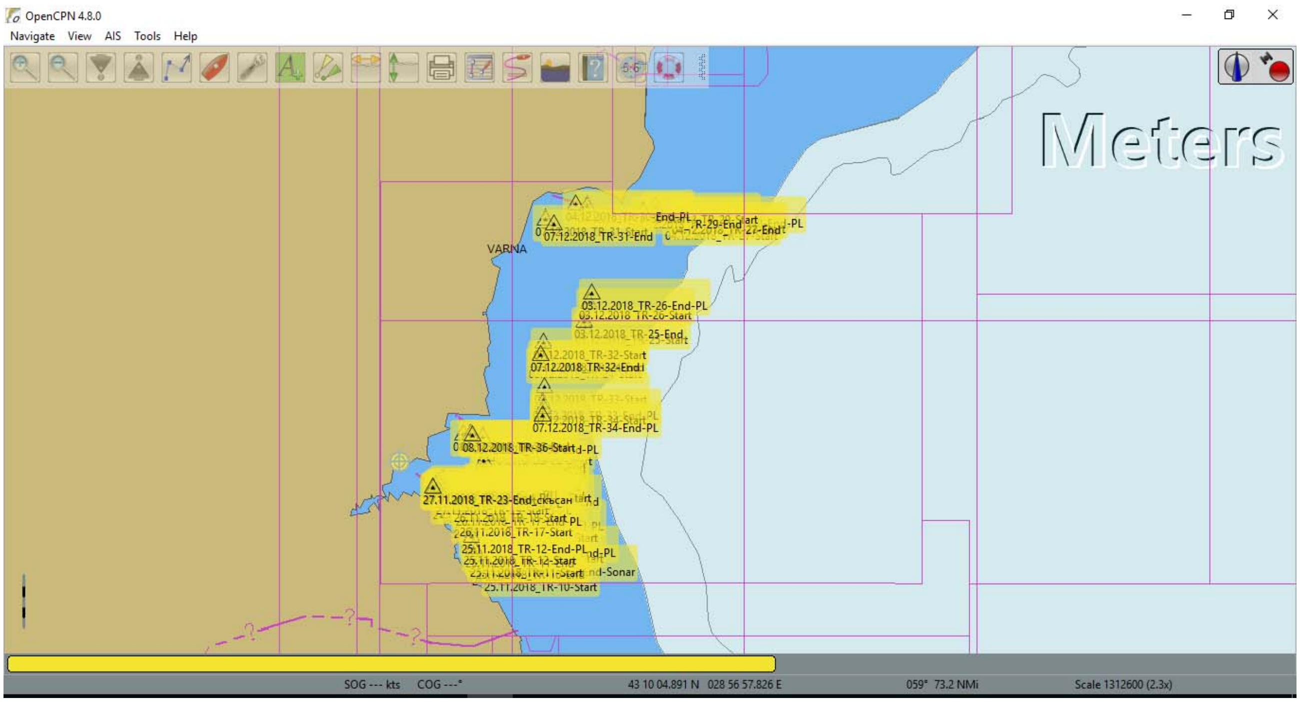

Fig. 3. Navigation map of the first expedition 2018 (OpenCPN 4.8.0.) [1]

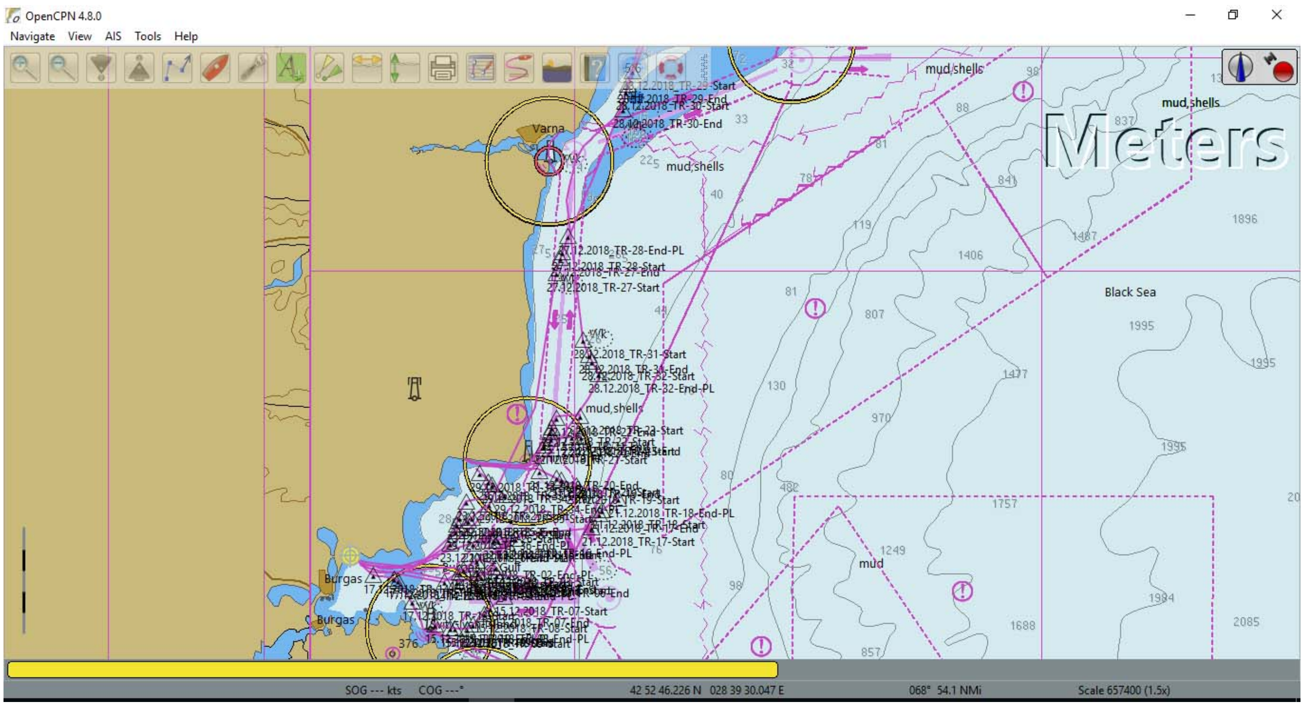

Fig. 4. Navigation map of the second expedition 2018 (OpenCPN 4.8.0.) [1]

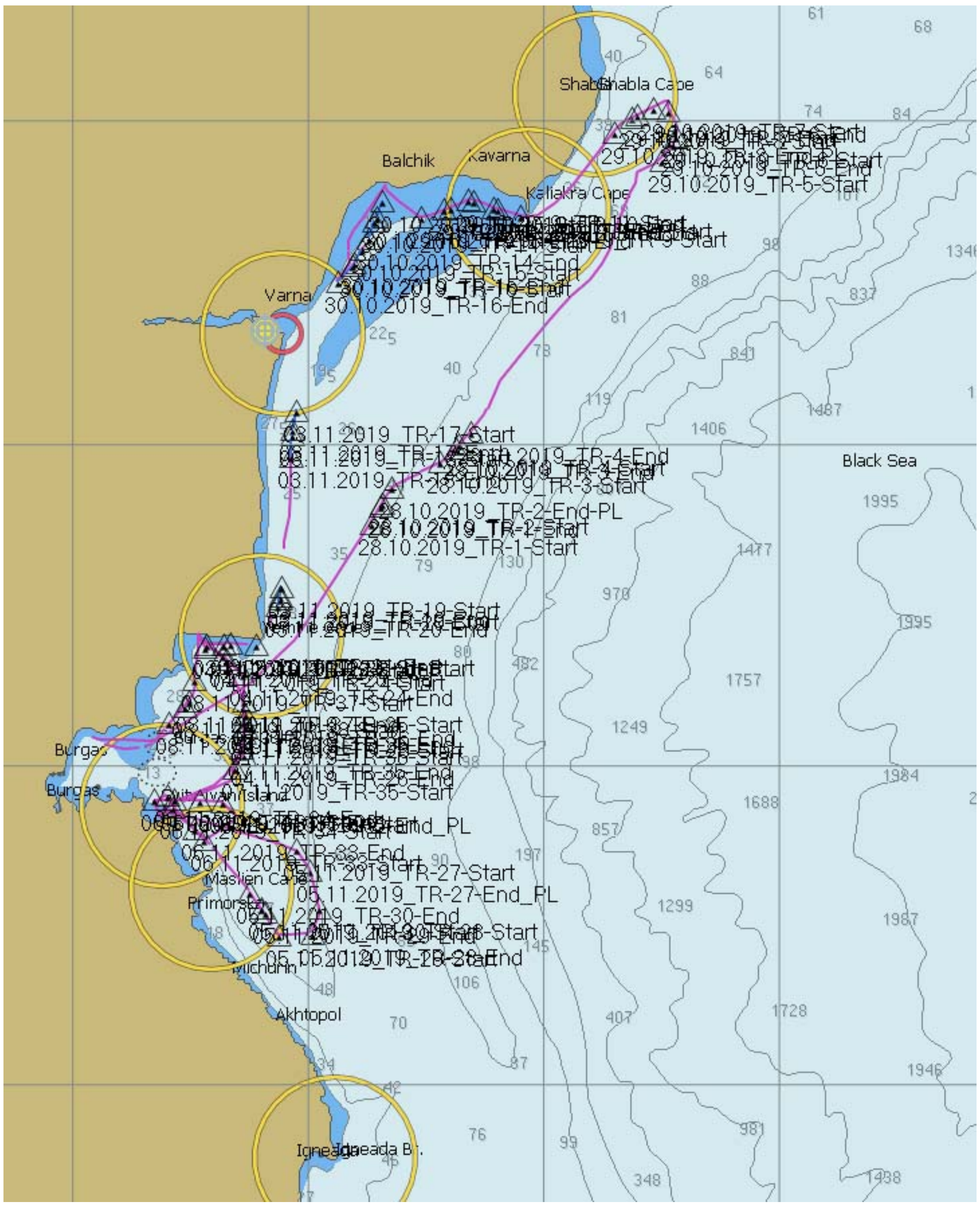

Fig. 6. Navigation map of the expedition in October-November 2019 (OpenCPN 4.8.0) [1]

For the more detailed depth measurements, determination of fish species and marine sediments was used Hydrographic Survey Echo Sounder **"**LituGraph 4F" (Fig. 7 - 12).

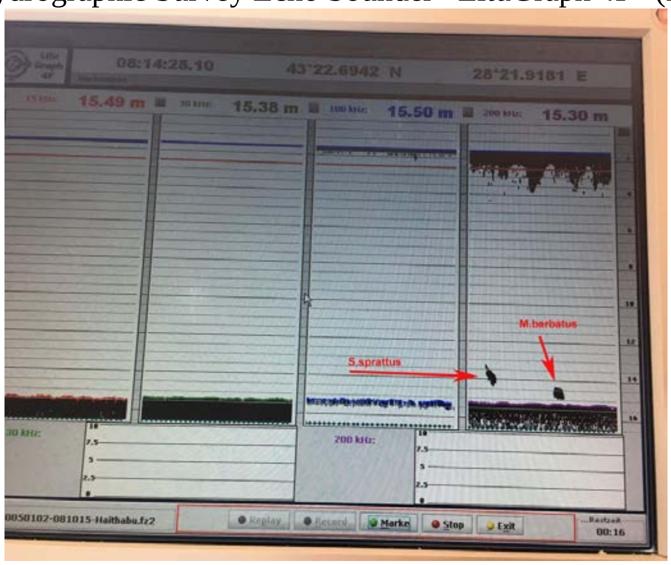

Fig. 7. Hydrographic Survey Echo Sounder **"**LituGraph 4F".
Trawl 31 (2019-1), *fish schools of S.sprattus*, *M.barbatus*, *Gobiidae.*

Fig. 8. Trawl 31 (2019-1), catch - 90 kg *S.sprattus*, 20 kg *M.barbatus*, 3 ind. *A.immaculata*, 20 kg *Gobiidae*, 70 kg *A.aurita*, 7 ind. *T. Mediterraneus*, 2 ind. *S.maximus*, 1 ind. *U.scaber*, 5 ind. *E.encrasicolus*

Project proposal № BG14MFOP001-3.003-0001 "Collection, management and use of data for the purposes of scientific analysis and implementation of the Common Fisheries Policy for the period 2017-2019", funded by the Maritime Affairs and Fisheries Program, co-financed by the European Union through the European Maritime and Fisheries Fund

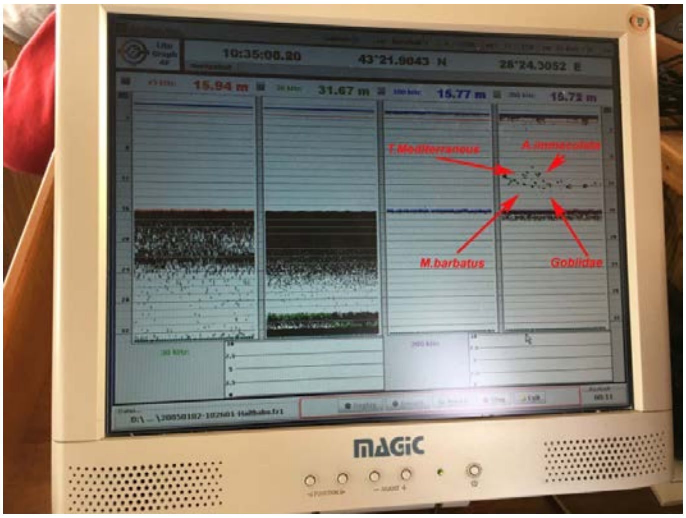

Fig. 9. Hydrographic Survey Echo Sounder **“**LituGraph 4F”.

***Trawl 10 (2019-2), fish schools of** T.mediterraneus, M.barbatus, Gobiidae, A.immaculata*

Fig. 10. Trawl 10 (2019-2), catch – 2.5 kg,
T.Mediterraneus, M.barbatus, Gobiidae, A.immaculata and Psetta maxima – 3,6 kg

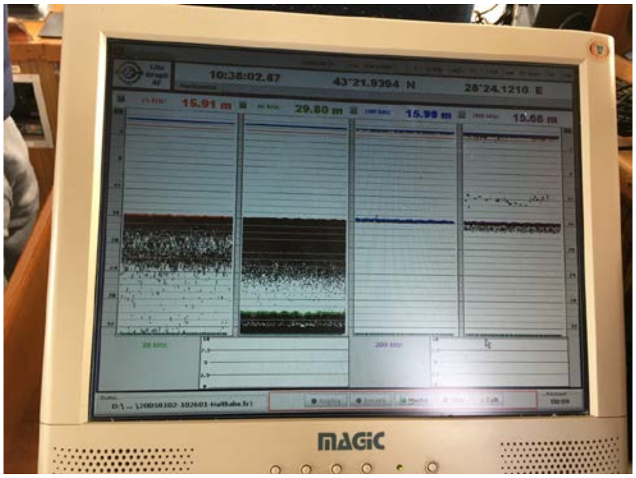

Fig. 11. Hydrographic Survey Echo Sounder “LituGraph 4F”.

Project proposal № BG14MFOP001-3.003-0001 "Collection, management and use of data for the purposes of scientific analysis and implementation of the Common Fisheries Policy for the period 2017-2019", funded by the Maritime Affairs and Fisheries Program, co-financed by the European Union through the European Maritime and Fisheries Fund

Trawl 12 (2019-2), ***fish schools of*** *T.Mediterraneus, M.barbatus, Gobiidae, A.immaculata.*

Fig. 12. Trawl 12 (2019-2), catch – 4.5 kg

T.Mediterraneus, M.barbatus, Gobiidae, A.immaculata

www.eufunds.bg

Project proposal № BG14MFOP001-3.003-0001 "Collection, management and use of data for the purposes of scientific analysis and implementation of the Common Fisheries Policy for the period 2017-2019", funded by the Maritime Affairs and Fisheries Program, co-financed by the European Union through the European Maritime and Fisheries Fund

For the purposes and tasks of the present study, hydro-acoustic equipment SIMRAD - NSO evo3 / HDS Carbon / LOWRANCE (Fig. 13, 14), [2, 3] was used.

Fig. 13. SIMRAD - NSO evo3 / HDS Carbon / LOWRANCE

Fig. 14. Probe of "SIMRAD - NSO evo3"

The hydroacoustic profiles make it possible to determine the quantitative and qualitative characteristics of the fish schools in combination with the macroscopic description of the trawl picture taken.

www.eufunds.bg

Project proposal № BG14MFOP001-3.003-0001 "Collection, management and use of data for the purposes of scientific analysis and implementation of the Common Fisheries Policy for the period 2017-2019", funded by the Maritime Affairs and Fisheries Program, co-financed by the European Union through the European Maritime and Fisheries Fund

NSO evo3 delivers the ultimate view with an ultra-bright display, available in 16, 19, or 24-inch widescreen sizes. Wide viewing angles keep the screen in view from anywhere in sight, even if you're wearing polarized sunglasses. See more than ever with Full HD resolution, and the option to combine up to six panels in a split-screen layout. Intuitively navigate charts, define waypoints, and take control of connected systems such as autopilot, radar, and sonar with a touch.

The Carbon HDS Series combines side imaging, downscan imaging, dual-channel CHIRP sonar, real-time underwater 3D mapping capabilities and ultra-bright displays to deliver the most advanced and easy-to-use fish finder/chart plotter on the market. The units' touch-screen interface works much like a smartphone with pinch-to-zoom and touch-and-move abilities for fast and intuitive control.

HDS Carbon units also feature the ability to create custom maps using recorded sonar logs. Anglers can add custom color layers, vegetation and bottom-hardness overlays. Each unit supports the most advanced marine technology and is easily updated to the most current software for optimal performance.

Featuring a powerful dual-core, high-performance processor, the HDS Carbon delivers accurate and definitive images with superior target separation. HDS Carbon multi-touch, super bright displays offer a wider viewing angle and feature an advanced anti-reflective coating for ultimate viewing in bright sunlight and while wearing polarized sunglasses.

HDS Carbon units remove the hassle of constantly monitoring and repositioning the boat with connectivity to certain autopilot trolling motors and shallow water anchors, freeing up anglers to concentrate on fishing. Both bow-mounted and console sonar can be displayed side-by-side with different zoom levels for a clear and precise view of schools or individual fish.

"SIMRAD - NSO evo3" provides the following data processing capabilities: navigation map, sonar and radar.

The Sonar feature provides an underwater view of the area, under and around the ship, allowing easy visualization of fish passages and geological - geomorphologic exploration of the sea floor. The format of the files is <*.sl3>, which includes the Sonar and StructureScan3D options. StructureScan HD provides a 328-meter wide-screen coverage with SideScan, while DownScan ™ provides a detailed view of the bottom structure and fish passages directly below the boat up to 92 m. StructureScan 3D is a multi-beam sonar technology that allows you to observe the structure and geomorphological features of the sea floor in 3D.

The "ReefMaster2.0.38.0" software was used to process and interpret hydroacoustic profile data (Fig. 15 - 17) [4].

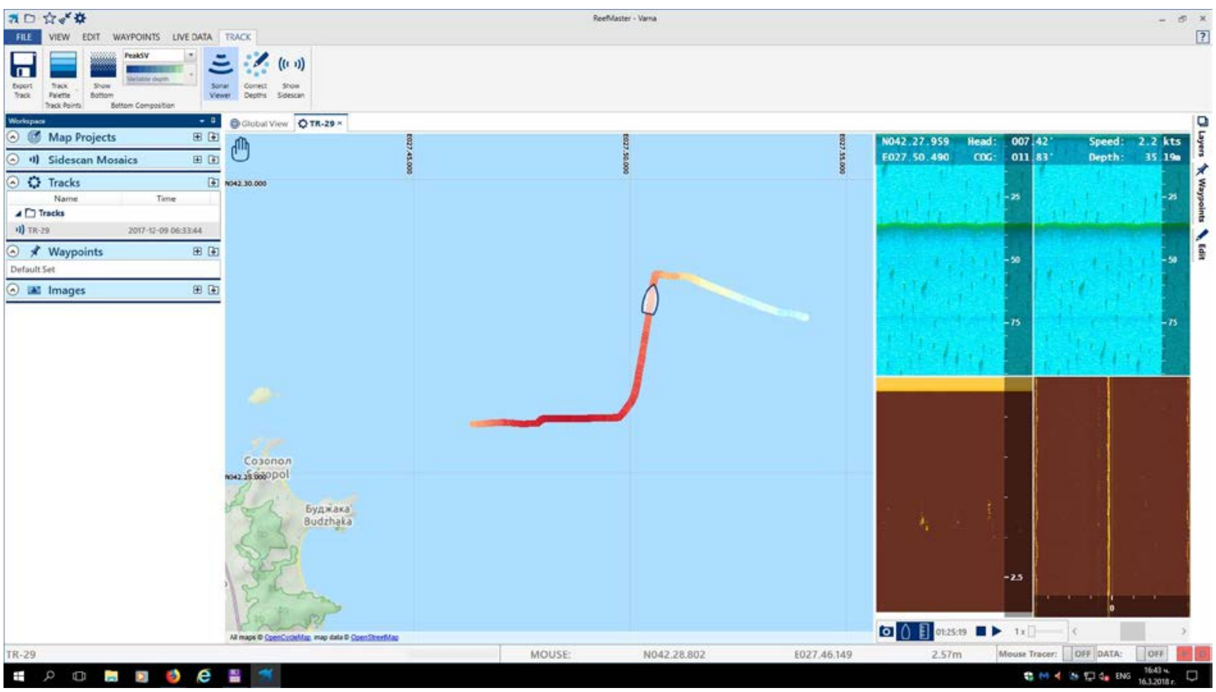

Fig. 15. Trawl 29 (2017-2)

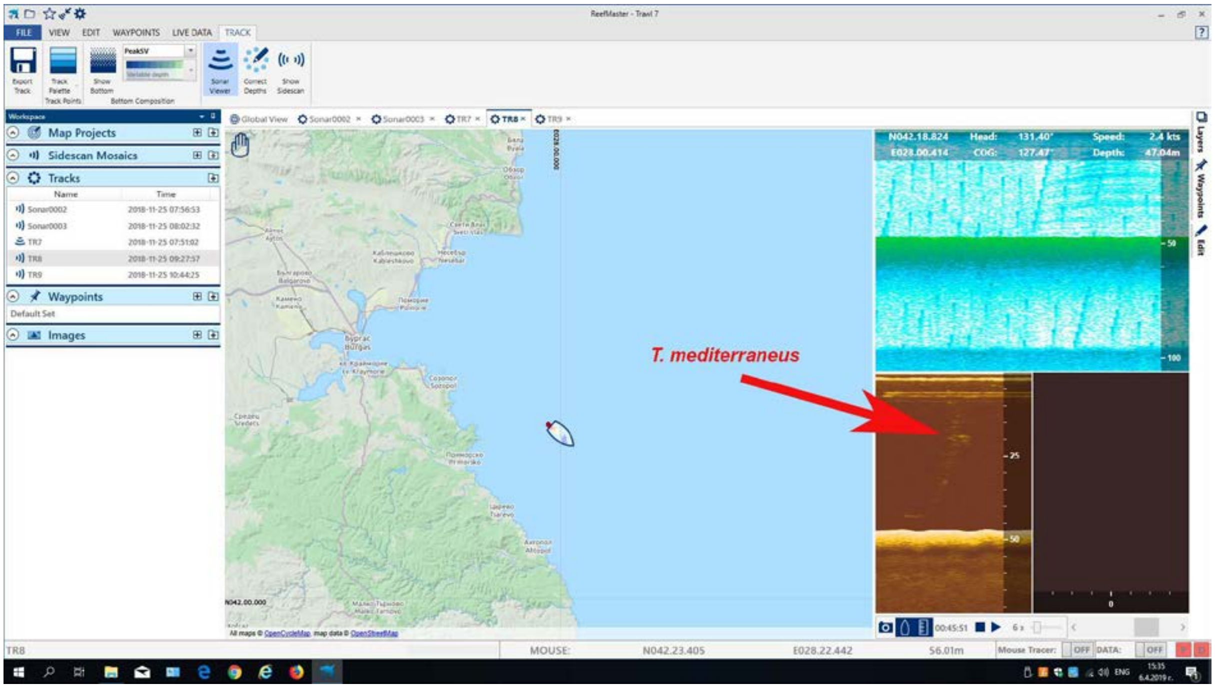

Fig. 16. Trawl 8 (2018-1), fish schools of *T.Mediterraneus*

Project proposal № BG14MFOP001-3.003-0001 "Collection, management and use of data for the purposes of scientific analysis and implementation of the Common Fisheries Policy for the period 2017-2019", funded by the Maritime Affairs and Fisheries Program, co-financed by the European Union through the European Maritime and Fisheries Fund

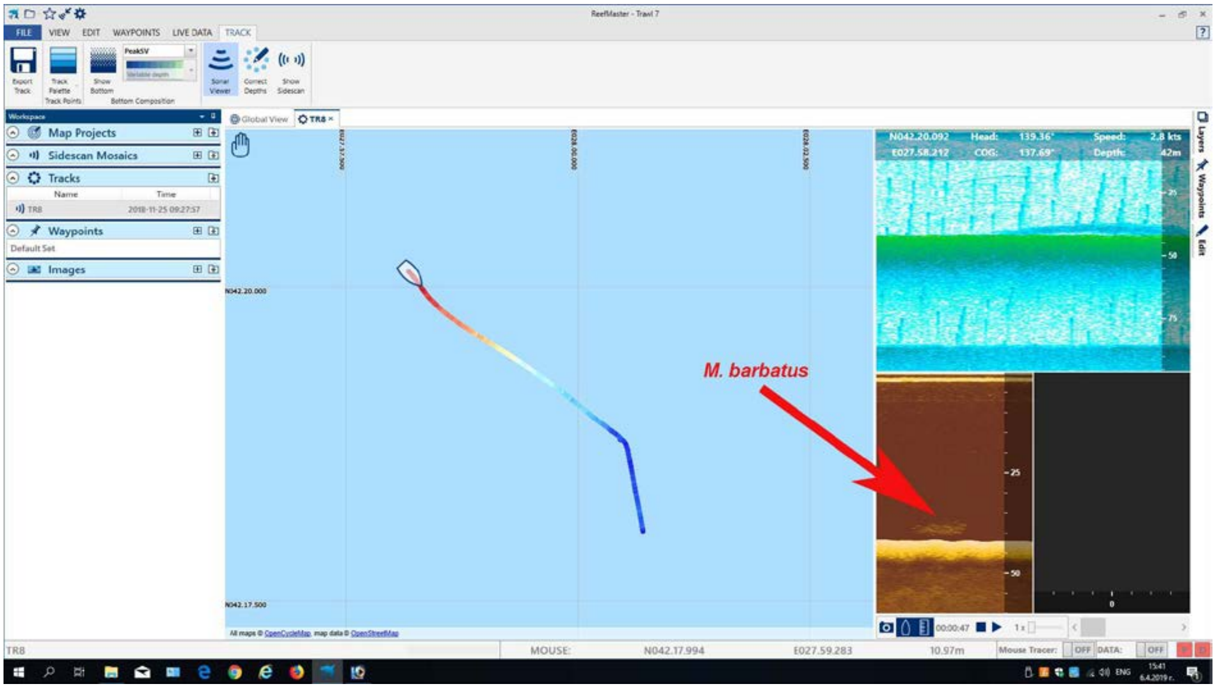

Fig. 17. Trawl 8 (2018-1), fish schools of *M.barbatus*

References

[1] OpenCPN 4.8.0. *https://opencpn.org/OpenCPN/about/ver480.html*

[2] Lowrance. 2018. *https://www.lowrance.com/lowrance/series/hds-carbon/*

[3] SIMRAD. 2018. *https://www.simrad-yachting.com/simrad/series/nso-evo3/*

[4] ReefMaster Software Ltd. 2018. *https://reefmaster.com.au/*